

EFFECTS OF SOIL SPATIAL VARIABILITY ON
SOIL-STRUCTURE INTERACTION

CENTRE FOR NEWFOUNDLAND STUDIES

**TOTAL OF 10 PAGES ONLY
MAY BE XEROXED**

(Without Author's Permission)

ARASH NOBAHAR



NOTE TO USERS

This reproduction is the best copy available.

UMI[®]



National Library
of Canada

Bibliothèque nationale
du Canada

Acquisitions and
Bibliographic Services

Acquisitions et
services bibliographiques

395 Wellington Street
Ottawa ON K1A 0N4
Canada

395, rue Wellington
Ottawa ON K1A 0N4
Canada

Your file *Votre référence*

ISBN: 0-612-93084-X

Our file *Notre référence*

ISBN: 0-612-93084-X

The author has granted a non-exclusive licence allowing the National Library of Canada to reproduce, loan, distribute or sell copies of this thesis in microform, paper or electronic formats.

L'auteur a accordé une licence non exclusive permettant à la Bibliothèque nationale du Canada de reproduire, prêter, distribuer ou vendre des copies de cette thèse sous la forme de microfiche/film, de reproduction sur papier ou sur format électronique.

The author retains ownership of the copyright in this thesis. Neither the thesis nor substantial extracts from it may be printed or otherwise reproduced without the author's permission.

L'auteur conserve la propriété du droit d'auteur qui protège cette thèse. Ni la thèse ni des extraits substantiels de celle-ci ne doivent être imprimés ou autrement reproduits sans son autorisation.

In compliance with the Canadian Privacy Act some supporting forms may have been removed from this dissertation.

Conformément à la loi canadienne sur la protection de la vie privée, quelques formulaires secondaires ont été enlevés de ce manuscrit.

While these forms may be included in the document page count, their removal does not represent any loss of content from the dissertation.

Bien que ces formulaires aient inclus dans la pagination, il n'y aura aucun contenu manquant.

Canada

**EFFECTS OF SOIL SPATIAL VARIABILITY ON SOIL-
STRUCTURE INTERACTION**

By

©Arash Nobahar, B.Eng., M.Sc.

A thesis submitted to the School of Graduate
Studies in partial fulfilment of the requirements
for the degree of

Doctor of Philosophy

Faculty of Engineering and Applied Science, Memorial
University of Newfoundland

July 2003

St. John's

Newfoundland

Canada

In memory of my father

ABSTRACT

Many physical systems in general, and soil materials in particular, exhibit relatively large spatial variability in their properties, even within so-called homogeneous layers. Physical descriptions of this spatial variability are not feasible owing to the prohibitive cost of sampling and uncertainty induced by measurement errors. This variability is widely dealt with as uncertainty in soil properties. Probabilistic methods currently used to represent this uncertainty often suffer from many limitations. For instance, they often only account for uncertainty in estimating the average soil properties. A probabilistic approach was developed here to investigate the effects of soil heterogeneity and provide practical recommendations and guidelines to account for these effects in routine engineering design.

There are still many unknown consequences of spatial variability. It is shown here that natural variability of soil properties within geologically distinct and so-called uniform layers affects soil behaviour. This study found that the phenomena governed by highly nonlinear constitutive relations are the most affected by spatial variability of soil properties. The bearing capacity of shallow foundations and lateral interaction loads of buried pipelines are functions of soil shear strength and, therefore, are governed by highly nonlinear stress-strain relationships.

The effects of soil heterogeneity were investigated for a strip foundation placed on elastic perfectly plastic soil and subjected to vertical loads. From a comparison of Monte Carlo simulations, accounting for the spatial variability of soil strength, and deterministic analyses assuming uniform soil properties, it was found that the soil heterogeneity changes

the mechanical behaviour of foundations. A parametric study was performed to quantify the effects of soil heterogeneity parameters on foundation response; the studied cases were pre-designed using statistical methods (Design of Experiments, DOE). It was observed that soil strength's degree of variation and probability distribution, which characterize the amount of weak pockets of soil, have the most effects on the foundation behaviour for the range of parameters considered. Correlation distances also affected the variability of foundation responses owing to local averaging effects.

The results of the parametric study are presented as simple regression equations (response surfaces) to estimate probabilistic characteristics of foundation responses - namely mean and coefficient of variation of bearing capacity and bearing pressures at damage criteria. They were used to calibrate partial design factors for limit state design methods, LSD, and estimate characteristic values for routine engineering design. The results, in terms of regression equations, can also be employed directly in level II & III reliability analysis methods.

A similar study with a limited scope was performed for lateral loading of a buried pipeline. Only one burial depth (geometrical configuration) was taken for the pipeline. Among the probabilistic characteristics of soil considered here, the degree of variability of soil strength was found to be the most significant factor affecting pipeline response. The response and failure mechanism of a laterally loaded buried pipeline is complicated and is dependent on several deterministic factors such as burial depth, pipe-soil interaction coefficients, and soil weight. The study could be further developed to account for other

probabilistic characteristics and deterministic parameters, and their corresponding interactions.

ACKNOWLEDGEMENTS

I would like to express my sincere appreciation to all those who have supported me in pursuing the degree of Doctor of Philosophy. In particular, I would like to thank my supervisor, Dr. Radu Popescu, for his academic guidance and financial support provided throughout the research program. I am also grateful to him for his patience, sincerity and expertise.

I am also indebted to Dr. Ryan Phillips, who is both my director and a member of my supervisory committee. He has been a source of knowledge and experience and I am grateful for his continuing support. I would also like to thank the other member of my supervisory committee, Dr. Leonard Lye, for his guidance and for introducing me to innovative statistical approaches.

I am also grateful for the financial support and assistance provided by Memorial University and C-CORE during the course of this study.

I would like to thank my professors at the University of Tehran. Their instruction was essential in fostering my desire to pursue a doctorate degree. Their steadfast support made it possible to continue my studies abroad.

I would also like to thank my friends living in various parts of the world and my colleagues at C-CORE for all their input, advice, and encouragement. Special thanks goes to Tanya Lopez for her help with editing and proofreading the thesis.

I would also like to thank my only brother, Abtin, my uncle, Behrooz Nobahar, and all my family members for their assistance and encouragement. Most importantly, I am

indebted to my parents, whose support has been invaluable. My mother's love and devotion has always motivated me to achieve my goals and she remains a constant source of inspiration. My father provided me with endless support and love and the memory of his dedication to his work as an engineer and to his family will always remain with me.

TABLE OF CONTENTS

ABSTRACT	III
ACKNOWLEDGEMENTS.....	VI
TABLE OF CONTENTS.....	VIII
LIST OF TABLES.....	XV
LIST OF FIGURES.....	XVII
LIST OF SYMBOLS.....	XXV
CHAPTER 1. INTRODUCTION	1
1.1. General Remarks	1
1.2. Objectives	2
1.3. Methodology	4
1.4. Organization of Thesis	5
CHAPTER 2. LITERATURE REVIEW	8
2.1. Effects of Soil Heterogeneity.....	8
2.1.1. Spatial Variability of Soil Properties.....	8
2.1.1.1. Characteristics of soil variability.....	8
2.1.1.2. Stochastic models	12
2.1.1.3. Probabilistic characteristics of the spatial variability of soil properties.....	15
2.1.2. Stochastic Finite Element Analysis.....	19
2.1.3. Effects of Soil Heterogeneity on Geotechnical System Behaviour.....	22
2.1.3.1. Settlement of shallow and deep foundations	22

2.1.3.2.	Seepage flow through heterogeneous soil.....	24
2.1.3.3.	Liquefaction potential.....	27
2.1.3.4.	Slope stability	28
2.1.3.5.	Effects of soil heterogeneity on bearing capacity of shallow foundations	30
2.2.	Bearing Capacity of Shallow Foundations	36
2.2.1.	Conventional Methods.....	38
2.2.2.	Analysis Methods.....	41
2.2.2.1.	Limit analysis method	41
2.2.2.2.	Limit equilibrium method	42
2.2.2.3.	Method of characteristics (slip-line method)	42
2.2.2.4.	Bearing capacity of foundations in engineering practice	42
2.2.2.5.	Some important issues in foundation design	43
2.2.3.	Numerical Methods for Bearing Capacity of Foundations.....	44
2.3.	Pipe–Soil Interaction.....	46
2.3.1.	Engineering Practical Methods.....	47
2.3.2.	Experimental Studies	51
2.3.2.1.	Lateral loading of buried pipeline	51
2.3.3.	Numerical Modelling of Pipe-Soil Interaction.....	54
2.3.3.1.	Numerical aspects.....	55
2.3.3.2.	Soil-pipeline interface.....	56
2.3.3.3.	Soil constitutive models	57
2.3.3.4.	Numerical results	58
2.4.	Design Approaches	59
2.4.1.	General Design Criteria	59
2.4.2.	Conventional Methods.....	62
2.4.2.1.	Characteristic (nominal) values.....	65
2.4.2.2.	Limitations of the conventional method	65
2.4.3.	Limit State Design Method.....	67

2.4.4.	Reliability and Probabilistic Design.....	73
2.4.4.1.	Application of response surface method.....	77
CHAPTER 3.	METHODOLOGY	79
3.1.	Introduction	79
3.1.1.	Elements of Proposed Methodology	82
3.1.2.	Monte Carlo Simulations	83
3.2.	Selection of Probabilistic Characteristics for Soil Variability	84
3.3.	Design of Experiments.....	87
3.3.1.	Introduction	87
3.3.2.	Design of Experiment Methods.....	88
3.3.2.1.	Two-level factorial design.....	89
3.3.2.2.	Central composite design	89
3.3.3.	Response Surfaces.....	90
3.3.4.	Design of Experiment Set-up	92
3.4.	Simulation of Random Fields	94
3.4.1.	General	94
3.4.2.	Theoretical Bases	95
3.4.2.1.	Digital generation of mV-nD Gaussian stochastic vector fields ..	95
3.4.2.2.	Digital generation of mV-nD non-Gaussian stochastic vector fields	98
3.4.3.	Generation of Sample Functions of a Stochastic Field.....	100
3.4.3.1.	Stochastic field mesh	100
3.4.3.2.	Generated sample functions of stochastic field	100
3.5.	Finite Element Analysis	106
3.5.1.	General Description	106
3.5.2.	Main Elements of the Finite Element Model	107
3.5.2.1.	Element type	107
3.5.2.2.	Mesh size	109
3.5.2.3.	Plasticity models.....	109

3.5.3.	Finite Element Code, ABAQUS/Standard	114
3.5.3.1.	Modelling soil-structure interaction	115
3.5.3.2.	Soil material behaviour modelling	116
3.5.4.	Finite Element Analysis with Stochastic Input – Issues	117
3.5.4.1.	Transfer and mapping of random data	117
3.5.4.2.	Automation of the generation and mapping of sample functions of a stochastic field.....	119
3.6.	Calibration of Results for Engineering design	120
3.6.1.	Introduction	120
3.6.2.	Characteristic Values/Percentiles	120
3.6.3.	Reliability Analysis and Required Safety Factors	122
3.6.4.	Calibration of Partial Design Factors	123
3.7.	Summary.....	126
CHAPTER 4. BEARING CAPACITY OF SHALLOW FOUNDATIONS		130
4.1.	Introduction	130
4.1.1	Description	130
4.1.2	Objectives.....	131
4.1.3	Limitations	132
4.2.	Deterministic Finite Element Analysis.....	133
4.2.1	Optimisation of Numerical Model.....	133
4.2.1.1.	Finite element domain and boundaries	133
4.2.1.2.	Selection of the finite element type.....	135
4.2.1.3.	Mesh size selection.....	136
4.2.1.4.	Numerical issues.....	140
4.2.2	Deterministic Finite Element Analysis.....	141
4.2.2.1.	Analysis set-up.....	141
4.2.2.2.	Results.....	142
4.2.2.3.	Effects of imperfection in deterministic analysis	143
4.3.	Stochastic Finite Element Analysis	145

4.3.1	The Studied Ranges of Probabilistic Characteristics for Soil Variability ..	145
4.3.2	Finite Element Analysis with Spatially Variable Soil	146
4.3.3	Monte Carlo Simulation Results	150
4.3.3.1.	Example of a typical analysis.....	150
4.3.3.2.	Effects of probability distribution of soil strength.....	153
4.3.3.3.	Effects of variance	155
4.3.3.4.	Effects of local averaging.....	157
4.3.3.5.	Sample size	161
4.3.4	Accounting for Three-Dimensional Soil Variability	165
4.4.	Parametric Studies.....	166
4.4.1	Design of Experiments.....	166
4.4.1.1.	Factorial design.....	167
4.4.1.2.	Central composite response surface	168
4.4.2	Statistical Analysis of Results	168
4.4.3	Results of Parametric Studies	172
4.4.3.1.	Mean bearing capacity.....	173
4.4.3.2.	Variability of predicted bearing capacity.....	177
4.4.3.3.	Characteristic bearing capacity	182
4.4.3.4.	Factor of safety for target failure probability.....	185
4.4.4	Design Recommendations	188
4.4.4.1.	Characteristic values.....	188
4.4.4.2.	Reliability analysis.....	192
4.4.4.3.	Calibration of partial design factors.....	192
4.4.4.4.	An illustration design example.....	194
4.5.	Differential Settlement and Damage Levels.....	199
4.5.1	Introduction	199
4.5.2	Damage Criteria	199
4.5.3	Experiment Design.....	201
4.5.4	Statistical Analysis and Results.....	201

4.5.4.1.	Regression equations for damage levels	204
4.6.	Application to Design and Reliability Analysis	210
4.7.	Summary.....	212
CHAPTER 5.	LATERAL LOADING OF A BURIED PIPE	215
5.1.	Introduction	215
5.1.1	Description	215
5.1.2	Objectives and Limitations	216
5.2.	Deterministic Finite Element Analysis.....	219
5.2.1	Finite Element Analysis Set-up	219
5.2.1.1.	Finite element mesh.....	219
5.2.1.2.	Material properties.....	221
5.2.1.3.	Analysis procedure	221
5.2.2	Finite Element Results	222
5.2.2.1.	Predicted force displacement results.....	222
5.2.2.2.	Failure mechanism.....	226
5.2.3	Validation of the Numerical Model.....	226
5.2.3.1.	Validation of finite element model based on full-scale experimental results	226
5.2.3.2.	Summary	229
5.3.	Stochastic Finite Element Analysis	233
5.3.1	Selection of Probabilistic Characteristics for Soil Variability.....	233
5.3.2	Monte Carlo Simulation Results	234
5.3.2.1.	Comparison with deterministic analysis	234
5.3.2.2.	Probabilistic analysis	235
5.4.	Illustrative Study for a Pipe Loaded in Clay	239
5.4.1	Statistical Analysis of Results – Rigid Pipe; 2D Analysis.....	239
5.4.1.1.	Regression equations	240
5.4.2	Lateral Loading of Flexible Pipeline, 3D Effects	241
5.5.	Conclusions	246

CHAPTER 6. SUMMARY AND CONCLUSIONS	248
6.1. Summary.....	248
6.1.1 Shallow Foundations.....	249
6.1.2 Lateral Loading of Buried Pipeline	250
6.2. Conclusions	251
6.3. Future Work	254
 REFERENCES	 256
 APPENDIX A. A SAMPLE FINITE ELEMENT INPUT FILE, A DETERMINISTIC FINITE ELEMENT ANALYSIS WITH STOCHASTIC INPUT	 275
 APPENDIX B. AUTOMATION OF MONTE CARLO SIMULATIONS	 281
B.1. Introduction	281
B.2. Automation of the Generation of Stochastic Sample functions.....	281
B.3. Finite Element Analyses: Input Files, Execution and Post-Processing	284
B.4. Automation of Probabilistic Analysis.....	286
 APPENDIX C. CALIBRATION OF RESISTANCE FACTORS FOR HETEROGENEOUS SOIL USING RELIABILITY THEORY	 303

LIST OF TABLES

<i>Number</i>	<i>Page</i>
Table 2.1	Ranges of global factor of safety commonly used for geotechnical engineering (Terzaghi and Peck, 1948, 1967; Terzaghi et al., 1996).....64
Table 2.2	Values of partial factors (after Meyerhof, 1995 [128]).....72
Table 4.1	Coefficient of variation: input for soil strength and resulting for predicted bearing capacity.156
Table 4.2	Results of Monte Carlo simulation for the effects of horizontal correlation distance.....158
Table 4.3	Required safety factors, FS obtained from 100 sample functions.....160
Table 4.4	Factorial design for foundation analysis on heterogeneous soil.....167
Table 4.5	Foundation responses for factorial and central composite design normalized by deterministic value (for $E = 1500c_u$) using 100 samples for each case.....170
Table 4.6	Parametric study for $E/c_u = 300$, design layout of Monte Carlo simulations and results for ultimate bearing capacity using 200 samples for each case. .172
Table 4.7	Statistical indices for significance of the fitted model for mean bearing capacity.....174
Table 4.8	Comparison of mean bearing capacity ratio, R_{BC} from Monte Carlo simulations and fitted response surface (Eq. 4.4 & Eq. 4.5).....176
Table 4.9	Statistical indices for significance of the fitted model for variability of predicted bearing capacity180
Table 4.10	Comparison of predicted values of C_V from Monte Carlo simulations with analytical approximations for soil shear strength with $C_V = 40\%$181
Table 4.11	Statistical indices for significance of the fitted model for characteristic bearing capacity183

Table 4.12	Comparison of safety factors obtained from Monte Carlo simulations and analytical approximations	188
Table 4.13	Assumptions for design example.....	195
Table 4.14	Parametric study for $E/c_u = 300$, design layout of Monte Carlo simulations and results for damage levels.....	202
Table 4.15	Parametric study for $E/c_u = 1500$, design layout of Monte Carlo simulations and results for damage levels.....	203
Table 4.16	Parameters a, b, c, d in Eq. 4.15 for Gamma probability distribution and $E/c_u = 1500$	205
Table 4.17	Parameters a, b, c, d in Eq. 4.15 for Beta probability distribution and $E/c_u = 1500$	205
Table 4.18	Parameters e, f, g, h in Eq. 4.16 for Gamma probability distribution and $E/c_u = 1500$	206
Table 4.19	Parameters e, f, g, h in Eq. 4.16 for Beta probability distribution and $E/c_u = 1500$	206
Table 4.20	Parameters for estimating mean limit bearing pressure at different damage levels (Eq. 4.17, for cases with $E/c_u = 300$).....	209
Table 4.21	Parameters for estimating coefficient of variation of bearing resistance at different damage levels (Eq. 4.18, for cases with $E/c_u = 300$).....	210
Table 5.1	Stochastic cases analysed for lateral loading of pipeline.....	234
Table 5.2	Results of lateral loading of pipe in terms of normalized mean and coefficient of variation of bearing pressure.....	240
Table 5.3	Parameters used for the pipeline in Section 5.4.2	243
Table 5.4	Soil and gouge characteristics	244

LIST OF FIGURES

<i>Number</i>	<i>Page</i>
Figure 2.1	Uncertainty in soil property estimates (after Kulhawy, 1992 [102])......9
Figure 2.2	Recorded <i>in-situ</i> cone tip resistance (after Popescu et al., 1997 [162]).12
Figure 2.3	Coefficient of variation (<i>COV</i>) of inherent variability of soil undrained shear strength (s_u) vs. mean s_u (after Phoon and Kulhawy, 1999a [154]).16
Figure 2.4	Coefficient of variation, C_v , of soil undrained shear strength vs. mean soil undrained shear strength, c_u (after Cherubini et al., 1993 [28])......17
Figure 2.5	Influence of coefficient of variation and correlation distances ($\theta = \theta_h = \theta_v$) on mean (m_Q) and its standard deviation (s_Q) (after Griffiths and Fenton, 1997 [75])......26
Figure 2.6	Influence of $C.O.V_{cu}$ on a slope with $FS = 1.47$ (after Griffiths and Fenton, 2000 [76]). $\theta_{in\ cu}/H$ is isotropic correlation distance normalized by the height of slope.30
Figure 2.7	Comparison of deterministic and Monte Carlo simulation results for average and 95 percentile: a. pressure-settlement relationships; b. pressure-rotation relationships (after Nobahar and Popescu, 2000 [137])......33
Figure 2.8	Typical deformed mesh. The darker regions indicate weaker soil (after Griffiths and Fenton 2001 [77])......35
Figure 2.9	Graphs showing the relationship between $p(Nc < 5.14/F)$ and F for a soil with $C_{vcu} =$ (a) 12.5%, (b) 25%, (c) 50% and (d) 100% (after Griffiths and Fenton, 2001 [77])......36
Figure 2.10	Spread foundation shapes and dimensions (Coduto, 2001 [35])......37
Figure 2.11	A general failure mode captured by finite element analysis: (a) contours of plastic strains and (b) schematic normalized pressure-normalized settlement relationship.38
Figure 2.12	Failure mechanism of a foundation: (a) general shear failure, (b) local shear failure, and (c) punching failure (after Coduto, 2001 [35]).40

Figure 2.13	Soil-pipeline interaction (a) continuum analysis, (b) idealised structural model and (c) soil load-displacement response (t_w , x_w , p_w , y_w , q_{uw} , z_{uw} , q_{ud} , z_{ud} are spring characteristics).	48
Figure 2.14	Transverse horizontal bearing interaction factors for cohesive sediment.	51
Figure 2.15	Dependency of soil force on loading rate: pipelines buried in saturated clay (after Paulin et al. 1998).	54
Figure 2.16	Risks for selected natural events and engineering projects designed in keeping with current practice (after Whitman, 1984 [218]; Boyd 1994 [18]).	61
Figure 2.17	Design values for loads and resistance (after Becker, 1996a [15]).	64
Figure 2.18	Possible load and resistance distributions (after Green, 1989 [72]): (a) very good control of R and S ; (b) mixed control of R and S ; (c) poor control of R and S	67
Figure 2.19	Typical variation of load and resistance for reliability analysis.	74
Figure 3.1	Illustration of the applied methodology.	81
Figure 3.2	Probability density functions of the Beta and Gamma distributions assumed for shear strength, with mean of 100 kPa and coefficient of variation $C_V = 40\%$	87
Figure 3.3	Illustration of experiment design layouts for a 3-factor problem: (a) Two-level factorial design, (b) Two level factorial design with central point, and (c) Central composite design (face-centred).	90
Figure 3.4	Flowchart for simulation of mV - nD non-Gaussian stochastic vector fields (after Popescu, 1995 [158]).	99
Figure 3.5	Exponential decaying SDF model: a. correlation functions, and b. spectral density functions for various values of the parameters b , and b_s ; c. correlation distance values (Popescu, 1995 [158]).	103
Figure 3.6	Comparison of generated and target spectral density functions for one sample function of a stochastic field with (a) Gamma probability distribution and (b) Beta probability distribution.	104
Figure 3.7	Comparison of resulting and target cumulative probability distributions for one sample function of a stochastic field with coefficient of variation	

	of 40%: (a) Gamma probability distribution and (b) Beta probability distribution.	105
Figure 3.8	Tresca yield surfaces (after Prevost, 1990 [171]). Von Mises yield criteria is shown by dashed line.	112
Figure 3.9	Deviatoric stress plane (after Prevost, 1990 [171])......	113
Figure 3.10	Comparison of Tresca and von Mises yield surfaces in 3 dimensional principal stress space (after Venkatraman and Patel, 1970 [211]).	114
Figure 4.1	Finite element mesh.	134
Figure 4.2	Effects of lateral boundary conditions.....	135
Figure 4.3	Comparison of the effects of element type on predicted bearing capacity of a shallow foundation.....	136
Figure 4.4	Finite element meshes for bearing capacity of foundation: (a) mesh size of 1.0 by 0.5 m (b) mesh size of 0.5 by 0.25 and (c) mesh size of 0.25 by 0.125m.....	139
Figure 4.5	Effects of mesh size on the predicted bearing capacity of foundation.	140
Figure 4.6	Predicted normalized pressure vs. normalized settlement curves for a strip foundation placed on uniform soil.....	143
Figure 4.7	Analysis of the effects of imperfection with ABAQUS/Standard: (a) finite element mesh (b) Predicted pressure-settlement relationship of the foundation on uniform soil and soil with imperfection; (c) Predicted pressure-rotation relationship of the foundation on soil with imperfection. .	144
Figure 4.8	Predicted deformed shape and contours of equivalent plastic strain, γ , for a foundation on uniform soil and soil with imperfection at settlement $d=40\text{ cm}$: a. uniform soil; b. soil with imperfection.	145
Figure 4.9	A finite element analysis with spatially variable soil input (one sample realization of Monte Carlo simulations) (a) realization of undrained shear strength – the contours shows the ratio of actual undrained shear strength to the average value used in the deterministic analysis, (b) contours of plastic shear strain showing the local failure and (c) contours of plastic shear strain – asymmetric general shear failure.	148

Figure 4.10	A typical finite element analysis of foundation on the sample realization of heterogeneous soil from Figure 4.9 (a) predicted pressure-settlement relationship, and (b) predicted pressure-rotation relationship.	149
Figure 4.11	Comparison of Monte Carlo simulations and deterministic analysis results: a. pressure-settlement curves; b. pressure-rotation curves (no rotation is predicted in the deterministic analysis).....	151
Figure 4.12	Predicted deformed shape and contours of equivalent plastic shear strain, γ : a. normalized average settlement $\Delta_n = 0.0125$; b. $\Delta_n = 0.0625$; c. $\Delta_n = 0.1$	152
Figure 4.13	Comparison of deterministic and Monte Carlo simulation results for average and 95 percentile: a. pressure-settlement relationships; b. pressure-rotation relationships.....	153
Figure 4.14	Comparison of Monte Carlo simulations: a. symmetric Beta distribution b. skewed Gamma distribution c. averages resulting from Monte Carlo simulations and deterministic analysis.	154
Figure 4.15	Influence of the coefficient of variation of soil strength on bearing capacity.....	156
Figure 4.16	Effects of sample size on predicted mean and standard deviation.	162
Figure 4.17	Fitting probability distribution to the empirical probability distribution function of the predicted bearing capacity for 1200 samples using method of moments: (a) Lognormal fit and (b) Gamma fit.	163
Figure 4.18	Fitting probability distribution to the empirical probability distribution function of the predicted bearing capacity for 1200 samples using method of moments: (a) Lognormal fit and (b) Gamma fit.	164
Figure 4.19	Scatter plot for Monte Carlo simulations and predicted (Eq. 4.4 & Eq. 4.5) values of mean bearing capacity ratio.	176
Figure 4.20	Scatter plot for the Monte Carlo simulations and predicted (Eq. 4.6 & Eq. 4.7) values of coefficient of variation of bearing capacity.	180
Figure 4.21	Variation of the coefficient of variation of bearing capacity with C_ν and $\theta h/B$ for Beta distributed soil shear strength.	181
Figure 4.22	Scatter plot for the Monte Carlo simulations and predicted (Eq. 4.8 & Eq. 4.9) values of characteristic bearing capacity.	184

Figure 4.23	Variation of characteristic bearing capacity vs. C_V and θ_v/B of soil shear strength having a Beta probability distribution.	185
Figure 4.24	Contours of the ratio of mean value to characteristic value for resistance vs. natural variability of soil, C_V and uncertainty from other sources, C_{Vu}	191
Figure 4.25	Contours of partial design factors vs. natural variability of soil, C_V and uncertainty from other sources, C_{Vu} , for design using mean shear strength. .	196
Figure 4.26	Contours of partial design factors vs. natural variability of soil, C_V and uncertainty from other sources, C_{Vu} , for design using characteristic bearing capacity (see Section 4.4.4.1).	197
Figure 4.27	Contours of reliability index, β , obtained using a constant partial factor of 0.5. A target reliability index of 3.5 was used in Calibration of National Building Code of Canada, NBCC (see NRC, 1995 [142]; Becker, 1996a [15]).	198
Figure 4.28	Scatter plot for Monte Carlo simulations and predicted (Eq. 4.15) values of mean bearing pressure at minor damage level.....	207
Figure 4.29	Scatter plot for Monte Carlo simulations and predicted (Eq. 4.15) values of mean bearing pressure at major damage level.	207
Figure 4.30	Scatter plot for Monte Carlo simulations and predicted (Eq. 4.16) values of coefficient of variation bearing pressure at minor damage level.	208
Figure 4.31	Scatter plot for Monte Carlo simulations and predicted (Eq. 4.16) values of coefficient of variation bearing pressure at major damage level.	208
Figure 5.1	Lateral movements of soil: (a) an observed landslide in cohesive material; and (b) schematic representation of landslide.	218
Figure 5.2	Typical finite element mesh and boundary conditions.	220
Figure 5.3	Predicted normalized pressure-normalized displacement for pipeline as shown in Figure 5.2 and comparison with Rowe & Davis (1982a) results: a. firm clay used in stochastic analysis with $c_u = 50$ kPa; b. soft clay with $c_u=10$ kPa.....	224
Figure 5.4	Effects of undrained shear strength on soil failure mechanism and p-y curves (H/D ratio of 2.5) – adapted from Popescu et al. 2002 [168].	225

Figure 5.5	Contours of plastic shear strain magnitude (PEMAG) demonstrating failure mechanism of firm clay subjected to lateral loading of rigid pipeline (uniform soil).	226
Figure 5.6	Finite element mesh for validation modelled according to large-scale experimental tank size.....	227
Figure 5.7	Recorded and predicted range of force-displacement relations for large-scale tests in clay, using the Tresca model: a. soft clay; b. stiff clay.	228
Figure 5.8	Comparison of predicted and observed failure in stiff clay: a. observed (after Paulin et al. 1998 [150]); b. predicted using a finite element model of the experimental tests; c. predicted using finite element model used for stochastic analysis.	230
Figure 5.9	Validation of a numerical model for pipe/soil interaction: a. finite element mesh; b. comparison of recorded and predicted force-displacement relations (from Popescu et al., 2002 [169]).	231
Figure 5.10	Comparison of predicted and observed behaviour of dense sand: a. post-tests deformation tubes (after Paulin et al. 1998 [150], printed with permission from the Canadian Geotechnical Society); b. predicted displacements; c. predicted contours of plastic strain magnitude (after Nobahar et al., 2000 [141]).	232
Figure 5.11	A sample finite element analysis with spatially variable input soil: a. contours of undrained shear strength over domain of analysis (with average shear strength of 50 kPa); b. contours of plastic shear strain (PEMAG) demonstrating failure mechanism for the corresponding soil realization; (c) predicted normalized force-displacement relationship for the corresponding soil realization.	236
Figure 5.12	Results of Monte Carlo simulations (MCS) and comparison with results obtained for uniform soil with shear strength, $c_u = 50$ kPa.	237
Figure 5.13	Lateral loading of pipeline in heterogeneous clay (case 6 in Table 5.1) – empirical probability distribution of interaction pressures and fitted lognormal distribution (The results are obtained for $c_u^{av} = 50$ kPa and are not normalized).	238
Figure 5.14	(a) schematic subscour soil deformation; (b&c) longitudinal strain distributions in the pipe section at point 1&2 – soil cover from scour base to top of pipe = 0.5 m, scour depth = 1.5 m, scour width = 16 m	245

Figure B.1	Generation table for sample functions of stochastic fields.	283
Figure B.2	A generated sample function of a stochastic field read by MATLAB routine, “main_spfn” – contours show spatially variable parameter, here undrained shear strength (in kPa), the distribution over the domain of interest.	285
Figure B.3	A sample of foundation responses read by MATLAB routine, “main_spfn”.	286
Figure B.4	Samples plot of pressure vs. settlement and differential settlement.	289
Figure B.5	A sample of plots provided by post processing program.	290
Figure B.6	An example of empirical probability distribution of foundation bearing capacity at reference settlement criterion (ultimate bearing capacity) using Lognormal fit for an experiment with Gamma distributed soil shear strength, $C_V = 25\%$, $\theta_{hn} = 2.5$, $\theta_{vn} = 0.25$, and $E/c_u = 1500$	291
Figure B.7	An example of empirical probability distribution of foundation bearing capacity at reference settlement criterion (ultimate bearing capacity) using Normal fit for an experiment with Gamma distributed soil shear strength, $C_V = 25\%$, $\theta_{hn} = 2.5$, $\theta_{vn} = 0.25$, and $E/c_u = 1500$	292
Figure B.8	An example of empirical probability distribution of foundation bearing capacity at reference settlement criterion (ultimate bearing capacity) using Gamma fit for an experiment with Gamma distributed soil shear strength, $C_V = 25\%$, $\theta_{hn} = 2.5$, $\theta_{vn} = 0.25$, and $E/c_u = 1500$	293
Figure B.9	An example of empirical probability distribution of foundation bearing capacity at minor damage level criterion using Lognormal fit for an experiment with Gamma distributed soil shear strength, $C_V = 25\%$, $\theta_{hn} = 2.5$, $\theta_{vn} = 0.25$, and $E/c_u = 1500$	294
Figure B.10	An example of empirical probability distribution of foundation bearing capacity at minor damage level criterion using Normal fit for an experiment with Gamma distributed soil shear strength, $C_V = 25\%$, $\theta_{hn} = 2.5$, $\theta_{vn} = 0.25$, and $E/c_u = 1500$	295
Figure B.11	An example of empirical probability distribution of foundation bearing capacity at minor damage level criterion using Gamma fit for an experiment with Gamma distributed soil shear strength, $C_V = 25\%$, $\theta_{hn} = 2.5$, $\theta_{vn} = 0.25$, and $E/c_u = 1500$	296

Figure B.12	An example of empirical probability distribution of foundation bearing capacity at medium damage level criterion using Lognormal fit for an experiment with Gamma distributed soil shear strength, $C_V = 25\%$, $\theta_{hn} = 2.5$, $\theta_{vn} = 0.25$, and $E/c_u = 1500$.	297
Figure B.13	An example of empirical probability distribution of foundation bearing capacity at medium damage level criterion using Normal fit for an experiment with Gamma distributed soil shear strength, $C_V = 25\%$, $\theta_{hn} = 2.5$, $\theta_{vn} = 0.25$, and $E/c_u = 1500$.	298
Figure B.14	An example of empirical probability distribution of foundation bearing capacity at medium damage level criterion using Gamma fit for an experiment with Gamma distributed soil shear strength, $C_V = 25\%$, $\theta_{hn} = 2.5$, $\theta_{vn} = 0.25$, and $E/c_u = 1500$.	299
Figure B.15	An example of empirical probability distribution of foundation bearing capacity at major damage level criterion using Lognormal fit for an experiment with Gamma distributed soil shear strength, $C_V = 25\%$, $\theta_{hn} = 2.5$, $\theta_{vn} = 0.25$, and $E/c_u = 1500$.	300
Figure B.16	An example of empirical probability distribution of foundation bearing capacity at major damage level criterion using Normal fit for an experiment with Gamma distributed soil shear strength, $C_V = 25\%$, $\theta_{hn} = 2.5$, $\theta_{vn} = 0.25$, and $E/c_u = 1500$.	301
Figure B.17	An example of empirical probability distribution of foundation bearing capacity at major damage level criterion using Gamma fit for an experiment with Gamma distributed soil shear strength, $C_V = 25\%$, $\theta_{hn} = 2.5$, $\theta_{vn} = 0.25$, and $E/c_u = 1500$.	302

LIST OF SYMBOLS

a_i, b_i	parameters of the SDF
B	foundation width (m)
C	cohesion (kPa)
c_u	undrained shear strength (kPa)
C_V	coefficient of variation, coefficient of variation of soil spatial variability
C_{VBC}	coefficient of variation of resulting bearing capacity
C_{V_o}	overall coefficient of variation of a response
C_{V_u}	coefficient of variation from uncertainty other than soil heterogeneity
D	diameter of pipe
D_o	effective diameter of pipe or height of anchor
E	deformation modulus (kPa)
F	applied load (kN)
$f(X)$	n-dimensional m-variate stochastic field
$F_B(X)$	non-Gaussian distribution function
$f_B(X)$	non-Gaussian stochastic field
F_G	Gaussian distribution function
$f_G(X)$	Gaussian stochastic field
FS	factor of safety
$f_x, f_y \text{ \& } f_z$	spring unit forces function (kN/m)
h	embedment depth defined as burial depth from bottom of pipe to soil surface (m)
H	height of slope, burial depth from soil surface to springline (m)

$H(K)$	lower triangular matrix resulted from Cholesky decomposition of $S^0(K)$
i	index for spatial dimension; iteration counter
I_i	set of indicators for the quadrants of wave-number space, taking values ± 1
k_R	ratio of mean value to characteristic (nominal) value for resistance
k_S	ratio of mean value to characteristic (specified) value for load effects
l_i	counter for the discretization in wave-number domain
m	number of variables, average value
M_i	number of simulation points in spatial domain
n	number of spatial dimension
N_c, N_q, N_γ	bearing capacity factors for foundation
N_{ch}	pipe transverse horizontal bearing interaction factor
N_{cv}	pipe vertical uplift factor
N_i	number of points to describe the spectral density function in direction i
p_n	normalized pressure defined as pressure divided by shear strength
p_u	transverse horizontal ultimate load (pipe, pile or anchor) per unit length (kN/m)
Q	ultimate bearing capacity of foundation (kN) from limit analysis
q_n	bearing capacity normalized by shear strength
q_s	surcharge or overburden pressure (kN/m ²)
q_u/ q_{ult}	ultimate bearing capacity (foundation or pipe) per unit length (kN/m)

q_{ud}	transverse downward vertical yield load per unit length of pipe (kN/m)
q_{uu}	transverse upward vertical yield load per unit length of pipe (kN/m)
r	index of spatial dimensions
R	resistance
\bar{R}	average resistance
$R^0(\xi)$	cross-correlation matrix
$R^0_{ij}(\xi)$	auto-correlation functions
R_{BC}	ratio of mean bearing capacity of a foundation on heterogeneous soil to that of a foundation on uniform soil with average shear strength (deterministic bearing capacity)
R_{nBC}	ratio of characteristic (nominal) bearing capacity to deterministic bearing capacity
R_{tBC}	ratio of bearing capacity at target probability level 10^{-4} to deterministic bearing capacity
S	load or action
\bar{S}	average load
$S^0(K)$	target cross-spectral density matrix (target spectrum)
$S^0_{jk}(K)$	diagonal term of the target spectrum (target SDF)
$S_{Brr}(K)$	resulted SDF of the r^{th} scalar component of $f_B(x)$
SDF	spectral density function
$S_{Grr}(K)$	resulted SDF of the r^{th} scalar component of $f_G(x)$
$T(X)$	deterministic trend function
t_u	axial ultimate load (pipe, pile or anchor) per unit length (kN/m)
u_x, u_y, u_z	soil displacements in axial, transverse horizontal, and transverse vertical directions respectively
V_R	coefficient of variation of resistance

V_S	coefficient of variation of load
X	position in the n dimensional spatial domain (space vector)
$Y(X)$	typical soil property at point X
y_u	ultimate transverse horizontal displacement of pipe (m)
z_{ud}	ultimate transverse downward vertical displacement (m)
z_{uu}	ultimate transverse upward vertical displacement of pipe (m)
Δ_n	normalized settlement defined as settlement divided by foundation width or pipe diameter
Δx_k	mesh size in spatial domain
$\Delta \kappa_i$	wave-number increment in direction i
K	position in the n dimensional wave-number domain (wave-number vector)
β	reliability index
$\varepsilon_n(X)$	residual due to measurement noise
$\varepsilon_r(X)$	residual due to natural inherent variability
ϕ	friction angle
$\Phi_{s,l_1,l_2,\dots,l_n}^{I_1,I_2,\dots,I_n}$	sets of uniformly distributed random phase angles
γ	soil unit weight, unit weight (kN/m^3)
$\gamma(T)$	variance reduction function
κ_{iu}	upper cut-off wave-number in direction i
μ	average value, axial interaction factor
ν	Poisson's ratio
θ	correlation distance (m), separation coefficient
θ_h	horizontal correlation distance (m)
θ_{hn}	normalized horizontal correlation distance defined by θ_h/B
$\theta_{ln\ cu}$	correlation distance of logarithm of undrained shear strength (m)
θ_v	vertical correlation distance (m)

θ_{vn}	normalized vertical correlation distance defined by θ_v / B
σ	normal stress (kPa), standard deviation
τ	shear stress (kPa)
τ_{crit}	limit shear stress at soil-pipe/foundation interface (kPa)
ξ	space-lag vector

CHAPTER 1

INTRODUCTION

1.1. GENERAL REMARKS

In the past few decades, engineering codes have tried to adopt rational analysis and design approaches to deal with uncertainties in design. Engineering design should provide satisfactory performance while securing desired levels of safety. A rational design is possible through quantifying the risk associated with every scenario and assessing probable damage costs. Hence, engineering codes have tried to employ reliability and risk concepts in defining appropriate safety levels by comparing the cost of damage from failure with the cost of a higher safety level; in addition, social and political factors are often considered. It is vital to establish robust design methods to secure the desired safety level. However, current design methods in geotechnical engineering are primarily based on engineering experience and suffer from an insufficient theoretical background.

Estimation of reliability levels requires quantification of the probabilistic characteristics of load and resistance. This study focused on the latter part; design loads and their probabilistic characteristics are independent of the studied subject and were not addressed here. In geotechnical engineering, resistance uncertainties are induced by various sources: natural inherent variability of soil properties, measurement errors, limited

availability of information about subsurface conditions, transformation errors, model uncertainty, etc. (see Lumb, 1974 [115]; Vanmarcke, 1977 [208]; DeGroot and Baecher, 1993 [45]; Phoon and Kulhawy, 1999a&b [154&155]). A major source of uncertainty in geotechnical systems is the natural variability of soil properties. For instance, Phoon and Kulhawy (1996) [153] studied the inherent soil variability as observed from some common *in-situ* soil test measurements. They expressed the observed degree of soil strength variability by means of the coefficient of variation. Coefficients of variation – $C_V = 20\%$ to 40% for clay materials, and $C_V = 20\%$ to 60% for sand materials – were found in a large number of cone tip resistance measurements. Some of the scatter might have been induced by measurement errors. However, in the case of cone penetration tests, the scatter in results produced by measurement errors is estimated as $C_V = 5\%$ for electrical cones and $C_V = 10\%$ for mechanical cones (ASTM, 1989 [7]). Remaining variability can be attributed to soil heterogeneity.

Natural variability of soil properties within geologically distinct and uniform layers has been proven to affect soil behaviour; heterogeneous materials may behave differently from homogeneous materials having the same average properties (e.g. Nobahar and Popescu, 2001c [140]).

1.2. OBJECTIVES

The influence of soil spatial variability on soil-structure interaction problems – namely bearing capacity of shallow footings and lateral loading of buried pipelines – was studied to quantify the soil heterogeneity effects and provide design recommendations. The

main objective is to provide design recommendations for the effects of spatial variability in phenomena involving soil-structure interaction (namely bearing capacity of shallow foundations and lateral loading of buried pipelines). For this purpose,

- a methodology for stochastic analysis of geotechnical systems has been developed,
- the effects of spatial variability of soil properties on bearing capacity of shallow foundations and lateral loading of buried pipelines have been assessed and quantified, and
- methodologies to incorporate the estimated effects of soil heterogeneity in Limit State Design (LSD) method and reliability analysis have been developed.

The aforementioned analyses were performed for bearing capacity of shallow strip foundations as discussed in chapters 3 and 4. An extensive parametric study, which included ranges of degree of variability, probability distribution shape and correlation structure of soil shear strength and soil stiffness, was performed to assess and quantify the effects of soil heterogeneity. Statistical methods were incorporated to optimise the parametric study by using Design of Experiment (DOE) methodology.

For lateral loading of buried pipelines, the study had a limited scope due to a higher level of complexity for pipeline behaviour and a higher number of relevant factors, and can be regarded as a starting point for an extensive parametric study. Factors affecting behaviour of pipelines are not well understood in a deterministic analysis and its failure mechanism in uniform soil remains a matter of contention. It is essential to first know all these deterministic factors and their contribution to pipeline response before starting an extensive parametric study on the effects of soil spatial variability.

For the sake of clarity and to strictly emphasize the effects of soil heterogeneity, this study is limited to analysis of overconsolidated clayey soils under undrained condition. In this way, a fairly straightforward elastic perfectly plastic model was used (namely Tresca) and a single soil heterogeneity parameter was considered (namely undrained shear strength, c_u). Variable deformation moduli, E , is assumed perfectly correlated with soil shear strength over the analysis domain. This study does not analyse specific geostatistical data for a particular site.

1.3. METHODOLOGY

A Monte Carlo simulation methodology combining generation of stochastic fields with finite element analyses was employed. The parametric study was statistically pre-designed and results were studied through a series of probabilistic calculations. SINOGA, a program for digital generation of multidimensional, multivariate non-Gaussian random fields (Popescu, 1995 [158]) was used to generate sample functions of stochastic fields. MATLAB® (MathWorks, 2000 [116]), Microsoft Excel® and Microsoft Visual Basic® were used to develop and automate the stochastic analysis and Monte Carlo simulations. ABAQUS/Standard, a general multi-purpose finite element program with large-deformation, finite-strain and nonlinear analysis capabilities was used to model geotechnical system behaviour and soil-structure interaction (Hibbitt et al., 1998 & 2001 [92&94]).

1.4. ORGANIZATION OF THESIS

This thesis is divided into three main sections. The first section comprises the literature review, which discusses the geotechnical engineering background, previous developments, and engineering and design materials related to this study. The second section describes the methodology customized, automated and used to quantify and assess the effects of soil heterogeneity in nonlinear soil-structure interaction problems. The third section includes applications of the methodology in geotechnical problems, results of parametric study, and design recommendations.

This thesis has six chapters. Chapter 1 is an introduction to the background, scope, methodology and organization of this study.

Chapter 2 presents the literature review, which is divided into four subsections. The first subsection discusses soil heterogeneity and includes quantification of the probabilistic characteristics of soil properties and uncertainties involved in geotechnical design. It also presents stochastic models to simulate the spatial variability of soil properties, available stochastic analysis approaches, and an overview of previous work in quantifying of the effects of soil heterogeneity on the geotechnical systems. The second and third subsections present related engineering background, and analyses and design methods for shallow foundations and buried pipelines. The fourth subsection discusses engineering design methods in geotechnical engineering, and their philosophy, advantages and shortcomings.

Chapter 3 introduces the methodology developed and used in the course of study for the assessment of the effects of soil spatial variability. This includes: 1) deterministic aspects of conventional finite element analysis of geotechnical systems involving soil-

structure interaction and failure mechanism; 2) methodology used to digitally generate sample functions of a non-Gaussian stochastic field, with each sample function representing a possible realization of the relevant soil properties over the domain of interest; 3) presentation of finite element analysis with stochastic input and its customisation, development, and automation; 4) main concepts of Monte Carlo simulation methodology used in this study; 5) statistical design of parametric studies using Design of Experiment (DOE); 6) statistical study, optimisation, and regression of the results of parametric studies; and 7) methods to calibrate the results for usage in engineering design and to provide design recommendations.

Chapter 4 presents the application of the aforementioned methodology to the bearing capacity of shallow foundations on heterogeneous soil. It describes the effects of soil heterogeneity on the bearing capacity from two aspects: changes in failure mechanism and statistical effects. An extensive parametric study was performed to address the effects of soil shear strength's degree of variability, probability distribution, and correlation structure. This study also addressed the effects of soil deformation moduli on serviceability criteria for foundations placed on heterogeneous soil. The results of the parametric study were statistically analysed and summarized in regression equations and are discussed in chapter 4; also, applications of the results to engineering design methods and the three levels of reliability analysis are demonstrated.

Chapter 5 presents the application of the methodology used in this study to lateral loading of a buried pipeline. It also presents issues related to the deterministic analysis of laterally loaded buried pipeline in uniform soil. It discusses the complexity of the behaviour

of a buried pipeline subjected to soil movement. The effects of soil heterogeneity on the response of buried pipelines are also presented.

Finally, Chapter 6 summarizes the results presented in earlier chapters and recommends areas for further research.

CHAPTER 2

LITERATURE REVIEW

2.1. EFFECTS OF SOIL HETEROGENEITY

2.1.1. Spatial Variability of Soil Properties

Uncertainty in prediction of geotechnical responses is a complex phenomenon resulting from many disparate sources. In this section, a classification of these sources is presented, and aspects of soil heterogeneity – one of the main sources of uncertainty in geotechnical engineering – are discussed.

2.1.1.1. *Characteristics of soil variability*

It is well known that soil properties are variable from point to point in so-called homogeneous soil layers. Variability in measured properties in these layers comes from different sources. Phoon and Kulhawy (1999a) [154] quantified the inherent variability, the measurement errors, and the transformation uncertainty as primary sources of geotechnical uncertainty, as illustrated in Figure 2.1. The inherent spatial variability originates from the natural geological process that produced and continually modify the soil mass. Tang (1994) [196] attributes this to small-scale variation in mineral composition, environmental conditions during deposition, past stress history, and variations in moisture content.

Measurement errors, including those caused by equipment, procedural-operators, and random testing effects constitute the second source of error. Collectively, these two sources can be classified as data scatter. The third source of uncertainty is introduced when field or laboratory measurements are transformed into design soil properties using empirical or other correlation models.

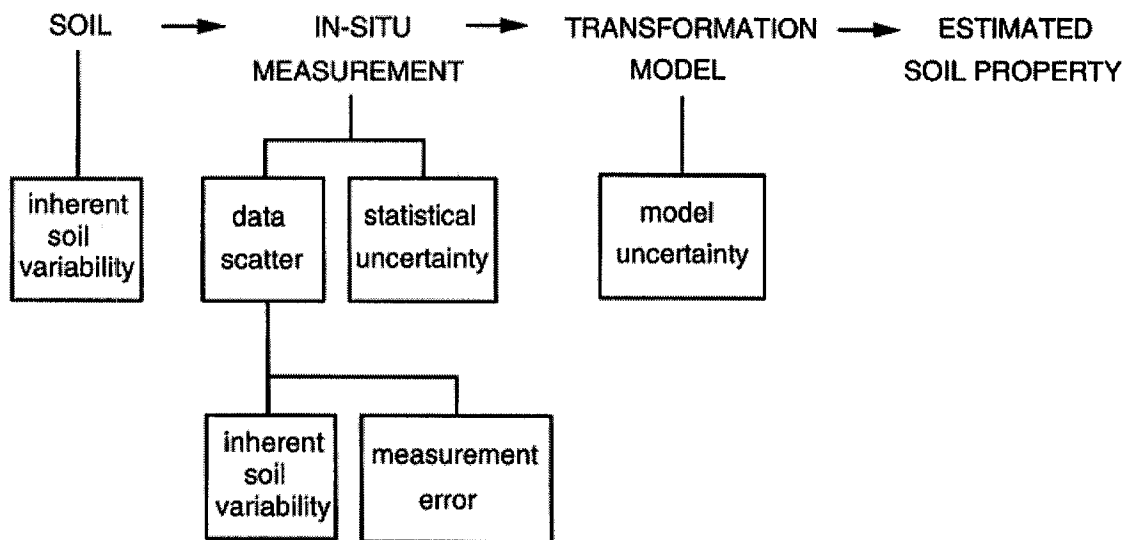


Figure 2.1 Uncertainty in soil property estimates (after Kulhawy, 1992 [102]).

Spatial variation of soil properties, as shown in Figure 2.2, can be represented by (e.g. Phoon and Kulhawy, 1999a [154]),

$$Y(X) = T(X) + \varepsilon(X) \quad \text{Eq. 2.1}$$

where $Y(X)$ is the soil property at point X ; $T(X)$ is the deterministic function giving the mean soil property at X ($T(X)$ is also called trend function); and $\varepsilon(X)$ is the residual (fluctuating component) at point X and can be defined as a homogeneous random function

or field (Vanmarcke, 1983 [209]). This function can be rewritten to account for random error (DeGroot and Baecher, 1993 [45]),

$$Y(X) = T(X) + \varepsilon_r(X) + \varepsilon_n(X) \quad \text{Eq. 2.2}$$

where $\varepsilon_r(X)$ is the residual of soil property due to natural inherent variability, and $\varepsilon_n(X)$ is the residual due to measurement noise. Separation of measurement errors from inherent variability of soil properties is an imprecise procedure, as discussed by Phoon and Kulhawy (1999a&b) [154&155]. One attribute of inherent variability of soil properties is the correlation structure, i.e. these properties do not vary randomly in space, but exhibit some coherence from one spatial location to another. Therefore, $\varepsilon_r(X)$ describes a set of correlated random variables. A rational means of quantifying inherent variability is to model $\varepsilon_r(X)$ as a homogeneous random field (Vanmarcke, 1983 [209]).

Using results of cone tip resistance records (Figure 2.2), Popescu et al. (1997) [162] showed that the probabilistic characteristics of inherent spatial variability of soil can be represented using stochastic fields with the following attributes (further discussion on stochastic models is presented in later sections):

- Mean values. These may follow a trend (such as an uniform increase of soil shear strength with depth). These systematic trends can be identified and separated.
- Variance. This represents the degree of scatter of the fluctuations about mean values.

- Correlation structure. This describes the similarity between fluctuations recorded at two points as a function of the distance between those points. As shown in Figure 2.2, some degree of coherence between the fluctuations can be observed, with this coherence becoming more noticeable as the measuring points become closer. This coherence between values of each material property at different locations can be described by auto-correlation functions (e.g. Vanmarcke, 1983 [209]; other models discussed in Section 2.1.1.2). The main parameter of the auto-correlation function is called correlation distance (or scale of fluctuation) – a length over which significant coherence is maintained.
- Probability distribution. Many researchers (e.g. Lumb, 1966 [113]; Shultze, 1971 [181]; Harr, 1977 [87]; Jefferies, 1989 [98], Griffiths and Fenton, 1993 [74]) have fitted various probability distributions for soil properties. Popescu et al. (1998a) [163] concluded that (1) most soil properties exhibit skewed, non-Gaussian distributions, and (2) each soil property can follow different probability distributions for various materials and sites. Therefore, in addition to mean and variance, it is also necessary to have more information about probability distributions of soil properties.

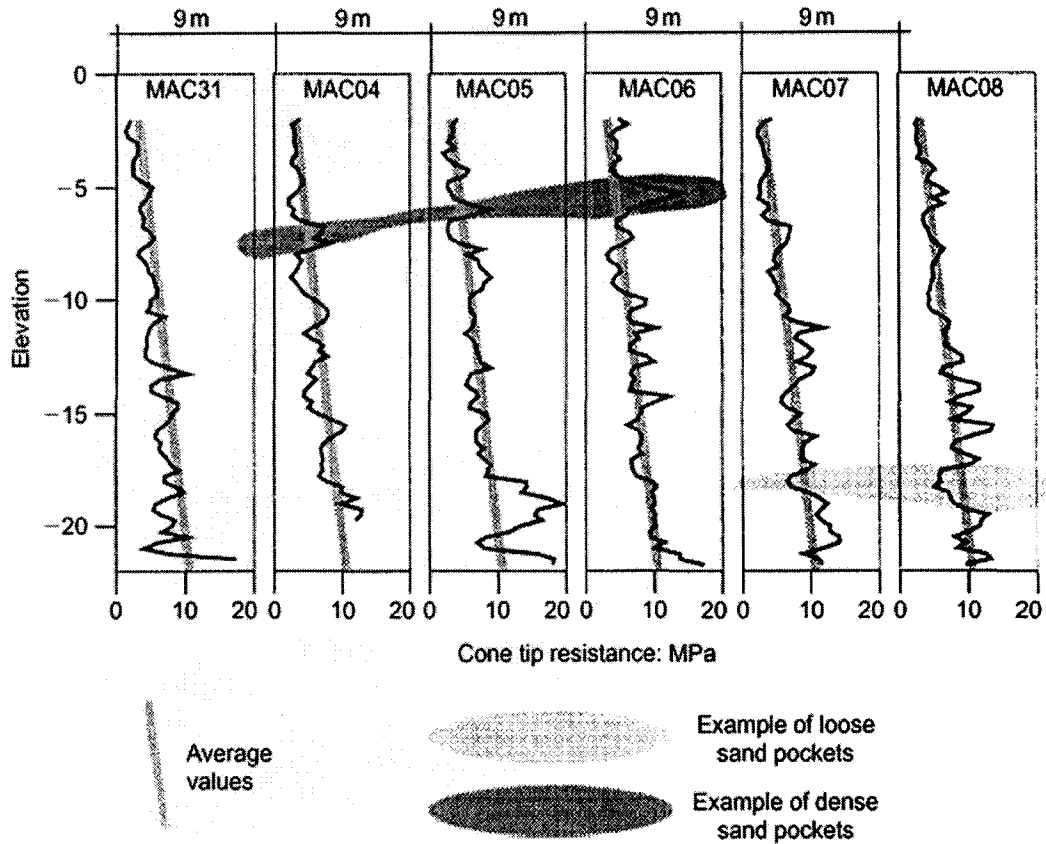


Figure 2.2 Recorded *in-situ* cone tip resistance (after Popescu et al., 1997 [162]).

2.1.1.2. Stochastic models

Various stochastic methods can be used to obtain and represent soil stochastic characteristics. Fenton (1999a) [62] pointed out the following methods as being commonly used in obtaining and representing stochastic characteristics of soil: the sample correlation or covariance function, the semi-variogram, the sample variance function, the sample wavelet coefficient variance function, and the periodogram. In addition, a decision should be made to use a finite-scale model (also known as a short memory model) or a fractal model (also known as statistically self-similar, long-memory model) to represent the

correlation structure of soil properties. Fenton (1999a&b) [62&63] compared different tools used in identifying stochastic models best suited to represent soil properties.

The most common stochastic model currently used in geotechnical engineering is the finite scale one (e.g. Vanmarcke 1983 [209]; Popescu 1995, 1997 & 1998b [158, 162&164]; Degroot, 1996 [44]; Hegazy et al., 1996 [91]; Ural, 1996 [206]; Fenton and Griffiths, 2002 [65] among others). However, the finite-scale stochastic model has several disadvantages because the scale of fluctuation is dependent on the size of analysis domain and on the sampling interval (see DeGroot and Baecher, 1993 [45]; Fenton, 1999b [63]). From studying the vertical variation of CPT q_c data, Fenton (1999a&b) [62&63] observed that soil properties seem to be fractal in nature. Fenton demonstrated that when sampling from a fractile process, the scale of fluctuation is dependent on the domain size. Hence, a fluctuation scale will become smaller/larger as the domain decreases/increases. Similarly, engineers interested in characterizing a very small/large domain should use small/large fluctuation scales in the site model. What this means is that if a researcher obtains a scale of fluctuation of 10 m for a 50-m wide domain, the scale may be much larger if the domain is 10 times larger. However, Fenton (1999b) [63] illustrated that using a fractal model does not eliminate the dependency on the domain size, but allows a better understanding of stochastic variation. Finally, there would be little difference between a properly selected finite-scale model and the real fractal model over the finite domain.

It is concluded that a finite-scale model using a correlation function is by far the most commonly used model (see Popescu, 1995 [158] for discussion of different types

correlation functions). Fractal models (long-memory), though theoretically more appropriate for soil properties, have yet to be developed and tested.

Stochastic models are also used in other areas of science and engineering. It is convenient to use independent mathematical-statistical theory to model physical processes. However, models that involve statistical dependence in time or space are often more realistic. A few examples of stochastic processes are (1) particle movement in Brownian motion, (2) emissions from a radioactive source, (3) fluctuating current in an electric circuit, (4) wave profile in the ocean, (5) response of an airplane to wind gusts, and (6) vibration of a building by an earthquake (Ochi, 1990 [143]). Cressie (1991) [39], among others, gathered literature and information on the development of statistics for spatial data. The notion that data close together in time or space are likely to be correlated is a natural one and has been used successfully by statisticians to model physical and social phenomenon (Cressie, 1991 [39]). Spatially correlated models have been developed in many areas of science, including geology, soil sciences, atmospheric science, and oceanography. Simply, spatially correlated models are used in every discipline that involves data collected from different spatial locations. For example, Peters and Bonelli (1982) [151] collected meteorological space-time data sets to study the effects of atmospheric pollution.

Soulie et al. (1990) [191], Chiasson (1995) [30], and Deutsch, 2002 [51] used variogram to represent the variability of clay deposits. The geostatistical model used in those studies is similar to the one used in this study, except this study used the covariance function, rather than variogram, to express spatial correlation. Variogram is the measure of

dissimilarity between two points in space separated by a distance h , according to the relation

$$2\gamma(h) = \text{Var}[Z(x+h) - Z(x)] \quad \text{Eq. 2.3}$$

where $2\gamma(h)$ is the variogram value at a separation distance h ; $Z(x)$ is the value of the random variable at location x . In this study, the covariance function is selected to represent the correlation structure; thus, readers are referred to Cressie (1991) [39] for more information on the use of variogram.

2.1.1.3. Probabilistic characteristics of the spatial variability of soil properties

After extensive research, Phoon and Kulhawy (1999a&b) [154&155] produced some “approximate guidelines” for ranges of uncertainty in geotechnical properties. They used a homogeneous random field to represent the inherent soil variability. They evaluated coefficients of variation, C_V , due to the inherent variability, ranges for scale of fluctuation of inherent variability, and C_V due to measurement error. For the undrained shear strength, c_u , of clayey soil deposits, they found a typical C_V range of between 10% and 55%, resulting solely from the inherent spatial variability of soil strength. This range was obtained from extensive study of data from cone penetration tests (CPT), vane shear tests (VST), and laboratory tests, which included: unconfined compression tests (UC); unconsolidated-undrained triaxial compression tests (UU); and consolidated isotropic undrained triaxial compression tests (CIUC). Figure 2.3 shows ranges of C_V (COV) of inherent variability from laboratory tests.

The undrained shear strength C_V from measurement errors is the result of equipment, procedural-operator, and random testing effects. It was found to range between about 5% to 45% for field and 5% to 40% for lab tests (However, they recommended a value of 5% to 15% for lab tests). Phoon and Kulhawy (1999b) [154] suggested a method for estimating the uncertainties in soil design properties resulting from transformation errors (from index to geomechanical properties).

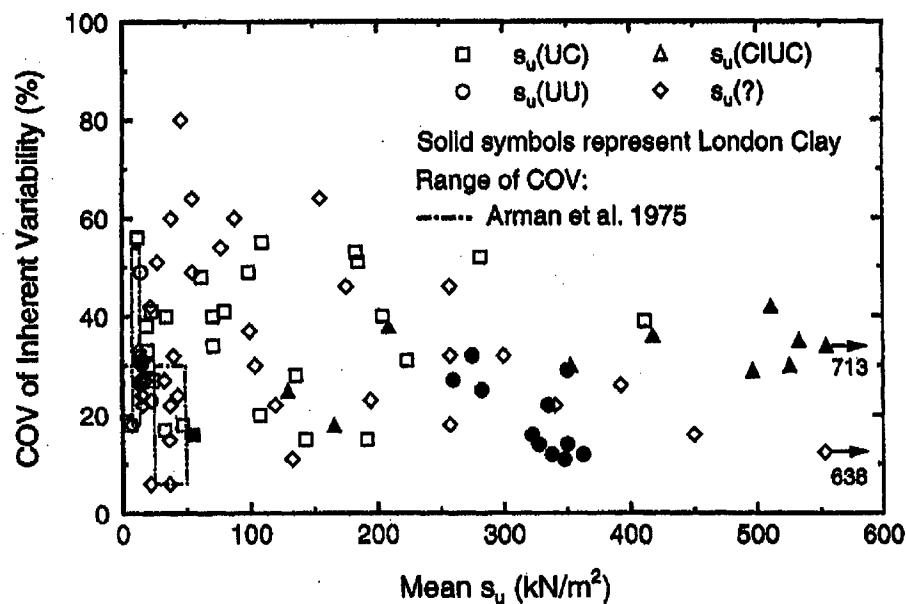


Figure 2.3 Coefficient of variation (COV) of inherent variability of soil undrained shear strength (s_u) vs. mean s_u (after Phoon and Kulhawy, 1999a [154]).

Cherubini et al. (1993) [28] collected the coefficient of variation of soil undrained shear strength. They found a very wide range of 12% to 145% for C_V of soil undrained shear strength. Figure 2.4 shows the reported values of C_V vs. mean undrained shear strength. Variability caused by measurement is not separated from these values (Figure 2.4). Cherubini et al. found that variability decreases as soil undrained shear strength increases; thus, they recommended a range of $C_V = 12\%$ to 45% for medium to stiff soil.

Soulie et al. (1990) [191] studied the structure of spatial variability of the undrained shear strength within a clay deposit. The site for that study is located on the shore of the Broadback River in the James Bay area of Quebec. The value of C_V of undrained shear strength for this site was about 22% and was determined using a series of vane tests.

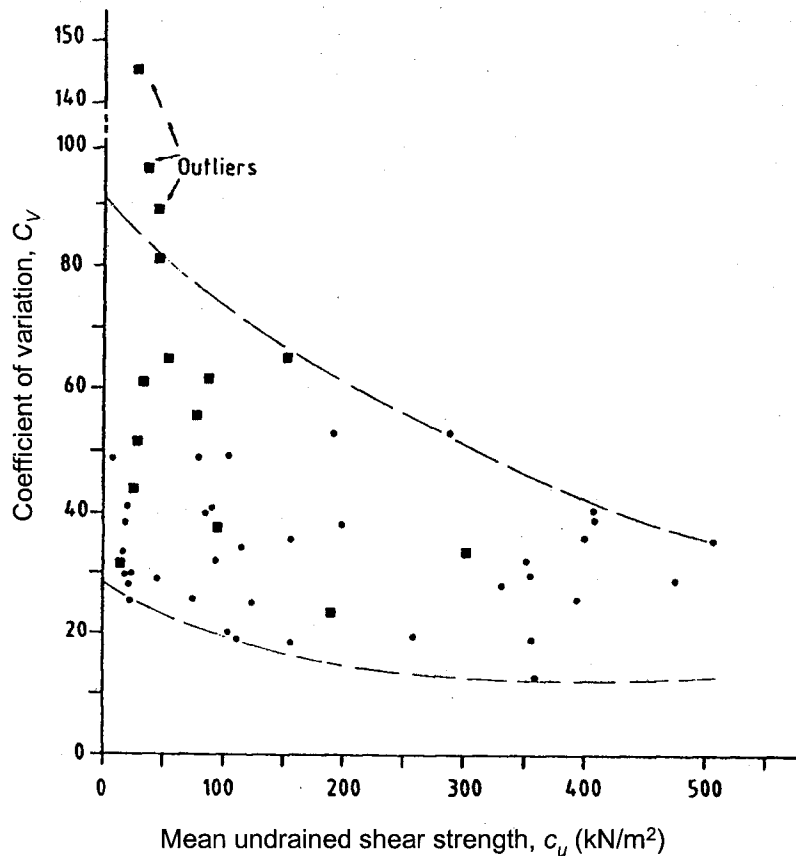


Figure 2.4 Coefficient of variation, C_V , of soil undrained shear strength vs. mean soil undrained shear strength, c_u (after Cherubini et al., 1993 [28]).

Fredlund and Dahlman (1972) [69], Lumb (1972) [114], Morse (1972) [131], and Matsuo and Kuroda (1974) [119] reported a range of 30% to 50% for C_V of unconfined compression strength of clayey soil deposits. Lumb (1972) [114] also reported values of C_V

in the range of 60% to 85% for extremely variable clay. Ejezie and Harrop-Williams (1984) [55] reported a range of $C_V = 28\%$ to 96% for undrained shear strength of clays.

Many other researchers have investigated the variability of natural soils. Based on studies by Harr (1984) [88], Kulhawy (1992) [102], and Lacasse and Nadim (1996) [105], Duncan (2000) [54] suggested a C_V of 13% to 40% for undrained shear strength. Similarly, Meyerhof (1993) [127] gave a range of 20% to 60% for C_V of soil undrained shear strength.

In conclusion, a range of $C_V = 10\%$ to 40% is suggested for inherent variability of undrained shear strength of medium to stiff clayey soil deposits. For highly variable soft soil, this variability may reach to a possible upper limit of $C_V = 80\%$. These ranges are inferred for soil inherent variability; the measured values of undrained shear strength may have higher variation due to measurement errors.

Ranges for scales of fluctuation for undrained shear strength have been estimated from both laboratory and field tests (Phoon and Kulhawy, 1999b [155]). In the vertical direction, θ_v , scales ranged from 0.5m to 6.0m (mostly between 1m to 2m), and in the horizontal direction, θ_h , scales ranged from 40m to 60m. Lacasse and Nadim (1996) [105] provided values of correlation distances obtained by various authors based on cone penetration records. The values ranged between 1m and 3m in the vertical direction and between 5m and 38m in the horizontal direction. Research suggests that the assessed scale of fluctuation depends on the sampling interval (e.g. DeGroot and Baecher 1993 [45]; Fenton, 1999b [63]). This issue is especially important for the horizontal direction, where a sufficient number of closely spaced measurements are rarely available. For example, based

on such closely spaced measurements, Popescu (1995) [158] found a horizontal scale of fluctuation of about 12m for a sandy soil deposit, and Przewlocki (2000) [173] found a horizontal scale of fluctuation of 5m for a clayey soil deposit. Soulie et al. (1990) [191] found autocorrelation distances of 7m and 30m in the horizontal direction and 3m in the vertical direction for clayey soil. Chiasson et al. (1995) [30] estimated an autocorrelation distance of 2m for a clay deposit in the vertical direction.

For physical reasons, soil properties follow non-Gaussian probability distributions; for example they do not assume negative values (See Harr, 1977 [87]; Popescu et al., 1998a [163]). Based on numerous studies reported in the literature, it can be concluded that each soil property can follow different probability distributions for different materials and sites. Several researchers recommended Beta distribution for soil shear strength, including Harr 1977 [87], Ejezie and Harrop-Williams (1984) [55], and Failmezger, 2001 [61]. Based on a limited number of soil deposits, Popescu et al. (1998a) [163] concluded that probability distributions of soil strength in shallow layers are skewed to the right, indicating a stronger influence of a lower bound, while strength of deeper soils tends to follow a more symmetrical distribution.

2.1.2. Stochastic Finite Element Analysis

Finite element approaches used for random media can be categorized into two main classes,

- Stochastic finite element method (SFEM): in these approaches statistical properties of the random variables are built into the finite element equations

(e.g. Baecher and Ingra, 1981 [11]; Righetti and Harrop-Williams, 1988 [177]; Brenner, 1991 [19]; Yeh and Rahman, 1998 [224]).

- Monte Carlo simulations using deterministic finite element analysis with stochastic input.

The first approach, is theoretically appealing and computationally effective, but suffers from several drawbacks when applied to soil mechanics problems. Most notably, it is not useful for analysis of highly nonlinear problems, nor can it address soil properties with non-Gaussian distribution and large variability. Soil properties exhibit a high degree of nonlinearity and follow a non-Gaussian distribution often with large degree of variability; therefore, the application of these approaches in most areas of geotechnical engineering is not recommended. Elkateb et al. (2000) [56] summarized the limitations of SFEM as follows:

- The shape of the probability distribution for input random variables does not affect the analysis results. Therefore, it is not able to capture the effects of skewness in distribution of soil properties. Furthermore, a distribution has to be assumed for the output response variable as SFEM provides only its mean and standard deviation.
- Element variance and the covariance matrix are functions of the finite element shape and geometry and their determination becomes quite complicated for irregular element shapes.
- Limited to small variability due to the error associated with the truncation of higher order terms in the Taylor expansion, which is used to determine the mean values of the response variables.

- Integration of the random variable field over each element may result in a change in the anisotropy ratio of the correlation structure of soil properties.

Yeh and Rahman (1998) [224] conducted a comparative study using four different SFEM approaches for seismic response of soil materials. They concluded that a direct Monte Carlo simulation is the most reliable stochastic finite element method for the analysis of seismic response of soils. They stated that stochastic finite element analyses other than Monte Carlo are unsuitable for when it comes to evaluation of nonlinearity in system responses.

The second approach was deemed as the most general and reliable approach. It has been widely used for geotechnical problems in the last decade (e.g. Griffiths and Fenton, 1993 [74]; Paice et al., 1995 [145]; Popescu, 1995 [158]; Fenton and Vanmarcke, 1998 [67]; Popescu et al., 1997 [162]; Rahman & Yeh, 1999 [174]; Nobahar and Popescu, 2001a [138]; Fenton and Griffith, 2002 [65]). It is capable of handling highly nonlinear geotechnical problems (e.g. Popescu et al., 1997 [162]) as well as capturing changes in behaviour of systems, such as changes in failure mechanism and triggering patterns (see Popescu, 1995 [158] and Nobahar and Popescu 2001a [138]). Its well-known drawback is high computational cost. However, rapid advances in the computer industry have alleviated this problem to some degree.

There are a few efficient sampling techniques such as Latin-Hypercube to optimise the number of Monte Carlo simulations. These sampling techniques are applicable for random variables, whereas sample functions of a random field are generated in this study.

2.1.3. Effects of Soil Heterogeneity on Geotechnical System Behaviour

It has been proven that natural variability of soil properties within geologically distinct and uniform layers affects soil behaviour. Previous work in this area addressed these effects on seepage through spatially random soils (e.g. Griffiths and Fenton, 1993 [73] and Gelhar, 1993 [70] among others), settlements (Phoon et al., 1990 [157]; Paice et al., 1994 [145]; Brzakala and Pula, 1996 [22]; Fenton and Griffiths, 2002 [65]), liquefaction potential (Popescu et al., 1997 [162]; Fenton and Vanmarcke, 1998 [67]), seismic response of soils (Rahman and Yeh, 1999 [174]), seismic wave propagation through heterogeneous soils (Assimaki et al., 2002 [6]), and slope stability (Griffiths and Fenton, 2000 [76]; Gui, 2000 [79]).

It was found that soil heterogeneity affects the system response in two ways: (1) by inducing a certain degree of variability in the response, and (2) by inducing changes in the mean response, as compared to the response obtained from deterministic analyses (i.e. assuming uniform soil properties).

2.1.3.1. Settlement of shallow and deep foundations

Paice et al. (1996) [146] used a random, spatially correlated field for soil stiffness to study the effects of soil heterogeneity on the total settlement of a uniformly loaded flexible-strip footing on an elastic soil. A parametric study was performed for a range of coefficients of variation and depths of the spatially variable soil layer. The study results indicated significant effects of soil heterogeneity on the response variability. However only a modest increase in average settlement was predicted for soil stiffness variability ranges of

10% to 40%. For soil stiffness with a coefficient of variation $C_V = 42\%$ (upper value recommended by Lee et al., 1983 [107]), the expected (average) settlement was observed to be 12% higher than the deterministic value calculated using a uniform Young's modulus with a mean value. Relatively small changes in results were due to the fact that elastic settlement is a linear phenomenon; therefore, the spatial variability effects on the resulting average settlements were modest. Fenton et al. (2002) [65] developed the study to assess total and differential settlements of strip foundations in a probabilistic framework.

Phoon et al. (1990) [157] presented a reliability analysis of pile settlement accounting for spatial variability of soil properties. They used a stochastic finite element method (SFEM), in which statistical properties of the random variables were built into the finite element equations. They modelled the soil as an elastic linear material, and characterized Young's modulus as a homogeneous random field (Vanmarcke, 1977 [208]). The mean and coefficient of variation, C_V , of the pile head settlement for single piles were evaluated using a first order second moment (FOSM) analysis. Subsequently, reliability analysis (Der Kiureghian and Ke, 1985 & 1988 [48&49]) was applied to obtain the reliability index and probability of unserviceable behaviour. In this study, Phoon et al. (1990) looked at the effects of Young's modulus variability for soil, its horizontal and vertical correlation distances, relative stiffness of soil/pile, and slenderness ratio of pile. Variation of C_V of pile head settlement and reliability index (Hasofer and Lind, 1974 [90]) versus the mentioned parameters were investigated and design charts were provided. Combining stochastic finite element analysis with reliability analysis provided a good means of assessing the effects of soil variability for geotechnical systems. The study

considered a very wide range of correlation distances. The ability of the coarse mesh used in capturing small correlation distances is questionable. No mention of decrease in mean settlement of pile was reported compared to deterministic analysis.

2.1.3.2. Seepage flow through heterogeneous soil

Fenton and Griffiths (1996) [64] performed a study on free surface flow through a stochastically heterogeneous earth dam. They assumed a stationary spatially random field for the soil permeability with a lognormal distribution and spatial correlation structure. It was concluded that the stochastic predictions were dependent on the ratio of the scale of fluctuation to the length of flow domain, for the given dam shape and soil variability.

Griffiths and Fenton (1997) [75] performed three-dimensional analyses for seepage through spatially random soils using Monte Carlo simulation methodology. Similar to the aforementioned study, a lognormally distributed random field generated by local average subdivision method (LAS) was used to characterize isotropic soil permeability. They studied seepage under single sheet-pile using 2D and 3D models. They concluded that for practical ranges of correlation distances (scales of fluctuation), the average flow rate fell consistently with increases in the coefficient of variation of the soil permeability. However, it should be mentioned that according to the results of analytical studies by Gelhar (1993) [70], the average flow rate increases as the variance of soil permeability (hydraulic conductivity) increases for a heterogeneous three-dimensional isotropic system. The results of 3-dimensional analysis were compared to the previous results of 2D analysis (Griffiths and Fenton, 1993 [74]). It was observed that the variability of response (i.e. flow rates) predicted from three-dimensional analysis was smaller than those predicted from two-

dimensional analysis. Also, the mean flow rates predicted from three-dimensional analysis were closer to deterministic values than those predicted from two-dimensional analysis. In other words, the effect of three-dimensionality was shown to be a reduction in overall response randomness. However, it was concluded that there was not a great difference between the 2D and 3D results, suggesting that the simpler and less expensive 2D approach may give acceptable accuracy for the cases considered. One of the drawbacks of this analysis is that it used equal correlation distances for vertical and horizontal direction. Usually correlation distances in a horizontal direction are much larger than those in a vertical direction.

For Griffiths and Fenton's (1997) study, changes in the mean flow rate were modest. For instance, at $C_V = 50\%$, for a wide range of correlation distance from 1m to 8m, the predicted mean flow rate had dropped by less than 8% (Figure 2.5). This was possibly due to the linearity of seepage phenomenon. It should also be mentioned that built-in first order second moment stochastic finite element methods (see first category Section 2.1.2 - e.g. Choot, 1980 [31] and Hachich, 1981 [81]) are deemed to provide reasonable results for linear problems and are numerically much less costly.

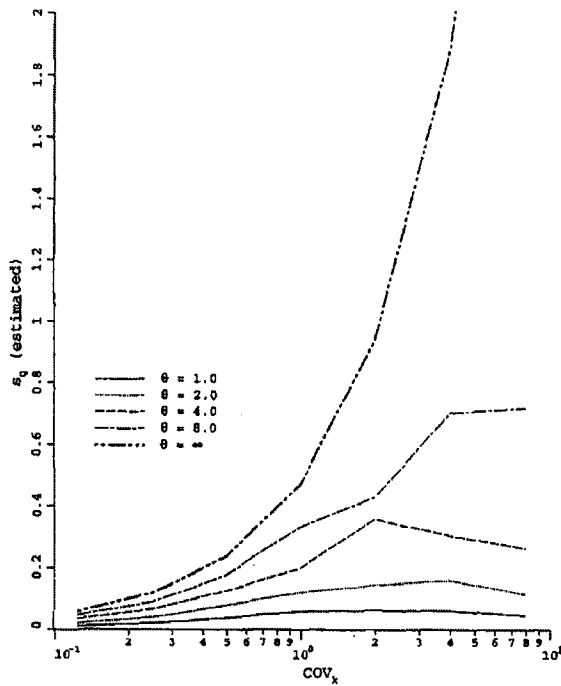
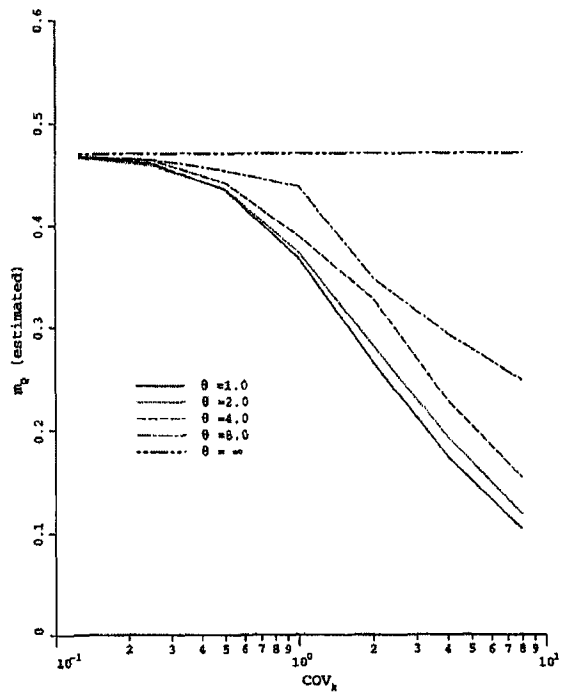


Figure 2.5 Influence of coefficient of variation and correlation distances ($\theta = \theta_h = \theta_v$) on mean (m_Q) and its standard deviation (s_Q) (after Griffiths and Fenton, 1997 [75]).

2.1.3.3. *Liquefaction potential*

Popescu (1995) [158] studied the effects of soil spatial variability on liquefaction. He concluded that both the pattern and the amount of dynamically induced pore water pressure build-up were strongly affected by spatial variability of soil properties. He concluded that the amount of predicted excess pore pressure was strongly affected by the probability distribution of soil parameters and, more specifically, by the left tail of the distribution, corresponding to presence of loose pockets in the soil deposit.

Popescu et al. (1997) [162] performed Monte Carlo simulations for soil liquefaction using experimental in-situ soil data accounting for spatial variability of soil. The predictions from the stochastic approach were compared with the deterministic ones based on average values and range of percentiles of soil strength. Using the characteristic percentile approach, it was possible to define a characteristic percentile of index soil properties (cone tip resistance that is directly related to soil strength) for a deterministic analysis that would predict a response equivalent to that predicted by more expensive Monte Carlo simulations. Comparisons were performed for various degrees of liquefaction of the soil deposit and for seismic excitations with various ranges of maximum spectral response amplitudes. For the soil analysed (loose to medium hydraulically placed sand) and for the range of input motions considered, the 80-percentile of soil strength was found to be a conservative enough characteristic value for equivalent deterministic analysis. It is mentioned that current design codes recommend use of 90 to 95 percentile of soil strength for soil liquefaction analysis (e.g. ENV, 1994 [59]). In subsequent studies (e.g. Prevost et al., 1997 [172] and Popescu et al., 1998c [165]), it was observed that the degree of

variability and the marginal probability distribution functions for soil parameters has significant effects on the predicted soil liquefaction.

2.1.3.4. *Slope stability*

Griffiths and Fenton (2000) [76] studied the stability of an undrained soil slope having spatially randomly varying shear strength. They characterized soil shear strength as an isotropic stochastic field with lognormal probability distribution. They performed parametric studies for a range of coefficients of variation and correlation distances. They used a Monte Carlo simulation methodology using deterministic finite elements with stochastic input. “Failure” was considered to have occurred if, for any given realization, the algorithm was unable to converge within 500 iterations. The probability of failure was defined as the ratio of non-converged simulations to the total number of simulations. It was concluded that for the considered slope with a factor of safety, $FS = 1.47$ (based on mean shear strength), the single random variable approach gave conservative estimates of the probability of failure for coefficient of variation values typically ranging from 0 to 50% (as marked in Figure 2.6). Single random variable analysis was defined as analysis using uniform soil at each simulation (common in most engineering probabilistic analysis) or in other words, using a correlation length $\theta_{ln\ cu}$ of infinity (Figure 2.6); $\theta_{ln\ cu}$ is the correlation distance of the logarithm of undrained shear strength. For higher values of the coefficient of variation (>50%); however, the single random variable approach gave non-conservative estimates. This conclusion may be affected by the assumption of failure based on numerical convergence. One would expect that the failure probability of a slope depends on the

average shear strength of the failure surface. Consequently, due to local averaging (Vanmarcke, 1983 [209]), a smaller failure probability is expected for small correlation distances. Contrary to this hypothesis, results from Fenton and Griffiths (Figure 2.6) show larger failure probabilities for smaller correlation distances for values of C_V higher than 50%. This may be caused by the assumption of failure - i.e. large presence of loose pockets of soil may cause numerical procedure not to converge. It should be noted that range of coefficient of variation used in this study – 10% to 1000% – is misleading as a C_V of undrained shear strength. Practical ranges are generally 10% to 60%, with most being from 10% to 40%.

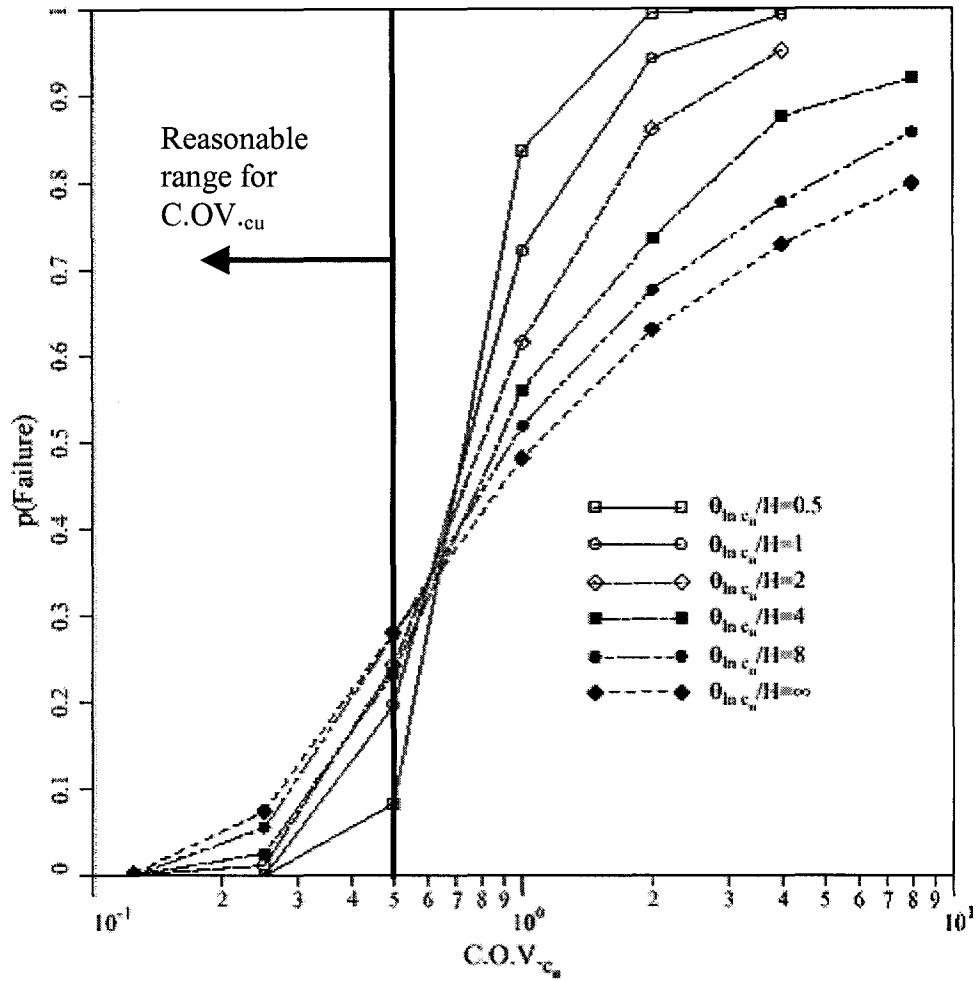


Figure 2.6 Influence of $C.O.V._{cu}$ on a slope with $FS = 1.47$ (after Griffiths and Fenton, 2000 [76]). $\theta_{\ln c_u}/H$ is isotropic correlation distance normalized by the height of slope.

2.1.3.5. Effects of soil heterogeneity on bearing capacity of shallow foundations

At the start of this research, no literature was found on the effects of soil heterogeneity on the bearing capacity of shallow foundation. Nobahar and Popescu (2000) [137] studied the effects of inherent spatial variability of soil properties on the bearing capacity of shallow foundations subjected to vertical loads, and placed on an elastic perfectly plastic soil deposit. The numerical model simulated the behaviour of an

overconsolidated clayey soil under undrained condition. A Monte Carlo simulation methodology combining deterministic finite element analysis with digital generation of stochastic fields was used. The undrained shear strength of soil was modelled as a random field with $C_V = 40\%$ following a Beta distribution. An exponential decay function for correlation structure was used.

Two-dimensional finite element analyses were performed for a strip foundation assuming undrained loading conditions. Bearing capacity, settlements, and foundation rotations predicted by Monte Carlo simulations that accounted for the spatial variability of soil strength were compared with deterministic analysis results that assumed uniform soil properties. Results showed that the bearing capacity of shallow foundations is strongly affected by the natural variability of soil strength in both resulting variability and average values. The predicted failure mechanism was unsymmetrical and significantly different for heterogeneous soil compared to uniform soil.

For the probabilistic characteristics of soil variability considered in that study, and for the numerical analysis assumptions (undrained loading of purely cohesive soil), the average ultimate bearing capacity predicted by Monte Carlo simulations was 25% lower than that predicted by a deterministic analysis assuming uniform soil with undrained shear strength, c_u , equal to the average c_u in Monte Carlo simulations. A characteristic percentile (nominal value) was proposed for use in design accounting for the effects of spatial variability. Despite a decrease in mean bearing capacity, the 95-percentile of bearing capacity predicted by Monte Carlo simulations was 38% higher than that obtained using the

95-percentile of soil strength (nominal value recommended by design codes), due to spatial averaging effects.

For the probabilistic characteristics of soil properties considered in that study, Nobahar and Popescu (2000) [137] concluded that a characteristic percentile of 88% of the soil strength used in a deterministic analysis would ensure 95% reliability. That study consisted a preliminary research and the effects of the degree of variability, probability distribution, and correlation distances were not addressed.

Foundation differential settlements resulting from spatial variability of soil were found to be likely to control the design. In deterministic analysis, due to the assumption of uniformity, there is no rotation for symmetrically loaded foundations. However, a more realistic analysis (Nobahar and Popescu, 2000 [137]) showed that limiting the slope of foundation to 0.5% imposes a limit of 240 kPa for bearing capacity (Figure 2.7b). This was 13% lower than the ultimate bearing capacity shown in Figure 2.7a (namely 280 kPa). In this case, the “nominal value” of soil strength (or characteristic percentile) for deterministic analysis is the 91-percentile.

Nobahar and Popescu (2001a) [138] continued their study of bearing capacity of shallow foundations by looking at range of coefficients of variation and two probability distributions. Results showed that the shape of the left tail of the distribution (i.e. amount of loose pockets in the soil mass) affected the predicted response variability and average bearing capacity values. This aspect will be further discussed in Section 4.3.3.2.

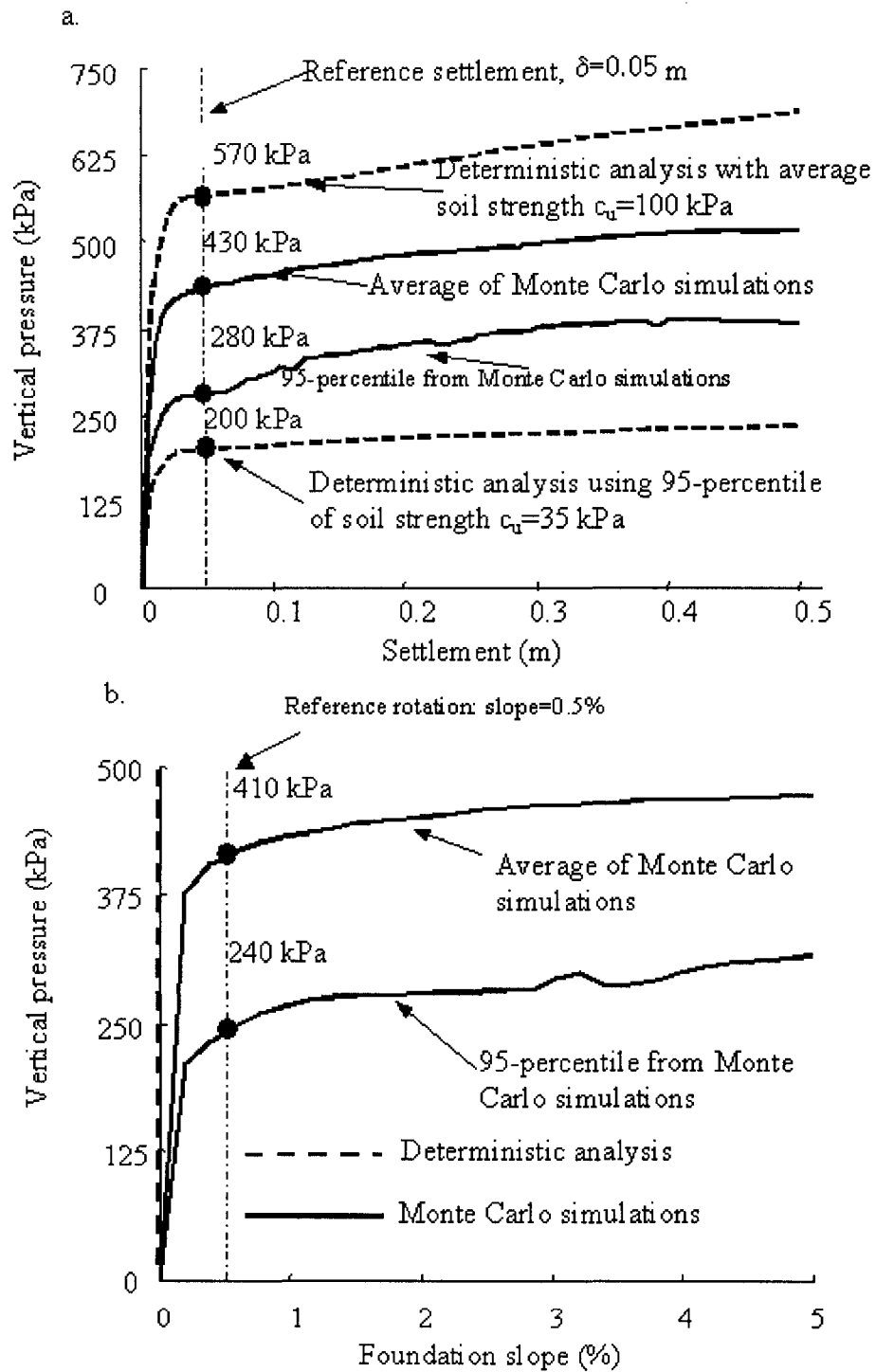


Figure 2.7 Comparison of deterministic and Monte Carlo simulation results for average and 95 percentile: a. pressure-settlement relationships; b. pressure-rotation relationships (after Nobahar and Popescu, 2000 [137]).

Griffiths and Fenton (2001) [77] performed a study on bearing capacity of spatially random soil placed on undrained clay. A Monte Carlo simulation methodology using elasto-plastic finite element analysis with stochastic input was used. A random field using a lognormal distribution, isotropic correlation distance and Markovian spatial correlation function represented the undrained shear strength. 2D plane strain finite element analyses were performed using 8-node reduced integration quadrilateral elements. An elastic perfectly plastic stress-strain law with a Tresca failure criterion was used to model the undrained soil behaviour. A local average process was used to map the random fields on the finite element mesh. Local averages preserved the mean, but reduced the standard deviation. For each case, 1000 simulations were performed. A typical deformed mesh is shown in Figure 2.8. Foundations on heterogeneous soil should exhibit asymmetric behaviour. However, as it can be seen in Figure 2.8, the foundation rotation was fixed in these analyses and may not represent the real behaviour of a foundation.

Griffiths and Fenton (2001) [77] studied the variation of the resulting bearing capacity and its coefficient of variation versus soil strength's coefficient of variation and correlation distance (see Figure 2.9 for an example). They concluded that a very high factor of safety (about 3) is required to reduce the probability of failure of foundation caused by natural variability of soil with the range of $C_v = 10\%$ to 50% . This is in agreement with standard geotechnical practice (Lambe and Whitman, 1969 [106]). They explained, in a probabilistic context, why factors of safety used in bearing capacity calculations are typically much higher than those used in other limit state calculations in geotechnical engineering, such as slope stability and earth pressures.

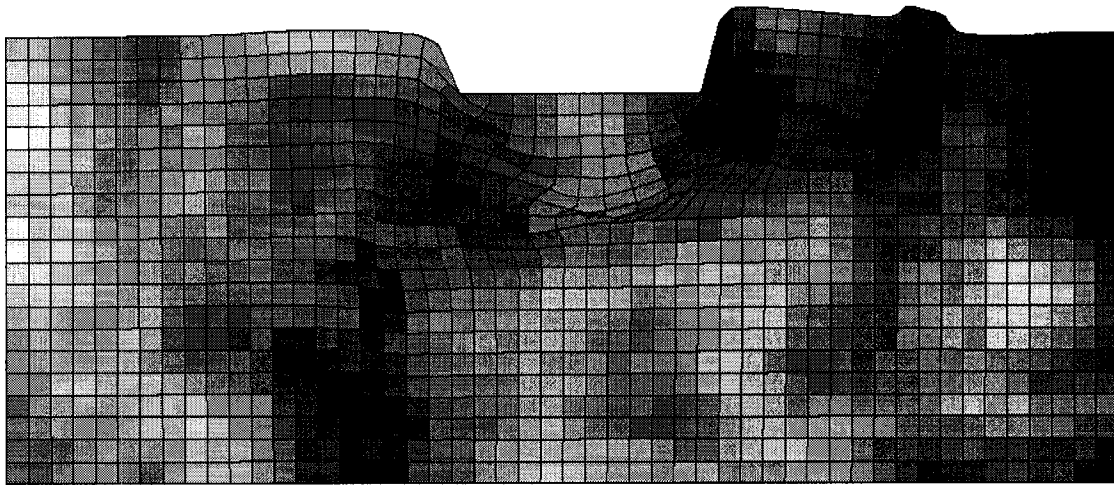


Figure 2.8 Typical deformed mesh. The darker regions indicate weaker soil (after Griffiths and Fenton 2001 [77]).

Though using high factors of safety, 2 or 3, is common for shallow foundations, there are other main sources of uncertainty (e.g. measurement error and uncertainty in model as discussed in Section 2.1.1). Therefore, attributing only these safety factors to the uncertainty caused by natural variability does not seem reasonable. There are researchers who believe that natural variability of soil has minimal effects on the uncertainty of geotechnical systems and that most uncertainty comes from uncertainty in models or measurement (e.g. Li and Lam, 2000 [110]). In the author's opinion, using different safety factors in geotechnical engineering may also be attributed to different target reliability levels in each area.

Fenton and Griffiths (2003) [66] extended their studies for bearing capacity of foundations placed on a soil with friction and cohesion. They used a two dimensional model to simulate strip foundations. They found that the geometric average of soil shear strength beneath the foundation in a domain with plastic deformations (taken to have a depth of B and length of $5B - B$ as the foundation width) may be used as a representative

value of soil shear strength. They found that a correlation distance of $\theta = B$ results in the lowest values for foundation bearing capacity; therefore, when sufficient data are not available, it can be used as a conservative value in calculations.

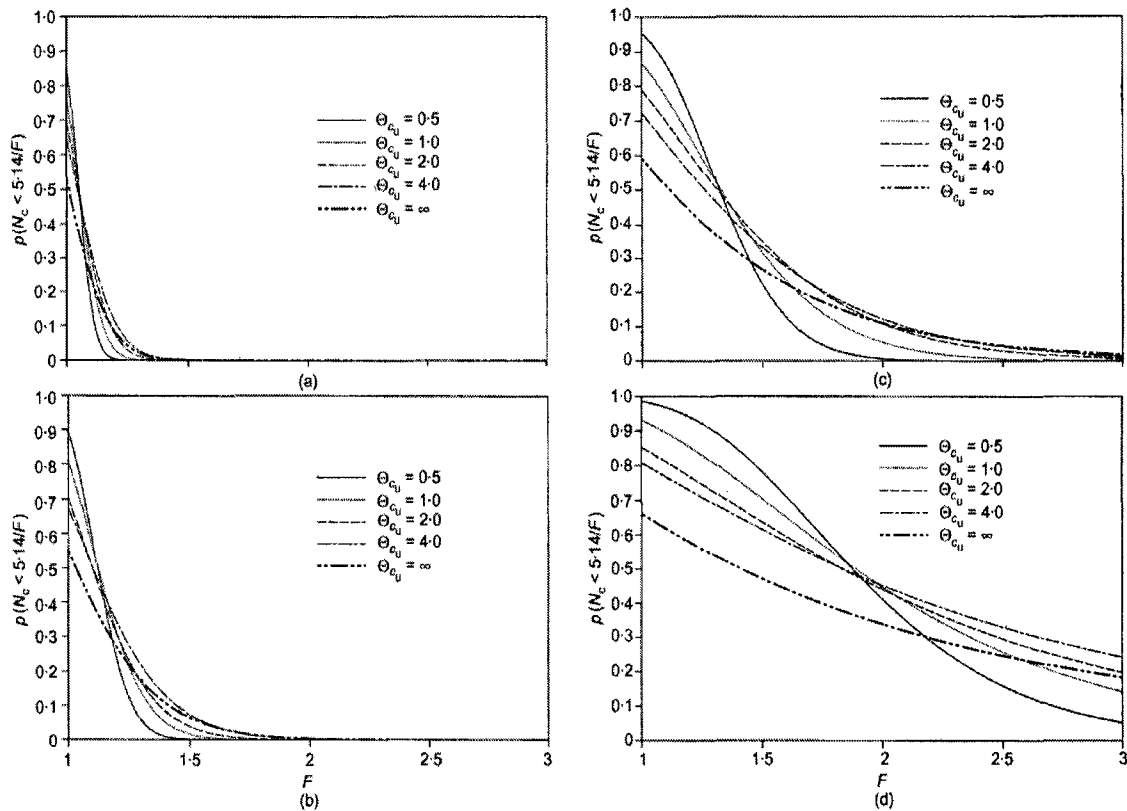


Figure 2.9 Graphs showing the relationship between $p(Nc < 5.14/F)$ and F for a soil with $C_{vcu} =$ (a) 12.5%, (b) 25%, (c) 50% and (d) 100% (after Griffiths and Fenton, 2001 [77]).

2.2. BEARING CAPACITY OF SHALLOW FOUNDATIONS

Foundations in civil engineering are divided into two main categories: 1) shallow foundations, and 2) deep foundations. This study investigated shallow foundations; hereafter the word “foundations” refers to “shallow foundations”.

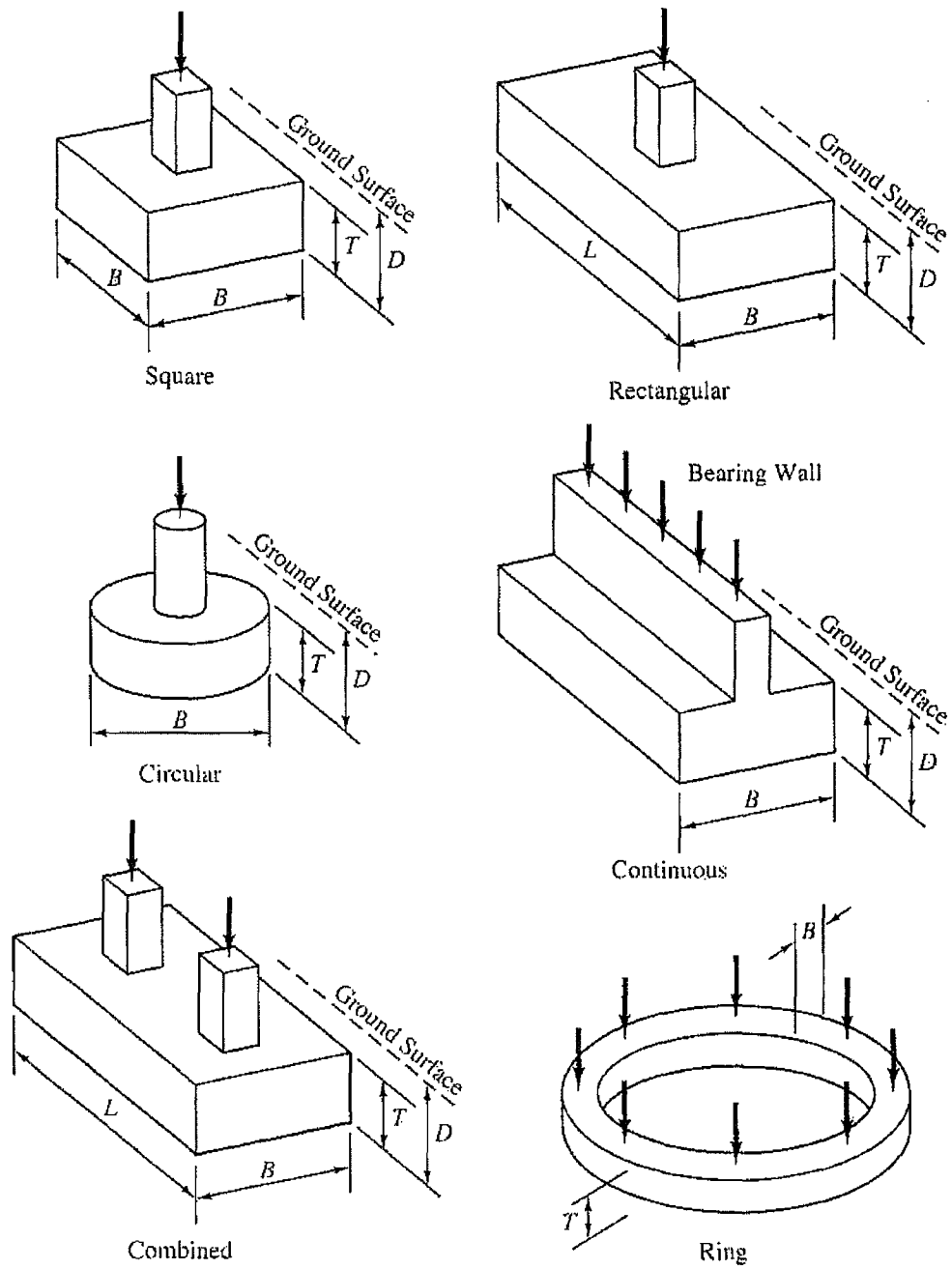


Figure 2.10 Spread foundation shapes and dimensions (Coduto, 2001 [35]).

Shallow foundations are those that transmit loads to near-surface soils. These can be classified as (1) spread footings, and (2) mat or raft foundations. Different types of spread footings are illustrated in Figure 2.10. A mat foundation is essentially a very large footing that usually encompasses the entire footprint of the structure. This study researched general methods of analysis for strip foundations to review their possible use in stochastic analysis, and for comparison with stochastic results.

2.2.1. Conventional Methods

This section presents a short review of behaviour of shallow foundations placed on clayey soil in undrained situation.

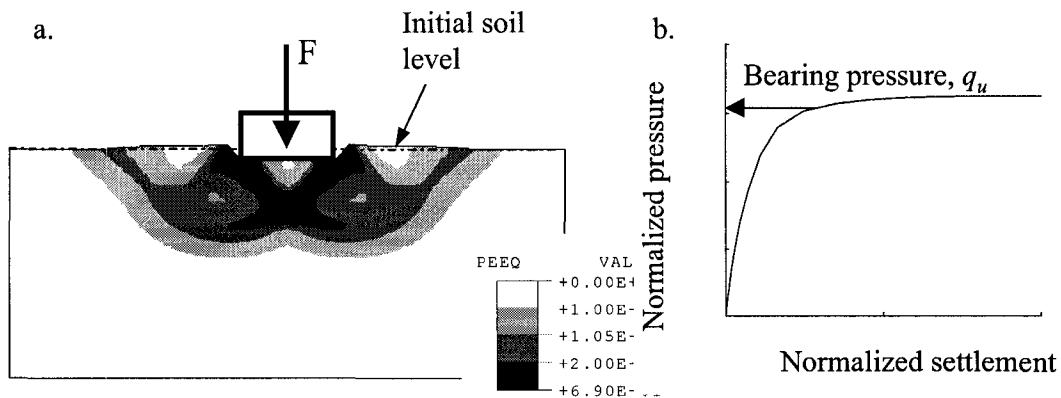
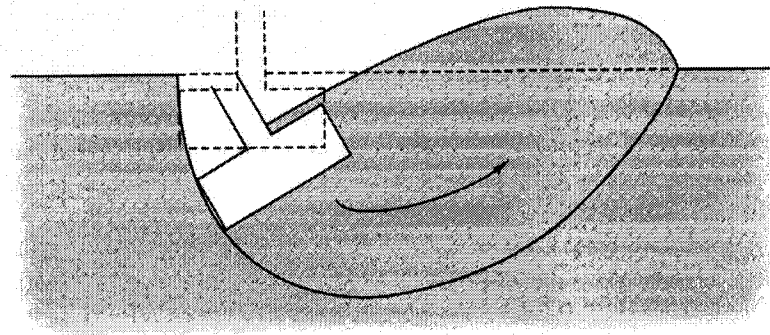


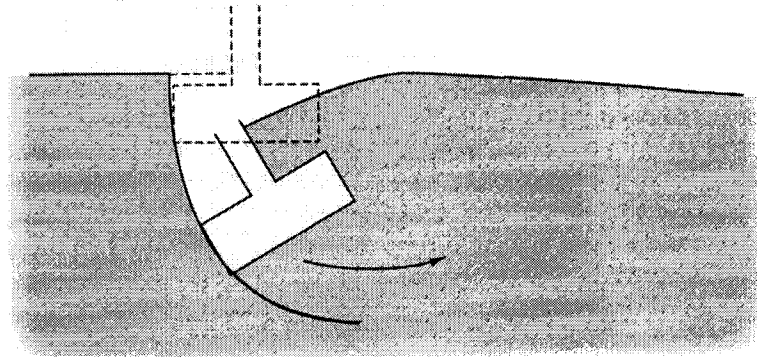
Figure 2.11 A general failure mode captured by finite element analysis: (a) contours of plastic strains and (b) schematic normalized pressure-normalized settlement relationship.

2.2.1 Failure mechanisms of shallow foundations

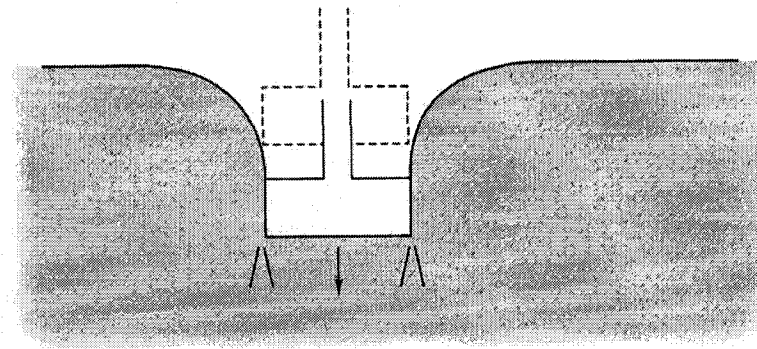
A foundation is said to have reached its ultimate bearing capacity when the settlement increases without significant changes or even with a decrease in applied load (Figure 2.11b). This behaviour is the result of failure. There are three possible failure mechanisms for a foundation (e.g. Vesic, 1973 [212]; Coduto, 2001 [35]): (1) general shear failure, (2) local shear failure, and (3) punching failure (Figure 2.12). The failure mode of a foundation depends on several factors, including soil strength and ductility, soil compressibility, stress state, foundation geometry, and loading conditions.



(a) General Shear Failure



(b)



(c)

Figure 2.12 Failure mechanism of a foundation: (a) general shear failure, (b) local shear failure, and (c) punching failure (after Coduto, 2001 [35]).

2.2.2. Analysis Methods

In engineering practice, usually bearing capacity problems are investigated assuming a perfectly rigid perfectly plastic behaviour for soil materials.

2.2.2.1. *Limit analysis method*

The solution of a boundary value problem in continuum mechanics involves satisfying 15 equations, including stress equilibrium equations, compatibility equations, and stress-strain relationships. In limit analysis method, the response is approximated using an idealized stress-strain relationship. Limit analysis methods are generally classified into upper and lower bound approaches. It is usually possible to bracket a true solution between upper bound and lower bound limit analysis solutions with desirable accuracy (Chen, 1975 [26]; Chen and Han, 1988 [27]).

In the upper-bound method, a velocity field (deformation mode), which satisfies the velocity boundary conditions as well as the strain and velocity compatibility conditions, is considered. The loads, determined by equating the external rate of work to the internal work rate of dissipation in a kinematically admissible velocity field, are not less than the actual collapse load (Chen, 1975 [26]).

For the lower-bound method, an admissible stress distribution, satisfying the equilibrium equations and the stress boundary conditions and not violating the yield criterion, is applied to the problem. The load determined from such an assumption is not greater than the actual collapse load. The lower-bound approach only considers the equilibrium equations and yield criterion (Chen, 1975 [26]).

2.2.2.2. *Limit equilibrium method*

In this method, failure surfaces are assumed, and minimum failure load is sought. Due to approximations induced by assuming the failure mechanism, the result is not necessarily a lower bound or an upper bound solution.

2.2.2.3. *Method of characteristics (slip-line method)*

In this method, a region of the soil mass near a foundation is considered. Equilibrium and yield criteria provide a set of differential equations. Imposing stress boundary conditions, the differential equations can be solved for specific problems. For more information, refer to Chen (1975 [26]).

2.2.2.4. *Bearing capacity of foundations in engineering practice*

The bearing capacity of a shallow foundation in engineering practice is usually calculated using formulas based on Terzaghi's (1943) [198] equation,

$$q_{ult} = cN_c + q_s N_q + \frac{\gamma B}{2} N_\gamma \quad \text{Eq. 2.4}$$

Terzaghi (1943) [198] (also see Terzaghi et al., 1996 [201]) assumed that friction, cohesion, and overburden pressure have separable effects and, therefore, the bearing capacity equation is comprised of the superposition of three separable components. N_c , N_q , and N_γ are three dimensionless bearing capacity factors for cohesion, overburden and friction effects in Eq. 2.4. Terzaghi proposed one set of bearing capacity factors. His values are frequently used in practice; however, there are many values from other authors (e.g.

Meyerhof, 1963 [124]; Hansen, 1970 [86]; Vesic, 1973 [212] & 1975 [213]). The main difference between the suggested values is the value of N_γ . N_γ has the widest suggested range of values of any of the bearing capacity factors (Bowles, 1997 [20]). A literature search reveals that the range of N_γ is:

$$38 < N_\gamma < 192 \quad \text{for } \phi = 40 \text{ degrees}$$

Terzaghi (1943) [198] realized that due to simple superposition, bearing capacity obtained from Eq. 2.4 has some errors. However, he concluded that these errors are on the conservative side and less than 10% to 20%.

2.2.2.5. *Some important issues in foundation design*

Practical plasticity methods usually postulate a rigid perfectly plastic model and a general failure system for soil. However, this assumption is suitable for dense sand and stiff clay, but is not necessarily logical for soft soil where there is a chance of punching shear failure. In large foundations, failures are also most likely to happen because of punching mode.

The roughness of the footing also has a significant impact on the bearing capacity. Meyerhof (1955) [123] concluded that the bearing capacity of a perfectly smooth foundation on the surface of sand is only half of that of a rough foundation. Currently, using the finite element method, it is possible to address these aspects in a more rational manner.

2.2.3. Numerical Methods for Bearing Capacity of Foundations

To obtain a more accurate solution for bearing capacity of foundations, the finite element method can be employed. The finite element method has been used successfully in many engineering applications and it can be adopted for bearing capacity problems as well. Chen (1975) [26], Zienkiewicz et al. (1975 & 1978) [231&232], Davidson and Chen (1976) [43], Christian (1977) [32], Griffiths (1982) [73], Britto and Gunn (1987) [21], Zhu (1998) [234], Merifield (1999) [122], and Taiebat and Carter (2000&2002) [193&194] among others applied the finite element method to estimate the bearing capacity of foundations. In comparison to other aforementioned methods, the finite element method uses relatively fewer assumptions; therefore, it is deemed to provide results that are more accurate.

In conducting a review of finite element analysis of shallow foundations, a number of studies were consulted (Nagtegaal et al., 1974 [132]; Griffiths, 1982 [73]; Sloan and Randolph, 1982 [189]; Sloan, 1988 [188]; Merifield et al., 1999 [122]; Taiebat and Carter, 2000 & 2002 [193&194]). Relatively few finite element solutions for bearing capacity of cohesionless soils are available due to the complex behaviour of frictional soil and numerical problems.

Griffiths (1982) [73] carried out finite element analysis of strip footings on frictional and cohesive materials, separately assessing N_c due to soil cohesion, c ; N_q due to overburden pressure, q ; and N_γ for cohesionless soil assuming weightless soil. He employed the Mohr-Coulomb failure criterion with zero plastic volumetric strain. The elastic properties were $E = 2 \times 10^5$ kN/m² and $\nu = 0.35$. Perfect plasticity was implemented

using the visco-plastic technique (Zienkiewicz and Corneau, 1972 & 1974 [229&230]). Bearing resistance was mobilized by applying a prescribed vertical displacement at the base of the foundation. For a smooth footing, those nodes are allowed to move horizontally; for rough footing, the horizontal displacement is fixed.

According to the finite element results presented by Griffiths (1982) [73] and the comparison with closed form solutions or well-known approximate solutions available for highly idealized soil properties, it was suggested that the finite element method could be used with confidence to estimate the bearing capacity factors N_c and N_q . The predicted values for N_γ had relatively good agreement with practical values. The dependence of N_γ on footing roughness was confirmed. The calculated values of N_γ decreased with increased footing size. A friction angle of 35 degrees appeared to be the limit for obtaining a reasonable resistance factor using the visco-plastic technique. Griffiths concluded that the finite element method enables bearing capacity problems involving collapse prediction to be tackled with confidence. Such problems would be those involving irregular boundaries or loading conditions.

However, applying finite element methods to geotechnical engineering has several drawbacks in practice. Practice has shown that the results obtained from the displacement finite element method tend to overestimate the true load limit (Nagtegaal et al., 1974 [132]; Sloan and Randolph, 1982 [189]; Merifield et al., 1999 [122]; Taiebat and Carter, 2000 & 2002 [193 & 194]).

Merifield et al. (1999) [122] applied a new plasticity solution for the bearing capacity of foundations. They provided numerical formulations for upper and lower bound

limit theorems, developing a new finite element formulation. Using this method, they bracketed the exact collapse load for the foundations placed on a two-layered soil within 12%.

In the past few decades, there have been several finite element studies on the bearing capacity of foundations. These studies usually did not address load eccentricity and inclination. In addition, only elastic perfectly plastic constitutive models were employed. This may be explained by the reasoning that these studies mainly aimed to show the efficiency of the finite element method by comparing it to conventional methods, such as limit analysis. Moreover, accurate modelling of soil behaviour requires sophisticated constitutive models that account for hardening and softening.

2.3. PIPE–SOIL INTERACTION

This section presents a literature review of significant issues related to modelling pipe-soil interaction. The study focused primarily on pipe-soil interaction in clay (mainly lateral loading of buried pipes). Experimental and empirical engineering methods, as well as numerical models were studied. The review has three parts: (1) engineering practical methods, which focus on parameters and methods used in engineering practice and guidelines based on previous studies and experience, (2) experimental studies, which review the parameters and findings of past experimental studies regarding lateral loading of pipeline, and (3) numerical modelling, which discusses numerical aspects of modelling of pipe-soil interaction and presents findings of some previous studies in this regard. These three parts were used to validate the deterministic finite element model used in this study

and to screen the main interaction parameters affecting lateral loading of pipeline. Since deterministic analysis of buried pipes is not the main goal of this study and is only used as a tool, the review presented here is limited and does not include all aspects of soil-pipe interaction.

2.3.1. Engineering Practical Methods

In engineering practice, the soil-pipeline system is represented by a numerical model including structural beam elements for the pipe and elasto-plastic spring elements for the soil in the axial (longitudinal), transverse horizontal, and transverse vertical directions (ASCE, 1984 [5]), Figure 2.13. The current state of practice is reflected in the ASCE (1984) [5] guidelines, Dutch Code NEN3650 [133], and more recently, in the PRCI guidelines (Honegger and Nyman, 2001 [95]). This simplification is derived from the concept of sub-grade reaction originally proposed by Winkler (1867) [219]. The maximum soil spring forces and associated relative displacement necessary to mobilize these forces are computed using different equations corresponding to assumed conditions.

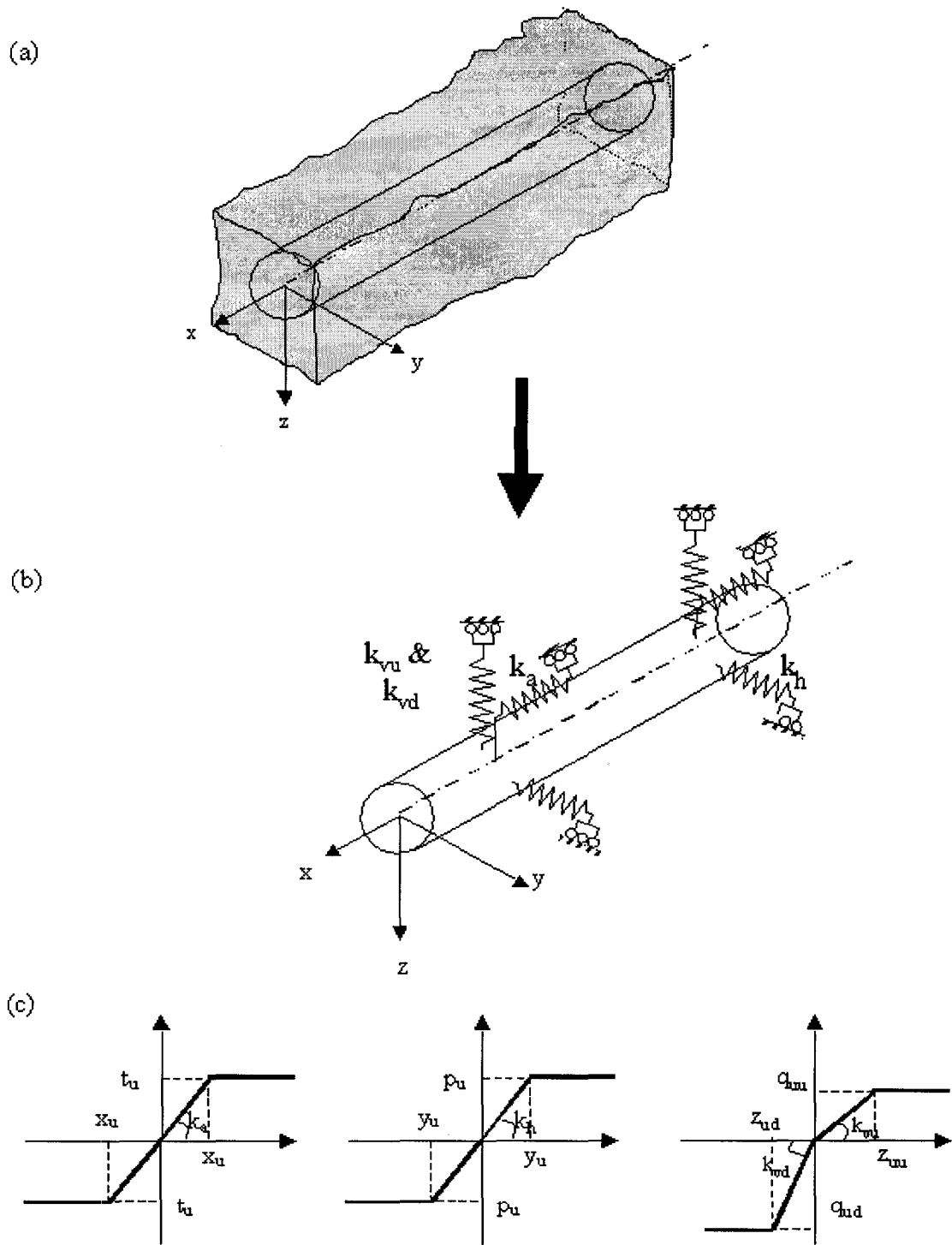


Figure 2.13 Soil-pipeline interaction (a) continuum analysis, (b) idealised structural model and (c) soil load-displacement response (t_u , x_u , p_u , y_u , q_{vu} , z_{vu} , q_{ud} , z_{ud} are spring characteristics).

The critical task in the beam/spring model for buried pipelines is determining the analytical expressions of soil resistance functions f_x , f_y and f_z . Various relationships have been proposed for axial t-x, transverse horizontal p-y, and transverse vertical interaction q-z. Hyperbolic and bilinear forms are the most widely used force-displacement relationships. The characterization of soil loads on pipeline is performed using three approaches: (1) use of theoretical soil mechanics to derive equivalent simplified relationships, (2) use of numerical modelling of soil media mainly using finite element method and (3) use of physical model test (small- or large- scales) data to develop empirical relationships.

In elastic continuum models (see Reissner, 1958 [176] and Vlazov & Leontiev, 1966 [214] among others), assumptions about the distribution of displacements and stresses are based on physical laws. The springs describing the soil resistance to deformation are usually assumed independent of one another; therefore, no connection between adjacent soil zones is considered. However, the assumption of independent soil slices does not truly replicate the observed behaviour (Kettle, 1984 [100]; Popescu and Konuk, 2001 [167]). Winkler-type soil models are unable to describe complicated soil behaviour, such as dilatancy, stress path dependency and, to some extent, strain softening. When soil is under large deformation, these phenomena may have significant effects on the soil loads and can only be simulated by using more sophisticated constitutive models and continuum numerical modelling techniques.

ASCE Guidelines (1984) [5] defined the transverse horizontal yield load (p_u) per unit length (kN/m) as,

$$p_u = N_{ch} D_o c_u \quad \text{Eq. 2.5}$$

where N_{ch} is the transverse horizontal bearing interaction factor adapted from Hansen (1961) [86] or Rowe and Davis (1982a) [179]. These bearing capacity factors recommended by ASCE are illustrated in Figure 2.14. Paulin's (1998) [149] experimental data are also plotted in Figure 2.14, which suggests that the later model was more appropriate. For H/D ratio greater than 1.5, the bearing capacity factor for Rowe and Davis (1982a) [179] can be expressed as,

$$N_{ch} = 4.3 + 0.32 \ln \left(\frac{H}{D_o} \right) \quad \text{Eq. 2.6}$$

The PRCI guidelines (Honegger and Nyman, 2001 [95]) consider the contributions of both soil friction and cohesion to lateral soil resistance in two separate terms for cohesive and frictional soil. For these guidelines, bearing capacity factors were derived from fits to the published empirical results.

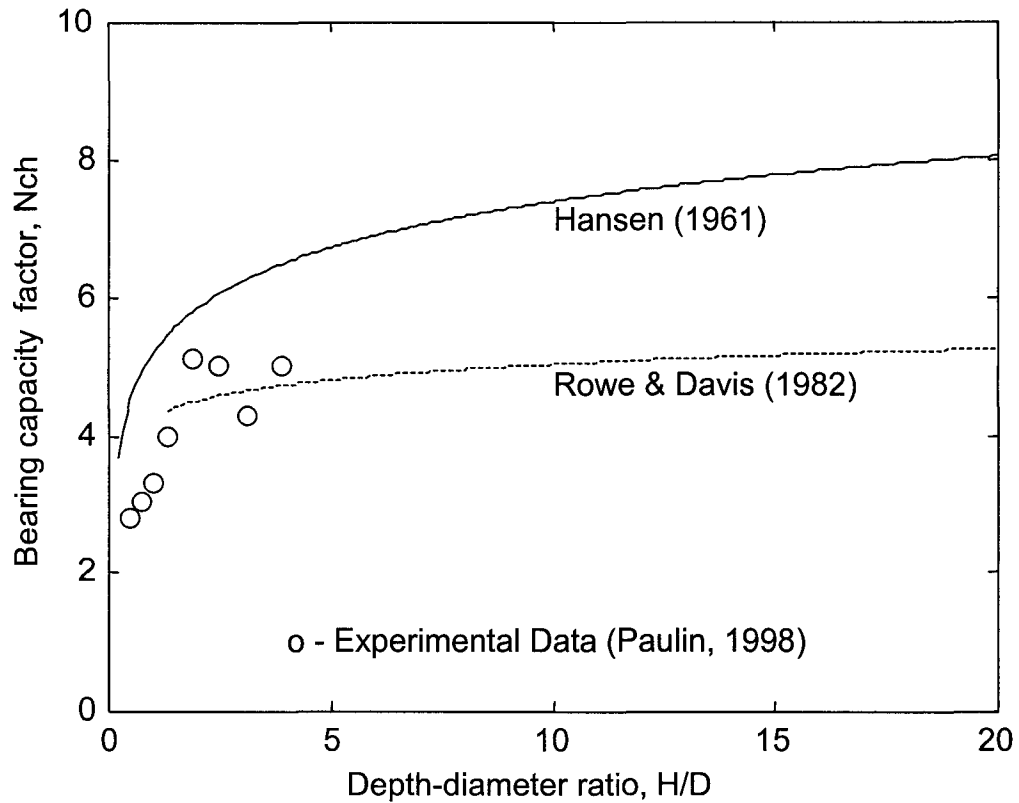


Figure 2.14 Transverse horizontal bearing interaction factors for cohesive sediment.

2.3.2. Experimental Studies

2.3.2.1. Lateral loading of buried pipeline

The format presented in equation Eq. 2.5 is advised by more recent researchers (e.g. Rizakalla et al., 1992 [178]). However, it lacks a weight term. For instance, early small-scale experimental work by Mackenzie (1955) [117] suggested the following equation for lateral resistance of shallow to medium depth buried anchors,

$$p_u = \sqrt{\frac{D_o}{H} \left(\frac{1}{2} \gamma (H + D_o)^2 + 2(H + D_o)c_u \right)} \quad \text{Eq. 2.7}$$

where $H+D_o$ is the burial depth of an anchor from its bottom. p_u is limited for deep burial by the following equation (Mackenzie, 1955 [117]),

$$p_u = 8D_o c_u \quad \text{Eq. 2.8}$$

Wantland et al. (1982) [216] conducted field and laboratory tests to determine the effect of pipe weight, pipe diameter, embedment depth, loading rate and type of soil on the lateral resistance to a pipeline buried in clay. The N_c values increased with the embedment ratio h/D_o , with an upper limit in the order of 5 to 6. For $h/D_o = 1, 2$ and 5 , the values of N_c (approximate average of test data) were about 2.2, 3.4 and 5.0 respectively. N_c was not significantly affected by pipeline diameter. It was suggested that lateral soil resistance to pipeline in clay is similar to the bearing capacity of a foundation and that an upper bound plasticity mechanism for bearing capacity could be applied to a laterally loaded pipeline. Using the foundation analogy, the maximum lateral resistance to a pipeline would be $5.14c_u D_o$ at $h = 2D_o$. Wantland et al. (1982) [216] recognized that the actual maximum lateral resistance for a pipeline may be different from the value suggested by the plasticity theory and, therefore, a deeper embedment may be necessary to achieve the maximum value. Finally, they advised using an average c_u from a distance of $2D_o$ above the pipe base.

Various centrifuge tests have been conducted to investigate soil-pipe interaction. Investigations included the effect of groundwater level on buried pipes (English and Schofield, 1973 [57]), the behaviour of flexible circular pipes subjected to surface loads (Valsangkar and Britto, 1979 [207]), thaw induced settlement of pipelines (Smith, 1991

[190]), influence of excavation on buried pipes (Kusakabe, 1984 [104]; Phillips, 1986 [152]), and the effect of earth pressure on buried flexible pipes (Tohda et al., 1985 [203]).

Paulin (1998) [149] conducted a full series of centrifuge tests of pipelines with a prototype diameter of 0.95m to investigate the effects of trench geometry, soil preconsolidation stress, pipeline displacement rate, and backfill type on the pipe-soil interaction. The pipes were placed in trenches with widths of 1.5m to 3m while the cover depth varied from 0 to 3.25m. The testbed soil was a kaolin-silt mixture preconsolidated to either 140kPa or 400kPa. The type of trench backfills included slurry, chunks of backfill, remoulded material and fine sand. The experimental data indicated that when the H/D_o ratio varied from 1.0 to 1.84, the normalized lateral load increased with H/D_o ; however, the effect of cover depth on lateral load was not significant when $H/D_o > 1.84$. On the other hand, when partial drainage was permitted or the loading velocity was decreased, the lateral load on pipeline increased (Figure 2.15). For the tests performed under undrained conditions (i.e. at high loading speed), experimental data appeared to be bounded by the interaction curves from Rowe and Davis (1982a) [179] and Hansen (1961) [86] for embedment ratios of H/D_o less than 2. For greater embedment ratios, the experimentally derived lateral soil resistance was similar to that found by Rowe and Davis (1982a) [179].

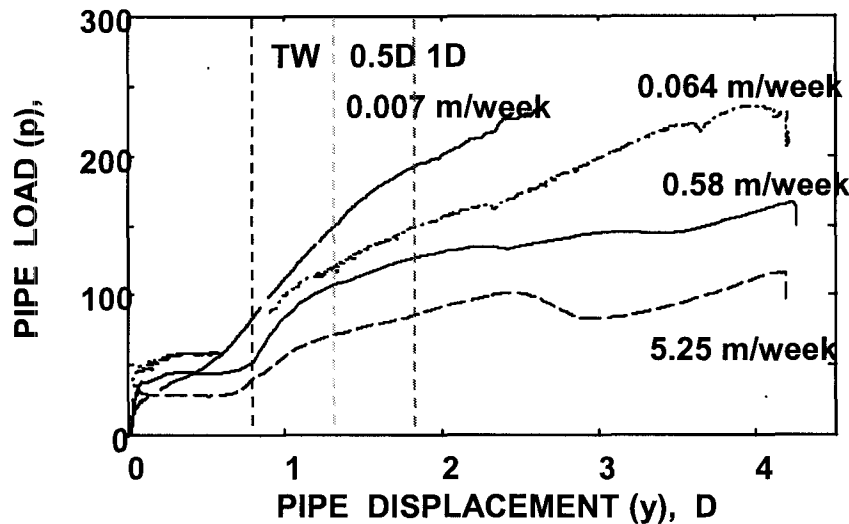


Figure 2.15 Dependency of soil force on loading rate: pipelines buried in saturated clay (after Paulin et al. 1998).

Based on experimental results of centrifuge tests, Rizakalla et al. (1992) [178] suggested a routine design of laterally loaded pipelines should incorporate Rowe and Davis' (1982a&b) [179 & 180] work, which was based on the elasto-plastic finite element analysis of vertical smooth anchors. It should also consider the recommendation of the ASCE Committee on Gas and Liquid Fuel Lifeline (ASCE, 1984 [5]), which was based on Hansen's (1961) [86] work of laterally loaded piles.

2.3.3. Numerical Modelling of Pipe-Soil Interaction

Practical engineering solutions, which often use structural finite element (numerical) analysis, are advantageous in terms of the simplicity, functionality and utility for conducting preliminary assessment of pipeline integrity and parametric analysis. The procedures, however, are limited by the underlying assumptions and idealizations considered. Furthermore, analytical difficulties are encountered for pipe-soil interaction

events considering non-uniform boundary conditions, spatial variation in characteristics of the pipeline and soil media, large amplitude, accumulated or cyclic deformational loading mechanisms, and nonlinear material behaviour. For these issues, numerical methods for continuum media provide a rational basis for conducting pipe-soil interaction studies. In addition, numerical and experimental studies have been used to calibrate parameters required for state of practice engineering solutions.

2.3.3.1. Numerical aspects

Continuum finite element models are robust and comprehensive numerical tools and can address a number of limitations in reproducing,

1. soil constitutive behaviour,
2. soil deformation mechanisms (e.g. shear load transfer),
3. soil-pipe interaction (e.g. variable circumferential or longitudinal pressure distribution), and
4. complex pipeline response mechanisms (e.g. ovalization, or wrinkling).

The significant disadvantages of continuum finite element modelling are the demands on computational resources, limited availability of realistic soil constitutive models, and the requisite experience and knowledge of the analyst. A number of studies have been conducted to investigate pipe-soil interaction using continuum finite element modelling, including studies conducted by Bruschi et al. (1995) [23], Altaee et al. (1996) [8], Popescu et al. (1999) [166], Nobahar et al. (2000) [141] and Popescu and Konuk (2001) [167]. Other researchers have studied pipeline research, including Yoshizaki et al. (1998) [227] and Yoosef-Ghodsi et al. (2000) [226].

2.3.3.2. *Soil-pipeline interface*

Correct modelling of soil-structure interaction is very important for accurate simulation of the load transfer to the pipeline. Relative movement often takes place at the interface, involving slip and/or separation. In a state-of-the-art approach, the pipe and the soil are discretized in 2D/3D finite elements. The pipe-soil interface is modelled with true interface elements that can account for relative displacements. Various types of interface elements have been used, including zero-thickness elements (e.g. double nodes with relative motion allowed), thin layer elements, and modified quadrilateral/brick elements. Ng et al. (1997) [134] compared the performance of three interface elements implemented in the finite element code CRISP. To test the ability of the interface element in simulating gapping, they upgraded one of them, and performed 2D simulations of lateral pipe loading in an elastic perfectly plastic soil. Using a three node contact element implemented in ABAQUS/Standard, Yin et al. (1993) [225] conducted a similar plane strain analysis that involved large relative displacements and gapping.

Popescu et al. (1999) [166], Nobahar et al. (2000) [141], Popescu and Konuk (2001) [167], and Popescu et al. (2002) [169] used the contact surface approach implemented in ABAQUS/Standard. It allowed for separation and sliding of finite amplitude and arbitrary relative rotation of the contact surfaces, and included an equivalent shear stress limit.

2.3.3.3. *Soil constitutive models*

Numerous constitutive models have been proposed for simulating the soil surrounding a buried pipeline. Some authors assumed linear behaviour, modelling the soil either with elastic springs (Zhou and Harvey, 1996 [233]; Karadeniz, 1997 [99]; Zhuang and O'Donoghue, 1998 [235], among others), or as an elastic continuum (e.g. Tohda et al., 1994 [204]; Fernando and Carter, 1998 [68]). However, the linear elastic assumption is only applicable to situations involving a relatively low strain level, such as compressor-induced vibrations, or moderate vertical loads on the backfill. The next step was to assume elastic perfectly plastic behaviour of the soil materials. Workman (1992) [221], Yin et al (1993) [225], Popescu and Konuk (2001) [167], and Guo and Popescu (2002) [80] simplified the soil as an elastic-plastic continuum. Several other studies have also used nonlinear hyperbolic soil models (e.g. Javanmard and Valsangkar, 1998 [97]).

However, to correctly simulate the pipe-soil interaction in problems involving large deformations, there must be an appropriate soil model that can reproduce both strain hardening and softening. Also, in the case of saturated soil materials, coupled field equations capabilities are required to reproduce pore water pressure build-up and suction phenomena induced by pipe movements through soil. The following are examples of such finite element analyses. Altaee and Boivin (1995) [8] and Altaee et al. (1996) [9] conducted 2D plane strain analyses of pipes moved laterally through soil. They investigated the performance of various nonlinear soil constitutive models implemented in CRISP and AGAC. Cam-Clay models were deemed to provide satisfactory results for normally consolidated and slightly overconsolidated clays. A boundary surface soil constitutive

model was recommended for overconsolidated clays. In those analyses, no special consideration was given to the soil-pipe interface.

Yang and Poorooshasb (1997) [223] studied the effects of ice scour on buried pipelines. Using the Drucker-Prager soil model implemented in ABAQUS/Standard, they carried out 3D finite element analyses to investigate the effects of ice scour on pipelines buried in a sandy seabed. The pipeline was modelled as an elastic beam, and no slip was allowed at the interface.

Extensive experimental and numerical research on interaction between soil and buried pipes subjected to very large relative deformations (e.g. Popescu et al. 1999 [166]; Nobahar et al., 2000 [141]; Nobahar and Popescu, 2001b [139]) indicated that: (1) a modified Cam-Clay model with isotropic hardening was adequate for analysing pipes loaded in clay under drained conditions, and (2) a non-associated Mohr-Coulomb model with isotropic hardening/softening provided good results for pipes loaded in sand. A contact surface approach, allowing for separation and sliding of finite amplitude and arbitrary relative rotation of the contact surfaces was used. It was mentioned, however, that kinematic hardening is needed for capturing hysteretic effects in saturated soils subjected to cyclic loading.

2.3.3.4. *Numerical results*

Rowe and Davis (1982a) [179] conducted an elasto-plastic finite element analysis of vertical anchor plates subjected to lateral loading in cohesive soil. The anchor under plane-strain conditions was thin and rigid, with a height of D and a depth of h (embedment depth). The effects of embedment depth, overburden pressure, breakaway conditions,

anchor roughness, thickness and shape were investigated. In the case of “immediate breakaway”, the back of the anchor separated from the surrounding soil. However, for the “no breakaway” condition, the back of the anchor remained in contact with the soil. The failure of a shallow anchor was characterized by plastic flow to the soil surface, while the failure of a deep anchor was characterized by local failure. The resistance of soil increased with depth up to a critical depth ratio (h/D). If the depth ratio was further increased, the anchor capacity did not change very much with depth. This critical depth ratio was about 3 for horizontally loaded anchors in both “immediate breakaway” and “no breakaway” conditions. Furthermore, the value of N_c was greatly influenced by breakaway conditions. For example, for depth ratios of 1, 2 and 3, the corresponding values of N_c were approximately 2, 4 and 5 for “immediate breakaway” and about 4, 9.5 and 11.5 for “no breakaway”. The results were found to be comparable with small-scale anchor tests conducted by Mackenzie (1955) [117] and Ranjan & Aurora (1980) [175].

2.4. DESIGN APPROACHES

2.4.1. General Design Criteria

Primary objectives of engineering design are safety, serviceability, durability, and economy. This is reflected in most engineering codes by two categories of limiting criteria: 1) ultimate limit states (ULS), and 2) serviceability limit states (SLS) – e.g. AASHTO (1992) [1], CSA (1992) [41], CGS (1992) [25], ENV (1994) [59], NRC (1995) [142], Z662 (1999) [228], and DNV (2000) [53]. An appropriate engineering design should satisfy both criteria considering the overall economy in design. Engineering systems as well as other

physical systems always deal with uncertainties and, therefore satisfying these two engineering limiting criteria requires certain tools to measure and quantify the degree of uncertainty. Eurocode 1 “Basis of Design” (ENV, 1999 [60]) states that the structural reliability against one or more potential risks must take into account the structural failure probabilities as well as the probabilities that these failures lead to prejudicial consequences.

These engineering uncertainties are generally caused by uncertainties in measuring parameters, uncertainties in loads or actions, and model uncertainties. Natural variability of parameters also contributes to uncertainty, both directly by increasing response variability and indirectly, by affecting the failure mechanism. Many physical, biological, and social systems exhibit complex patterns of variation in space and time. In many cases, the consequences of this spatial variability have not yet been well understood. In addition, deterministic approaches may not be able to appropriately describe the true physical behaviour due to the large number of parameters involved.

Engineering codes demand safe design and the application of safety factors. There are many design approaches in engineering. However, it is possible to divide them into two main categories: 1) conventional method of overall safety factor (FOS), and 2) limit state design method (LSD). More recently, advanced methods based on reliability theory have also been recommended in engineering codes. In these methods, the probability of failure is limited to a sufficiently low level. The goal is to achieve an appropriate safety level. An appropriate safety level should be selected taking into account the consequences of failure. Therefore, it is possible to define the desired reliability level by comparing the probable damage costs with the extra expenses demanded by a higher degree of reliability. This can

be done through a risk analysis, though still there are many difficulties associated with such calculations. Becker (1996a) [15] stated that design should be based on a probability of failure that is comparable to risks that people (i.e. society) are willing to accept in specific situations or from natural and man-made work. Figure 2.16 summarizes observed risks associated with both natural events and engineering projects.

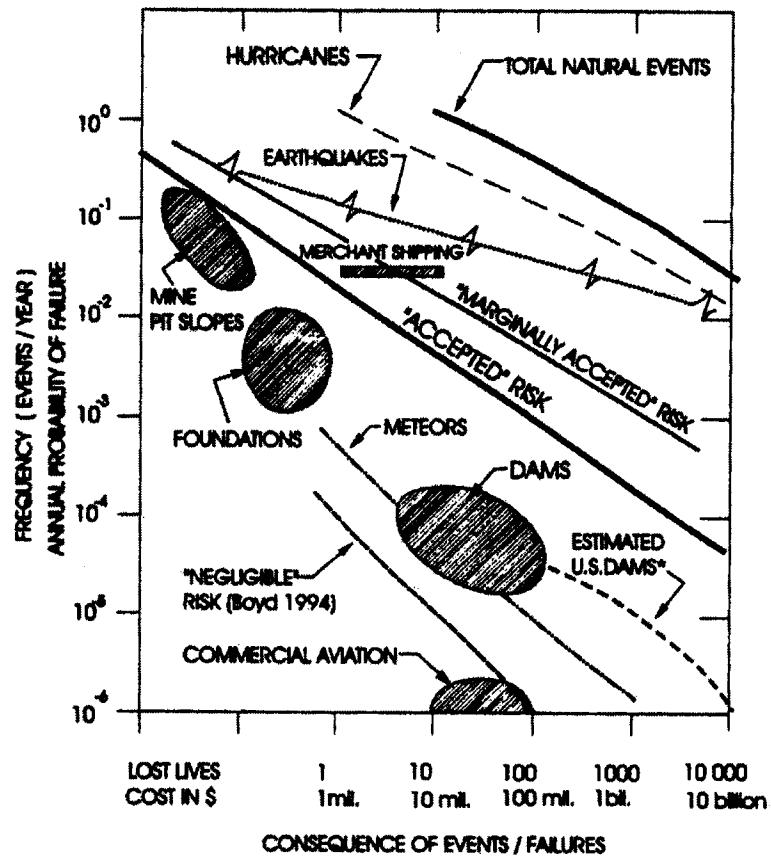


Figure 2.16 Risks for selected natural events and engineering projects designed in keeping with current practice (after Whitman, 1984 [218]; Boyd 1994 [18]).

Design codes usually reflect this concept by using safety class methodology. For example, in Canadian Standard Association (CSA, 1992 [41]), three safety levels are defined: 1) safety class I, where there is a great risk to life or high potential for

environmental pollution or damage, 2) safety class II, where there is small risk to life and low potential for environmental pollution or damage, and 3) serviceability. For these classes, reliability levels of 10^{-5} , 10^{-3} and 10^{-1} respectively are required.

2.4.2. Conventional Methods

Using a conventional method, engineers apply a factor of overall safety (FOS) to secure the desired safety level. This is similar to the concept of allowable stress (or working stress design, WSD), in which engineers estimate the expected stress in the structure and compare it with an allowable stress, often defined as a portion of ultimate or yield stress. All the uncertainties involved in the design process are addressed by means of a single global safety factor. FOS and WSD have been the traditional design basis in civil engineering since they were first introduced in the early 1800's (Becker, 1996a) [15]. The values of the global factor of safety selected for design reflect past experience and consequence of failure. A more serious consequence of failure and/or a higher uncertainty require a higher factor of safety. Some values of global factors of safety used in geotechnical engineering, as suggested by Terzaghi and Peck (1948, 1967) [199&200] and Terzaghi et al. (1996) [201] are shown in Table 2.1.

A global factor of safety represents a relationship between allowable and applied quantities. It can be written as,

$$FS = \frac{R}{S} \qquad \text{Eq. 2.9}$$

where R and S are resistance and actions (loads). A single global safety factor would have unambiguous meaning if carefully prescribed standard procedures for estimating resistance and load were always used in design. However, in geotechnical engineering, engineers use different approaches and select different values of strength for design. Some engineers may use mean value for strength, while others may use a conservative assessment of strength based on their own experience. Still, others may use statistics and use a certain percentile of resistance. Therefore, for the same factor of safety value, the actual reliability of the same structure would be different (see Becker, 1996a&b [15&16] for more discussion). Moreover, various components of the “resistance” or of the “load” may have various degrees of uncertainty.

It is possible to define two formats for the global safety factor. The mean factor of safety using mean resistance and loads,

$$\overline{FS} = \frac{\overline{R}}{\overline{S}} \quad \text{Eq. 2.10}$$

And nominal factor of safety using nominal (characteristic) resistance and nominal (specified) load values in design,

$$FS = \frac{R_n}{S_n} \quad \text{Eq. 2.11}$$

This is demonstrated graphically in Figure 2.17 (from Becker, 1996a [15]). Nominal (characteristic) resistance is defined in next section.

Table 2.1 Ranges of global factor of safety commonly used for geotechnical engineering (Terzaghi and Peck, 1948, 1967; Terzaghi et al., 1996)

Failure type	Item	Factor of safety, FS
Shearing	Earthworks	1.3-1.5
	Earth retaining structures, excavations	1.5-2
	Foundations	2-3
Seepage	Uplift heave	1.5-2
	Exit gradient, piping	2-3
Ultimate pile loads	Load tests	1.5-2.0
	Dynamic formulae	3

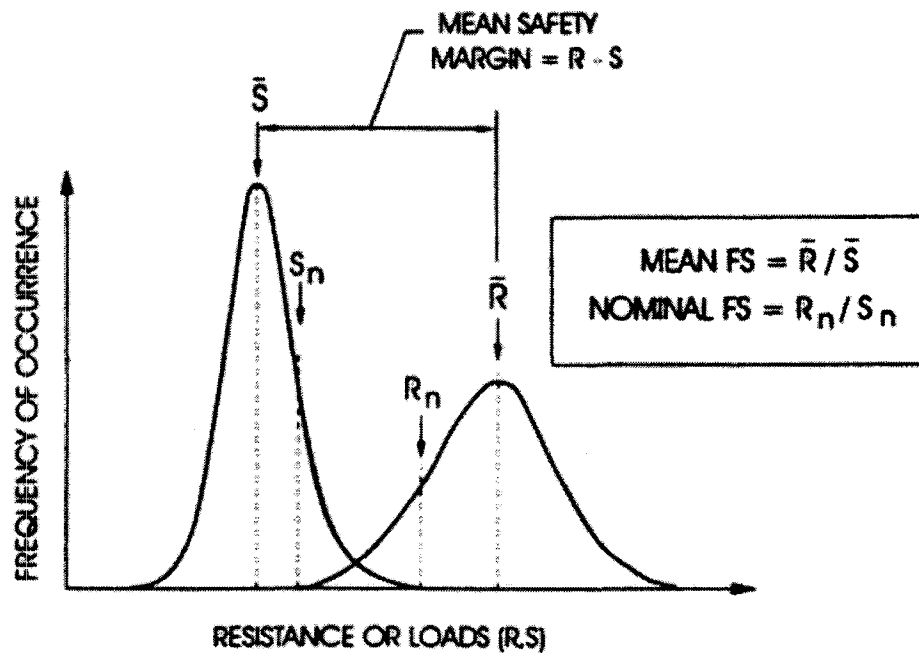


Figure 2.17 Design values for loads and resistance (after Becker, 1996a [15]).

2.4.2.1. Characteristic (nominal) values

Usage of conservative values instead of mean strength is common in many engineering fields. These conservative values are so-called nominal, specified, or characteristic values in structural engineering. The characteristic values have significant importance in ensuring a uniform safety level in engineering design because they reflect not only mean resistance values, but also the variability of resistance (See Li et al., 1993 [108] and Cardoso and Fernandes, 2001 [24] for discussion of nominal values in geotechnical design).

It is very important to have a unified definition for characteristic values (see Becker, 1996a [15]; Cardoso and Fernandes, 2001 [24]). Attempts have been made to unify the definition of these values. Structural codes have prescribed procedures to define these values. The characteristic values are also related to statistical indices. Most structural codes use 95-percentile as characteristic values (95-percentile is a value of resistance with 95% reliability). In other words, it is a value derived such that the calculated probability of a worse value governing the occurrence of limit state is not greater than 5%.

2.4.2.2. Limitations of the conventional method

The main shortcoming of this method is illustrated in Figure 2.18. In all three plots, the factor of safety has the same value. However, there is a very low probability of failure for Case 1. Case 2 is a common case in foundation engineering, where structural loads applied on foundations are well estimated and involve small amounts of uncertainty, but foundation resistance involves much higher uncertainty. The third case involves load and

resistance, both of which are quite uncertain. Examples of Case 3 are earthquake loading and bearing capacity of piles. Although the factor of safety is the same for all three cases, the probability of failure increases from case one to case three. The overlapping area, which is shaded, is related to the probability of failure. Hence, it is obvious that an overall safety factor cannot guarantee a uniform safety level. Conventional methods are deterministic by nature and the probability of failure cannot be directly inferred from them. As aforementioned, all uncertainty is dealt with by one lumped factor of safety; there is no distinction between different sources of uncertainty and their magnitude.

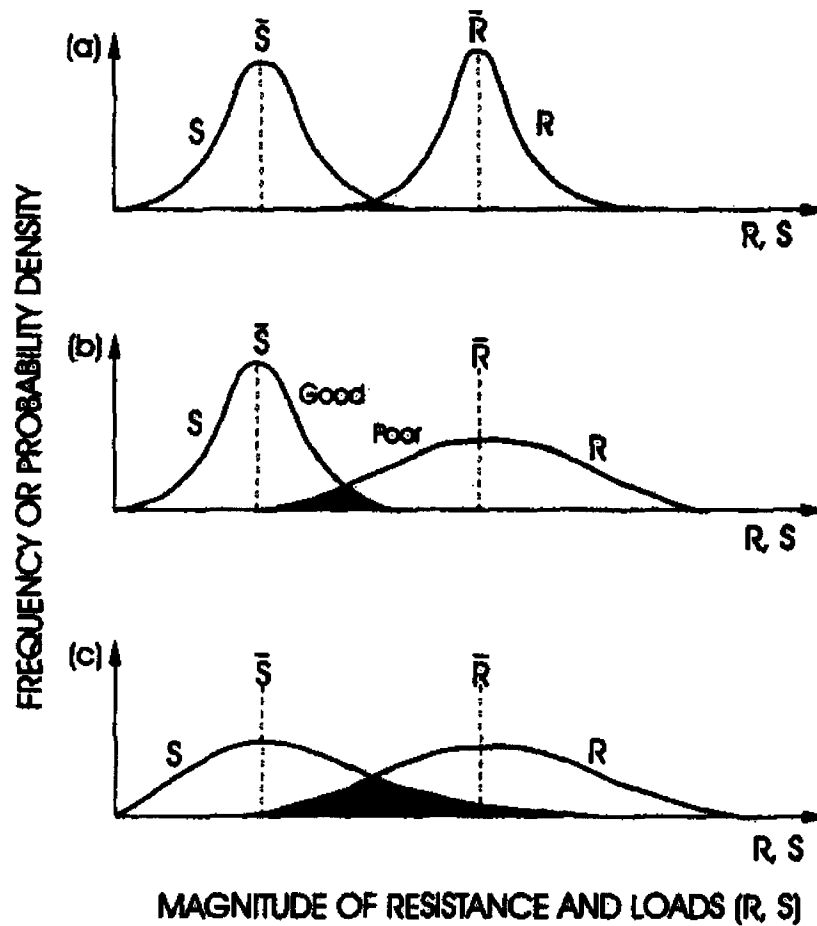


Figure 2.18 Possible load and resistance distributions (after Green, 1989 [72]): (a) very good control of R and S ; (b) mixed control of R and S ; (c) poor control of R and S .

2.4.3. Limit State Design Method

Overall safety factor (conventional method) does not seem appropriate in all cases due to variability in the nature of engineering problems. It may lead to over-designed structures in some cases or it may fail to achieve the desired reliability level in others. Therefore, in recent decades and in conjunction with other engineering and scientific advancements, there has been a trend towards the use of reliability concepts in design (e.g.

Duncan, 2000 [54]). Limit state design (LSD) method was introduced to engineering practice as a simple method to overcome some of the problems in conventional approaches, and to introduce reliability bases for design. LSD method provides a more logical framework to deal with uncertainties in engineering design. Thus, it is expected to provide a more uniform design reliability level due to its use of different load and resistance factors (Meyerhof, 1982 [125]).

Limit states are defined as conditions under which a structure or its component members no longer perform their intended functions. Limit state design (LSD) is a formal way of stating the design criteria in a performance-based way. As previously mentioned, two classes of limit states are normally considered: (1) ultimate limit states (ULS) and, (2) serviceability limit states (SLS).

There are two main approaches in LSD methods: the factored strength and the factored resistance. The format for the first LSD method, the factored strength, is as follows (e.g. Becker, 1996a [15] and Baikie, 1998 [12]):

$$R_{Nf} > \sum \alpha_N S_N \quad \text{Eq. 2.12}$$

where R_{Nf} is the resistance obtained using factored strength parameters (The factored strength parameters are obtained by applying strength reduction factors on nominal strength parameters) and S_N are the nominal loads, dead load, and live load; α_N are the load factors for the corresponding loads.

The format for the second LSD method, the factored resistance, is (e.g. Becker, 1996a [16] and Baikie, 1998 [12]):

$$\phi R_N > \sum \alpha_N S_N \quad \text{Eq. 2.13}$$

where ϕ is a resistance factor and R_N is the nominal resistance calculated using characteristic soil parameters. This study focuses on undrained shear strength of soil. The bearing capacity of a foundation or the lateral load on a buried pipeline is directly related to undrained shear strength (e.g. $q_u = N_c c_u$); therefore, there would be no practical difference between using the factored strength and the factored resistance here.

The following are advantages of the LSD concept in geotechnical engineering (Meyerhof, 1982 [125]):

- Facilitates a greater degree of compatibility between the geotechnical and structural design, which are now codified in Canada and in many other countries based on LSD.
- Sets up a rational way to obtain safety factors.
- Obtains a consistent approach leading to a more uniform margin of safety for different types and components of earth structures and foundations under different loading conditions.

The importance of the first and second points is obvious. The second and third points also have a significant value. The factoring of separate sources of uncertainties, particularly if derived from statistical data reflecting the probability of their occurrences, is a qualitatively more accurate concept. However, the application of LSD method in geotechnical engineering has faced critical problems. For instance, Been et al. (1993) [17], Lin (1996) [111] and Nobahar (1999 & 2000) [135&136] investigated the problem of

dependence between loads and resistance in foundations. Li et al. (1993) [108] showed that the constant partial factor LSD methods, commonly used in structural codes, are not suitable for geotechnical design owing to the wide range of uncertainty involved. Based on probabilistic analysis, they advised on use of a lumped, variable partial factor for resistance. This factor varies as a function of uncertainty involved in geotechnical design – i.e. a larger reduction in resistance for a higher uncertainty. Day (2001) [42] demonstrated a more noticeable lack of physical interpretation for LSD methods in geotechnical engineering compared to structural engineering. Due to the complex behaviour of soil, strength or resistance reduction factors have often been obtained by direct calibration from available conventional design methods (Meyerhof, 1984 & 1995 [126&128]; Baikie, 1998 [12]). They are not based on strong theoretical or systematic experimental studies aimed at securing a uniform target reliability level. Therefore, there is a need to establish strong theoretical and experimental bases to obtain strength or resistance design factors.

Becker (1996b) [16] proposed the following methodology for deriving resistance factors corresponding to a given set of load factors based on a calibration methodology using reliability theory:

1. Estimate the level of safety or reliability inherent in current design methods.
2. Select a target reliability index based on the level of safety or probability of failure used in current designs.
3. Calculate resistance factors consistent with the selected target reliability index. It is also important to couple experience and judgment with the

calibration results in the final decision process of selecting appropriate values of resistance factors for various design situation or problems.

4. Validate or verify the new design approach by comparing actual designs based on the resistance factors resulting from the calibration, with designs obtained from current (conventional) approach.
5. Recalibrate and modify resistance factors as required.

Some partial design factors used in design codes are summarized in Table 2.2 (see Meyerhof, 1982, 1984, 1993&1995 [125, 126, 127&128]; Baikie, 1998 [12]).

Table 2.2 Values of partial factors (after Meyerhof, 1995 [128])

	Hansen (1953) [84]	Hansen (1956) [85]	Denmark DS 415 (DI, 1965 [52])	Eurocode 7 (ENV, 1993 [58])	Canada CGS (1992) [25]	Canada NBCC (NRC, 1995 [142])	U.S.A. ANSI A58 (ANSI, 1980 [4])
LOADS							
Dead loads, soil weight	1.0	1.0	1.0	1.1	1.25	1.25	1.2-1.4
Live loads	1.5	1.5	1.5	1.5	1.5	1.5	0.5-1.6
Water pressure	1.0	1.0	1.0	1.0	1.25	1.25	
Accidental loads		1.0	1.0	1.0			
Shear strength							
Friction ($\tan \phi$)	1.25	1.2	1.25	1.25	1.25	Resistance factor of 1.25-2.0 on ultimate resistance using unfactored strength	Resistance factor of 1.25-2.0 on ultimate resistance using unfactored strength
Cohesion (c) Slope, earth pressures	1.5	1.5	1.5	1.4-1.6	1.5		
Cohesion (c), Spread foundations		1.7	1.75	1.4-1.6	2.0		
Piles		2.0	2.0	1.4-1.6	2.0		
Ultimate pile capacities							
Load tests		1.6	1.6	1.7-2.4	1.6-2.0	1.6	
Dynamic formulas		2.0	2.0		2.0	2.0	
Penetration tests					2.0-3.	2.5	
Deformations*							
		1.0	1.0	1.0	1.0	1.0	1.0

* For deformations (serviceability criteria), engineering codes often apply a partial factor of unity.

2.4.4. Reliability and Probabilistic Design

Reliability and probabilistic design methods have attracted increasingly more interest in recent years (e.g. Harr, 1987 [89]; Phoon et al., 1990 [157] & 2000 [156]; Li and Lo, 1993 [109]; Tang, 1993 [197]; Christian et al., 1994 [33] etc.). In reliability-based design, the parameters are treated as random variables rather than as constant deterministic values. The measure of safety is the probability of failure, which can be computed directly if the actual probability density function or frequency distribution curves are known or measured for the loads and resistance. The probability of failure is related to the shaded area representing the overlap between load and resistance curves as shown in Figure 2.19. In a formal format, it is possible to define a performance function,

$$g(X) = R - S \quad \text{Eq. 2.14}$$

And the probability of failure is,

$$p(g(X) < 0) \quad \text{Eq. 2.15}$$

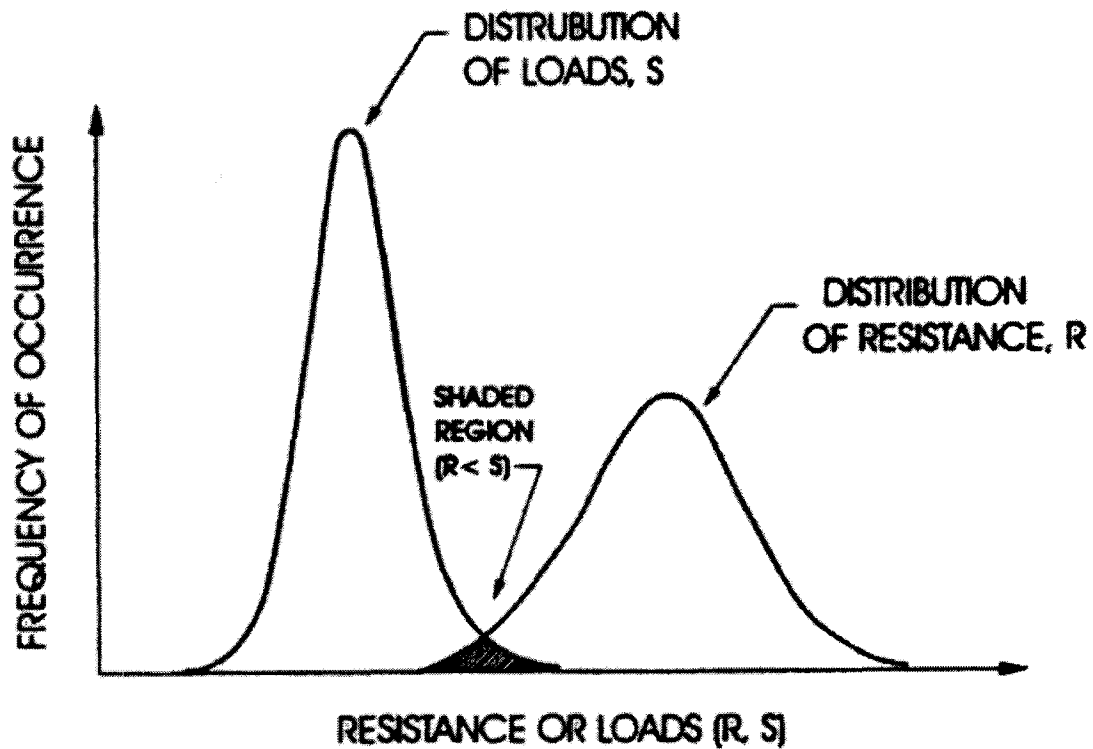


Figure 2.19 Typical variation of load and resistance for reliability analysis.

Conventional structural reliability methods are usually concerned with probabilities that every specified limit state will not be reached during the design life of a structure. However, they do not account for failures caused by human errors or other gross errors.

Reliability based design has important potential advantages, such as being more realistic, rational, consistent, and widely applicable. It is capable of systematically analysing the uncertainties associated with each design parameter. However, statistical data are needed for each parameter, and sufficient data are often scarce. Palmer (1996) [147] examined the applicability of reliability theory in offshore pipeline design. He showed how exact values of reliability and failure probability cannot be determined because of the lack of complete understanding and lack of data. Data pertaining to the tail of probability

distributions are not reliable due to too small samples. This is a well-known reality in reliability analysis. Melchers (1992) [121] stated that the tail sensitivity problem is merely a reflection of the various uncertainties, which arise in quantifying the variables to be considered in reliability analysis. However, Melchers suggested considering the failure probability as a “formal” measure of structural reliability. In this way “failure probability” is not a quantitatively actual value, but demonstrates the level of reliability.

Alternatively, a reliability index can be used. The reliability index shows the distance between load and resistance in terms of their standard deviations. It can be related to failure probability by assuming probability distributions for load and resistance.

Thoft-Christian and Baker (1982) [202] discussed different application levels for structural reliability and categorized them into the following levels:

- Level I design method, in which appropriate degrees of structural reliability are provided on a structural element basis by use of a number of partial safety factors or partial coefficients, is related to pre-defined characteristic or nominal values of the major structural and loading variables. This is merely a reliability analysis; it is the same as limit state design (discussed in Section 2.4.3).
- Level II methods or approximate probabilistic methods involve approximation of distribution curves of load and resistance. Usually the actual probability distributions of random variables are not available, but their shapes and types are assumed. Typically normal or lognormal distributions are used in this type of analysis.

- Level III reliability method is also known as the fully probabilistic method. In this category, the actual probability distribution curves are already known or are measured for each random variable. Theoretically, this is the most complete treatment of safety. The main problem associated with Level III is lack of complete statistical data. Statistical data analysis and full probabilistic calculations are also time-consuming and complicated.

An example of level II reliability method is the second moment probabilistic method, in which the random nature of the variables is defined using only the mean and the coefficient of variation. In this method, safety is defined by the reliability index (Allen, 1975 [3]; CSA, 1981 [40]; Harr, 1987 [89]; Li et al., 1993 [108]). The reliability index provides a simple quantitative basis for assessing risk/failure probability and/or comparing the relative safety of various design alternatives. The reliability index can be obtained simply and avoids many difficulties inherent in applying complete statistical analysis. It can also be connected with failure probability by assuming probability distributions for random variables.

Duncan (2000) [54] presented simple reliability analyses, which do not involve complex theory or unfamiliar terms, and can be easily used in practice. Duncan showed how simple reliability analyses can provide means of evaluating the combined effects of uncertainty in parameters involved in the calculations. The presented reliability analyses calculated uncertainty in safety factor; therefore, they can be easily used together with factor of safety method as complementary of acceptable design. Duncan showed how additional parameters needed for reliability analyses (e.g. standard deviation of parameters)

can be evaluated using the same amount of data and types of correlation that are widely used in geotechnical engineering practice.

As discussed in Section 2.4.1 design methods have changed to account for reliability concepts during the past few decades. There is a trend to provide reliability/risk bases for engineering design. It should be emphasised that the design methods always should be calibrated and validated based on past experience and conventional approaches.

2.4.4.1. Application of response surface method

Performance (failure) functions (Eq. 2.14) are often either complex or cannot be explicitly expressed. For many problems, the only practical reliability solution is the use of Monte Carlo simulations. A Monte Carlo approach needs a large number of replications, which have considerable computational costs. One solution is to approximate the complex response over the region of interest with simple functions (e.g. Cox and Baybutt, 1981 [38], Kim and Na, 1997 [101]; Tadjiria et al., 2000 [195]; Mohamed et al., 2001 [129]). These simple explicit functions can be used as a replacement model in reliability analysis. Han and Wen (1997a&b) [82&83] describe response surface as a method of approximating an unknown function of multiple variables (response surface in n-dimensional space) by a polynomial that facilitates solution procedures such as in finding the minimum values of the function.

Bauer and Pula (2000) [14] used a mathematically simple function to approximate foundation settlements for reliability analysis using the FORM (first-order reliability method) and the SORM (second order reliability method). First, they approximated the response (foundation settlement) on a large interval (two standard deviations) of random

variable (here Young's modulus and Poisson's ratio). Then they reduced the interval in the proximity of the design points. This increases the accuracy of FORM and SORM, since most contribution to failure probability comes from the vicinity of design points.

It is concluded that Response Surface Method (RSM) is a useful tool to study and approximate complex behaviours in the region of interest. A statistical design is required to minimize the number of points for surface fitting. This technique was used in this study and its application is discussed in Section 3.3.

CHAPTER 3

METHODOLOGY

3.1. INTRODUCTION

Rapid advances in computers have made numerical methods, such as finite element and finite difference analyses, the state of practice in many civil engineering fields. Recently, probabilistic methods have become more common in many areas, partly due to decreases in their numerical costs, as well as more demands for risk analysis from industry. There are several methods available for solving problems in continuum mechanics involving uncertain quantities described by stochastic processes or fields. However, Monte Carlo methodology is the only universal approach for engineering problems involving material and geometrical nonlinearity, such as those encountered in soil mechanics. As discussed in Section 2.1, this approach was found to be the only practical method for highly nonlinear problems in geotechnical engineering involving soil heterogeneity. The main drawback of Monte Carlo simulation methodology using finite element method to analyse the effects of soil spatial variability on soil-structure interaction is its computational cost. However, recent advances in computer technology have alleviated this problem.

The methodology illustrated in Figure 3.1 combined deterministic analyses with Monte Carlo simulations. It was not intended to study geostatistical data from a specific

site. This research evaluated the effects of stochastic variability of soil properties on bearing capacity through a series of parametric studies. Thus, the results of the study can be used to evaluate the effects of soil heterogeneity for every site having soil heterogeneity parameters within the studied ranges. These effects can be incorporated in engineering design. Design methods are based on many years of engineering practice and this research can be only regarded as a more accurate study of various sources of uncertainty. This could lead to a better understanding and identification of uncertainty sources, as well as improvement and optimisation in design.

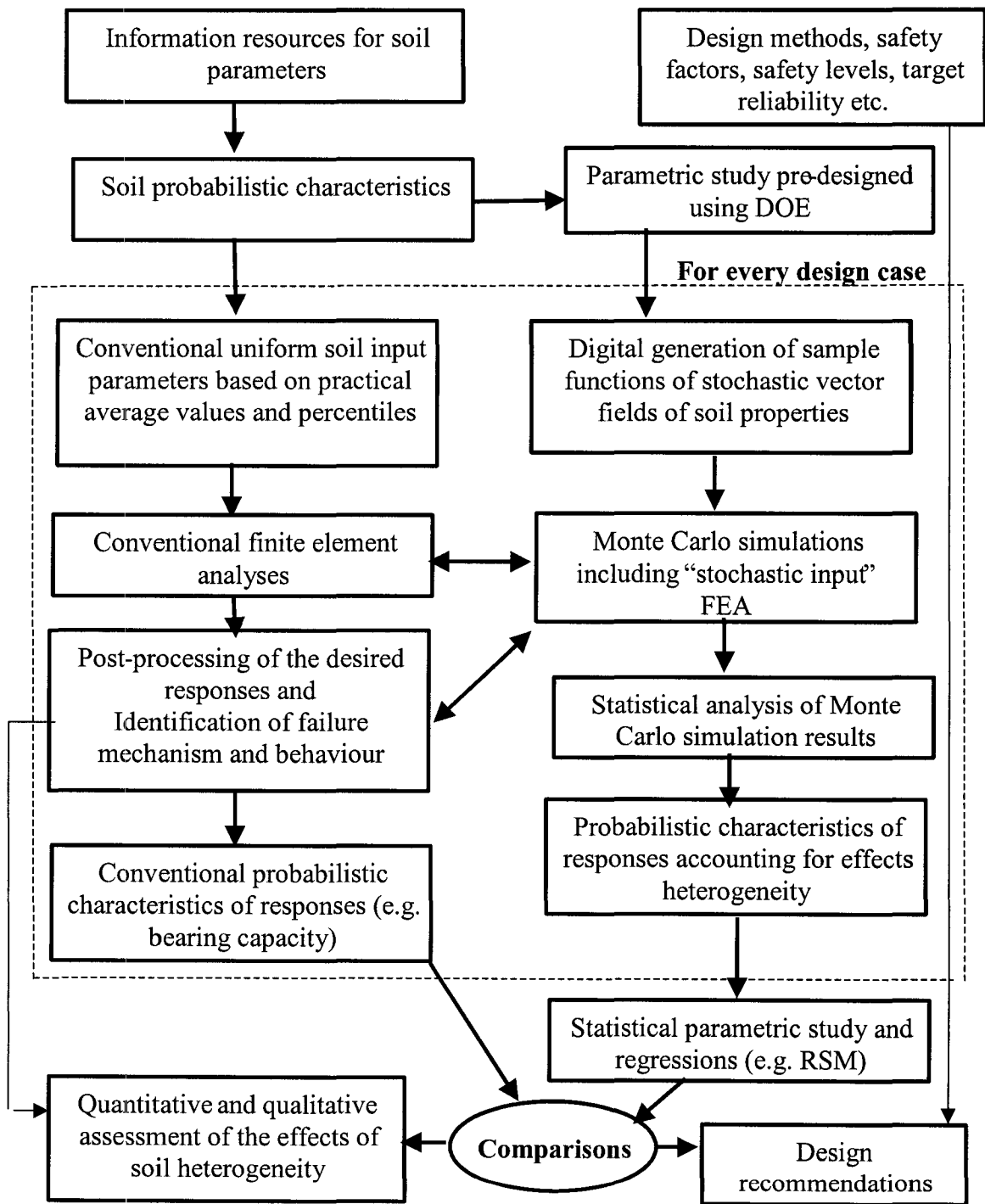


Figure 3.1 Illustration of the applied methodology.

3.1.1. Elements of Proposed Methodology

The methodology used in this research had the following elements, as shown in Figure 3.1,

- Design of parametric studies for Monte Carlo simulations (Section 3.3).
- Digital generation of sample functions of a non-Gaussian stochastic field. Each sample function represented a possible realization of the relevant soil properties (here, the soil property was the undrained shear strength) over the domain of interest. Generation of random samples is the most important part of Monte Carlo simulations (Section 3.4)
- Nonlinear finite element model (or more generally, numerical model) of the soil and structure accounting for their interaction. The numerical model is capable of analysing the system using stochastic input parameters (Section 3.5).
- Automation of the Monte Carlo simulation procedure and finite element analysis using stochastic input functions (Section 3.5.4 & Appendix B).
- Analysis and processing of the results of Monte Carlo simulations for each case of parametric study, including post processing of the finite element results, statistical analysis of the responses, and comparison with corresponding deterministic analysis (see Appendix B).
- Statistical analysis and regression of parametric study results (Section 3.3).
- Processing of results by various reliability and probabilistic analysis methods, for providing practical design recommendations (Section 3.6).

Each of the above items is described in the following sections.

3.1.2. Monte Carlo Simulations

Monte Carlo simulations were performed for each set of probabilistic characteristics for parametric studies; the parametric studies were designed using statistical approaches (design of experiments, DOE). The Monte Carlo simulation method used here accounted for the effects of the stochastic spatial variability of soil properties on the system performance. The ensemble of soil properties over the domain of interest was modelled as a bi-dimensional, non-Gaussian stochastic field. The Monte Carlo procedure has three steps (see Popescu, 1995 [158]):

1. Obtain the probabilistic characteristic of the spatial variability of soil properties. Here these values were determined from design of parametric study.
2. Digitally generate sample functions of a non-Gaussian stochastic field, with each sample function representing a possible realization of the relevant soil properties (here the undrained shear strength values) over the domain of interest (step 2 in Section 3.1.1).
3. Nonlinear finite element analyses using stochastic input parameters obtained from the generated sample functions of soil strength (part of step 3 in Section 3.1.1).

The simulation methodology in step 2 (Popescu, 1995 [158]; Popescu et al., 1998b [164]) is based on the spectral representation method as discussed in Section 3.4. It

combines the work by Yamazaki and Shinozuka (1988) [222], Shinozuka and Deodatis (1996) [186], and Deodatis (1996) [47], and extends it to the simulation of multivariate, multidimensional non-Gaussian stochastic fields. Bi-dimensional, non-Gaussian stochastic fields were generated as documented in Section 3.4 to represent the variability of soil undrained shear strength. “SINOGA”, a Fortran program written by Popescu (1995) was used for this purpose. In step 3, the undrained shear strength determined from step 2 at each spatial location (finite element centroid) is employed for stochastic input finite element analyses for each sample function.

2D plane strain total stress analyses were performed for each sample function using the ABAQUS/Standard code (Hibbitt et al. 1998a) [93]. A series of issues were addressed in this study, including: (1) data transfer from the discretization used for stochastic field generation to the finite element mesh was carried out using the mid-point method (Benner 1991) [19] to preserve the prescribed (non-Gaussian) probability distribution function; (2) an appropriate size of the finite element mesh was used to capture the essential features of the correlation structure; (3) the soil Young’s modulus (E) was assumed perfectly correlated with the shear strength, and the Poisson’s ratio (ν) was assumed constant over the analysis domain (see Sections 3.5 & 3.5.4 for details).

3.2. SELECTION OF PROBABILISTIC CHARACTERISTICS FOR SOIL VARIABILITY

As shown in Figure 3.1, the first task was to determine ranges for probabilistic characteristics of soil properties based on available sources of information. These

probabilistic characteristics included degree of variability, probability distribution of soil strength and correlation structure.

Based on the literature review presented in Section 2.1.1.3, the coefficient of variation of undrained shear strength can take values as high as $C_V = 60\%$ (and sometimes even higher) for clay materials (Meyerhof, 1995 [128]; Phoon and Kulhawy, 1996 [153] and 1999b [155]; Duncan, 2001 [54]; also see Section 2.1). Some scatter is caused by measurement errors, as discussed in Section 2.1.1. In the case of cone penetration tests, the scatter in results produced by measurement errors is $C_V = 5\%$ to 15% for electrical cones, $C_V = 15\%$ to 25% for mechanical cones, and $C_V = 15\%$ to 45% for standard penetration tests (Orchant et al., 1988 [144]; Kulhawy and Trautmann 1996 [103]). Also discussed in the literature review (Section 2.1.1.3), C_V of undrained shear strength decreases with increases in mean undrained shear strength. Therefore, a range of $C_V = 10\%$ to 40% was assumed for undrained shear strength of medium to stiff clay and $C_V = 20\%$ to 80% was assumed for soft clay.

Based on numerous studies reported in the literature, it can be concluded that each soil property can follow different probability distributions for different materials and sites, but for physical reasons, they are non-Gaussian distributed (see also Section 2.1.1.3). Beta, Gamma and Lognormal are common distribution models meeting this requirement. For given mean and standard deviation of the field data, Gamma and Lognormal models are one-parameter distributions – lognormal can be shifted to have a minimum value (three-parameter or shifted lognormal distribution). They are both skewed to the right. Beta is a

two-parameter distribution, and therefore more flexible in fitting empirical data. Moreover, it can model data that are symmetrically distributed, or skewed to the left.

To assess the effects of the probability distribution of soil strength, a symmetrical Beta probability distribution function with shape parameters $p = q = 2.5$, and a skewed Gamma probability distribution with shape parameter, $\lambda = 1.73$ were selected to describe the variability of undrained shear strength in this study. These two distributions were deemed to cover the field situation in terms of the extension of the left tail, which represents the presence of loose pockets in the soil mass. The selected probability density functions are shown in Figure 3.2.

An important feature of stochastic fields is the concept of statistical correlation between field values at different locations in space. In this study, an exponentially decaying model, discussed by Shinozuka and Deodatis (1988) [184] among others, was selected for the auto-correlation function (see also Section 2.1.1). This model was found to describe relatively well the correlation structure recorded in various soil deposits (Popescu, 1995 [158]). The main parameter of the auto-correlation function is called scale of fluctuation (or correlation distance). It represents a length over which significant coherence is still manifested. The mechanisms of soil deposit formation lead to different spatial variability characteristics in vertical direction (normal to soil strata) compared to those in horizontal direction. Therefore, a separable correlation structure based on the exponentially decaying model is deemed to capture the main characteristics of soil spatial variability (see Section 2.1.1 for discussion). Due to the effects of geological layer deposition, soil properties have significantly different correlation distances in horizontal and vertical directions. Often

correlation distances in the horizontal direction are one order of magnitude larger than the correlation distances in the vertical direction. As discussed in Section 2.1.1, wide ranges are reported for horizontal and vertical correlation distances and many factors affect the estimation of these values. A literature review showed that vertical correlation distances are in the order of a 0.5m to 2m while horizontal correlation distances can take values in the order of tens of meters.

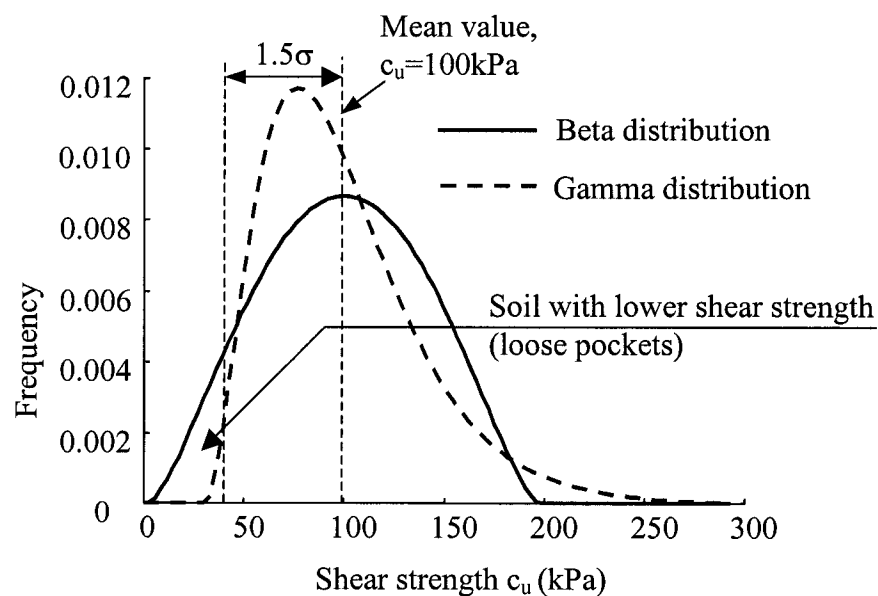


Figure 3.2 Probability density functions of the Beta and Gamma distributions assumed for shear strength, with mean of 100 kPa and coefficient of variation $C_V = 40\%$.

3.3. DESIGN OF EXPERIMENTS

3.3.1. Introduction

As shown in Figure 3.1, after deciding on the probabilistic characteristic parameters and their ranges, experiments were designed based on statistical principles for the

parametric study. Generally, an experiment is a test or a series of tests in which purposeful changes are made to the input variables or factors of a system so that we may observe and identify the reasons for changes in the output responses (Montgomery, 1997 [130]). Experiments in this study were Monte Carlo simulations, which were performed for each set of input variables (here input variables included: coefficient of variation, probability distribution function, correlation distances and ratio of soil stiffness to soil undrained shear strength, E/c_u). A sound strategy for experimental design was required to minimize the number of experiments, screen main factors, build a mathematical model, obtain prediction equations, and capture interaction between various factors. Statistically designed experiments allowed for efficiency and economy. The use of statistical methods in examining the data results in scientific objectivity when drawing conclusions. However, use of statistical designs has remained limited in geotechnical and structural engineering.

The results obtained from these experiments were fitted by linear combinations of simple functions, with the coefficients being determined by least squares fitting. These functions are called response surfaces.

3.3.2. Design of Experiment Methods

In practice, engineers and scientists often design experiments using the best guess approach and one-factor-at-a-time (Montgomery, 1997 [130]). Though these methods may often seem rational and the easiest way to do the study, they have disadvantages. These shortcomings include (1) inability to guarantee the best solutions, (2) failure to capture interaction, and (3) requirement of a high number of experiments. Scientific methods for

design of experiments are based on statistical principles. Two of the most used methods in this area are two-level factorial and central composite designs.

3.3.2.1. *Two-level factorial design*

The factorial approach is the modern and most efficient method of experimental design. It allows factors to be varied together and has been used widely in some engineering areas. It is a very efficient method to study the effects of several factors on the output. There are different classes of factorial methods such as 2-level, 3-level and general factorial method (see Montgomery, 1997 [130]; Atkinson and Donev, 1992 [10]; Cornell, 2002 [36]). In the 2-level factorial method, the effects of k factors are studied at only two levels for each factor. A complete replicate of such a design require $2 \times 2 \times \dots \times 2 = 2^k$ tests and is called a 2^k factorial design. A fractional method can be used to reduce the number of sampling for cases where the number of the input factors is high (see Montgomery, 1997 [130] for details). A 2-level factorial design for a 3-factor problem is illustrated in Figure 3.3. It is possible to add a centre point to the 2-level factorial design as shown in Figure 3.3b.

3.3.2.2. *Central composite design*

Central composite design is another method of experiment design. It has more flexibility in capturing responses with curvature and is used for fitting second order models. It consists of a 2^k factorial runs plus $2k$ axial runs, and n_c centre runs as illustrated in Figure 3.3. Figure 3.3c shows a face centred central composite design. This allowed for more flexibility in the expansion of the analysis domain.

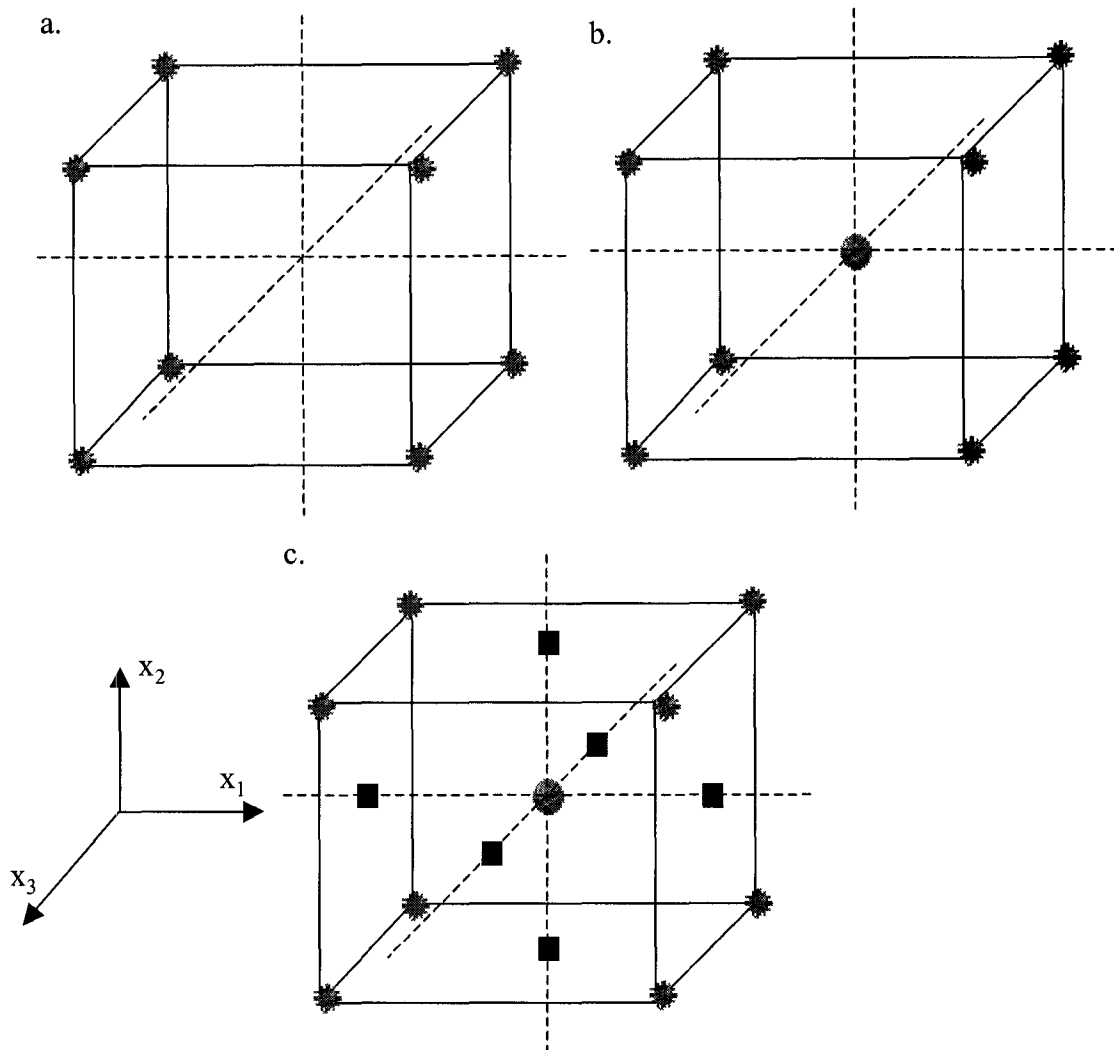


Figure 3.3 Illustration of experiment design layouts for a 3-factor problem: (a) Two-level factorial design, (b) Two level factorial design with central point, and (c) Central composite design (face-centred).

3.3.3. Response Surfaces

Many times an analytic output function does not exist for a problem. It may require a costly numerical analysis or physical testing to obtain the response for every combination of the input parameters. Thus, it is either impossible or too costly to perform a large number of experiments or numerical analyses to obtain responses for all ranges of

variables. The idea is to approximate the original complex and/or implicit function using a simple and explicit function (Kim and Na, 1997 [100]), a so-called response surface. To obtain this surface a series of experiments or numerical analyses is performed. These experiments should be designed according to a statistical experimental design, as discussed in Section 3.3.2.

The suitability of the response surface obtained relies mainly on the proper location of so-called sampling points, from which response functions are approximated using a conventional regression technique. Many algorithms have been proposed to select appropriate sampling points, which promise to yield better response function fitting. In addition, the basic function shape adapted for fitting is also known to be another major factor that influences the accuracy of the response surface method. Response surfaces suitable for design schemes discussed in section 3.3.2 are presented.

In a two-level factorial method, the fitted response is,

$$y = \beta_0 + \sum_{j=1}^k \beta_j x_j + \varepsilon \quad \text{Eq. 3.1}$$

The above equation is linear and therefore is not able to capture the curvature in the true response. The interaction terms can be added to Eq. 3.1 to give,

$$y = \beta_0 + \sum_{j=1}^k \beta_j x_j + \sum_{i < j} \beta_{ij} x_i x_j + \varepsilon \quad \text{Eq. 3.2}$$

It is possible to check the curvature of response by adding a centre point to the factorial design (Figure 3.3b). The above model is capable of capturing some curvature in

the response function. This curvature results from twisting of the response plane induced by the interaction terms, $\beta_{ij}x_i x_j$. In some cases, the curvature in response cannot be adequately modelled using Eq. 3.2. A central composite design can be used as a solution, as explained in Section 3.3.2.2. A logical model to consider is,

$$y = \beta_0 + \sum_{j=1}^k \beta_j x_j + \sum_{i < j} \beta_{ij} x_i x_j + \sum_{j=1}^k \beta_{jj} x_j^2 + \varepsilon \quad \text{Eq. 3.3}$$

In cases of higher nonlinearity, none of the above models works for the whole domain. As a solution, the domain may be divided into several regions or more points can be added to the experiment and a higher order polynomial be used for fitting (See Atkinson and Donev, 1992 [10] and Montgomery, 1997 [130] for more details). Special approaches are also developed for particular applications. For instance, Kim and Na (1997) [101] proposed a gradient projection technique to force the sampling points in the region close to the original failure surface in reliability analysis.

3.3.4. Design of Experiment Set-up

Design-Expert® software version 6.05 was used as an aid in design the experiments (points for series of Monte Carlo simulations). It is a powerful statistical tool with the following capabilities, among others,

- Two-level factorial screening studies: identify the vital factors that affect a process or product
- General factorial studies: suitable for categorical studies (categorical factors are factors that do not possess a numerical range but they can be at level A

or B – e.g. a probability distribution of shear strength can be Lognormal or Beta).

- Response surface method (RSM).

In this study, the experiment – defined as a set of Monte Carlo simulations using sample functions from a single stochastic field (see Figure 3.1) – was performed for each design point. Each design point is defined by a set of probabilistic characteristics including coefficient of variation, probability distribution and correlation distances of soil strength, c_u and ratio of E/c_u (E is soil Young's modulus). As mentioned before, the experiment consisted of performing and processing a set of Monte Carlo simulations, as illustrated in Figure 3.1 (the blocked area for every designed case). Details of the Monte Carlo procedure are described in the following sections.

Next, Design-Expert was used to fit a response surface to the results. This involved identifying significant factors and then performing an analysis of variance, ANOVA. Statistical criteria were checked to ensure the assumptions of ANOVA were met. In some cases, the experiment may also have to be redesigned or points added. Design-Expert provided equations for each response, which were in terms of simple analytical expression. The predictions from the equations were compared with the experimental data (here Monte Carlo simulations – see Figure 3.1). These equations could replace the costly Monte Carlo simulations for the range being studied.

3.4. SIMULATION OF RANDOM FIELDS

3.4.1. General

As discussed in the previous section, for every design case with a given set of probabilistic characteristics, corresponding sample functions of a stochastic field were generated for Monte Carlo simulations, as shown in Figure 3.1. This section describes the generation of these sample functions. These sample functions were used for finite element analysis in with stochastic input and discussed in Section 3.5.4.

The generation of sample functions of a random field representing possible realizations of the soil properties over the analysis domain is an important part of the Monte Carlo simulation methodology used here. In the past few decades, several methods were established to digitally generate sample functions of a random field, which may be stationary or non-stationary, homogeneous or non-homogeneous, one-dimensional or multidimensional, univariate or multivariate and Gaussian or non-Gaussian.

There are several ways to generate sample functions of Gaussian homogeneous stochastic fields, including (1) spectral representation method; (2) covariance decomposition; and (3) autoregressive moving average (ARMA) models.

The methodology described by Popescu et al. (1998b) [164] based on the spectral representation method, was used to generate sample functions of a 2D non-Gaussian stochastic vector field, according to prescribed cross spectral density matrix and a prescribed (non-Gaussian) probability distribution function. First, a Gaussian vector field was generated according to the target spectral density function. Next, it was transformed

into the desired non-Gaussian field using a memory-less nonlinear transformation coupled with an iterative process.

3.4.2. Theoretical Bases

3.4.2.1. Digital generation of mV - nD Gaussian stochastic vector fields

Let $f_{G^r}(X)$ be a mV - nD , homogeneous, non-Gaussian stochastic field with mean value equal to zero, autocorrelation matrix $R^0(\xi)$ and cross-spectral density matrix $S^0(K)$.

In the general case the cross-spectral density function and the autocorrelation matrix can be expressed as:

$$S^0(K) = \begin{bmatrix} S_{11}^0(K) & \cdots & S_{1m}^0(K) \\ \vdots & \ddots & \vdots \\ S_{m1}^0(K) & \cdots & S_{mm}^0(K) \end{bmatrix} \quad \text{Eq. 3.4}$$

$$R^0(\xi) = \begin{bmatrix} R_{11}^0(\xi) & \cdots & R_{1m}^0(\xi) \\ \vdots & \ddots & \vdots \\ R_{m1}^0(\xi) & \cdots & R_{mm}^0(\xi) \end{bmatrix} \quad \text{Eq. 3.5}$$

where:

$$S_{rs}^0(K) = \frac{1}{(2\pi)^n} \int_{-\infty}^{+\infty} \int_{-\infty}^{+\infty} \cdots \int_{-\infty}^{+\infty} R_{rs}^0(\xi) e^{-iK\xi} d\xi \quad \text{Eq. 3.6}$$

and,

$$R_{rs}^0(\xi) = \int_{-\infty}^{+\infty} \int_{-\infty}^{+\infty} \cdots \int_{-\infty}^{+\infty} S_{rs}^0(K) e^{iK\xi} dK \quad \text{Eq. 3.7}$$

with,

$$E[f_{Gr}(X)] = 0 \quad \text{Eq. 3.8}$$

and,

$$E[f_{Gr}(X)f_{Gr}(X + \xi)] = R^0(\xi) \quad \text{Eq. 3.9}$$

where $S_{rs}^0(K)$ is the complex cross-spectral function, $S^0(K)$ is hermitian and non-negative definite (Shinozuka, 1987 [182]), $K = (\kappa_1, \kappa_2, \dots, \kappa_n)$ is the n-dimensional wave number vector, $R^0(\xi)$ is autocorrelation matrix and $\xi = (\xi_1, \xi_2, \dots, \xi_n)$ is space-lag vector (separation vector). The cross-spectral density matrix is real, symmetric and non-negative, and therefore, under certain conditions, Cholesky decomposition can be applied and results in:

$$S^0(K) = H(K)H^T(K) \quad \text{Eq. 3.10}$$

where $H(K)$ is a lower triangular matrix and $H^T(K)$ is its transpose. The off-diagonal elements of $H(K)$ are generally complex and, therefore, can be written as:

$$H_{rs}(K) = |H_{rs}(K)| \exp\{i\theta_{rs}(K)\} \quad \text{Eq. 3.11}$$

where,

$$\theta_{rs}(K) = \tan^{-1} \left\{ \frac{\text{Im}[H_{rs}(K)]}{\text{Re}[H_{rs}(K)]} \right\} \quad \text{Eq. 3.12}$$

is the angle of $H_{rs}(K)$ in complex representation. Combining the simulation for $1V-nD$ stochastic fields and $mV-1D$ stochastic fields, the r^{th} component of a homogeneous $mV-nD$

Gaussian stochastic vector field with mean value equal to zero can be expressed by the following series as $N_1, N_2, \dots, N_n \rightarrow \infty$ simultaneously (Popescu et al., 1998b [164]):

$$f_{Gr}(X) = 2 \sum_{s=1}^r \sum_{l_1=1}^{N_1} \sum_{l_2=1}^{N_2} \dots \sum_{l_n=1}^{N_n} \sum_{\substack{I_i=1; \\ i=2,3,\dots,n}} \sum_{I_i=\pm 1} |H_{rs}(I_1 \kappa_{1sl_1}, I_2 \kappa_{2sl_2}, \dots, I_n \kappa_{nsl_n})| \sqrt{\Delta \kappa_1 \Delta \kappa_2 \dots \Delta \kappa_n} \cdot \\ \cos \left[I_1 \kappa_{1sl_1} x_1 + I_2 \kappa_{2sl_2} x_2 + \dots + I_n \kappa_{nsl_n} x_n - \theta_{rs}(I_1 \kappa_{1sl_1}, I_2 \kappa_{2sl_2}, \dots, I_n \kappa_{nsl_n}) + \Phi_{s,l_1 l_2 \dots l_n}^{I_1 I_2 \dots I_n} \right] \\ r = 1, 2, \dots, m$$

Eq. 3.13

where,

$$\Delta \kappa_i = \frac{\kappa_{iu}}{N_i}$$

Eq. 3.14

is the wave number increment in the κ_i direction with κ_{iu} denoting cut-off wave number (Shinozuka and Deodatis, 1996 [186]), the subscript G in $f_{Gr}(X)$ is for a Gaussian field, $X=(x_1, x_2, \dots, x_n)$ is the n -dimensional vector of space coordinates, and $\Phi_{s,l_1 l_2 \dots l_n}^{I_1 I_2 \dots I_n}$ are $m \cdot 2^{n-1}$ sequences of independent random phase angles uniformly distributed between 0 and 2π .

According to the central limit theorem, the simulated scalar fields are asymptotically Gaussian as $N_1, N_2, \dots, N_n \rightarrow \infty$.

The fast Fourier transform technique (FFT) is applied to speed-up the process. For more information in this regard, refer to Shinozuka and Deodatis (1996) [186], and Popescu et al. (1998b) [164].

3.4.2.2. Digital generation of mV - nD non-Gaussian stochastic vector fields

First, having the target spectral density $S^0(K)$, Gaussian sample functions are generated as described in section 3.4.2.1. Next, the simulated sample functions $f_{Gr}(X)$ are mapped to non-Gaussian sample functions having a marginal cumulative distribution function, F_{Br} , prescribed for all the scalar components of the non-Gaussian vector field:

$$f_{Br}(X) = F_{Br}^{-1}\{F_G[f_{Gr}(X)]\}; \quad r = 1, 2, \dots, m \quad \text{Eq. 3.15}$$

where F_G denotes the Gaussian cumulative distribution function. The transformation in Eq. 3.11 is nonlinear, and therefore the cross-spectral density matrix resulting from obtained non-Gaussian sample functions will not match the target cross-spectral density matrix. To solve the problem, Yamazaki and Shinozuka (1988) [222] proposed an iterative scheme. Figure 3.4 presents the flowchart to generate a random non-Gaussian mV - nD sample functions, after Popescu (1995) [158].

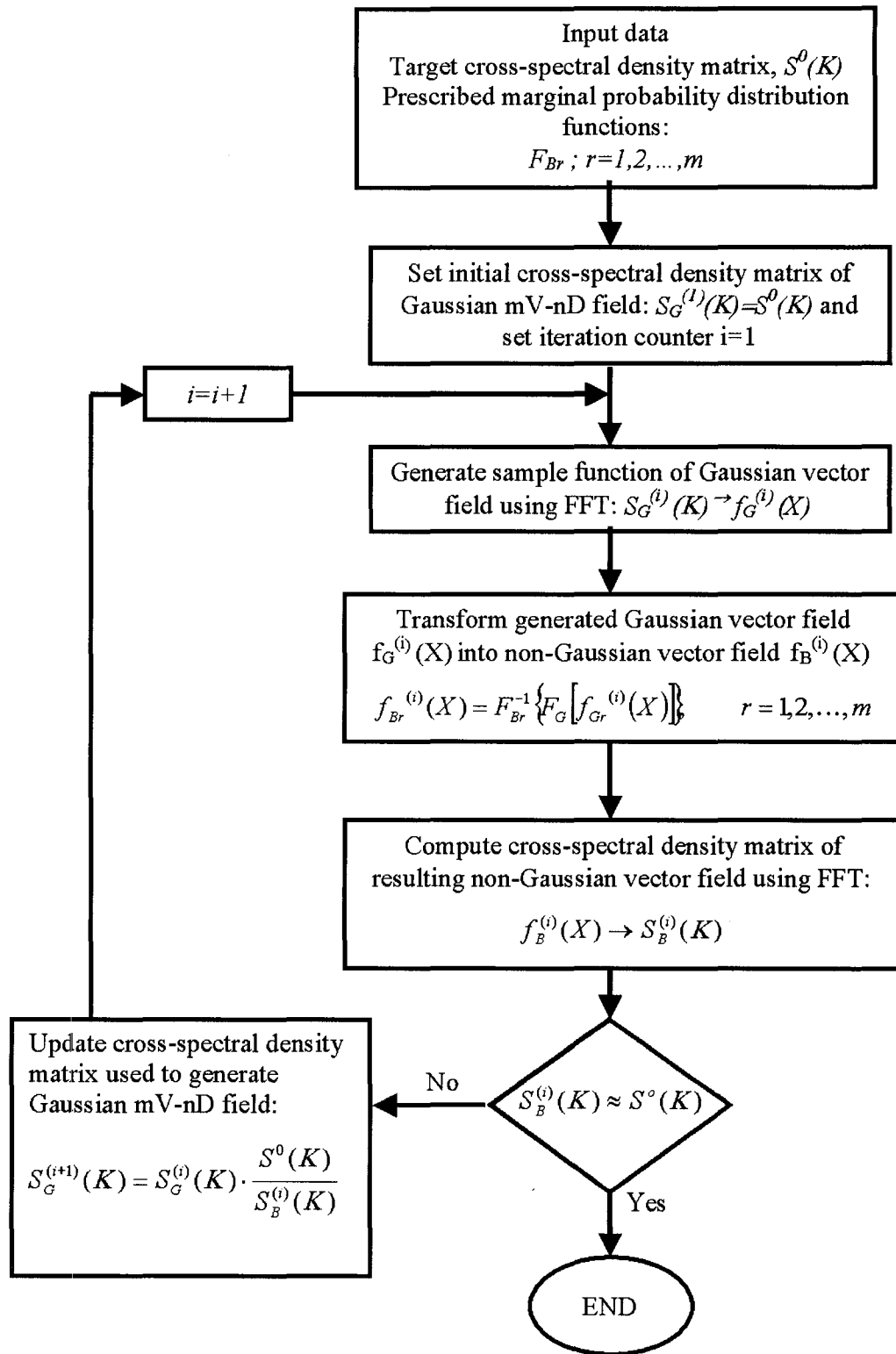


Figure 3.4 Flowchart for simulation of mV - nD non-Gaussian stochastic vector fields (after Popescu, 1995 [158]).

3.4.3. Generation of Sample Functions of a Stochastic Field

3.4.3.1. Stochastic field mesh

As described in Section 3.4.2, the continuous stochastic field describing the spatial variability of soil properties was estimated at predefined spatial locations. The distances Δx_i , which are referred to as “stochastic field mesh size”, depend on the upper cut-off frequency, k_{iu} , and the ratio between N_i and M_i – the number of simulation points in wave number domain and in spatial domain, respectively,

$$\Delta x_i = \frac{2\pi}{\Delta k_i} \cdot \frac{1}{M_i} = \frac{2\pi}{k_{iu}} \cdot \frac{N_i}{M_i} \quad i = 1, 2, \dots, n \quad \text{Eq. 3.16}$$

where the subscript i is the index for spatial dimensions and Δk_i is the mesh size in the wave number domain. The ratio of M_i/N_i shall be greater than two (Shinozuka and Deodatis (1991) [185]). On the other hand, a large value of N_i is required for a reliable discretization in the wave number domain. The values of M_i are limited by memory size. The upper cut-off frequency, k_{iu} , shall be selected according to the correlation structure of the stochastic field.

3.4.3.2. Generated sample functions of stochastic field

An exponentially decaying model, discussed by Shinozuka and Deodatis (1988) [184] among others, was selected for the auto-correlation function. This model is derived from the Exponential Decaying (ED) spectral density function,

$$s_{ED}(\kappa) = \frac{1}{2\Gamma(b_2+1)} b_1^{b_2+1} \kappa^{b_2} e^{-b_1|\kappa|} \quad \text{Eq. 3.17}$$

The expression for the corresponding correlation function is derived using the Wiener-Khinchine relation in the form of Fourier cosine transform (Popescu, 1995 [158]),

$$\rho_{ED}(\xi) = 2 \int_0^{\infty} s(\kappa) \cos(\kappa\xi) d\kappa = \frac{\cos \left[(b_2 + 1) \tan^{-1} \frac{\xi}{b_1} \right]}{\left[1 + \left(\frac{\xi}{b_1} \right)^2 \right]^{(b_2+1)/2}} \quad \text{Eq. 3.18}$$

The spectral density function is shown in Figure 3.5. Its spectral density function has a zero value at $\kappa=0$ and, therefore, is appropriate for the digital simulation procedure used in this study (Section 3.4). None of the classical expressions for evaluation of correlation distance (Vanmarcke, 1983 [209]) are appropriate for this model. Popescu (1995) [158] concluded that the model has finite correlation distance for $b_1 > 0$ and $b_2 > 0.3$. Popescu (1995) [158] studied the variation of correlation distance with parameters b_1 and b_2 , as shown in Figure 3.5c and approximated the correlation distance by,

$$\frac{\theta}{b_1} = 1.04 - 1.3 \log b_2 \quad 0.1 \leq b_2 \leq 2 \quad \text{Eq. 3.19}$$

Eq. 3.19 was used for selecting the parameters of the target SDF as a function of correlation distances. The cut-off frequency, κ_{iu} , was selected by limiting $s(\kappa_{iu}) < \varepsilon$ ($\varepsilon \sim 10^{-3}$ to 10^{-4}) obtained from Eq. 3.17. For two generated sample functions of the stochastic field, the spectral density functions are compared in Figure 3.6 with the target SDFs and the

cumulative probability distributions are compared in Figure 3.7 with the target cumulative probability distributions. Every generated sample function of soil shear strength followed the target probability distribution.

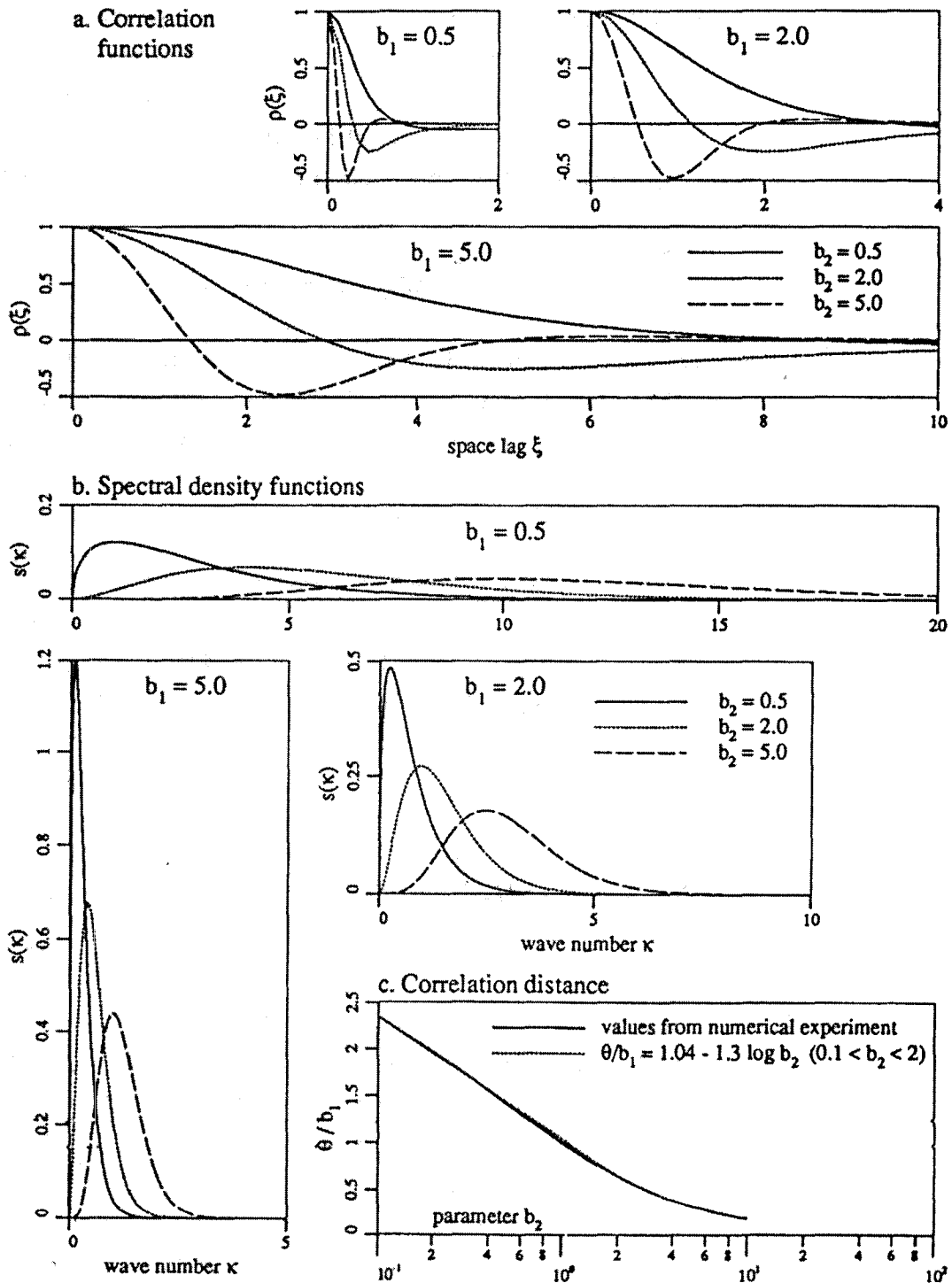


Figure 3.5 Exponential decaying SDF model: a. correlation functions, and b. spectral density functions for various values of the parameters b_1 and b_2 ; c. correlation distance values (Popescu, 1995 [158]).

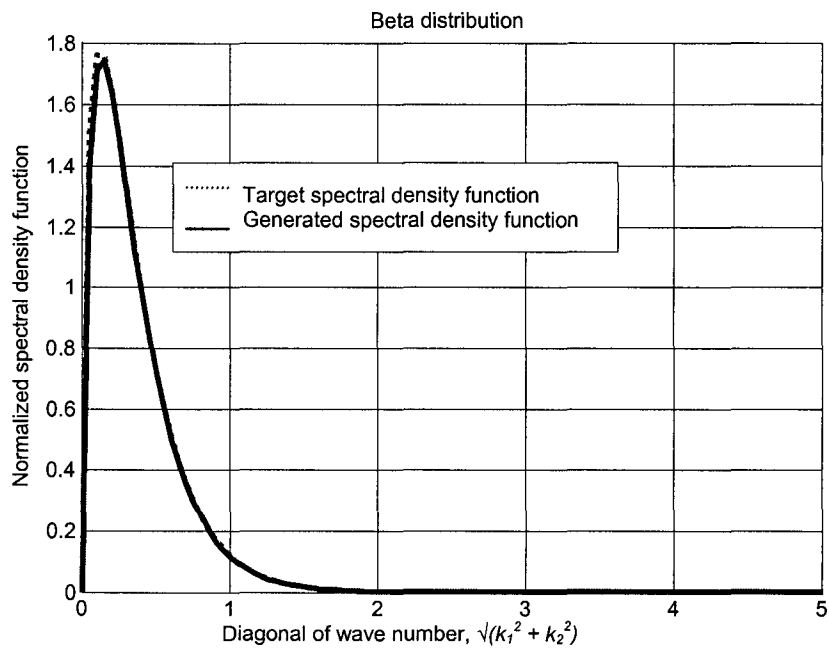
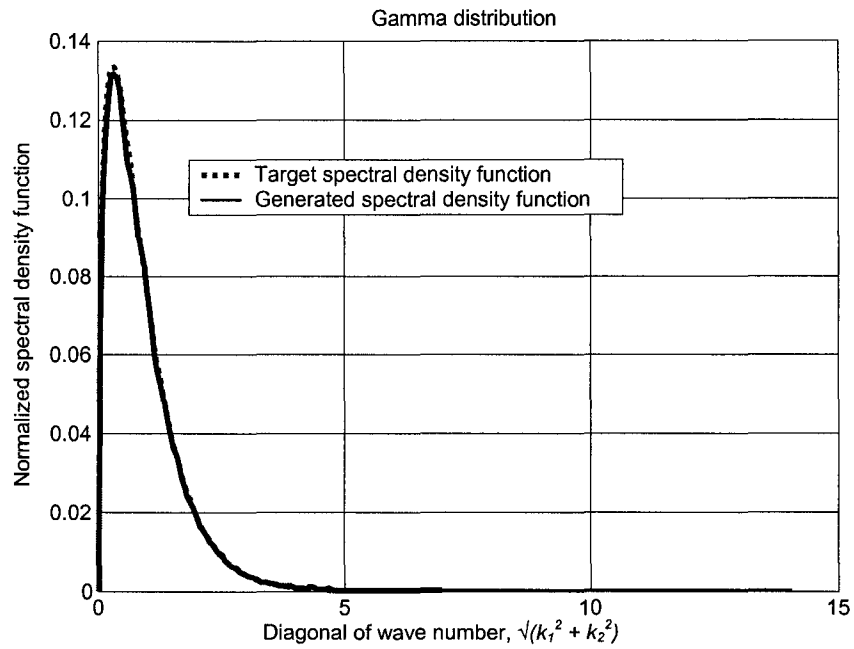


Figure 3.6 Comparison of generated and target spectral density functions for one sample function of a stochastic field with (a) Gamma probability distribution and (b) Beta probability distribution.

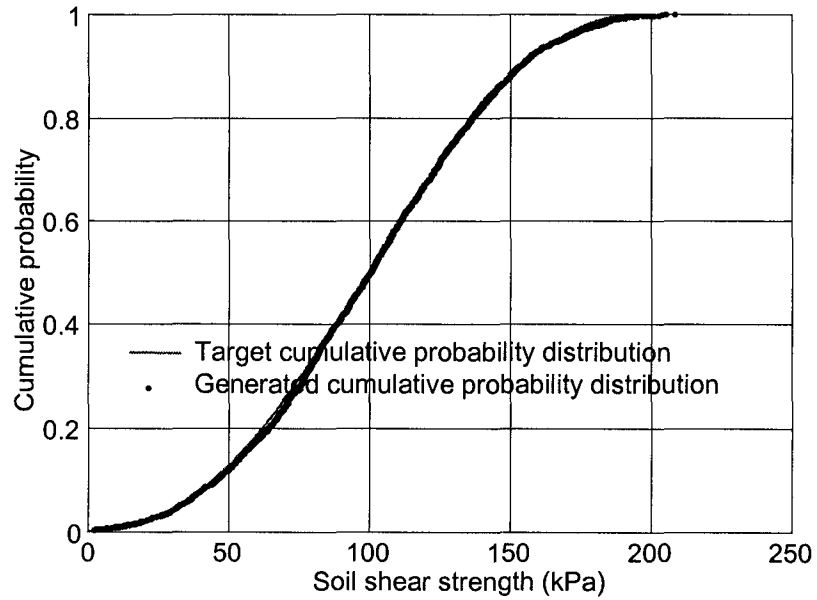
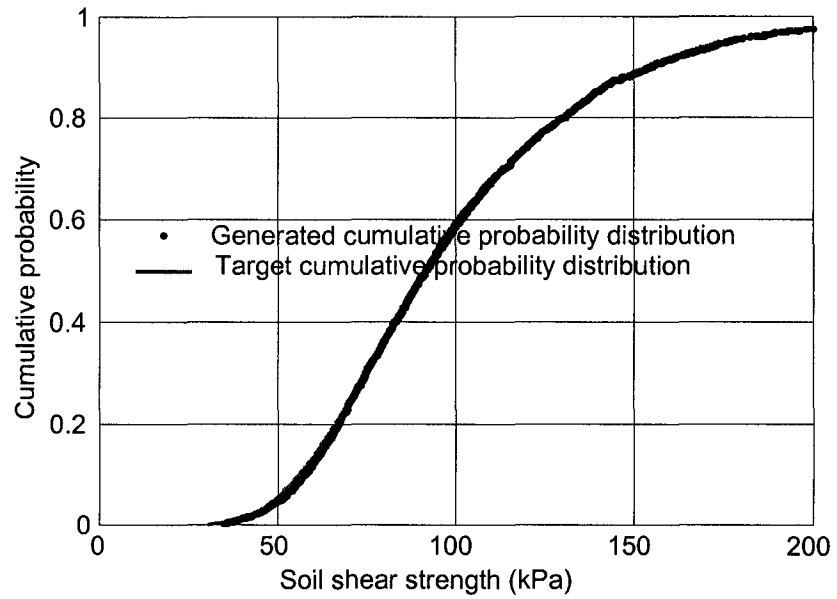


Figure 3.7 Comparison of resulting and target cumulative probability distributions for one sample function of a stochastic field with coefficient of variation of 40%: (a) Gamma probability distribution and (b) Beta probability distribution.

3.5. FINITE ELEMENT ANALYSIS

3.5.1. General Description

The finite element (FE) method has been widely used in engineering analysis in the last few decades. The origins of finite element method can be traced back to three different branches of research: applied mathematics (see Courant, 1943 [37]), (2) physics (see Synge, 1957 [192]), and (3) engineering (see Agyris and Kelsey, 1954 [2]). The development of FE method for practical engineering problems is closely connected with the development of digital computers. Though finite element was initially developed in structural mechanics (Hrennikoff, 1941 [96] and McHenry, 1943 [120]), it was soon applied to other engineering problems in virtually all fields of engineering analysis, including heat transfer and fluid mechanics. FE is a numerical method for solving engineering and mathematical problems (differential equations), such as stress-strain analysis, heat transfer, fluid flow and electromagnetic potential. Continuum finite element method is widely used in geotechnique as a general tool for stress and displacement analysis.

This study used finite element analysis to obtain responses for spatially variable soil in Monte Carlo simulations, as well as uniform soil for comparison and validation purposes (Figure 3.1). This section discusses some general aspects of the finite element analysis method used here and presents its application for spatially variable soil.

3.5.2. Main Elements of the Finite Element Model

3.5.2.1. Element type

Overconsolidated clay materials were studied in undrained condition. Soil undrained loading exhibits an almost incompressible behaviour, which is similar to the behaviour of metals at large strains (plastic region). Many researchers have studied the application of finite element methods to analysis of incompressible materials. It is known that except for plane stress cases, conventional finite element meshes often exhibit too stiff behaviour with such material behaviour. The finite element solution of a structure with a perfectly plastic material cannot exhibit a limit load; instead, it shows a steadily rising load-displacement curve attaining load values far in excess of the true limit load (Hibbitt et al., 1998a [93]).

The cause of this problem is that the volume at each integration point must remain fixed, which puts severe constraints on the kinematically admissible displacement fields. For instance, in a refined three-dimensional mesh of 8-node hexahedra, there is one node with three degrees of freedom per element on average. The volume at each integration point must remain fixed. Since full integration uses 8 points per element, we have as many as 8 constraints per element but only 3 degrees of freedom, resulting in overconstrained mesh (it locks). A similar problem arises in almost all fully integrated meshes.

There are several methods to overcome this problem among others,

- Using reduced integration elements
- Using irregularity in meshes

- Selective reduced integration element
- Using hybrid (mixed) elements

As discussed in the literature review, there are also special finite element formulations developed for this purpose (e.g. Merifield et al., 1999 [122]). Using reduced-integration elements is a common approach to overcoming this behaviour. Reduced integration elements result in meshes that are less constrained and, therefore, are less likely to become overconstrained. Hibbitt et al. (1998 & 2001) [93 & 94] expressed that usage of reduced integration elements effectively eliminates volumetric locking. ABAQUS/Standard uses a modified form of selectively reduced integration approach for “fully integrated” first order elements (4-node elements in two dimensions and 8-node elements in three dimensions). This approach is known as B-approach since the strain-displacement relationship matrix (the B matrix, $[\varepsilon]=[B].[u]$) is modified.

Another approach is use of hybrid (mixed) elements. In this approach, incompressibility constraints on each element are imposed in some average sense by a Lagrange multiplier technique. This approach allows for modelling of fully incompressible material behaviour, due to the fact that coupling only involves the inverse of the bulk modulus.

The reduced integration elements were selected for the finite element analyses described in Chapters 4 & 5 for two-dimensional plane strain analysis. Also, the behaviour of material is assumed approximately incompressible ($\nu=0.49$) to simulate undrained loading condition.

3.5.2.2. *Mesh size*

Mesh size effects are well known, particularly in prediction of collapse loads. An accurate prediction of failure loads needs very fine meshes or use of remeshing (adaptive meshing) in areas where failure surfaces develop. However, using a fine mesh is numerically very expensive, particularly for this research where thousands of finite element analyses were performed. Use of new techniques, such as adaptive meshing, is sophisticated and costly as well.

It is acknowledged that regular meshes fail to predict the collapse load precisely; however, they are able to predict the collapse load by very good approximation. The main goal in this research was to investigate the effects of soil spatial variability on predicted loads. Hence, rather than using finer meshes or sophisticated approaches, a comparison study was conducted. The results of the finite element analyses with stochastic input were compared to results from the finite element analyses with uniform soil. In both analyses, identical meshes were used to compensate for the mesh effects. This is detailed for foundation and pipe analysis in Chapters 4 & 5.

3.5.2.3. *Plasticity models*

Tresca (Tresca, 1867 [205]) and von Mises (von Mises, 1913 [215]) – simple pressure independent plasticity models – were considered to model undrained behaviour of overconsolidated clay. Tresca's yield criterion stipulates that yielding occurs when the maximum shear stress reaches the critical intensity, k . Tresca's criterion states that for plastic flow, the largest of the differences of principal stresses has the value of c_u ($k = 2c_u$).

This is graphically demonstrated in terms of principal stress in Figure 3.8. If $\sigma_1 > \sigma_2 > \sigma_3$, this can be written in terms of principal stress,

$$\sigma_1 - \sigma_3 = k \quad \text{Eq. 3.20}$$

It can be expressed in terms of stress invariants according to Figure 3.9,

$$\begin{aligned} \sigma_1 &= p + \frac{2}{\sqrt{3}} \sqrt{J_2} \sin\left(\theta + \frac{2\pi}{3}\right) \\ \sigma_2 &= p + \frac{2}{\sqrt{3}} \sqrt{J_2} \sin(\theta) \\ \sigma_3 &= p + \frac{2}{\sqrt{3}} \sqrt{J_2} \sin\left(\theta - \frac{2\pi}{3}\right) \end{aligned} \quad \text{Eq. 3.21}$$

Thus, Tresca criterion can be written as,

$$2\sqrt{J_2} \cos\theta = k \quad \text{Eq. 3.22}$$

where θ can be measured from Figure 3.9. θ is the polar angle measured from the plane of pure shear or undrained loading and can be written as,

$$\sin 3\theta = -\frac{3\sqrt{3}J_3}{2J_3^{3/2}} \quad \text{for} \quad -\frac{\pi}{6} \leq \theta \leq +\frac{\pi}{6} \quad \text{Eq. 3.23}$$

where stress invariants J_2 and J_3 can be defined in terms of principal stresses as,

$$J_2 = \frac{1}{6} [(\sigma_1 - \sigma_2)^2 + (\sigma_2 - \sigma_3)^2 + (\sigma_3 - \sigma_1)^2] \quad \text{Eq. 3.24}$$

$$J_3 = \frac{1}{27} (2\sigma_1 - \sigma_2 - \sigma_3)(2\sigma_2 - \sigma_3 - \sigma_1)(2\sigma_3 - \sigma_1 - \sigma_2) \quad \text{Eq. 3.25}$$

For axial loading, $\theta = -\pi/6$, and for undrained loading in plane strain condition, $\theta = 0$. In terms of stress invariants, Tresca's yield surface can be expressed by,

$$f(J_2, J_3) = 4J_2^3 - 27J_3^2 - 9k^2J_2^2 + 6k^4J_2 - k^6 = 0 \quad \text{Eq. 3.26}$$

Another yield surface frequently used for pressure independent material is von-Mises criterion,

$$\sqrt{3J_2} = k \quad \text{or} \quad F_y \quad \text{Eq. 3.27}$$

For axial loading condition, k is the yield stress measured in axial experiment and is similar to Tresca's criterion. However, the model is different for pure shear or undrained loading. Looking at Figure 3.8 and Figure 3.9, it is possible to determine that the model has about 15% difference for undrained loading ($\sqrt{4/3} = 1.15$). Differences between Tresca and von Mises models are shown in Figure 3.10. Concerning soil materials, the maximum shear stress usually governs the behaviour. Consequently, the Tresca model was selected in this study to model soil behaviour.

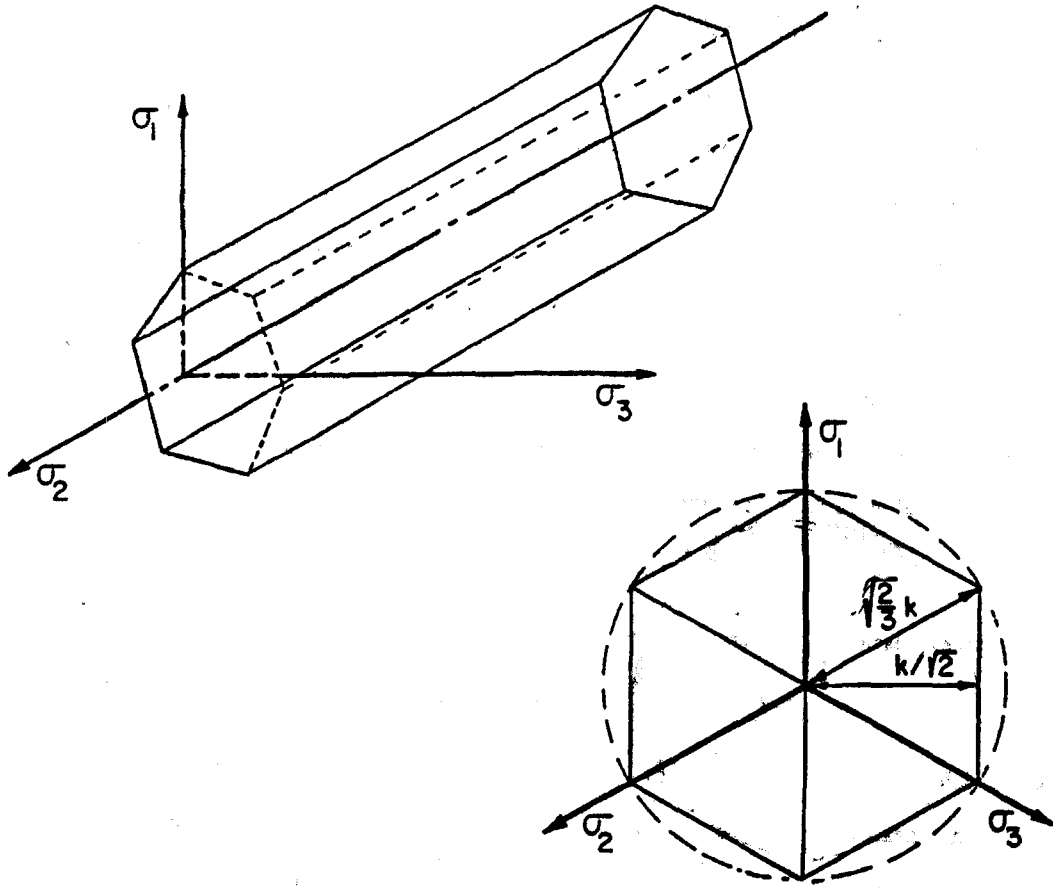


Figure 3.8 Tresca yield surfaces (after Prevost, 1990 [171]). Von Mises yield criteria is shown by dashed line.

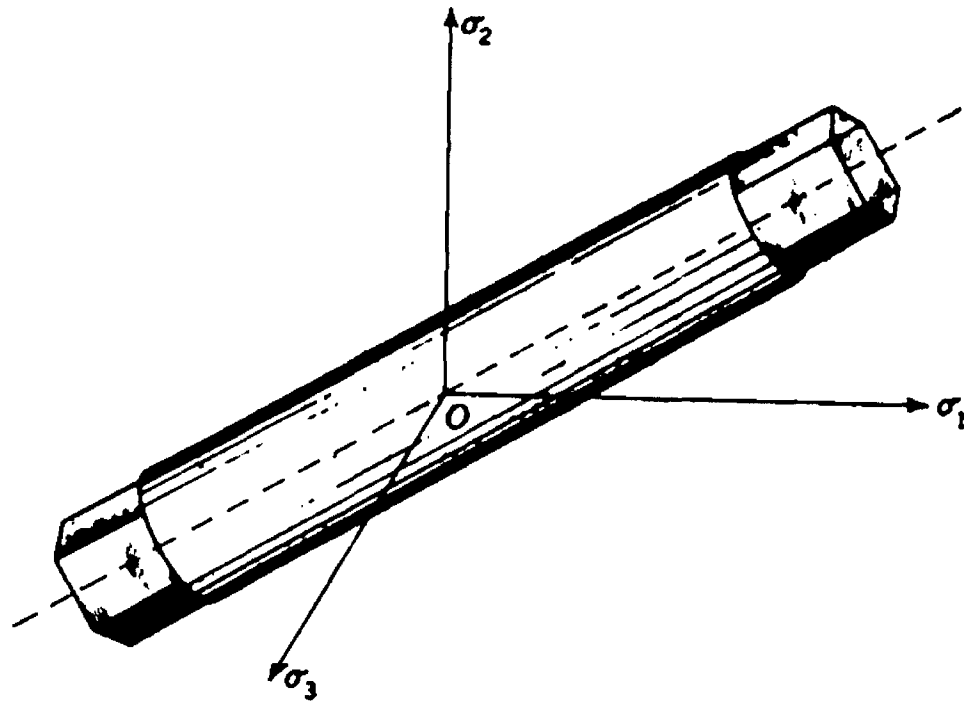


Figure 3.10 Comparison of Tresca and von Mises yield surfaces in 3 dimensional principal stress space (after Venkatraman and Patel, 1970 [211]).

3.5.3. Finite Element Code, ABAQUS/Standard

The finite element code, ABAQUS/Standard v5.8, 6.1 and 6.2, was used in the study. ABAQUS is a general purpose program for the static and transient responses of two and three-dimensional systems; it offers standard options, or can be customized to address many of the challenges involved in a study of geotechnical structures, such as: (1) 3D soil-structure analysis, using complex finite strain constitutive models and accounting for large deformation effects; (2) coupled field equations capabilities for two phase media; (3) contact analysis capabilities for simulating the soil-structure interface; and (4) large deformation formulation capable of capturing collapse mechanisms and strain localisation.

ABAQUS/Standard is widely available, and its use is well documented. The program has been widely used for 2D and 3D finite element analyses of soil-structure interaction involving large relative deformations, and it has been validated based on results of full-scale tests (Popescu et al., 1999 [166]; Nobahar et al., 2000 [141]; Popescu et al., 2001 [160]).

3.5.3.1. Modelling soil-structure interaction

ABAQUS offers very general contact capabilities and can model possible interaction, sliding, and loss of contact between soil and structure bodies. One approach is to define contact surfaces and then pair surfaces that are in contact or may potentially contact each other. Surface interaction properties, such as friction, can be defined for each contact pair. Several types of contact problems can be defined using the general approach that follows (Hibbitt et al., 2001 [94]),

- Contact between two deformable bodies. The structures can be either two- or three-dimensional, and they can undergo either small or finite sliding. Examples of such problems are 2D and 3D analysis of buried pipelines (Popescu et al., 2001 [160] and Nobahar et al., 2000 [141]).
- Contact between a rigid surface and a deformable body. The structures can be either two- or three-dimensional, and they can undergo either small or finite sliding. For example, contact between a rigid foundation or pipe and a deformable soil can be modelled using this option.

- Contact between a set of points and a deformable surface. These models can be either two- or three-dimensional. An example of this class of contact problem is a building model by structural beams on a deformable soil.
- Problems where two separate surfaces need to be “tied” together so that there is no relative motion between them. This modelling technique allows for joining dissimilar meshes.

Structure-soil (foundation-soil or pipe-soil) contacts can be included in the first category. When surfaces are in contact, they usually transmit shear as well as normal forces across their interface. There is generally a relationship between these two force components. The relationship, known as the friction between the contacting bodies, is usually expressed in terms of the stresses at the interface of the bodies. The friction model in ABAQUS is an extended version of the classical isotropic Coulomb friction model. It allows the friction coefficient to be defined in terms of slip rate, contact pressure, average surface temperature at the contact point, and field variables. A shear stress limit, which is the maximum value of shear stress that can be carried by the interface before the surfaces begin to slide, can be prescribed. The method is implemented with a stiffness (penalty) method. It has several other capabilities and can be customized using user subroutines.

3.5.3.2. Soil material behaviour modelling

Both von-Mises and Tresca plasticity models are available in ABAQUS/Standard. The Von Mises plasticity criterion is developed in ABAQUS/Standard as a classic isotropic metal plasticity model, which may have several yield surfaces with associated plastic flow.

It can be used in crash and general collapse studies. The Tresca model in ABAQUS is developed based on Mohr Coulomb plasticity model.

3.5.4. Finite Element Analysis with Stochastic Input – Issues

As discussed in Section 2.1.2, stochastic finite element methods are a class of methodologies used to analyse structures with spatial uncertainty in loads, material properties and/or geometry. As mentioned, the only universal SFEM that can be used for any structure (e.g. involving material and geometric nonlinearity, large parameter variability and non-Gaussian distribution of parameters) appears to be the Monte Carlo simulation technique.

In this regard, a conventional deterministic finite element method with spatially variable input was used for each realization of the soil properties over the analysis domain (a sample function of a stochastic field). As described in Section 3.4, sample functions of uncertain quantities were digitally generated to be compatible with prescribed probabilistic characteristics. These generated sample functions were used to define input parameters for each finite element analysis. Each finite element analysis was taken as one realization of foundation failure on heterogeneous soil in the framework of Monte Carlo simulation methodology.

3.5.4.1. Transfer and mapping of random data

There are substantial restrictions for the stochastic field mesh size in spatial domain. The finite element mesh used in analysis should be selected according to numerical needs for modelling of the physical problem and its behaviour. Hence, it is very

likely to have different meshes for the random field discretization and the finite element analysis of the structural or geotechnical systems. Thus, a transfer of data may be required from one mesh to another mesh. In this study, this transfer was avoided as much as possible. However, in the case of the lateral loading of buried pipeline, this was not possible due to geometric restrictions.

Numerous transfer methods are available (see Brenner, 1991 [19]). The following two methods were evaluated,

- The midpoint method (e.g. Shinozuka and Dasgupta, 1986 [183]; Yamazaki et. al. 1988; Der Kiureghian and Ke, 1988 [49]; Deodatis, 1989 [46]) is a point discretization type method. The random field is represented by its values at centroids of each finite element (or closest point to the centre of element).
- The local averaging (or spatial averaging) method, proposed by Vanmarcke (1977) [208] and Vanmarcke and Grigoriu (1983) [210], assigns to each element a value obtained as an average of stochastic field values over the element domain.

Popescu (1995) [158] performed a study for comparison of these two methods, and concluded that for non-Gaussian fields, the midpoint method is more appropriate, as it preserves the probability distribution of the original field. Der Kiureghian and Ke (1988) [48] concluded that the midpoint method over-represents the variability of the random field while the spatial averaging method tends to under-represent the true variability. They also demonstrated that for Gaussian fields, the spatial averaging method seems to be a more

logical approach to random field discretization; it was proven to provide better accuracy than the midpoint approach. In this study, non-Gaussian probability distributions were considered for soil properties, so the midpoint method was selected here. Geometrically similar finite element and stochastic mesh were used to facilitate the transfer of data between the two meshes.

3.5.4.2. Automation of the generation and mapping of sample functions of a stochastic field

For the parametric studies, a large number of sample functions of various stochastic fields were simulated for each case. Next, these sample functions were used to create input files for finite element analysis (see Figure 3.1). A sample of this input file is presented in Appendix A. For each case, 100 to 1200 finite element input files were executed and post-processed. Results were used in the framework of Monte Carlo simulation to obtain probabilistic characteristics of the desired response. These procedures were automated using Microsoft Excel® spreadsheets, Microsoft Visual Basic® for Application and MATLAB®. Appendix B provides an explanation of the automation of these procedures.

3.6. CALIBRATION OF RESULTS FOR ENGINEERING DESIGN

3.6.1. Introduction

After performing Monte Carlo simulations, the results were analysed to assess the effects of soil heterogeneity on bearing capacity. This included systematic parametric studies. Probabilistic characteristics of response (e.g. mean and coefficient of variation of bearing capacity) were obtained for every design case. These results can be directly used in reliability analysis level II and level III. Also it is possible to use them in the limit state design method (reliability level I) and incorporate them with other routine engineering concepts. In this section, it is shown how the results of the study can be used to evaluate characteristic values, evaluate the required safety factor for desired reliability levels, and to account for them in a formal limit state design format.

3.6.2. Characteristic Values/Percentiles

As mentioned, usage of conservative values instead of mean strength is common in engineering design. These values are so called nominal or characteristic values (see Section 2.4). As mentioned in Section 2.4, it is very important to have a unified definition for characteristic values (see Becker, 1996a [15]; Cardoso and Fernandes, 2001 [24]). As noted in the literature review (Section 2.4.2.1), characteristic values are defined based on engineering experience and statistical percentiles. A 95-percentile is a value of resistance with 95% reliability. In other words, 5% fractile of resistance is taken as characteristic resistance.

Soil strength has high point variability, however this high variability itself is not important. Soil strength average value on the failure surface and its corresponding variability are important for design. Here results of Monte Carlo simulations are used to obtain characteristic values of bearing capacity for each case analysed. These values are defined as bearing capacity values with 95% reliability. These values are curve fitted as functions of parameters of soil spatial variability (coefficient of variation, probability distribution and correlation distances). The results can be used to estimate the characteristic bearing capacity or corresponding characteristic value of soil shear strength to be used in a conventional analysis (assuming uniform soil), resulting in an equivalent bearing capacity with the one of the heterogeneous soil for a given confidence interval (here 95%). The calculations are detailed in Chapter 4 for investigated cases.

It is also possible to define a certain percentile of soil shear strength to be used in design. As mentioned, some design codes advise on use of resistance with 95% of reliability. However, due to high point variability of soil strength, using a 95% of soil strength would be too conservative. In addition, as discussed in the literature review, behaviour of heterogeneous materials differs from uniform materials. For example, Nobahar and Popescu (2000) concluded that 88-percentile of recorded soil strength used in a deterministic finite element analysis will provide similar results with the 95-percentile of the bearing capacity resulting from Monte Carlo simulations for a specific set of probabilistic characteristics of soil properties. However, using another set of probabilistic characteristics results in a different characteristic percentile.

3.6.3. Reliability Analysis and Required Safety Factors

Using the results of Monte Carlo simulations, it is possible to estimate the required safety factor to secure probability of failure at target probability level or target reliability index. The number of samples in Monte Carlo simulations performed in this regard was not sufficient for estimating the target reliability levels in the range of 10^{-3} to 10^{-5} . Therefore, theoretical probability distributions are fitted to the predicted results, and the results are extrapolated to the target level. Such extrapolations are common in risk and reliability analysis. Load variability was not considered here.

Also, two types of reliability indices can be used here (e.g. Thoft-Christian and Baker [202]; Barker and Puckett, 1997 [13]): (1) reliability indices based on normal distribution,

$$\beta = \frac{\bar{R} - \bar{S}}{\sqrt{\sigma_R^2 + \sigma_S^2}} \quad \text{Eq. 3.28}$$

and (2) reliability indices based on lognormal distributions,

$$\beta = \frac{\ln\left(\frac{\bar{R}}{\bar{S}}\right)}{\sqrt{V_R^2 + V_S^2}} \quad \text{Eq. 3.29}$$

where σ_R , V_R , σ_S , and V_S are the standard deviation and the coefficients of variation for resistance, R , and load, S , respectively. \bar{R} is average resistance and \bar{S} is average load; both are assumed to be independent variables.

3.6.4. Calibration of Partial Design Factors

Calibration of design factors should be conducted to ensure a specific goal. This goal may be to optimise safety, risk, economic indices etc. The selection of a structural reliability level against one or more potential risks takes into account the structural failure probabilities as well as the probabilities that these failures may lead to prejudicial consequences. So, a non-uniform reliability level may lead to optimal solutions from an economical point of view. As a matter of fact, the complete calibration process should take into account complex criteria such as failure modes, the expected consequences, the risk prevention methods, the fluctuating construction costs, the expected failures costs as well as the maintenance and the repair costs.

Design codes have roots in engineering experience, which is very valuable and continues to empirically address design needs. As such, design codes have steadily been improved. To provide a unified and scientific approach, design codes have been calibrated to secure some target reliabilities. An appropriate set of load and resistance factors together with a clear method of estimation of nominal or characteristic value shall be used to secure a desired reliability level. The goal usually is to have a uniform reliability in structure. This goal is used here to calibrate resistance factors.

Reliability is often presented by a reliability index in engineering codes. In general a reliability index β of 3 to 4 is considered suitable in structural and geotechnical design. Using a calibration technique, the weighted average of corresponding values of β in Canadian structural design specifications, for most practical or typical combinations of

loads, was found to range from 2.5 to slightly greater than 4.0 (MacGregor, 1976 [118]; Allen, 1975 [3]).

This study focused on the uncertainty in the resistance. The goal was assumed to be the calibration of partial design factors to satisfy a uniform reliability index of 3.5. It is possible to separate the effects of load and resistance uncertainty on reliability index in the approach presented hereafter. In this way, partial load factors are only functions of load uncertainty and partial design factors are only functions of resistance uncertainty. In this study, only soil undrained shear strength was addressed. Thus, only one partial factor was calibrated based on uncertainty in undrained shear strength.

Assuming Eq. 3.29 for the reliability index, Becker (1996b) [16] has shown that resistance and load factors can be obtained by,

$$\Phi = k_R e^{-\theta \beta V_R} \quad \text{Eq. 3.30}$$

$$\alpha = k_S e^{\beta \theta V_S} \quad \text{Eq. 3.31}$$

where Φ , α are resistance and load factors. k_R and k_S are reduction and increase factors used to obtain the characteristic (nominal) resistance and load,

$$R_n = \frac{\bar{R}}{k_R} \quad \text{Eq. 3.32}$$

$$S_n = \frac{\bar{S}}{k_S} \quad \text{Eq. 3.33}$$

where R_n , \bar{R} , S_n , \bar{S} are nominal and average resistance and load, respectively. θ is separation coefficient defined as,

$$\theta = \frac{\sqrt{1 + \left(\frac{V_R}{V_S}\right)^2}}{1 + \frac{V_R}{V_S}} \quad \text{Eq. 3.34}$$

where V_R , V_S are the coefficients of variation for resistance and load. It was found that θ varies from a minimum of about 0.7 to maximum of 1.0. For an expected practical range of V_R/V_S of 0.5 to 5, the value of θ varies within a relatively narrow range of 0.7 to 0.85. Becker (1996b) [16] stated that, in view of the complexity of the analysis and the insufficient geotechnical database, a value of $\theta = 0.75$ can be taken. This value was used for calibrating the resistance factor.

The average resistance in Eq. 3.31 should be the predicted mean resistance on heterogeneous soil from Monte Carlo simulations. It can be expressed as resistance on uniform soil divided by a heterogeneity factor,

$$\bar{R} = \frac{R_U}{k_H} \quad \text{Eq. 3.35}$$

Therefore, Eq. 3.30 should be changed to,

$$\Phi = \frac{k_R}{k_H} e^{-\theta\beta V_R} \sim \frac{k_R}{k_H} e^{-0.75\beta V_R} \quad \text{Eq. 3.36}$$

Similarly, if normal distributions are assumed for load and resistance,

$$\Phi = \frac{1 - \theta \beta V_R}{k_H} \cdot k_R \sim \frac{4 - 3 \beta V_R}{4 k_H} \cdot k_R \quad \text{Eq. 3.37}$$

See Appendix C for details of calculations.

Using the described approach, the required partial design factor for resistance is calculated using the fitted response surface equations. The partial design factor for soil undrained shear strength was obtained using two different methodologies to satisfy a reliability index of 3.5. In the first approach, it was assumed that the value of $k_R = 1$ in Eq. 3.36. In other words, it was assumed that average resistance is taken as a characteristic value (common in geotechnical design). Next, the required partial resistance factor was determined from the described approach. In the second approach, characteristic values suggested in section 3.6.1 were used to obtain the required resistance factor at each point. This means that a variable k_R depending on uncertainty involved was used.

3.7. SUMMARY

The methodology used here is presented in Figure 3.1. The methodology, as presented in this chapter combined a deterministic finite element model with stochastic input (sample function of a stochastic field) and Monte Carlo simulation approach to evaluate the effects of stochastic variability of soil properties in geotechnical design (namely bearing capacity problem) through a series of parametric studies. The integration of the Monte Carlo simulations and the methodology is detailed in Figure 3.1. From *in-situ* tests, it is possible to extract the characteristics of soil spatial variability. Here, the ranges of the characteristics of soil spatial variability (coefficient of variation, shape of probability

distribution, and correlation distances) were evaluated based on a literature review (Phoon and Kulhawy, 1999b [155]; Popescu, 1998b [163] – see Section 2.1). Parametric studies were designed using the design of experiment (DOE) methodology as described in Section 3.3. Then, sample functions of the stochastic field were digitally generated for every case as detailed in Section 3.4. Monte Carlo simulations were performed for every case. For each replication of Monte Carlo simulations, a sample function of the stochastic field was generated. This sample function was used to define soil properties (here shear strength) at each point over domain of interest and mapped to an appropriate finite element mesh. Conventional finite element analysis was performed to obtain the structural response (e.g. bearing pressure vs. settlement). The procedure was replicated for the required number of simulations. The results of the Monte Carlo simulations were studied through the investigation of the system's behaviour and failure mechanism on heterogeneous soil, as well as statistical analysis. Having a sufficient number of results of Monte Carlo simulations based on realistic data, it was possible to determine probabilistic characteristics of bearing capacity, such as mean and standard deviation. The influence of various probabilistic characteristics of soil strength on the geotechnical system could then be assessed.

Since Monte Carlo simulations are complicated and numerically very costly, the goal was to compare the results of stochastic analysis with conventional deterministic analysis to provide some design recommendations to account for the effects of soil heterogeneity in conventional analysis. This has been done through:

- Providing characteristic values. Design codes account indirectly for variability of soil properties by using a “conservatively assessed nominal value” of soil strength. This value, in structural engineering (advised in general in Eurocode and Canadian LSD code) is taken as the 95-percentile soil strength, determined from a number of measurements. This conservative value is not established based on strong theoretical or experimental studies.

It is also possible to define a characteristic percentile of soil strength that, when used in deterministic analysis, will provide a similar pressure-settlement relationship as was obtained from Monte Carlo simulations for a given confidence interval.

- Calibration of the required safety factor for the desired reliability levels.
- Calibration of the partial resistance factor as detailed in Section 3.6.

Consequently, the conventional methods can be verified and adjusted to provide a more realistic reliability level. Of course, it should be mentioned that design methods are based on many years of engineering practice, and this research can help provide a better assessment of uncertainties involved in geotechnical problems with high natural variability and nonlinear behaviour.

It is also possible to use the results of the study in terms of probabilistic characteristics of foundation response on heterogeneous soil in reliability analysis level II and III. This can be done through back calculations of partial design factors for reliability level II analysis (Section 3.6) and through the use of cumulative distribution functions of resistance for reliability level III analysis.

Finally, it is possible to provide a more accurate assessment of reliability level of geotechnical structures accounting for the effects of spatial variability. Such assessments can become fundamental in establishing a robust theoretical approach for verifying design methods based on the target reliability level, which may lead to adjustment and verification of current safety factors and/or design approaches to secure a more uniform desired reliability level.

CHAPTER 4

BEARING CAPACITY OF SHALLOW FOUNDATIONS

4.1. INTRODUCTION

4.1.1 Description

The effects of inherent spatial variability of soil properties on the bearing capacity of strip footings subjected to vertical loads, and placed on a perfectly elastic-plastic soil deposit were investigated through a series of parametric studies. A Monte Carlo simulation methodology, discussed in the previous chapter, was used here. Results from Monte Carlo simulations accounting for the spatial variability of soil strength, and deterministic analyses assuming uniform soil properties were compared. Effects of the probability distribution, soil strength variability, and correlation distances were investigated through parametric studies. As described in Section 3.3, the studied cases were designed using statistical approaches (DOE). The results were statistically analysed to draw scientific conclusions. The main parameters of probabilistic characteristics of heterogeneous soil affecting foundation responses and their contributions were determined. Based on the results, some design recommendations were put forward. In this Chapter, the word ‘foundation’ refers to a strip foundation placed at the ground level.

4.1.2 Objectives

Monte Carlo simulation approach and other adequate probabilistic approaches are complicated and numerically expensive for routine design. Thus, the aim of this study was to determine the effects of spatial variability of soil on bearing capacity and behaviour of a foundation and consequently provide necessary design recommendations for engineering application. This provides a tool to assess the effects of soil heterogeneity with minimal analysis efforts and limited statistical information. The objectives of this study were:

- To investigate the effects of soil heterogeneity on differential settlement and bearing capacity of shallow foundations.
- To screen and determine the contributions of the main factors influencing soil spatial variability characteristics (degree of variability of the soil strength, probability distribution functions, horizontal and vertical correlation distances and ratio of soil Young's modulus to its shear strength, E/c_u).
- To provide simple regression equations for bearing capacity and foundation responses based on soil stochastic characteristics and demonstrate their applicability in design and reliability analysis.
- To provide design recommendations by (1) proposing characteristic values of soil properties and characteristic resistance values for use in design and assessment of reliability level of geotechnical systems, (2) regression of partial design factors, and (3) back calculation of safety factors.

4.1.3 Limitations

The main limitation of the study was the relatively small number of samples in Monte Carlo simulations. This was due to the numerical cost. Monte Carlo simulation results can be confidently used to obtain probabilistic characteristics of structural resistance (e.g. mean and standard deviation). However, in order to estimate reliability levels of the order of 10^{-3} to 10^{-4} , common probabilistic distributions were fitted to the results of Monte Carlo simulations and extrapolated for the tails. An alternative way is the second moment probabilistic method, which only uses mean and standard deviation of the results (e.g. Becker 1996a&b [15&16]). As discussed in Section 3.6, this method is identical to using a normal/lognormal fit.

To counter the above limitation, different theoretical probabilistic distributions (normal, lognormal, and gamma) were fitted to the results of Monte Carlo simulations. However, no single distribution was found to be the most suitable for all studied cases. Lognormal distribution was selected to be the overall best representative. This was another limitation of study and it was related to the first limitation. It requires further investigation by using a much larger number of replications for Monte Carlo simulations and statistical analysis.

4.2. DETERMINISTIC FINITE ELEMENT ANALYSIS

4.2.1 Optimisation of Numerical Model

4.2.1.1. Finite element domain and boundaries

A study was performed for a strip shallow foundation on homogeneous soil to find the necessary extent of the analysis domain. A 4m wide strip foundation was placed on the surface of a 10m deep layer of over-consolidated clay, as shown in Figure 4.1. The soil was discretized using 4-node linear finite elements with reduced integration (CPE4R) in ABAQUS/Standard. A rigid layer was assumed at the base of the analysis domain. This rigid layer had minimal effect on the bearing capacity of the foundation. According to a study performed by Merifield et al. (1999) [122], the rigid layer at the base of the analysis domain for a two-layered soil deposit does not have a noticeable effect on the static response of the foundation for depths of rigid layer larger than the foundation width, B . In this study, the rigid boundary was assumed at a depth, $z = 2.5B$.

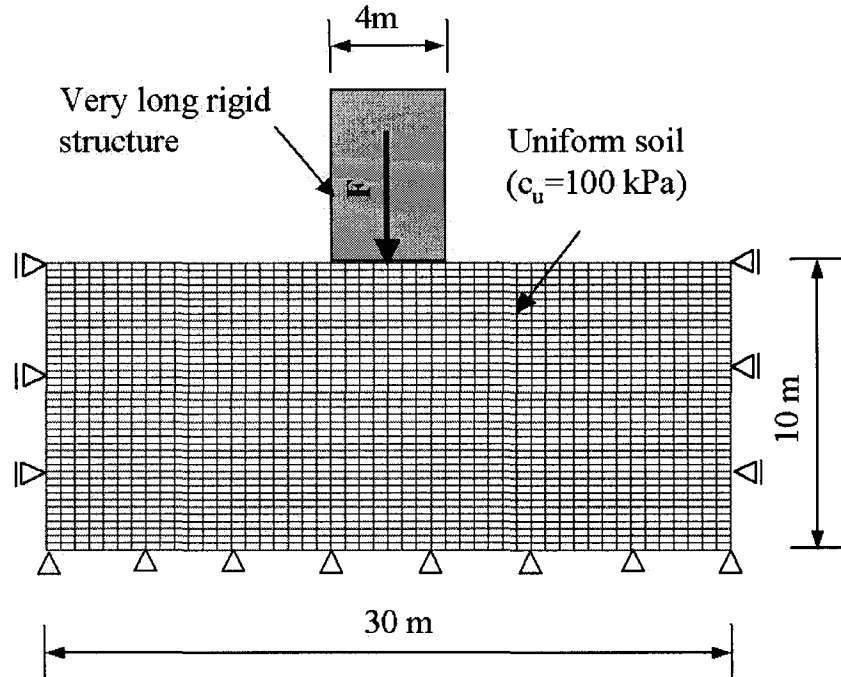


Figure 4.1 Finite element mesh.

The effects of the lateral boundary condition on the foundation response were investigated (see Figure 4.2). The length of the analysis domain, L , varied from 24m to 48m. The results showed almost no difference in the predicted bearing pressure-settlement curves. The results in terms of bearing pressure and settlements were normalized. The normalized pressure was defined as the ratio of the average pressure beneath the foundation to the mean undrained shear strength. The normalized settlement was defined as the ratio of the average settlement to foundation width. A width of 30m for the analysis domain is considered hereafter.

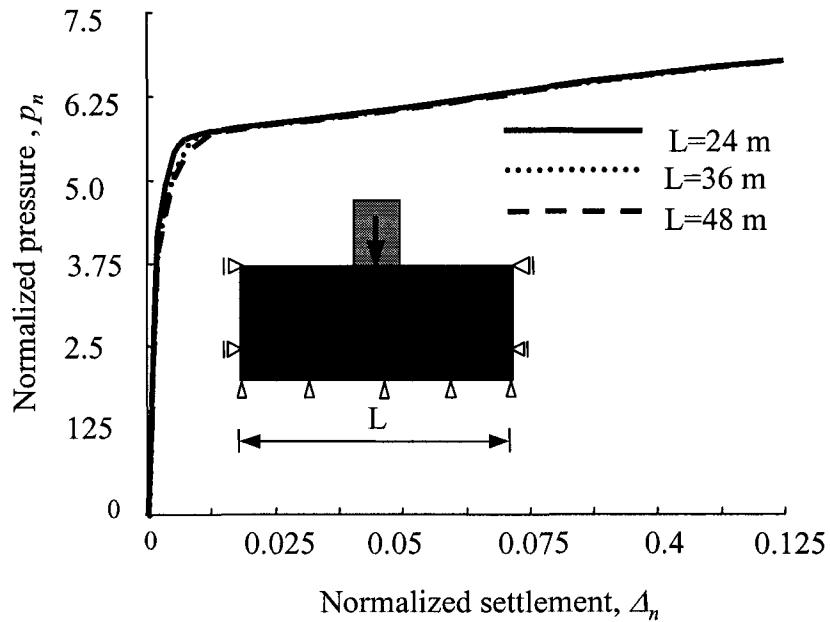


Figure 4.2 Effects of lateral boundary conditions.

4.2.1.2. Selection of the finite element type

Deterministic finite element analyses of a strip foundation on undrained soil stratum were performed using several types of 2-D plane strain elements, as discussed hereafter. An elastic perfectly plastic model with a Tresca yield criterion was selected. According to Hibbitt et al. (1998 & 2001) [92&94], a finite element analysis of a perfectly plastic material cannot predict a limit load, rather will predict a steady increasing load displacement curve attaining loads far in excess of the true limit load. This behaviour is due to volumetric locking. Reduced integration elements have fewer constraints for volumetric locking and, therefore, are recommended for this type of analysis. An alternative approach is to use a selectively reduced integrated approach. This method is available for 4-node full-integrated elements in ABAQUS/Standard. A comparison was performed to study these elements. Figure 4.3 shows the predicted force-displacement curves in terms of

normalized pressure vs. normalized settlement from four types of finite elements. The 4-node reduced integration element had the best performance (among elements available in ABAQUS/Standard for plane strain analysis) and the lowest computational cost; thus, it was selected for this study.

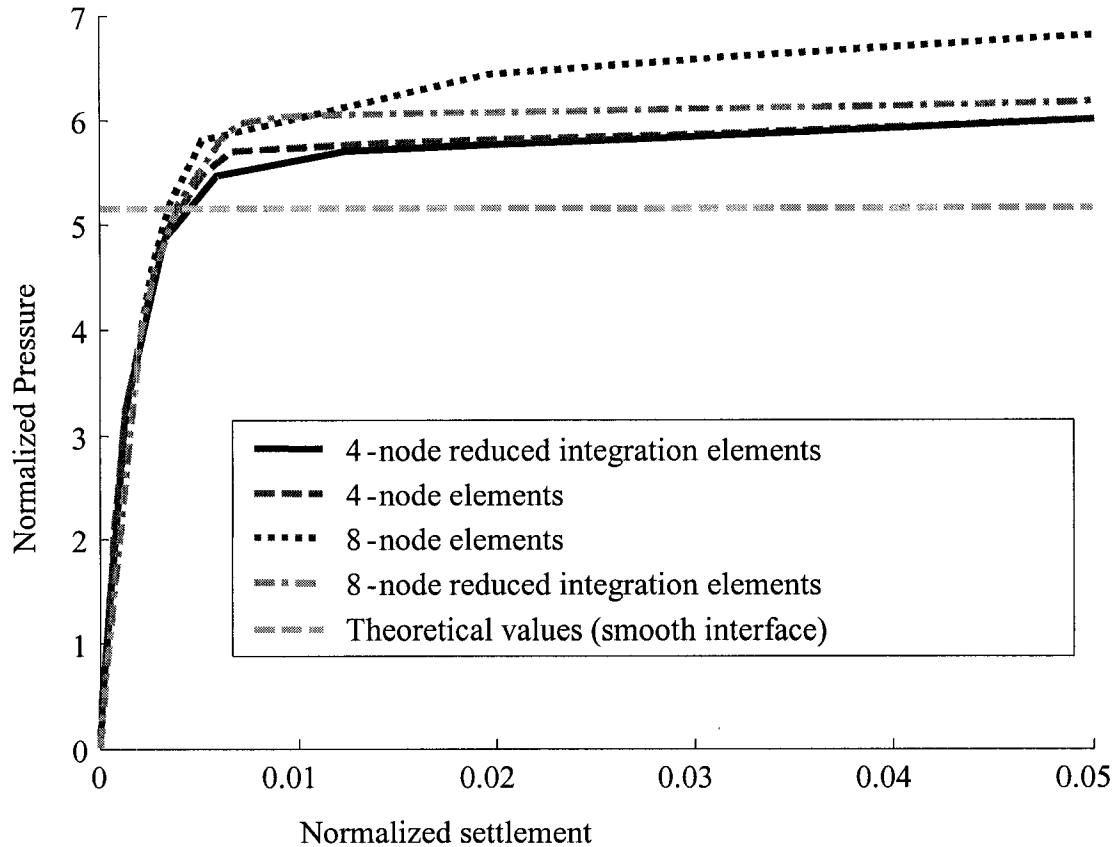


Figure 4.3 Comparison of the effects of element type on predicted bearing capacity of a shallow foundation.

4.2.1.3. Mesh size selection

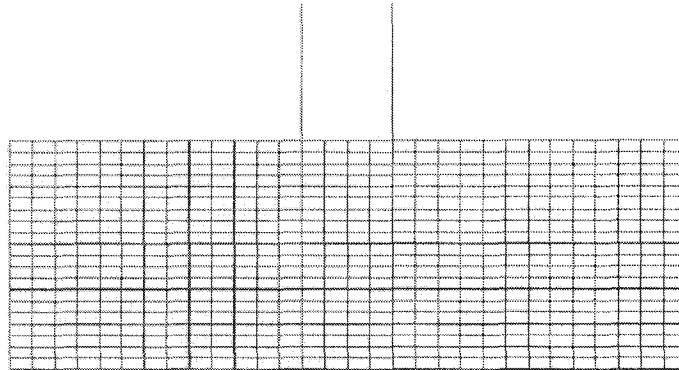
An appropriate size of the finite element mesh should be selected to correctly capture the failure mechanism and the failure load of the foundation. In addition, the mesh size should be capable of capturing the essential features of the correlation structure (e.g.

Popescu, 1995 [158]). Therefore, this mesh size depends on the correlation distances of the soil properties. Der Kiureghian and Ke (1988) [48] suggested that 0.25 to 0.5 of the correlation distance should be taken as maximum mesh size. The correlation distances in the vertical directions were assumed in range of 1m to 4m (minimum of 1 m). Therefore, a finite element size of 0.25m in the vertical direction was selected. Assumed horizontal correlation distances were larger than or equal to 4 m, imposing an upper limit of 1m to 2m on the finite element size in the horizontal direction.

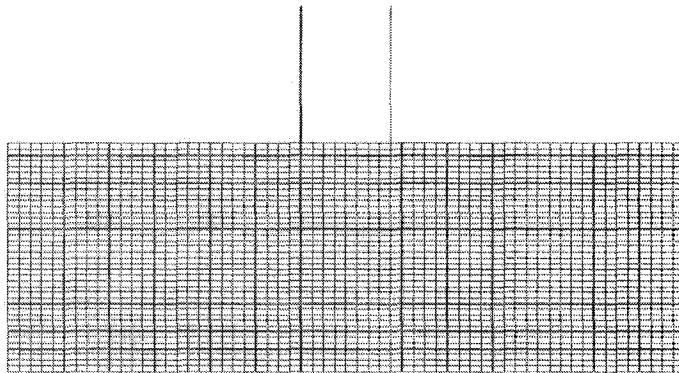
A study was performed on the effects of the mesh size on the predicted bearing capacity of the foundation. The different meshes used are shown in Figure 4.4. The results of foundation response in terms of normalized pressure vs. normalized settlement (p_n vs. Δ_n) are shown in Figure 4.5. The bearing capacity predicted by the numerical model was higher than the theoretical value obtained assuming a rigid perfectly plastic behaviour with a smooth contact surface between foundation and soil (shown by a dashed line in Figure 4.5). This difference was due to a number of reasons, including: 1) elastic perfectly plastic behaviour postulated here resulted in a gradual increase of plastic zones, which caused a steady increase in bearing capacity, and 2) use of a frictional contact surface below the foundation increased the bearing capacity due to its rough behaviour. It can be seen that the fine mesh yielded results that were closer to the theoretical value of 5.14. An explanation is the capability of a finer mesh to reproduce plastic strain concentration in narrower zones. In this study, a large number of finite element analyses were required. Exact numerical prediction of collapse load was not the main goal, rather its relative variation due to soil heterogeneity. Therefore, a finite element mesh size of 0.25m in the vertical direction and

0.5m in the horizontal direction was selected. This was labelled as “standard mesh” in Figure 4.5.

a.



b.



c.

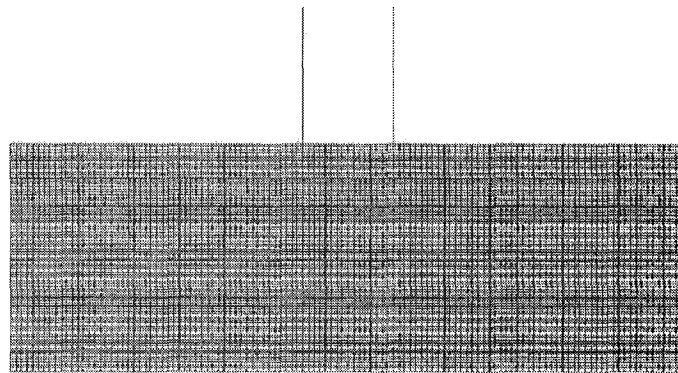


Figure 4.4 Finite element meshes for bearing capacity of foundation: (a) mesh size of 1.0 by 0.5 m (b) mesh size of 0.5 by 0.25 and (c) mesh size of 0.25 by 0.125m.

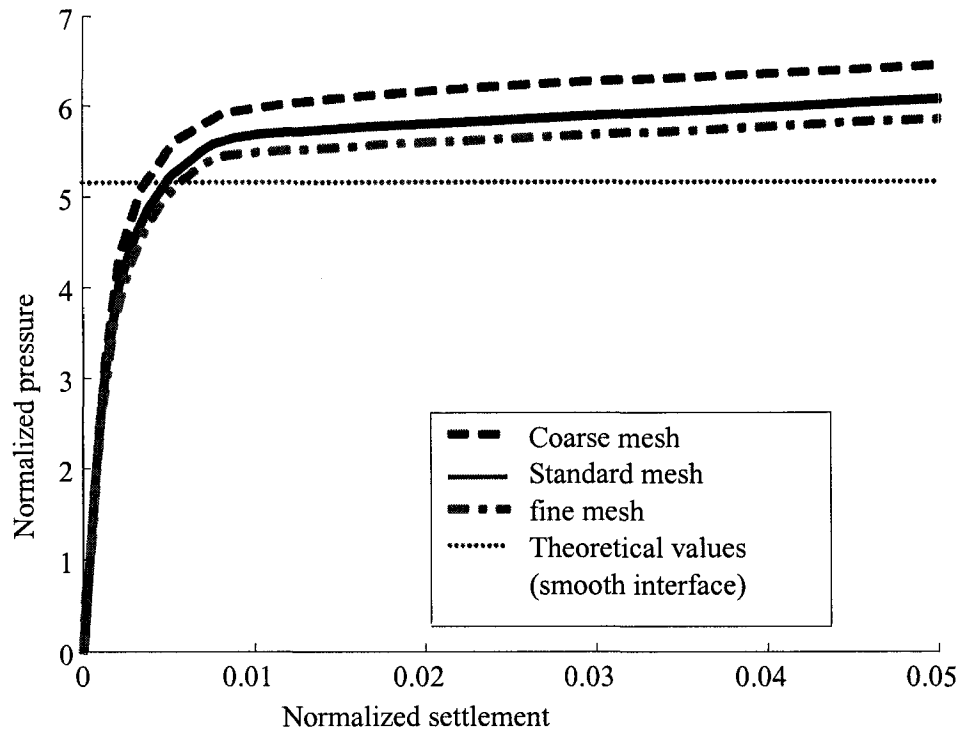


Figure 4.5 Effects of mesh size on the predicted bearing capacity of foundation.

4.2.1.4. Numerical issues

Bearing capacity of a strip footing on a uniform cohesive soil can be obtained using the theory of plasticity. However, estimation of the failure loads of geotechnical systems using the displacement finite element method faces numerical difficulties. It is well known that displacement-based finite element methods tend to over-predict the failure load of geotechnical systems. Many researchers have investigated the predictions of failure load of geotechnical systems and their difficulties particularly in an undrained situation (e.g. Nagtegaal et al, 1974 [132]; Merifield et al., 1999 [122]; Taiebat and Carter 2000 & 2002 [193&194]). Capturing a definite failure point for purely elastic perfectly plastic material is not possible. Taiebat and Carter (2000) [193] stated that for elastic perfectly plastic finite

element analyses of foundation subjected to vertical loading, it is very difficult to find a point at which the overall failure can be deemed to occur. They attributed this to gradual development of plastic zones. They used a small horizontal force to capture the failure point and defined the point of decrease in horizontal load as the failure load. In this study, a certain displacement was taken as the failure point after studying hundreds of finite element runs. The aim was to compare the results of uniform and heterogeneous soil; the bearing capacity at the same displacement for uniform and heterogeneous soil was obtained – i.e. at normalized settlement $\Delta_n = 0.0125$.

4.2.2 Deterministic Finite Element Analysis

4.2.2.1. Analysis set-up

Based on the study described in Section 4.2.1, the finite element mesh shown in Figure 4.1 was used in analysis hereafter. The lateral and horizontal boundary conditions are illustrated in Figure 4.1 and discussed in Section 4.2.1.1. The interface between soil and strip foundation was modelled using the contact surface capability implemented in ABAQUS/Standard. A frictional Coulomb interface with separation capability was considered between the foundation and soil. The limiting value for the shear resistance at the interface was taken to be about one third of the undrained shear strength of soil (Paulin, 1998 [150]). The soil was discretized using 2400 4-node linear finite elements with reduced integration (CPE4R). Vertical displacements were gradually imposed to the centre of the foundation base to simulate a vertical central load at the foundation level. Some researchers suggest that imposing vertical displacements instead of loads tends to overestimate collapse

load. However, applying force creates numerical difficulties related to softening of the foundation. The model had large deformation/strain formulations and was capable of capturing unsymmetrical behaviour.

An elastic perfectly plastic model with a Tresca yield criterion was selected for this study (see Section 3.5.2.3 for discussion). The model required the following constitutive parameters: Young's modulus (E), Poisson's ratio (ν), and cohesion (c_u). A uniform overconsolidated soil stratum with average undrained shear strength, c_u of 100kPa is considered in deterministic analysis. A range for the Young's modulus for undrained loading was assumed by considering two extreme values: $E = 300 c_u$ and $E = 1500 c_u$ (see Bowles, 1997 [20] for typical values of soil stiffness). A value $\nu = 0.49$, appropriate for undrained conditions, was assumed for the Poisson's ratio.

4.2.2.2. *Results*

Finite element results in terms of normalized pressure vs. normalized settlement are presented in Figure 4.6 for two cases: (a) high E , using Young's modulus $E = 1500 c_u$ and (b) low E , using Young's modulus $E = 300 c_u$. Pressure beneath the foundation and foundation settlement were normalized by dividing by soil shear strength and foundation width respectively. Figure 4.6 shows that failure load may not be exactly the same for the foundation placed on stiff soil and soft soil. To avoid the interference of these effects with the effects of soil heterogeneity, Monte Carlo simulation results were always compared relative to their corresponding base cases – namely deterministic analysis results.

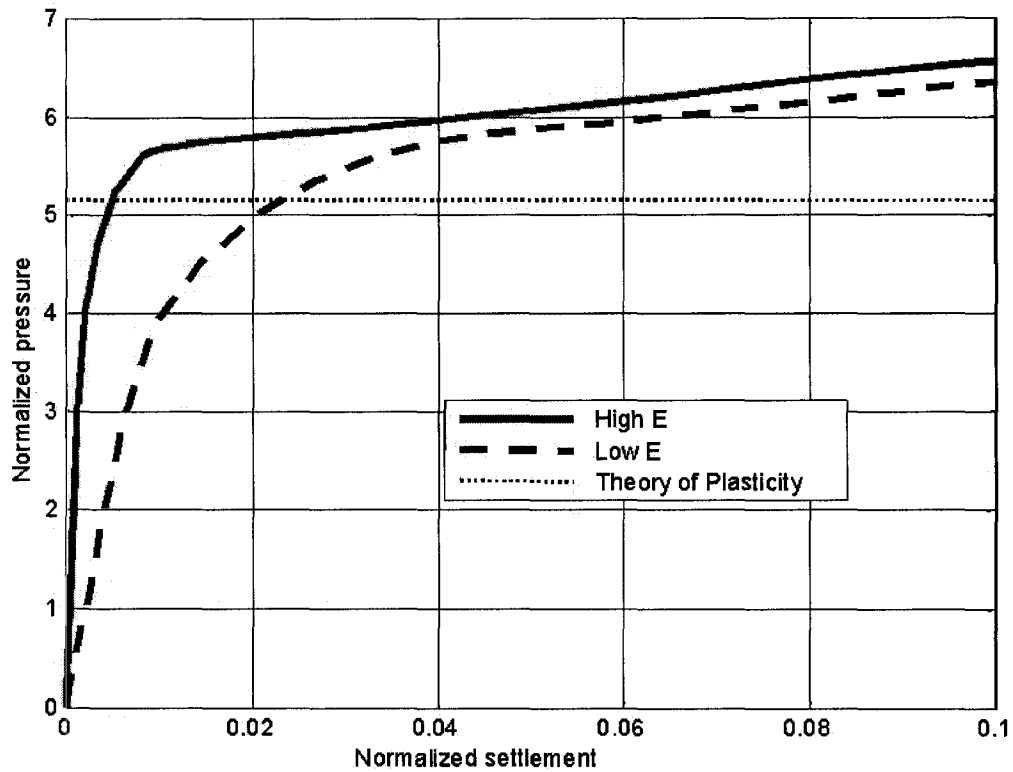


Figure 4.6 Predicted normalized pressure vs. normalized settlement curves for a strip foundation placed on uniform soil.

4.2.2.3. *Effects of imperfection in deterministic analysis*

The effects of an imperfection in the soil were investigated by considering a uniform soil with an imperfection presented by a small portion of the soil comprised of four finite elements with $c_u = 200$ kPa, as shown in Figure 4.7a. The results of the two analyses are compared in Figure 4.7b&c. The imperfection imposed significant changes in the behaviour of the soil-structure system. Obviously, there was no rotation in the uniform soil but the soil with imperfection induced a significant rotation of the foundation, which could become a governing criterion from serviceability aspect. The evolution of equivalent plastic strain contours (Figure 4.8) illustrates the predicted failure mechanism. Results showed that

ABAQUS/Standard is able to capture the effects of imperfection in failure mechanism and soil spatial variability may cause significant changes in the response of the foundation.

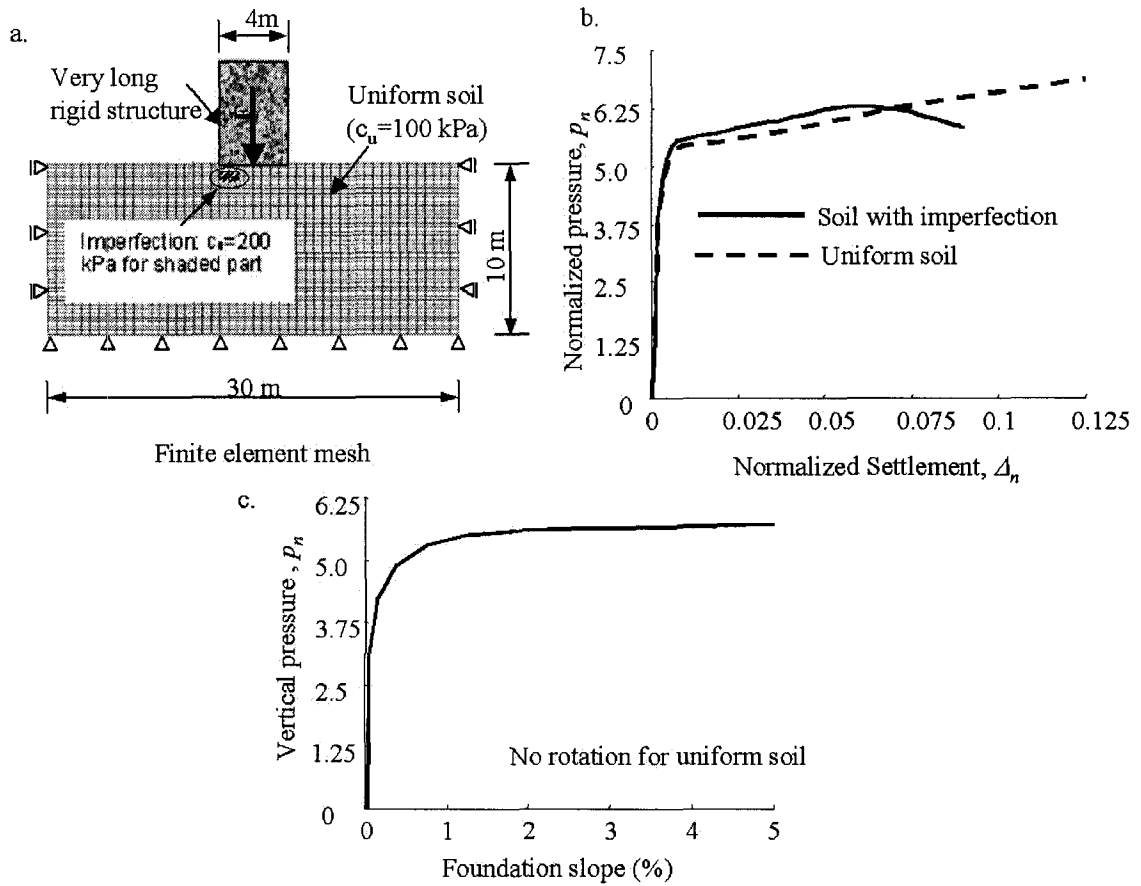


Figure 4.7 Analysis of the effects of imperfection with ABAQUS/Standard: (a) finite element mesh (b) Predicted pressure-settlement relationship of the foundation on uniform soil and soil with imperfection; (c) Predicted pressure-rotation relationship of the foundation on soil with imperfection.

The equivalent plastic strain, γ , is expressed as (Hibbitt et al. 1998),

$$\gamma(t) = \gamma_0 + \int_0^t \sqrt{\frac{2}{3} d\gamma : d\gamma} \quad \text{Eq. 4.1}$$

where $\gamma_0 = 0$ is the initial equivalent plastic strain and $d\gamma$ is the plastic strain rate tensor – the operator “:” represents the trace of two tensors.

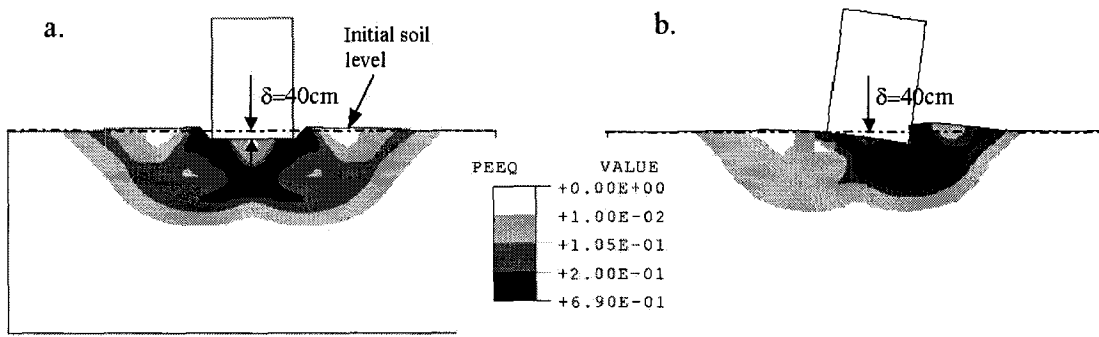


Figure 4.8 Predicted deformed shape and contours of equivalent plastic strain, γ , for a foundation on uniform soil and soil with imperfection at settlement $d=40$ cm: a. uniform soil; b. soil with imperfection.

4.3. STOCHASTIC FINITE ELEMENT ANALYSIS

4.3.1 The Studied Ranges of Probabilistic Characteristics for Soil Variability

Soil probabilistic model and its parameters were selected based on values published in the literature review (as discussed in Section 2.1 and 3.2). Since shallow foundations are usually placed on medium to stiff clays, a range of $C_V = 10\%$ to 40% was selected for soil

beneath shallow foundations. This was based on findings in the literature review (Section 2.1.1.3). A separable correlation structure with ranges of scale of fluctuations, $\theta_{nn} = \theta_h/B = 1.0$ to 4.0 , and $\theta_{vn} = \theta_v/B = 0.25$ to 1.0 , was considered in the parametric study (where B is the width of the foundation, and θ_h and θ_v are correlation distances in the horizontal and vertical directions). Two different probability distribution functions were assumed for the soil strength: (1) a Gamma distribution skewed to the right, and (2) a symmetrical Beta distribution (see Figure 3.2).

4.3.2 Finite Element Analysis with Spatially Variable Soil

Figure 4.9b and Figure 4.9c show the results of a finite element analysis with spatially variable soil properties in terms of plastic shear strains. Figure 4.9a shows the point variability of shear strength over the domain of interest. This point variability was mapped to the finite element mesh using the mid-point method, as discussed in Section 3.5.4. Figure 4.9b and Figure 4.10b show how a local shear failure develops below the foundation at a much lower bearing pressure than the general symmetric failure in Figure 4.8a does. Subsequently, increasing the imposed foundation settlement caused another asymmetric general shear failure to develop. It should be mentioned that both failure surfaces were developed mainly through the loose pockets of soil, indicated by darker patches in Figure 4.9a. Figure 4.10 shows the predicted normalized pressure/normalized settlement and normalized pressure/slope for the sample realization of heterogeneous soil shown in Figure 4.9. The effects of soil heterogeneity were clearly captured by the finite

element model. Spatial variability of soil shear strength affected the failure mechanism and response of the foundation.

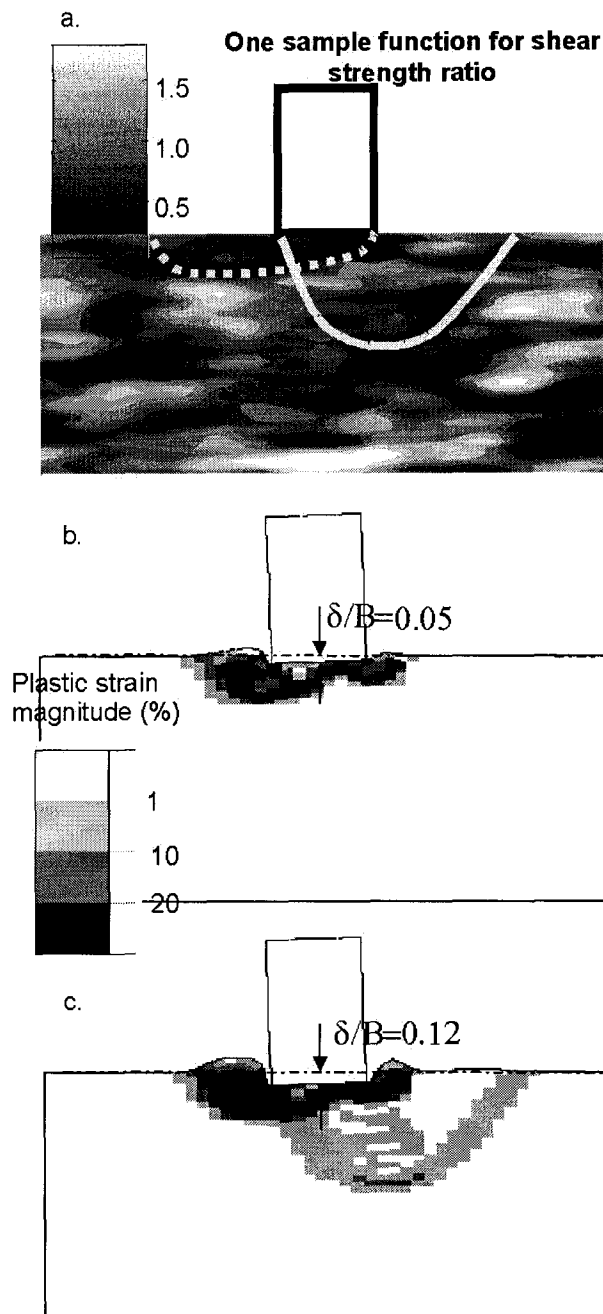


Figure 4.9 A finite element analysis with spatially variable soil input (one sample realization of Monte Carlo simulations) (a) realization of undrained shear strength – the contours shows the ratio of actual undrained shear strength to the average value used in the deterministic analysis, (b) contours of plastic shear strain showing the local failure and (c) contours of plastic shear strain – asymmetric general shear failure.

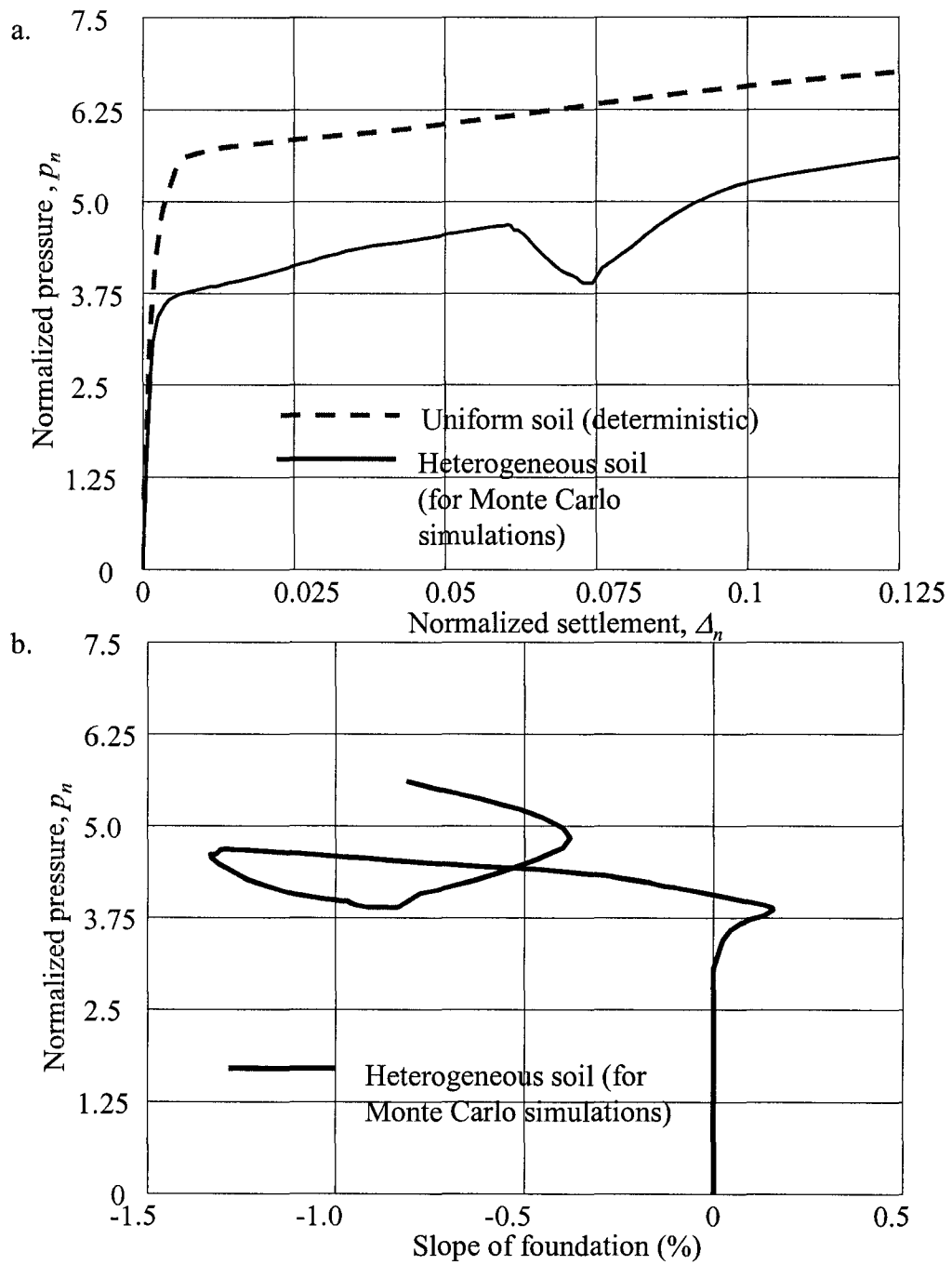


Figure 4.10 A typical finite element analysis of foundation on the sample realization of heterogeneous soil from Figure 4.9 (a) predicted pressure-settlement relationship, and (b) predicted pressure-rotation relationship.

4.3.3 Monte Carlo Simulation Results

4.3.3.1. Example of a typical analysis

Results of a study by Nobahar and Popescu (2000) [137] assuming a Beta distribution with $C_V = 40\%$ for undrained shear strength and correlation distances: $\theta_{hn} = 1.25$ and $\theta_{vn} = 0.25$, are summarized in Figure 4.11. This figure presents the results of Monte Carlo simulations for 100 sample functions representing possible realizations of soil strength distribution over the domain of analysis by thin lines in terms of normalized-pressure vs. normalized-settlement. A similar curve resulting from a deterministic analysis is represented by a thick dashed line. The Monte Carlo simulations, accounting for spatial variability of soil strength, yielded bearing capacity values that were generally lower than those predicted by the deterministic analysis. It is mentioned that the average soil strength used in the Monte Carlo simulations was equal to the uniform soil strength used in the deterministic analysis. Asymmetric foundation failure mechanisms, as captured in the Monte Carlo simulations (Finite element analysis with variable soil as shown in Figure 4.12), lead to earlier shear failure than predicted by the deterministic analysis assuming perfect symmetry. In addition, the deterministic analysis did not produce any foundation rotation. On the other hand, the Monte Carlo simulations, accounting for spatial variability of soil properties, resulted in significant rotations in foundation. These rotations may become the main criterion for the foundation design. Figure 4.11b shows the normalized pressure versus rotation relations predicted by Monte Carlo simulations. The predicted deformed mesh and the contours of equivalent plastic strains are shown in Figure 4.12 for

one of the samples used in Monte Carlo simulations (pressure-settlement and pressure-rotation curves for that sample function are shown by thick continuous lines in Figure 4.11).

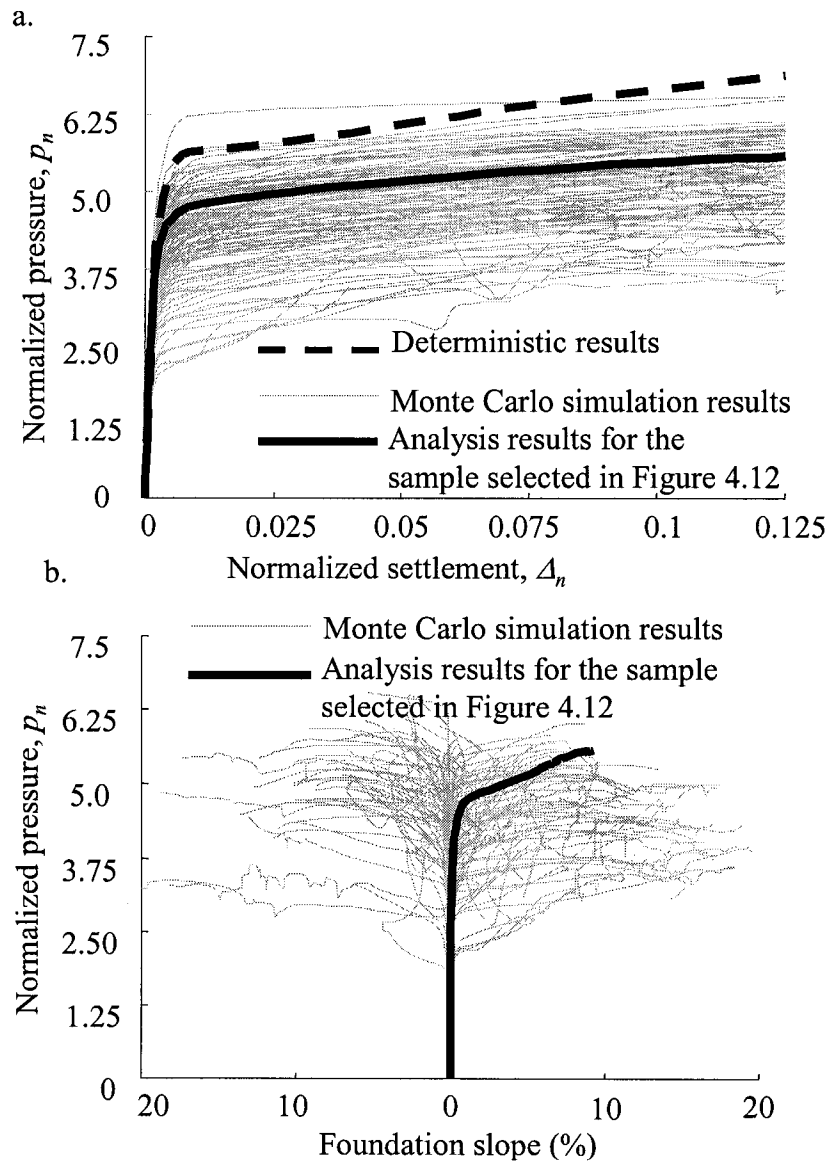


Figure 4.11 Comparison of Monte Carlo simulations and deterministic analysis results: a. pressure-settlement curves; b. pressure-rotation curves (no rotation is predicted in the deterministic analysis).

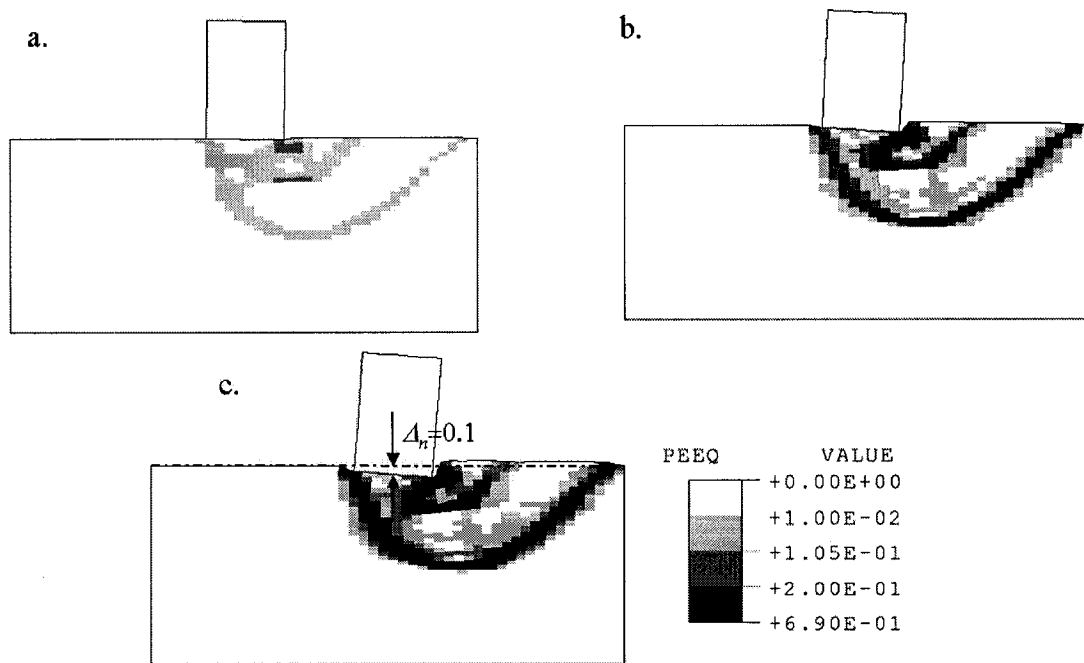


Figure 4.12 Predicted deformed shape and contours of equivalent plastic shear strain, γ :
a. normalized average settlement $\Delta_n = 0.0125$; b. $\Delta_n = 0.0625$; c. $\Delta_n = 0.1$.

Next, the average and 95-percentile of these results were calculated at each displacement or foundation slope value (Figure 4.13). Based on the assumptions in this study and considering a value $\Delta_n = 0.0125$ as the reference settlement (corresponding to ultimate bearing capacity), the average bearing capacity value resulting from Monte Carlo simulations was 25% lower than that predicted by the deterministic analysis. As in conventional approaches, a deterministic analysis was performed using a nominal soil strength value considerably lower than the average value (namely the 95-percentile of soil strength) and the results were compared with Monte Carlo simulation results. As seen in Figure 4.13, the 95-percentile value of bearing capacity resulting from the Monte Carlo

simulations exceeds by 38% the bearing capacity resulting from a deterministic analysis using the 95-percentile of soil shear strength.

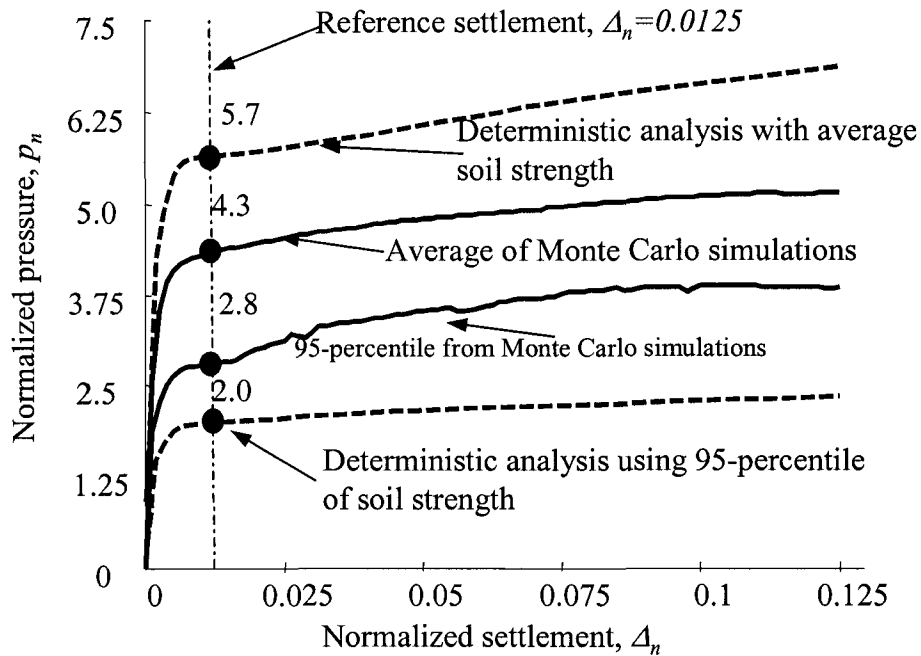


Figure 4.13 Comparison of deterministic and Monte Carlo simulation results for average and 95 percentile: a. pressure-settlement relationships; b. pressure-rotation relationships.

4.3.3.2. Effects of probability distribution of soil strength

A series of Monte Carlo simulations was performed assuming a Gamma distribution for the soil shear strength. The distribution is skewed to the right (shape parameter $\lambda = 1.73$ and skewness coefficient $\sqrt{\beta_1} = 1.15$). The same degree of variability ($C_V = 40\%$) and correlation structure were assumed as for the Beta-distributed soil strength (described in the previous section). The two probability density functions are presented in Figure 3.2. The ranges of results for the two series of Monte Carlo simulations, as well as the predicted average pressure-settlement relations are presented in Figure 4.14. The results

showed that the shape of the left tail of the distribution (i.e. amount of loose pockets in the soil mass, see Figure 3.2) affected both the predicted variability (Figure 4.14a&b) and the predicted average values (Figure 4.14c) of bearing capacity.

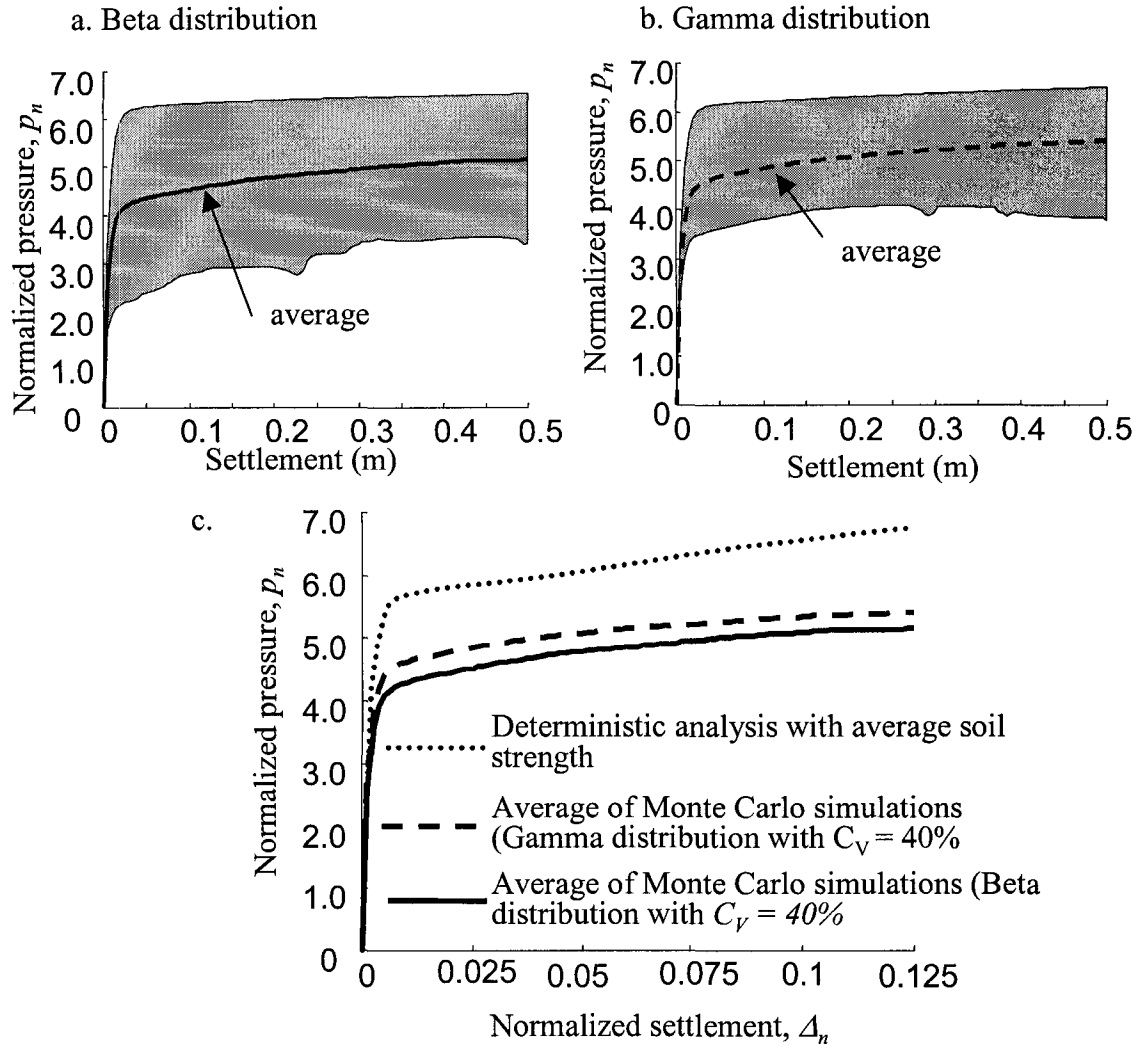


Figure 4.14 Comparison of Monte Carlo simulations: a. symmetric Beta distribution b. skewed Gamma distribution c. averages resulting from Monte Carlo simulations and deterministic analysis.

Nobahar and Popescu (2001) found that the shape of the left tail of probability distribution function, which indicates presence of loose pockets in the soil mass, has a significant impact on the predicted mean bearing capacity. Figure 3.2 shows the Beta and Gamma probability distribution functions used for simulating the undrained shear strength in the two examples presented here (both have the same mean and coefficient of variation). It can be seen that the Beta distribution has a much fatter left tail than Gamma distribution, which represents the amount of loose pockets in the soil mass. The effects of probability distribution were statistically studied in a parametric study, as discussed in Section 4.4.

4.3.3.3. *Effects of variance*

It was observed in the literature review (e.g. Popescu et al. 1998c [165]) that the degree of variability (variance) of soil strength was the most important factor affecting soil behaviour. A parametric study was performed here to investigate its effects on bearing capacity. Five sets of Monte Carlo simulations were carried out for a range of coefficients of variation of shear strength. The Gamma probability distribution was assumed for the soil strength with $\theta_m = 1.25$ and $\theta_m = 0.25$ (A similar study was performed using Beta-distributed soil shear strength. Similar results were obtained, but are not reported here). Monte Carlo simulations were performed for five different coefficients of variation ($C_V = 10\%, 20\%, \dots, 50\%$) using 100 sample functions for each value of the coefficient of variation. The results of Monte Carlo simulations in terms of average values are presented in Figure 4.15. As the coefficient of variation of shear strength increases, the average predicted bearing capacity decreases. This again emphasizes the effects of the loose

pockets in the soil mass on the predicted bearing capacity. Also, it was observed in all cases that the scatter in the predicted bearing capacity was significantly lower than those assumed for the shear strength (Table 4.1). This effect of decrease in the response variance is well known to be the effect of local averaging (Vanmarcke, 1977 & 1983 [208 & 209]). Local averaging effects are further discussed in the next section.

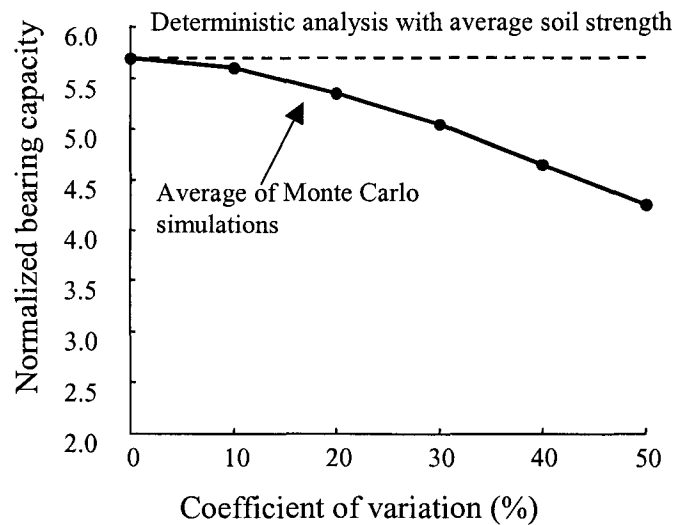


Figure 4.15 Influence of the coefficient of variation of soil strength on bearing capacity.

Table 4.1 Coefficient of variation: input for soil strength and resulting for predicted bearing capacity.

C_V (soil shear strength) %	10	20	30	40	50
C_{VBC} (predicted bearing capacity) %	2	6	9	13	16

4.3.3.4. *Effects of local averaging*

The study was further developed to investigate the effects of horizontal correlation distances. The ratio of horizontal correlation distance to foundation width can take a large range of values. Here a range of 1.25 to 4.0 was investigated. The Gamma-distributed soil shear strength (Figure 3.2) with coefficient of variation of 40% is considered. The results of Monte Carlo simulation are presented in Table 4.2. The reduction in coefficient of variation of bearing capacity was also calculated using the variance reduction function (Vanmarcke, 1983 [209]) and reported in the table. The mean bearing capacity ratio, R_{nBC} was defined as the ratio of the mean bearing capacity of heterogeneous soil resulting from Monte Carlo simulations to that of uniform soil having the same average shear strength. It can be seen in Table 4.2 that both the mean and the coefficient of variation of the predicted bearing capacity increase with increasing horizontal correlation distance. The last line represents the results that would be obtained using a large number of sample functions in which the undrained shear strength of the soil is uniform over each sample, but varies from one sample to another according to the probability density function shown in Figure 3.2.

The decrease in the coefficient of variation of the resulting bearing capacity leads to a higher reliability of a foundation. This is the effect of local averaging (e.g. Vanmarcke, 1977 & 1983 [209]). Failure occurs along a slip surface, therefore, there is a variability reduction in the predicted bearing capacity due to spatial averaging. This phenomenon is known and accounted for in reliability assessment of geotechnical structures (See Li and Lam, 2001 [110], Cherubini, 2000 [29], Casrdozo and Fernandes, 2001 [24]).

Table 4.2 Results of Monte Carlo simulation for the effects of horizontal correlation distance

θ_{hm}	Mean bearing capacity ratio, R_{nBC}	Coefficient of variation of bearing capacity (%)	Coefficient of variation of bearing capacity (analytical approximations – Eq. 4.2)
1.25	0.81	13.1	13.4
2.0	0.82	14.9	16.1
4.0	0.838	17.3	19.5
Uniform soil	1.0 (*)	40 (*)	40

(*) Theoretical values, not resulting from actual Monte Carlo simulations

A sample calculation for variance reduction factor based on Vanmarcke (1983) [209] is presented. For local averaging theory, the reduction in variance over a two-dimensional domain having length of T_1 and width of T_2 was defined by,

$$\sigma_T^2 = \gamma(T_1, T_2) \sigma^2 \quad \text{Eq. 4.2}$$

where $\gamma(T_1, T_2)$ is the variance reduction function, σ_T^2 is the reduced variance, and σ^2 is the point variance. The variance reduction function for a homogeneous (quadrant symmetry) is defined as,

$$\gamma(T_1, T_2) = \frac{4}{T_1 T_2} \int_0^{T_1} \int_0^{T_2} \left(1 - \frac{\tau_1}{T_1}\right) \left(1 - \frac{\tau_2}{T_2}\right) \rho(\tau_1, \tau_2) d\tau_1 d\tau_2 \quad \text{Eq. 4.3}$$

The correlation function is separable here ($\rho(\tau_1, \tau_2) = \rho(\tau_1) \cdot \rho(\tau_2)$) and is defined in Eq. 3.18. The domain for averaging was selected based on Prandtl theoretical solution for cohesive soil as $3B$ in length and $0.7B$ in depth (B is the foundation width). The above

integral was numerically solved for the cases presented in Table 4.2 and the values of obtained coefficients of variation are reported. These values were generally in agreement with results of Monte Carlo simulations. The difference can be attributed to changes in failure mechanism and the fact that the resulting variability depends on variability on failure surface, which cannot be captured exactly with a theoretical solution.

However, the effects of spatial variability on mean bearing capacity should also be considered in a reliability assessment. To illustrate these effects, a required overall safety factor was calculated to secure a probability of failure of 10^{-4} . For this calculation, a theoretical probability distribution was fitted to predicted results, as discussed in Section 4.3.3.5. Then it was extrapolated to the target level; load variability was ignored for simplification. Similarly, the required safety factor was calculated accounting only for the reduction in the predicted coefficient of variation (using Eq. 4.2). The results are presented in Table 4.3. The table illustrates the importance of changes in failure mechanism. Accounting only for the effects of local averaging on bearing capacity variability, the required safety factors are about 20% lower in Table 4.3. Not accounting for spatial averaging may lead to overestimating the probability of failure, while only considering the beneficial effects of local averaging and ignoring the changes in failure mechanism that would induce a significant reduction in the mean bearing capacity, may result in underestimating the failure probability. For example, the required safety factor is $FS = 3.1$ for uniform soil with variable mean shear strength (the last line in Table 4.3). Whereas assuming $\theta_h/B = 2$, the required safety factor from Monte Carlo simulations accounting for

changes in failure mechanism is $FS = 2.3$ and in the case where only the reduction of soil variability due to local averaging is considered, the required safety factor is $FS = 1.84$.

Table 4.3 Required safety factors, FS obtained from 100 sample functions

θ_v/B	Factor of safety for target failure probability of 10^{-4} (Monte Carlo simulation)	Factor of safety for target failure probability of 10^{-4} (analytical approximations)
1.25	2.1	1.66
2.0	2.3	1.84
4.0	2.5	2.09
Uniform soil	3.1 (*)	3.1

(*) Theoretical value, not resulting from actual Monte Carlo simulations

Limit state design methods can be used to obtain a uniform safety level. The resulting failure probability from limit state design methods depends on the selection of characteristic values and the partial safety factors. Eurocode 7 (ENV 1997-1, 1994 [59]) states that statistical methods may be used in the selection of characteristic values for ground properties, which should be derived such that the calculated probability of a worse value governing the occurrence of a limit state is not greater than 5%. Using 95-percentile values of soil strength as characteristic values is often too conservative and practically not acceptable in many geotechnical applications due to the large natural variability of soil properties. The Monte Carlo simulation method used here accounted for both the beneficial effects of local averaging and the decrease in mean predicted bearing capacity, and could, therefore, produce reasonable characteristic values for undrained shear strength.

The factors of safety reported in Table 4.3 only account for the effects of natural variability of soil properties, while ignoring other sources of uncertainty, such as measurement errors, model uncertainty and load variability.

4.3.3.5. *Sample size*

One hundred sample functions were used for each analysed case reported in this section (Section 4.3). For $C_V = 40\%$, a Gamma probability distribution and $\theta_{nn} = 1.25$, 1200 sample realizations were analysed to investigate the effects of sample size. Figure 4.16 shows the effects of sample size on the predicted mean and coefficient of variation; it can be seen that the predicted mean and variance remain practically constant for sample sizes larger than 100. In addition to the mean and standard deviation, the cumulative probability distribution of the predicted bearing capacity was analysed. Lognormal and gamma probability distributions were fitted to the empirical probability distribution function of the predicted bearing capacities (Figure 4.17). Figure 4.18 shows the same fits in logarithmic scale for cumulative probability distributions. The left tail, representing the presence of loose zones in the soil mass, has significant importance in design. Therefore, the left tails of these probability distributions are also illustrated in Figure 4.17 (similar plots are shown for cases with 100 sample functions in Appendix B). Both Gamma and lognormal distributions seem to be acceptable at least for inferring the mean and coefficient of variation of the response. Use of this type of extrapolation in risk analysis with high reliability levels (e.g. probability of failure of 10^{-3} to 10^{-4}) is, however, debatable (probability distribution of the response at tails is not known). A Gamma fit was used to extrapolate the results of predicted bearing capacity to obtain factors of safety in Table 4.3.

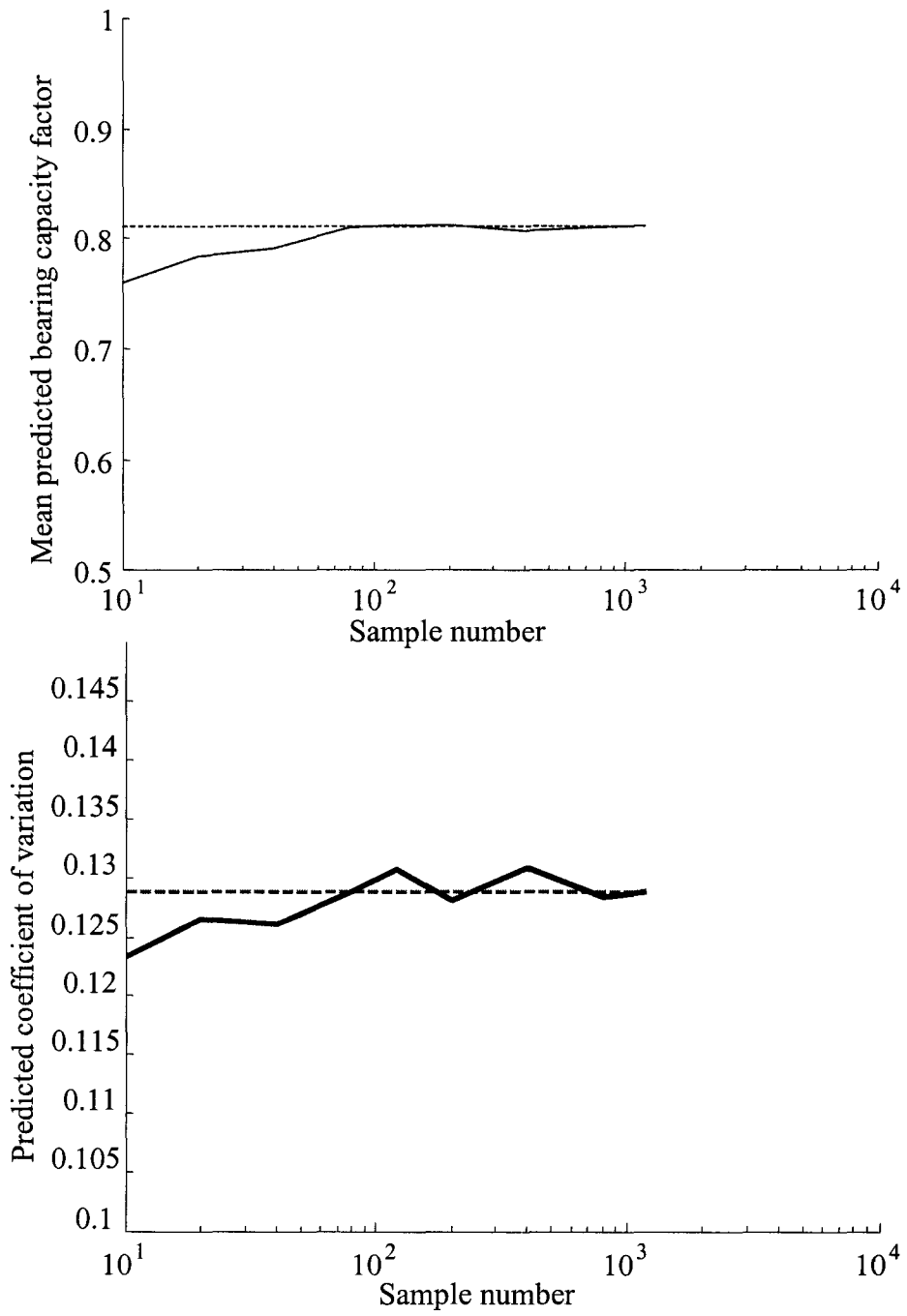


Figure 4.16 Effects of sample size on predicted mean and standard deviation.

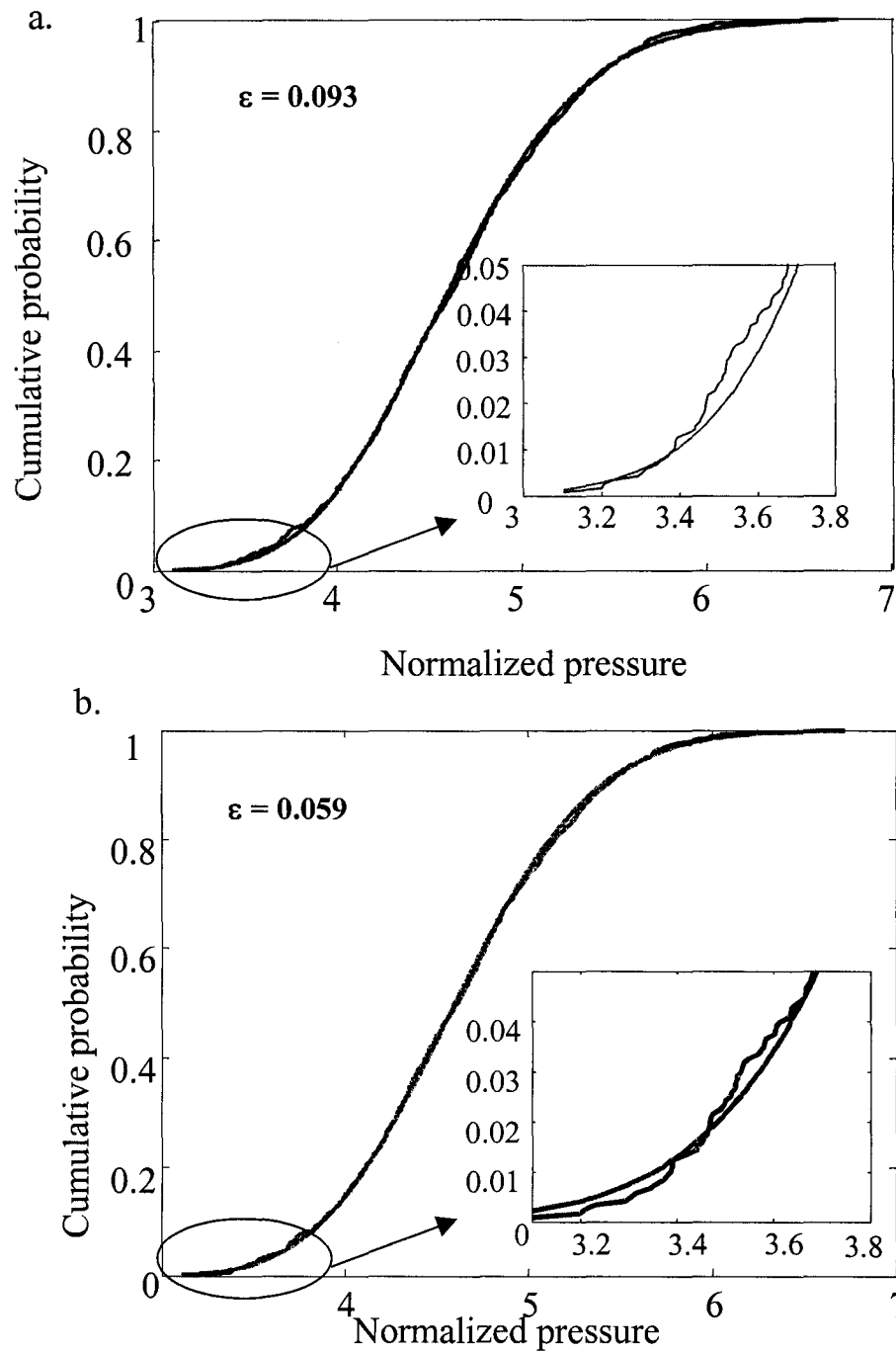


Figure 4.17 Fitting probability distribution to the empirical probability distribution function of the predicted bearing capacity for 1200 samples using method of moments: (a) Lognormal fit and (b) Gamma fit.

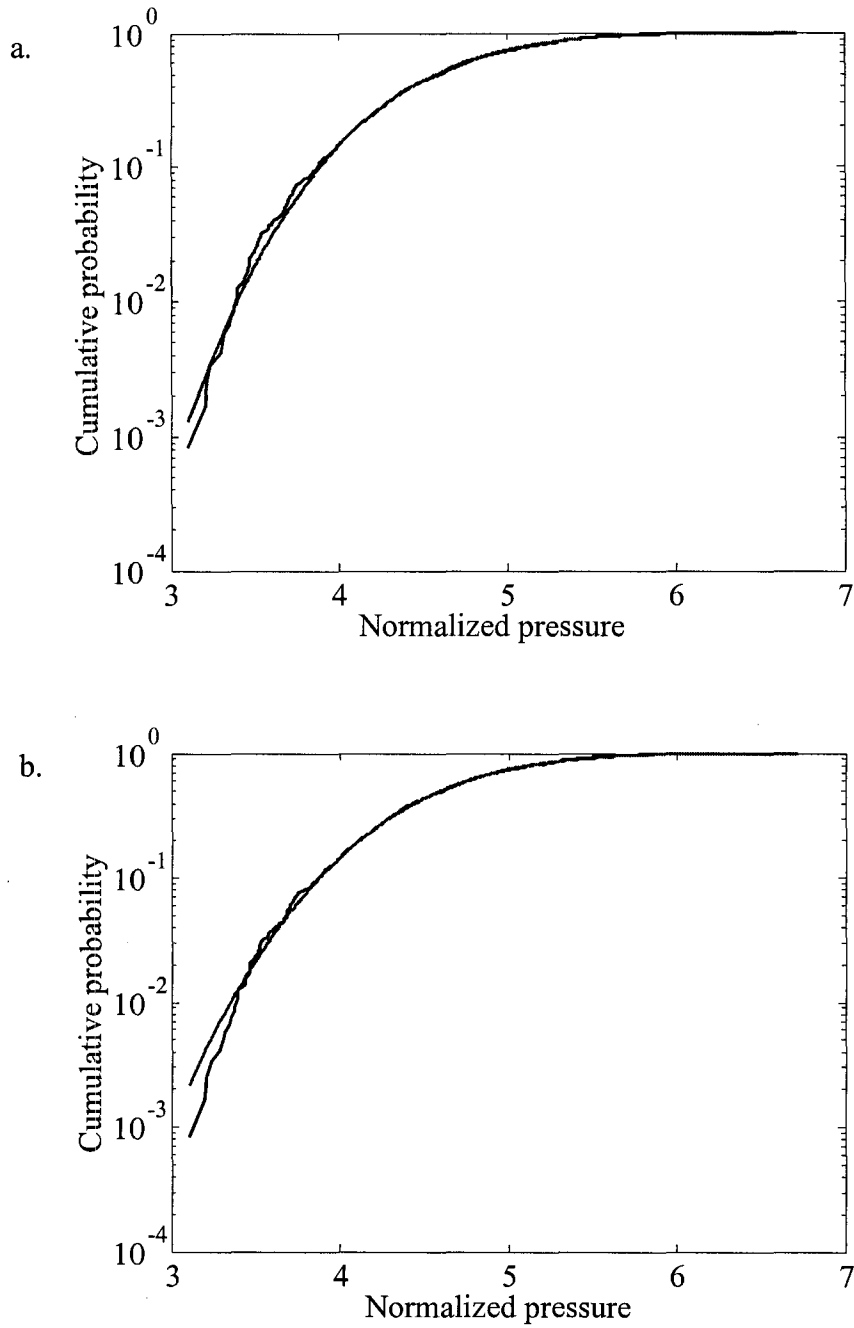


Figure 4.18 Fitting probability distribution to the empirical probability distribution function of the predicted bearing capacity for 1200 samples using method of moments: (a) Lognormal fit and (b) Gamma fit.

4.3.4 Accounting for Three-Dimensional Soil Variability

This study investigated the effects of soil heterogeneity for a rigid strip footing assuming two-dimensional plane strain condition. This implied that an infinite correlation distance was considered in one horizontal direction. These assumptions are commonly acceptable in foundation engineering.

It was shown in this study that accounting for soil heterogeneity resulted in variability of predicted structural response as well as decrease of average predicted bearing capacity (due to changes in failure mechanism).

It is deemed that when adding the 3rd direction in the analysis, the variability of predicted response will be reduced. As shown in Sections 4.3.3 & 4.4.3, at finite correlation distances, θ_h/B , the variability in the predicted response resulted in significantly lower values than input variability (i.e. variability of actual soil strength). This is due to local averaging of soil strength over the length of the failure surface. Based on those results, it is deemed that, for the real situation with soil variability in the third direction ($\theta_h/L < \infty$, where L is the actual length of foundation), the predicted response variability will be smaller than that predicted for 2D assumption. In this respect, 2D results are conservative.

With respect to average bearing capacity, when accounting for real 3D variability, the predicted failure surface will have more degrees of freedom, so it is expected that the average shear strength over the failure surface will be lower than for the 2D case. However, the 3D layout will generally result in a larger area per meter of foundation length for the failure surface than the 2D one due to end effects, with an expected increase in predicted overall bearing capacity. In conclusion, it is expected that the 2D approach gives

conservative results for a real situation. A more accurate evaluation of 3D effects can be further studied using 3D Monte Carlo simulations in the future.

4.4. PARAMETRIC STUDIES

4.4.1 Design of Experiments

As described in Section 3.3.2, a statistical methodology called design of experiments (DOE) was used here to pre-design the parametric studies. Two design approaches were used: (1) factorial method with central point and (2) face-centred central composite design. The Design-Expert® software (2000) [50] was used to design the experiments. Next, a set of Monte Carlo simulations was performed for each experiment – 18 cases for factorial and 30 cases for central composite design. For each experiment, 100 finite element runs were executed. It should be mentioned that 18 points of the factorial design were included among the 30 points of the central composite design. Therefore, 3000 nonlinear finite element analyses were performed for the parametric study using $E/c_u = 1500$. A similar study was also performed for $E/c_u = 300$. However, for this case, based on the results obtained for $E/c_u = 1500$, the vertical correlation distance was screened out from the study. It was also concluded in the first study (with $E/c_u = 1500$) that factorial design adequately captured the curvature in the responses. Thus, using a factorial design, only 10 cases were analysed in the second study, with $E/c_u = 300$.

4.4.1.1. Factorial design

The design layout for factorial method is presented in Table 4.4 (see Figure 3.3 for illustration of the factorial design). Factorial design is one of the most efficient designs. It is very useful in screening the main influencing factors. However, it may fail to capture curvatures in the response surface. To monitor the curvature, a central point was added to the factorial design (experiments 17 and 18 in Table 4.4).

Table 4.4 Factorial design for foundation analysis on heterogeneous soil

	Factor 1 (Numerical)	Factor 2 (Numerical)	Factor 3 (Numerical)	Factor 4 (Categorical)
Experiment #	Coefficient of variation, C_V (%)	Normalized horizontal correlation distance, θ_{hn}	Normalized vertical correlation distance, θ_{vn}	Probability distribution
1	10	1	0.25	Gamma
2	40	1	0.25	Gamma
3	10	4	0.25	Gamma
4	40	4	0.25	Gamma
5	10	1	1	Gamma
6	40	1	1	Gamma
7	10	4	1	Gamma
8	40	4	1	Gamma
9	10	1	0.25	Beta
10	40	1	0.25	Beta
11	10	4	0.25	Beta
12	40	4	0.25	Beta
13	10	1	1	Beta
14	40	1	1	Beta
15	10	4	1	Beta
16	40	4	1	Beta
17	25	2.5	0.625	Gamma
18	25	2.5	0.625	Beta

4.4.1.2. *Central composite response surface*

The central design approach needed a higher number of experiments. A face-centred design was used here. The design, together with results of Monte Carlo simulations, is presented in Table 4.5; see Figure 3.3 for illustration of the central composite design. It had 12 additional points compared to the factorial method. This method is believed to be capable of capturing higher degrees of curvature in the results.

4.4.2 **Statistical Analysis of Results**

Using the results of Monte Carlo simulations, a cumulative probability distribution of ultimate bearing capacity was obtained for each case. From these CDFs, four responses were estimated for ultimate bearing capacity: (1) mean bearing capacity ratio, R_{BC} , (2) standard deviation, (3) characteristic bearing capacity (95-percentile), and (4) bearing capacity at failure probability of 10^{-4} by fitting a lognormal probability distribution using the method of moments, as shown in Table 4.6. It should be mentioned that the values of bearing resistance at failure probability level as low as 10^{-4} may have significant errors due to extrapolation of the fitted probability distributions. In other words, the number of replications of Monte Carlo simulations was insufficient, as discussed in Section 4.1.3. These values were normalized respectively as (1) mean bearing capacity ratio, R_{BC} , defined as the ratio of bearing capacity of heterogeneous soil to the bearing capacity of uniform soil having the same average shear strength, (2) coefficient of variation of bearing capacity from heterogeneity effects C_V , (3) characteristic (nominal) bearing capacity ratio, R_{nBC} , defined similar to R_{BC} , and (4) normalized bearing capacity at target probability level 10^{-4} ,

R_{iBC} , also defined similar to R_{BC} . The results are shown in Table 4.5 for $E = 1500c_u$ and in Table 4.6 for $E = 300c_u$. These results are discussed and analysed in the next section. As discussed earlier, the results of the first study ($E = 1500c_u$) were used to screen out unnecessary experiments for the second study ($E = 300c_u$). Hence, the number of experiments was reduced from 30 to 10.

Similarly, cumulative distributions of bearing pressure for the three serviceability criteria discussed in Section 4.5.2 were obtained. A lognormal fit was used for these curves; therefore, bearing pressure CDF curves at the reference rotation criteria can be expressed in terms of the mean and standard deviation of bearing pressure at damage criteria. The mean values and coefficients of variation of bearing pressures at damage criteria were also taken as responses. Design-Expert® was used to statistically analyse the responses and fit the response surfaces.

The Design-Expert software was used to fit the response surface and to check the significance of fits through several statistical procedures (Design-Expert, 2000 [50]). For each response, non-significant factors were screened out and appropriate surfaces were fitted. These surfaces could be plane or curved, and have interaction terms and/or quadratic terms. The procedure is discussed in Section 3.3. Each of these responses is discussed in detail in the next section. These response surfaces (fitted equations) are only valid in the studied ranges and can only be used in practical engineering applications to approximate complex behaviour in these ranges.

Based on the study reported in Section 4.3.3.5, it was observed that the lognormal distribution is an appropriate fit for the results of Monte Carlo simulations. For all studied

cases, three different probability distributions – lognormal, Gamma, and normal – were fitted. Lognormal distribution was observed to be the best fit. Gamma fits were close to lognormal; hence, they are not reported here. However, for a few cases with highly variable Beta-distributed input soil, the empirical distribution had a richer left tail than that predicted by the lognormal fit. For those cases, the normal distribution provided a better fit. This issue still needs to be further studied by employing a larger sample of Monte Carlo simulations and statistical analysis. However, usage of larger samples for Monte Carlo simulations in parametric study was impractical. The results reported here for a probability level of 10^{-4} show the bearing capacity at a very low failure probability level; however, they should not be used quantitatively.

Table 4.5 Foundation responses for factorial and central composite design normalized by deterministic value (for $E = 1500c_u$) using 100 samples for each case.

	Factor 1	Factor 2	Factor 3	Factor 4	Response 1	Response 2	Response 3	Response 4
Exp. #	Coeff. of variat., C_V (%)	Norm. horiz. correl. dist., θ_{hn}	Norm. vert. correl. dist., θ_{vn}	Prob. dist.	Mean bearing capacity ratio, R_{BC}	Coefficient of variation of bearing capacity, C_{VBC} (%)	Characteristic (nominal) bearing capacity ratio, R_{nBC}	Normalized bearing capacity @ target probability level 10^{-4} , R_{tBC}
								Log. fit
1	10	1	0.25	Gamma	0.98	2.7%	0.94	0.89
2	40	1	0.25	Gamma	0.82	11.3%	0.67	0.54
3	10	4	0.25	Gamma	0.98	5.1%	0.90	0.80
4	40	4	0.25	Gamma	0.81	21.4%	0.52	0.36
5	10	1	1	Gamma	0.98	2.7%	0.94	0.89
6	40	1	1	Gamma	0.82	13.1%	0.61	0.50
7	10	4	1	Gamma	0.98	5.9%	0.90	0.79
8	40	4	1	Gamma	0.83	25.1%	0.50	0.32
9	10	2.5	0.625	Gamma	0.98	4.7	0.91	0.82

	Factor 1	Factor 2	Factor 3	Factor 4	Response 1	Response 2	Response 3	Response 4
Exp. #	Coeff. of variat., C_V (%)	Norm. horiz. correl. dist., θ_{hn}	Norm. vert. correl. dist., θ_{vn}	Prob. dist.	Mean bearing capacity ratio, R_{BC}	Coefficient of variation of bearing capacity, C_{VBC} (%)	Characteristic (nominal) bearing capacity ratio, R_{nBC}	Normalized bearing capacity @ target probability level 10^{-4} , R_{tBC}
								Log. fit
10	40	2.5	0.625	Gamma	0.80	19.4	0.55	0.39
11	25	1	0.625	Gamma	0.91	6.0	0.82	0.73
12	25	4	0.625	Gamma	0.91	14.3	0.73	0.53
13	25	2.5	0.25	Gamma	0.91	11.0	0.75	0.60
14	25	2.5	1	Gamma	0.91	11.7	0.75	0.58
15	25	2.5	0.625	Gamma	0.90	11.6	0.75	0.58
16	10	1	0.25	Beta	0.98	2.9	0.93	0.88
17	40	1	0.25	Beta	0.76	19.0	0.54	0.37
18	10	4	0.25	Beta	0.98	6.6	0.88	0.77
19	40	4	0.25	Beta	0.78	30.7	0.33	0.24
20	10	1	1	Beta	0.98	3.0	0.93	0.88
21	40	1	1	Beta	0.76	19.0	0.49	0.37
22	10	4	1	Beta	0.98	6.6	0.87	0.77
23	40	4	1	Beta	0.79	29.7	0.38	0.26
24	10	2.5	0.625	Beta	0.99	5.3	0.90	0.81
25	40	2.5	0.625	Beta	0.81	24.4	0.48	0.32
26	25	1	0.625	Beta	0.90	8.2	0.78	0.66
27	25	4	0.625	Beta	0.89	18.3	0.64	0.45
28	25	2.5	0.25	Beta	0.88	15.2	0.64	0.50
29	25	2.5	1	Beta	0.89	14.4	0.65	0.52
30	25	2.5	0.625	Beta	0.92	13.7	0.71	0.55

Table 4.6 Parametric study for $E/c_u = 300$, design layout of Monte Carlo simulations and results for ultimate bearing capacity using 200 samples for each case.

Exp. #	Factor 1	Factor 2	Factor 3	Ultimate bearing capacity			Normalized bearing capacity @ target probability level 10^{-4} , R_{IBC}
	Coefficient of variation, C_V (%)	Normalized horizontal correlation distance, θ_{hm}	Probability distribution	Mean ratio, R_{BC}	Coefficient of variation, C_{VBC} (%)	Characteristic ratio, R_{nBC}	Log. fit
1	10	1	Gamma	0.98	2.0	0.95	0.90
2	40	1	Gamma	0.83	10.0	0.71	0.57
3	10	4	Gamma	0.98	6.0	0.90	0.79
4	40	4	Gamma	0.81	23.0	0.51	0.34
5	10	1	Beta	0.98	3.0	0.94	0.89
6	40	1	Beta	0.76	19.0	0.55	0.37
7	10	4	Beta	0.97	6.0	0.86	0.77
8	40	4	Beta	0.75	31.0	0.30	0.23
9	25	2.5	Gamma	0.91	10.0	0.78	0.63
10	25	2.5	Beta	0.89	14.0	0.70	0.53

4.4.3 Results of Parametric Studies

The results of the Monte Carlo simulations were studied using the factorial and central composite methods. Both methods yielded close results, which indicated that there was little curvature in the response surfaces. The regression equations obtained from the factorial design, which use only 18 points (Table 4.4), were able to closely predict the responses of an additional 12 points in the central composite design. This was a confirmation of the applicability of the regression analysis. Since the central composite

method used a larger number of points, the results from this approach are shown and discussed here.

4.4.3.1. Mean bearing capacity

The coefficient of variation, C_V , and the probability distribution of soil shear strength were found to be the most important factors affecting the bearing capacity of foundation on heterogeneous soil. As expected, C_V had the largest contribution of all factors. It can be inferred that the amount of loose pockets was the most significant factor controlling the mean bearing capacity. Variation of mean bearing capacity R_{BC} vs. coefficient of variation and horizontal correlation distance of a Beta distributed soil shear strength is plotted in Figure 4.19. The effects of the horizontal and vertical correlation distances were found to be negligible on the mean bearing capacity for the ranges considered in this study. Regression equations were obtained for the mean bearing capacity ratio, R_{BC} , (reported in Table 4.5) for each probability distribution of soil shear strength. The equations are as follows:

For Gamma-distributed shear strength,

$$R_{BC} = 1.01 - 2.7 \times 10^{-3} C_V - 5.4 \times 10^{-5} C_V^2 \quad \text{Eq. 4.4}$$

For Beta-distributed shear strength,

$$R_{BC} = 1.03 - 4.1 \times 10^{-3} C_V - 5.4 \times 10^{-5} C_V^2 \quad \text{Eq. 4.5}$$

where C_V is the coefficient of variation of soil shear strength in the range of 10% to 40%.

The accuracy of the fitted equations (Eq. 4.4 and Eq. 4.5) was statistically checked ($R^2 =$

0.98 and predicted $R^2 = 0.975$). The predicted R^2 is a measure of how the equations fits each point in the design (here each case in Table 4.5), computed by first predicting where each point should be from a model that contains all other points except the one in question. Statistical indices were also checked for significance of the fitted model and its terms (e.g. C_V , probability distribution, interaction terms in the fitted equations) in Table 4.7. The F value, in Table 4.7, for a term is the test for comparing the variance associated with that term with the residual variance. It is the Mean Square for the term divided by the Mean Square for the Residual. The third column in Table 4.7 (Prob. > F) is the probability value associated with the F value for a term. It is the probability of getting an F value of this size if the term did not have an effect on the response. In general, a term that has a probability value less than 0.05 would be considered a significant effect (all the terms in Table 4.7 are significant). A probability value greater than 0.10 is generally regarded as not significant. The first row in Table 4.7 shows these values for the fitted model.

Table 4.7 Statistical indices for significance of the fitted model for mean bearing capacity

	F value	Prob. > F
Model	359.8	< 0.0001
C_V	1396.7	< 0.0001
Probability distribution	17.0	0.00036
C_V^2	8.2	0.0085
Interaction between C_V and probability distribution	17.2	0.00034

The results obtained from Eq. 4.4 and Eq. 4.5 were compared with the results of Monte Carlo simulations in Table 4.8. Figure 4.19 shows the scatter plots for Monte Carlo simulations and predicted values of mean bearing capacity ratio. The two points, shown by

circles, were obtained from Monte Carlo simulations for two cases assuming Gamma distributed soil shear strength with $C_V = 20\%$ and 30% , $\theta_{hn} = 1.25$, and $\theta_{vn} = 0.25$. These two points were not used in obtaining the regression equations. The scatter plots show the accuracy of regression equations in the studied ranges. Eq. 4.4 and Eq. 4.5 are regression equations and are only valid for a range of $C_V = 10\%$ to 40% . Many researchers only account for the effects of soil heterogeneity on the variability of bearing capacity through use of variance reduction function (e.g. Li and Lam, 2001 [110]). These effects are discussed in the next section. Griffiths et al. (2002) [78] studied the effects of correlation distance on mean bearing capacity using equal correlation distances in the horizontal and vertical directions. From their results, it can also be inferred that for the practical range of coefficient of variation ($C_V < 50\%$) and for correlation distance in the range studied here, the effects of correlation distance on mean bearing capacity is small. Thus, the observed negligible effects of correlation distances on the mean bearing capacity for the studied ranges is reasonable.

For example if soil shear strength has $C_V = 30\%$ and follows a Beta distribution, and knowing the bearing capacity factor of uniform soil, $N_c = 5.14$ (Prandtl solution), then the average bearing capacity factor for the heterogeneous soil is,

$$N_{cH} = R_{BC} \cdot N_c = (1.03 - 4.1 \times 10^{-3} \times 30 - 5.4 \times 10^{-5} \times 30^2) \times 5.14 = 4.41$$

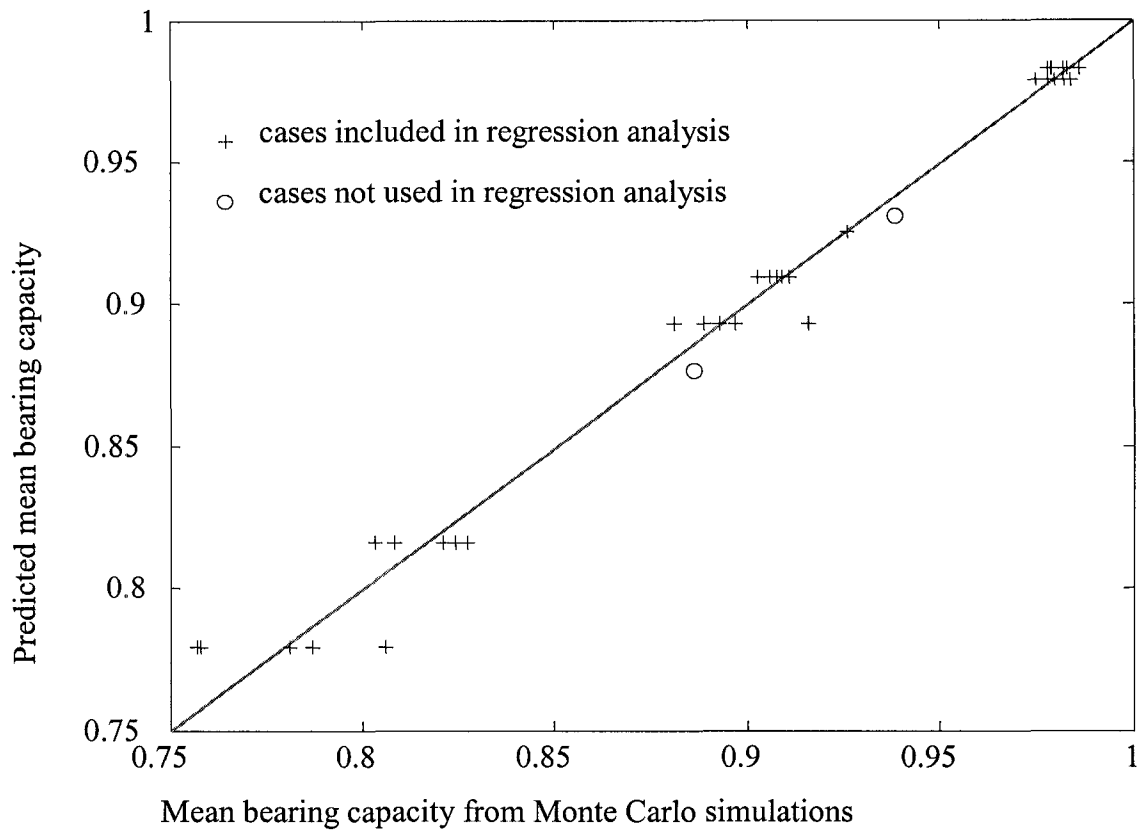


Figure 4.19 Scatter plot for Monte Carlo simulations and predicted (Eq. 4.4 & Eq. 4.5) values of mean bearing capacity ratio.

Table 4.8 Comparison of mean bearing capacity ratio, R_{BC} from Monte Carlo simulations and fitted response surface (Eq. 4.4 & Eq. 4.5)

Experiment number (as given in Table 4.5)	Monte Carlo simulation values	Predicted values	Error (%)
1	0.982	0.979	0.3%
2	0.821	0.816	0.7%
3	0.975	0.979	0.4%
4	0.808	0.816	0.9%
5	0.984	0.979	0.5%
6	0.824	0.816	1.0%
7	0.980	0.979	0.1%
8	0.827	0.816	1.4%
9	0.978	0.979	0.0%

Experiment number (as given in Table 4.5)	Monte Carlo simulation values	Predicted values	Error (%)
10	0.803	0.816	1.6%
11	0.908	0.909	0.1%
12	0.909	0.909	0.0%
13	0.911	0.909	0.1%
14	0.906	0.909	0.4%
15	0.903	0.909	0.7%
16	0.978	0.983	0.4%
17	0.757	0.779	2.9%
18	0.982	0.983	0.1%
19	0.781	0.779	0.3%
20	0.979	0.983	0.4%
21	0.758	0.779	2.7%
22	0.983	0.983	0.0%
23	0.787	0.779	1.0%
24	0.986	0.983	0.4%
25	0.806	0.779	3.4%
26	0.897	0.893	0.4%
27	0.893	0.893	0.0%
28	0.881	0.893	1.3%
29	0.889	0.893	0.5%
30	0.916	0.893	2.5%

4.4.3.2. *Variability of predicted bearing capacity*

Another important response obtained from Monte Carlo simulations was the variability of predicted bearing capacity of a strip foundation on heterogeneous soil. A study was performed that was similar to the one for mean bearing capacity presented in Section 4.4.3.1. The response surface fitted on the coefficient of variation of bearing capacity, C_{VBC} is shown in Figure 4.21 for Beta distributed soil shear strength. The coefficient of variation, probability distribution and normalized horizontal correlation

distance, θ_{hn} , of soil undrained shear strength were deemed significant. The coefficient of variation of soil shear strength was the most important contributor to the variability of foundation bearing capacity on heterogeneous soil. The amount of variability significantly decreased due to local averaging phenomenon, which was more pronounced for small correlation distances. The regression equations obtained for C_{VBC} from the values in Table 4.5 are:

For Gamma distributed soil shear strength,

$$C_{VBC} = -1.3 + 0.24C_v + 0.33\theta_{hn} + 0.09C_v\theta_{hn} \quad \text{Eq. 4.6}$$

For Beta distributed soil shear strength,

$$C_{VBC} = -2.8 + 0.44C_v + 0.33\theta_{hn} + 0.09C_v\theta_{hn} \quad \text{Eq. 4.7}$$

R^2 was 0.988 and predicted R^2 was 0.981 for the fitted model. Similar to mean bearing capacity, statistical indices were also checked for significance of the fitted model and its terms in Table 4.9. The model and all the terms were significant.

For example, taking $C_v = 30\%$, Beta distribution, and $\theta_{hn} = 2$, the coefficient of variation of bearing capacity results as,

$$C_{VBC} = -2.8 + 0.44 \times 30 + 0.33 \times 2 + 0.09 \times 30 \times 2 = 16.5\%$$

Again regression equations are only valid for the range of probabilistic characteristics considered here. For example, if a value of $C_v = 0$ is used in Eq. 4.6, it results in negative coefficient of variation for bearing capacity, which is impossible. The reason is that the above equations are only applicable for the studied ranges ($C_v = 10\%$ to 40% , $\theta_{hn} = 1$ to 4 and $\theta_{vn} = 0.25$ to 1). Figure 4.20 shows the scatter plots for Monte Carlo

simulations and predicted (Eq. 4.6 & Eq. 4.7) values of coefficient of variation of bearing capacity. Again, the two points, shown by circles, were obtained from Monte Carlo simulations for two cases assuming Gamma distributed soil shear strength with $C_V = 20\%$ and 30% , $\theta_{hm} = 1.25$, and $\theta_{vm} = 0.25$. These two points were not used in obtaining regression equations. The scatter plots show the accuracy of regression equations in the studied ranges.

The values obtained here were compared with values obtained using variance reduction factor based on the theory of random fields (Vanmarcke, 1983 [209]), as discussed in Section 4.3.3.4 and presented in Table 4.10. The results showed a general agreement. However, due to changes in failure mechanisms, the resulting coefficients of variation of bearing capacity were not solely dependent on correlation distances and input coefficients of variation of soil strength; the probability distributions of input soil strength also affected the resulting coefficients of variation. The numerical model, used in the study, has captured all these effects. Accounting only for the effects of local averaging does not capture the changes in response variance produced by changes in failure mechanisms of heterogeneous soil.

Table 4.9 Statistical indices for significance of the fitted model for variability of predicted bearing capacity

	F value	Prob. > F
Model	387.6	< 0.0001
C_V	1444.1	< 0.0001
Horizontal correlation distance, θ_{hn}	296.5	< 0.0001
Probability distribution	88.8	< 0.0001
Interaction between C_V and the horizontal correlation distance	64.3	< 0.0001
Interaction between C_V and probability distribution	44.2	< 0.0001

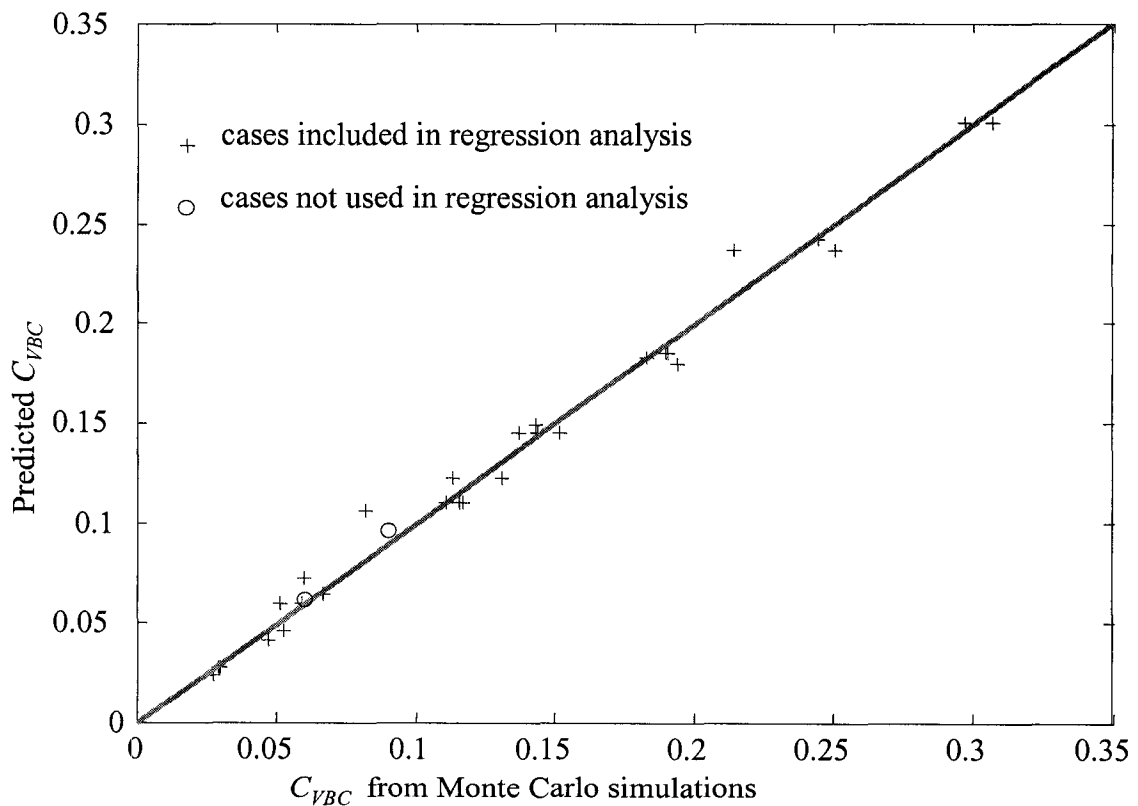


Figure 4.20 Scatter plot for the Monte Carlo simulations and predicted (Eq. 4.6 & Eq. 4.7) values of coefficient of variation of bearing capacity.

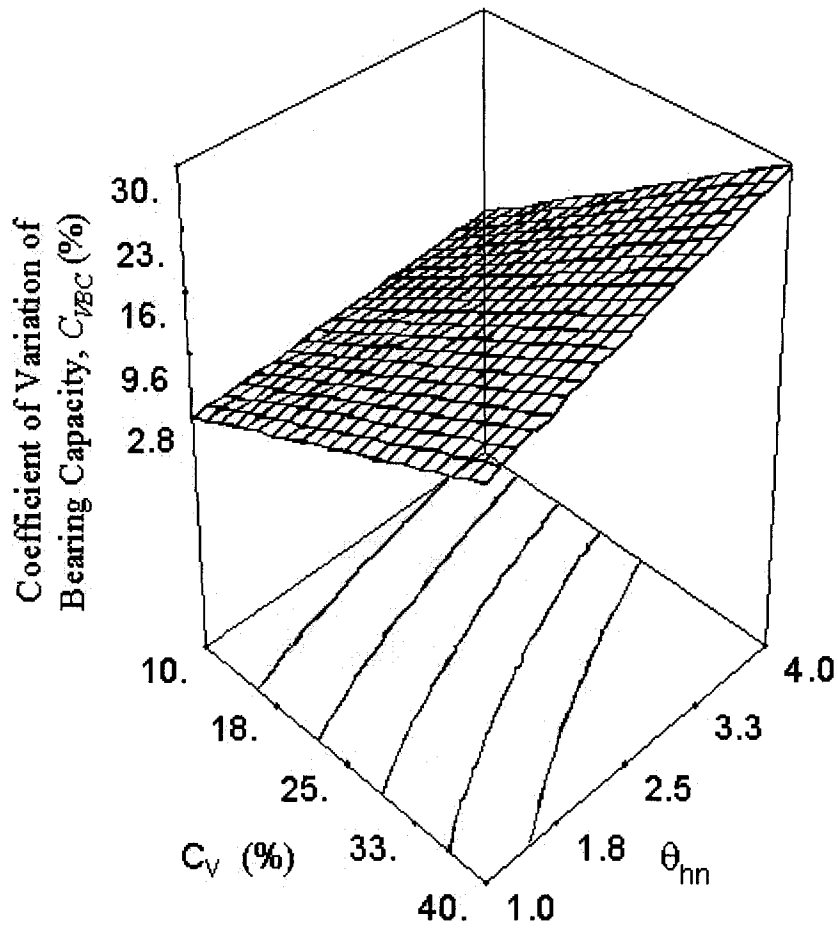


Figure 4.21 Variation of the coefficient of variation of bearing capacity with C_V and θ_h/B for Beta distributed soil shear strength.

Table 4.10 Comparison of predicted values of C_V from Monte Carlo simulations with analytical approximations for soil shear strength with $C_V = 40\%$.

Norm. horiz. correl. Dist., θ_{hn}	Norm. vert. correl. dist., θ_{vn}	Coefficient of Variation of Bearing Capacity, C_V (%)		
		Gamma	Beta	Analytical approximations
1	0.25	11.3%	19.0%	12.2%
4	0.25	21.4%	30.7%	19.5%
2.5	0.625	19.4%	24.4%	24.1%
1	1	13.1%	19.0%	19.1%
4	1	25.1%	29.7%	30.4%

4.4.3.3. Characteristic bearing capacity

Characteristic values play an important role in design (see Section 2.4). As previously mentioned, it is possible to define a characteristic percentile of soil strength that, when used in deterministic analysis, will provide a similar bearing capacity to that obtained from Monte Carlo simulations for a given confidence interval. Characteristic values of soil strength were obtained for every case with 95% reliability and then a response surface was fitted to them. The soil shear strength variability, its probability distribution and horizontal correlation distance were significant factors. The coefficient of variation had the highest contribution. Figure 4.23 shows the variation of characteristic bearing capacity vs. C_v and θ_{hn} of soil shear strength having a Beta probability distribution. The response equations obtained for R_{nBC} from the values in Table 4.5 are:

For Gamma distributed soil shear strength,

$$R_{nBC} = 1.06 - 0.009C_v - 0.006\theta_{hn} - 0.001C_v\theta_{hn} \quad \text{Eq. 4.8}$$

For Beta distributed soil shear strength,

$$R_{nBC} = 1.07 - 0.013C_v - 0.006\theta_{hn} - 0.001C_v\theta_{hn} \quad \text{Eq. 4.9}$$

R^2 was 0.984 and predicted R^2 was 0.981 for the fitted model. Similar to mean bearing capacity, statistical indices were also checked for significance of the fitted model and its terms in Table 4.11. The model and all the terms were significant. Again the above equations are only valid for the range studied ($C_v=10\%$ to 40% , $\theta_{hn}=1$ to 4 and $\theta_{vm}=0.25$ to 1). Figure 4.22 shows the scatter plots for Monte Carlo simulations and predicted (Eq. 4.10

and Eq. 4.11) values of characteristic bearing capacity. Again, the two points, shown by circles, were obtained from Monte Carlo simulations for two cases assuming Gamma distributed soil shear strength with $C_V = 20\%$ and 30% , $\theta_{hn} = 1.25$, and $\theta_{vn} = 0.25$. These two points were not used in obtaining regression equations. For example, taking $C_V = 30\%$, Beta distribution, $\theta_{hn} = 2$ and bearing capacity factor of uniform soil $N_c = 5.14$, the characteristic bearing capacity with 95% confidence is,

$$R_{nBC} = 1.07 - 0.013 \times 30 - 0.006 \times 2 - 0.001 \times 30 \times 2 = 0.608$$

Thus, the bearing capacity factor to obtain characteristic (nominal) bearing capacity is,

$$N_{nc} = R_{nBC} \times N_c = 0.608 \times 5.14 = 3.12$$

It should be mentioned that due to a limited number of Monte Carlo simulations, the 95-percentile values obtained here may not be accurate.

Table 4.11 Statistical indices for significance of the fitted model for characteristic bearing capacity

	F value	Prob. > F
Model	299.4	< 0.0001
C_V	1315.8	< 0.0001
Horizontal correlation distance, θ_{hn}	81.2	< 0.0001
Probability distribution	61.8	< 0.0001
Interaction between C_V and the horizontal correlation distance	15.4	0.00065
Interaction between C_V and probability distribution	22.7	< 0.0001

As detailed in Section 3.6.2, it is possible to obtain a characteristic percentile of soil strength to be used in design. It should be mentioned that characteristic bearing capacity (resistance) corresponds to a certain confidence interval (here 95%).

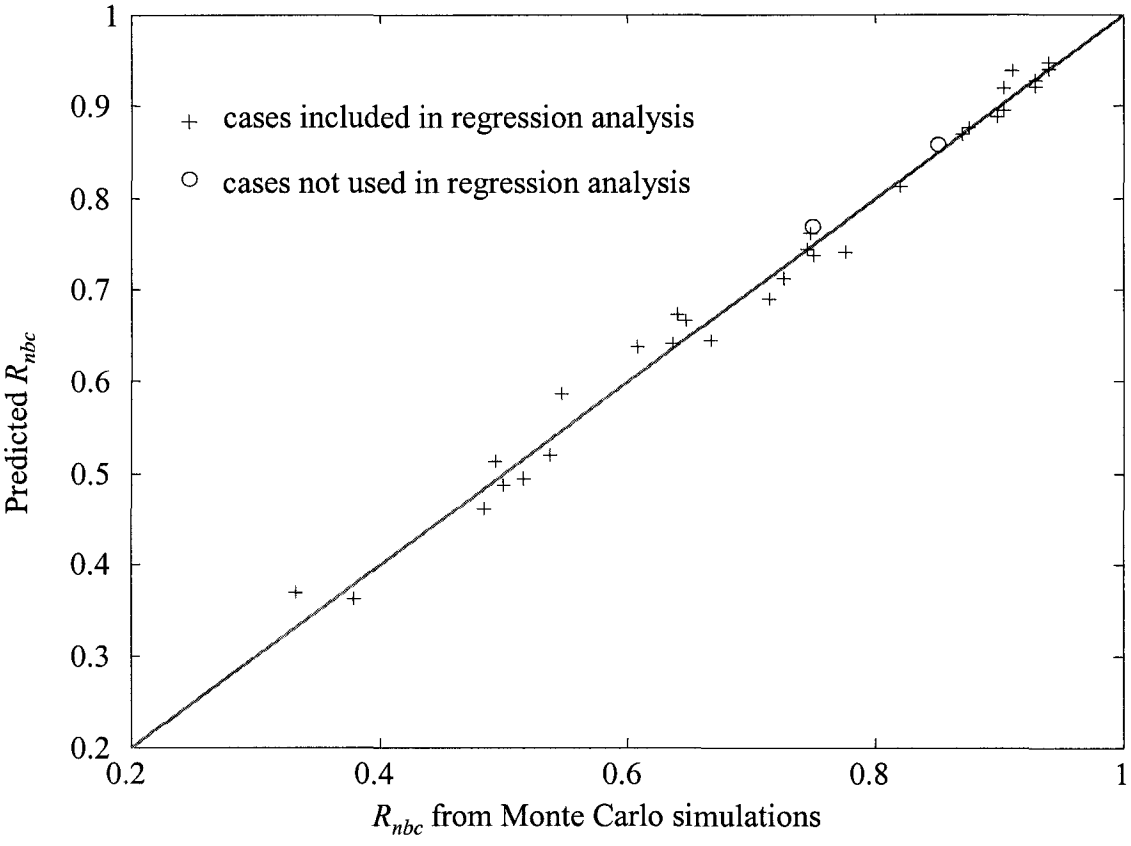


Figure 4.22 Scatter plot for the Monte Carlo simulations and predicted (Eq. 4.8 & Eq. 4.9) values of characteristic bearing capacity.

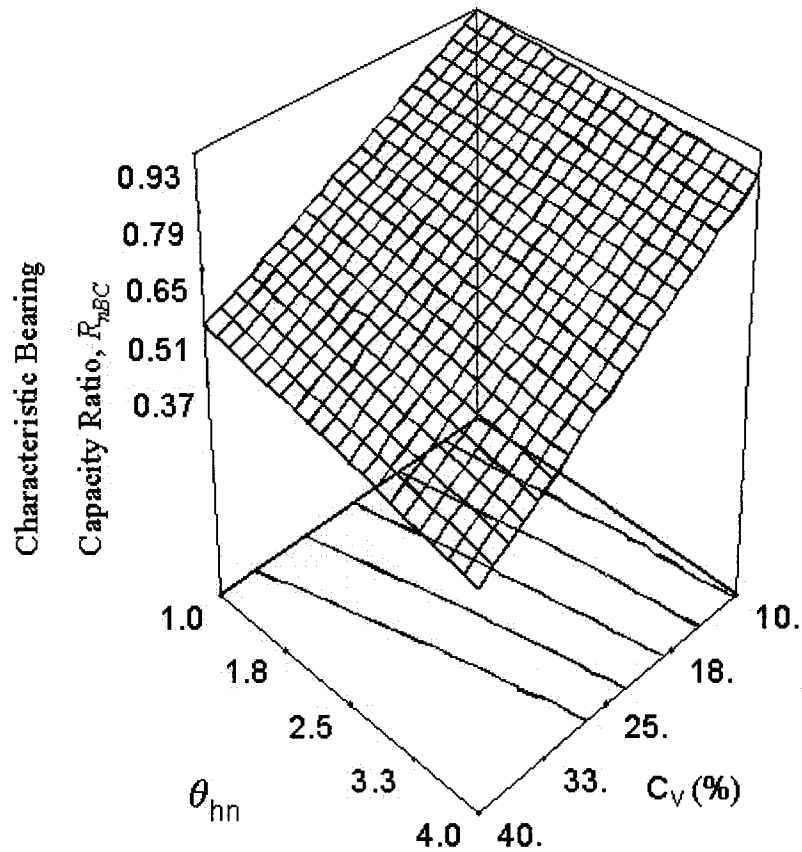


Figure 4.23 Variation of characteristic bearing capacity vs. C_v and θ_{hn}/B of soil shear strength having a Beta probability distribution.

4.4.3.4. Factor of safety for target failure probability

Theoretical distributions were fitted to the resulting empirical probability distributions of bearing capacity and extrapolated to a desired probability level to obtain bearing capacity at desired reliability levels (see Section 4.3.3.4). It should be mentioned that the results obtained so far accounted only for the variability in response caused by soil heterogeneity. However, it is easy to add uncertainty from other sources. These additional uncertainties can be added by summation of the variability. For example, assuming

independence between different sources of uncertainty, Failmezger (2001) [61] presented the following equation,

$$\sigma_{overall} = \sqrt{\sigma_{spatial}^2 + \sigma_{noise}^2 + \sigma_{model}^2} \quad \text{Eq. 4.10}$$

where $\sigma_{overall}$, $\sigma_{spatial}$, σ_{noise} , σ_{model} are the resulting (overall) standard deviation of the response, standard deviation of soil natural variability, standard deviation of noise in measurement, and standard deviation of model accuracy. It is possible to simplify the above equation by assuming that there are two categories of uncertainty. The first category is the uncertainty caused by measurement errors, simplification used in modelling of soil behaviour, transformation errors, etc. These uncertainties are taken to have a coefficient of variation denoted as C_{Vu} . The second category is the uncertainty caused by assuming uniform soil instead of modelling the realistic spatially variable soil. Furthermore, the errors can be biased. In this context, errors were assumed to have no bias. However, it is possible to account for bias in results in the same framework. In this study, the spatial variability of soil was shown to change the behaviour of geotechnical system. The empirical probability distribution of the bearing capacity was obtained. The effects of soil heterogeneity on mean bearing capacity and its variation were addressed. C_{VBC} denotes the bearing capacity's coefficient of variation due to the natural variability of soil. Thus, using a first-degree approximation and assuming independence between different sources of uncertainty, the overall coefficient of variation of bearing capacity is,

$$C_{Vo} = \sqrt{C_{VBC}^2 + C_{Vu}^2} \quad \text{Eq. 4.11}$$

See Tang (1984) [196] for derivation of Eq. 4.11. Assuming $C_{vu} = 0$, the bearing capacities at target probability level of 10^{-4} were estimated by fitting lognormal distributions to the resulting bearing capacities and extrapolating the fitted distributions.

For Gamma distributed soil strength,

$$R_{tBC} = 1.09 - 0.0139C_v - 0.0471\theta_{hn} \quad \text{Eq. 4.12}$$

For Beta distributed soil strength,

$$R_{tBC} = 1.1 - 0.0169C_v - 0.0471\theta_{hn} \quad \text{Eq. 4.13}$$

R^2 was 0.981 and predicted R^2 was 0.974 for the fitted model. It is also possible to add the additional uncertainty caused by other sources by direct numerical integration, as discussed in Section 4.6. It should be mentioned that, assuming no load variability, the required factor of safety at target probability level of 10^{-4} is,

$$FS = \frac{1}{R_{tBC}} \quad \text{Eq. 4.14}$$

The values of factors of safety were calculated and compared to values obtained theoretically that only accounted for variance reduction due to local averaging effects, as presented in Table 4.12 (similar to the ones calculated in Table 4.3). This shows that only accounting for the effects of local averaging may lead to a non-conservative design, reconfirming the conclusion in Section 4.3.3.4

Table 4.12 Comparison of safety factors obtained from Monte Carlo simulations and analytical approximations.

Norm. horiz. correl. dist., θ_{hn}	Norm. vert. correl. Dist., θ_{vn}	Safety factors, F_S		
		Gamma	Beta	Analytical approximations
1	0.25	1.86	2.71	1.59
4	0.25	2.78	4.09	2.09
2.5	0.625	2.59	3.13	2.49
1	1	1.99	2.71	2.06
4	1	3.12	3.90	3.16

4.4.4 Design Recommendations

The behaviour of soil and soil-structure systems in the nonlinear regime was found to be strongly affected by the natural spatial variability of soil strength within geologically distinct and uniform layers. The average bearing capacities of heterogeneous soils obtained from Monte Carlo simulations were consistently lower than the ones predicted assuming uniform soil strength. The predicted bearing capacities had a lower coefficient of variation than that input for the soil shear strength. These effects were incorporated in engineering design recommendations in this section.

4.4.4.1. Characteristic values

As discussed in the literature review (Section 2.4), design codes account indirectly for variability of materials by using “conservatively assessed values” of strength known as nominal or characteristic values. Statistically, these values are often taken as the 95-percentile of strength resulting from a number of measurements. For example, a specified

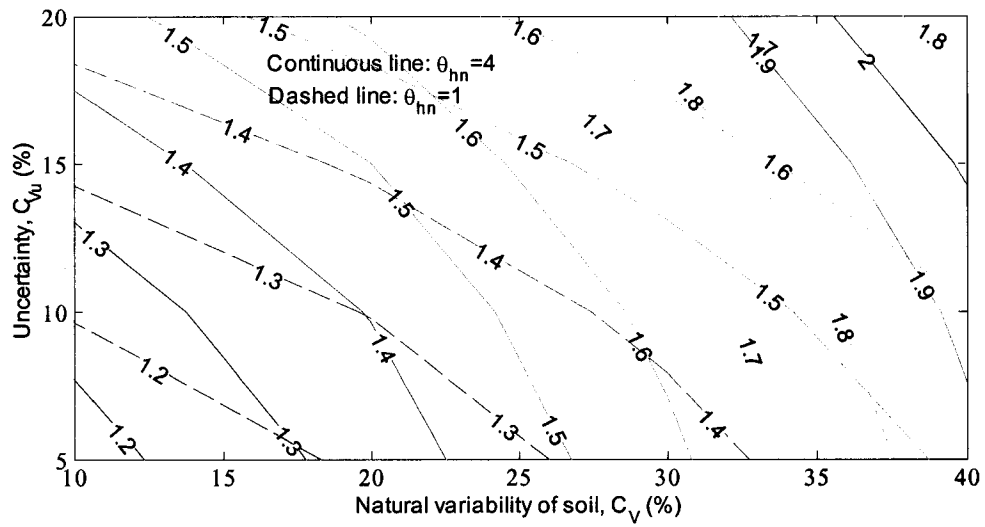
Grade X65 for pipeline means that it is expected that from 20 tests performed for strengths of this pipeline, 19 of them will yield a value larger than 65 ksi (~448 MPa). In geotechnical engineering, the nominal or characteristic values are not well established (See Section 2.4). Selection of those values has great importance in securing a uniform safety level in LSD (see e.g. Cardoso and Fernandes, 2001 [24]). This deficiency in geotechnical engineering can be partly attributed to high point variability of soil properties. Other causes may be: insufficient soil data, relatively large measurement errors, relatively large uncertainties related to modelling of soil behaviour, etc. Section 4.4.3.3 explains how the characteristic bearing capacity values were obtained accounting only for the effects of soil heterogeneity

It is also possible to estimate uncertainty from other sources and then use the equations provided in Section 4.4.3.1 & 4.4.3.2 to calculate bearing capacity with 95-percentile reliability as nominal value. For this purpose, Eq. 4.4 and Eq. 4.5 can be used to estimate mean bearing capacity. Eq. 4.6 and Eq. 4.7 can estimate the coefficient of variation of bearing capacity resulting from soil heterogeneity. This value should be added to uncertainty from other sources using Eq. 4.11. Assuming a lognormal distribution, the bearing capacity at every confidence level (here 95%) can be calculated easily. For example, for given values of $C_V = 30\%$ (variability due to soil heterogeneity), Beta distributed shear strength, and $\theta_{hm} = 2$, a resulting R_{BC} and C_V (of bearing capacity) were 0.846 and 16.5% (see Sections 4.4.3.1 & 4.4.3.2). Assuming a $C_{Vu} = 15\%$, from Eq. 4.11,

$$C_{Vo} = \sqrt{16.5^2 + 15^2} = 22.3\%$$

Assuming a lognormal distribution with mean of 0.846 and $C_V = 22.3\%$, the bearing capacity with 95% confidence is $R_{nBC} = 0.57$. In other words, the calculated bearing capacity using uniform average shear strength shall be divided by a reduction factor $k_R = 1.74$. The values of reduction factors to obtain bearing capacity with 95% confidence are contoured in Figure 4.24 for the range of soil heterogeneity parameters studied here ($C_V = 10\%$ to 40% , Gamma and Beta distributed soil shear strength, and $\theta_{nn} = 1$ to 4) and $C_{vu} = 5\%$ to 20% . This approach was used to calculate the characteristic values for Calibration of partial factors, as discussed in Section 4.4.4.3.

For Gamma distributed soil strength



For Beta distributed soil strength

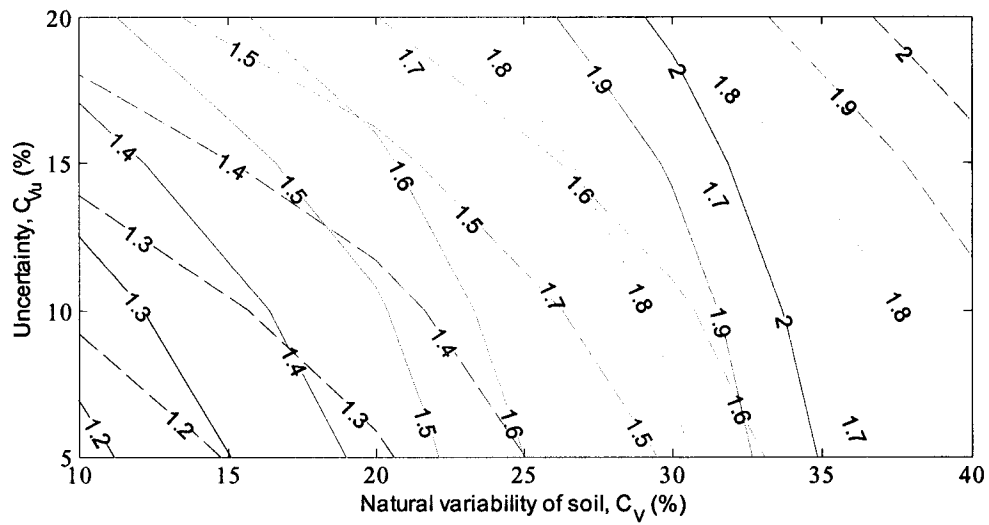


Figure 4.24 Contours of the ratio of mean value to characteristic value for resistance vs. natural variability of soil, C_V and uncertainty from other sources, C_{Vu} .

4.4.4.2. Reliability analysis

The equations recommended in Section 4.4.3 for the resulting mean and coefficient of variation of bearing capacity can be used in a framework of reliability analysis. A lognormal probability distribution was found in most cases to fit the resulting bearing capacity well. The reliability analysis can be implemented through approximate methods, such as FOSM or through direct use of numerical integration. Direct use of numerical integration is explained in Section 4.5.4. The approximate method is demonstrated in Section 3.6.4 and is applied in the next section to calibrate partial design factors.

4.4.4.3. Calibration of partial design factors

Partial design factors (resistance reduction factors) can be estimated using the methodology described in Section 3.6.4. For heterogeneous soil, mean bearing capacity and its coefficient of variation can be calculated using Equations 4.4, 4.5, 4.6, 4.7, and 4.11, similar to the calculations in Section 4.4.4.1. The partial design factors were estimated in two ways: (1) assuming use of mean shear strength in design, and (2) using a characteristic bearing resistance based on Section 4.4.4.1.

Using the first approach (i.e. using the mean shear strength as a design value), partial reduction factors were estimated for the range of parameters of spatial variability adopted here – $C_V = 10\%$ to 40% , a right skewed Gamma probability distribution or a symmetric Beta probability distribution, a range of horizontal correlation distances of $\theta_{hn} = 1.0$ to 4.0 . A range of $C_{Vu} = 5\%$ to 20% was assumed for other sources of uncertainty. A target reliability index, $\beta = 3.5$ (using Eq. 3.29), was considered (Section 3.6.4). This target

reliability index is a typical value used in many codes (see AASHTO, 1992 [1]; NRC, 1995 [142], etc.).

The estimated partial design factors using the first methodology – using mean shear strength- are contoured in Figure 4.25. It shows that a highly variable partial reduction factor should be used in design to keep a uniform reliability index if mean soil shear strength is used in design. A variable reduction factor is suggested for different applications (see Li et al., 1993 [108] and CSA, 1992 [41]).

However, there is often a tendency to use a constant reduction factor in design. To provide a constant partial design factor that will also result in a uniform reliability level, one may use characteristic resistance values instead of mean resistance values. Figure 4.26 shows the required partial design factors using the second approach. Here the characteristic resistance values defined in Section 4.4.4.1 were used as design values. The ratios of mean resistance values to characteristic (nominal) resistance values used for calculation of partial factors are contoured in Figure 4.24. The required partial design factors in Figure 4.26 show relatively small variability. A constant value of approximately 0.85 can be taken for the range of probabilistic characteristics considered here. A lower reduction factor is required, only for Beta distributed shear strength with very high variability. It should be mentioned that both methodologies are very close; they are just two different formal ways of design.

Using Eq. 3.36, the values of reliability index were back calculated assuming a constant partial reduction factor of 0.5 (CGS, 1992 [25]; Meyerhof, 1984 [126]), using mean shear strength ($k_R = 1$) and load partial factor from Eq. 3.31. Contours of the

estimated reliability indices are shown in Figure 4.27. A reliability index smaller than 3.5 is assumed undesirable. This shows the high non-uniformity of reliability index if a constant partial factor and mean shear strength is used. This problem can be solved by using one of the two methodologies presented here: (1) using variable partial factors, or (2) using a characteristic bearing resistance and a constant partial factor. This leads to a reduction in the non-uniformity of reliability index and consequently, it may result in safer and more economical designs.

Using variable partial factors (the first methodology) is potentially capable of securing a more uniform reliability index. It also does not need the estimation of characteristic values. However, the second approach also has its own advantages (e.g. using a constant partial resistance factor for design). Therefore, both methodologies have been discussed here.

4.4.4.4. *An illustration design example*

Using a design example, application of the calibrated partial resistance factors in Section 4.4.4.3 is demonstrated here. It is intended to design a strip foundation for a long structure placed on clayey soil deposit with assumptions given in Table 4.13.

Using values in Table 4.13, the factored load is,

$$\alpha S = 1.25 \times 1500 + 1.5 \times 500 = 2625 \text{ kN/m}$$

Given $C_V = 25\%$ and $C_{Vu} = 10\%$ from Figure 4.25, the partial resistance factor, $\phi = 0.65$ and 0.56 for $\theta_{hm} = 1$ and 4 respectively. Using a linear interpolation, $\phi = 0.62$ for $\theta_{hm} = 2$. Thus, the factored resistance is,

$\phi R = \phi N_c c_u B = 0.62 \times 5.14 \times 140B = 446B$ kN/m (assuming bearing capacity factor $N_c = 5.14$ for uniform soil; B is the foundation width)

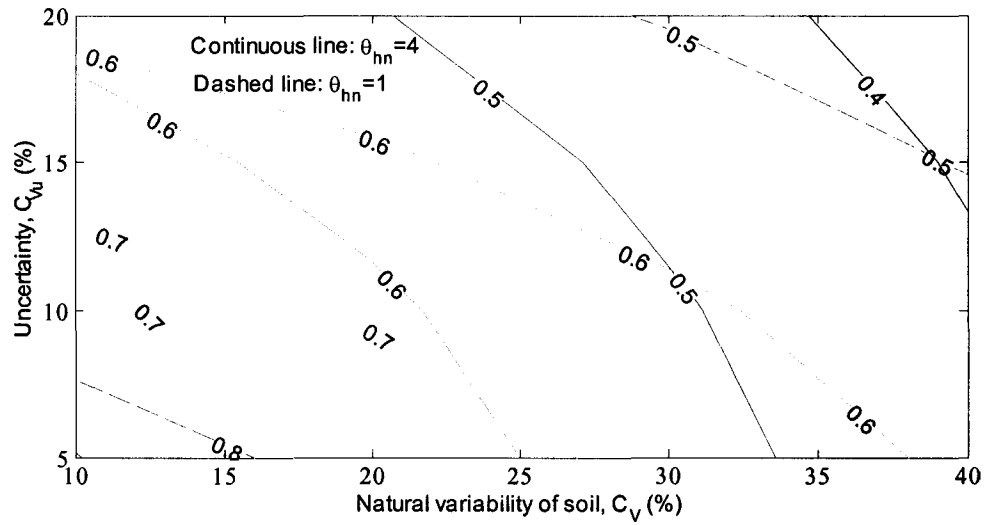
$$\phi R > \alpha S \Rightarrow 446B > 2625 \Rightarrow B > 5.88\text{m (say } B = 6.0\text{m)}$$

Table 4.13 Assumptions for design example

Load		Resistance	
Dead load (DL)	1500 kN/m	Mean undrained shear strength, c_u	140 kPa
Live Load (LL)	500 kN/m	C_V (variability due to soil heterogeneity)	25%
α_D (partial load factor for DL), CGS, 1992 [25]	1.25	C_{Vu} (variability due to other sources of uncertainty – see Section 4.4.3.4)	10%
α_L (partial load factor for LL), CGS, 1992 [25]	1.5	θ_{hn} (normalized horizontal correlation distance)	2

A required foundation width of 6.0m was obtained; this foundation width satisfies a target reliability index of 3.5. If the above foundation were designed based on current practice (CGS, 1992) using $\phi=0.5$, the required foundation width would be $B = 7.3\text{m}$ (say $B = 7.5\text{m}$). The values of the degree of variability assumed in this example are in the low ranges; therefore, the foundation width obtained here is smaller than what is calculated using current practise. If higher values for variability – namely C_V and C_{vu} in Table 4.13 – were considered, the calculated foundation width from the calibrated partial design factor (Figure 4.25) would be larger than those estimated from current practise. A foundation designed using the calibrated partial design factor would satisfy a more uniform reliability index.

For Gamma distributed soil strength



For Beta distributed soil strength

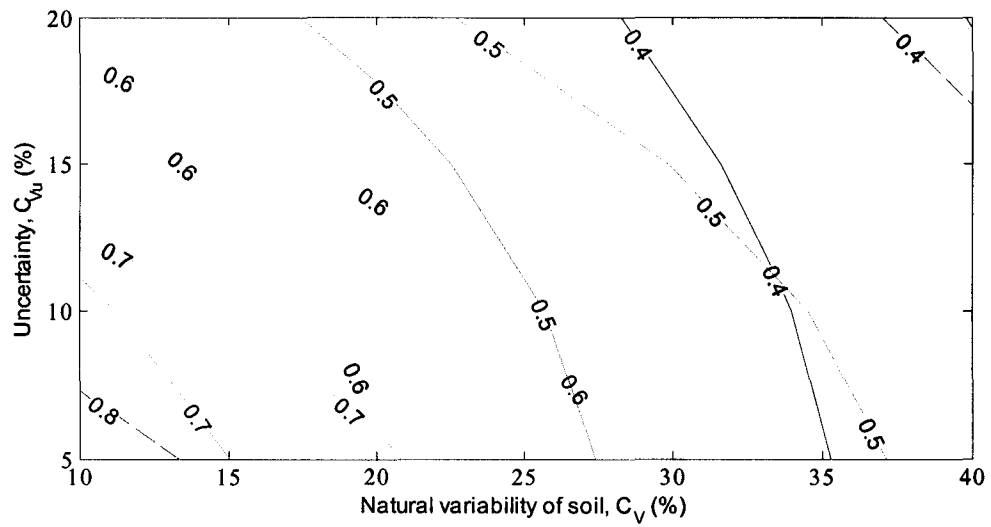
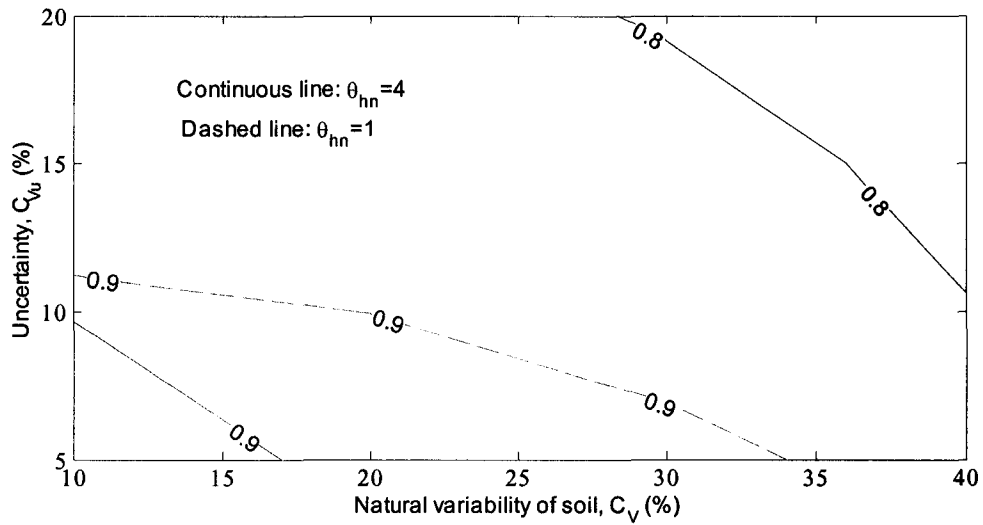


Figure 4.25 Contours of partial design factors vs. natural variability of soil, C_V and uncertainty from other sources, C_{Vu} , for design using mean shear strength.

For Gamma distributed soil strength



For Beta distributed soil strength

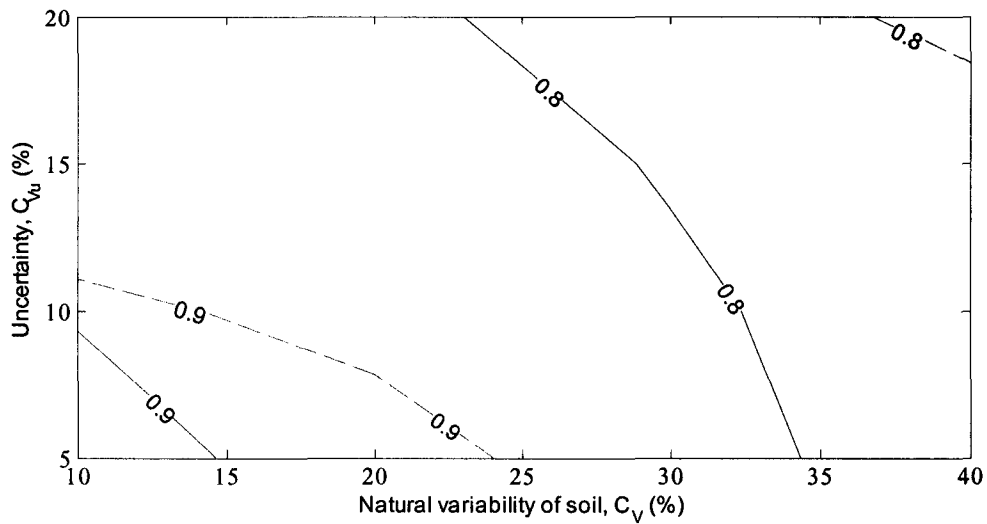
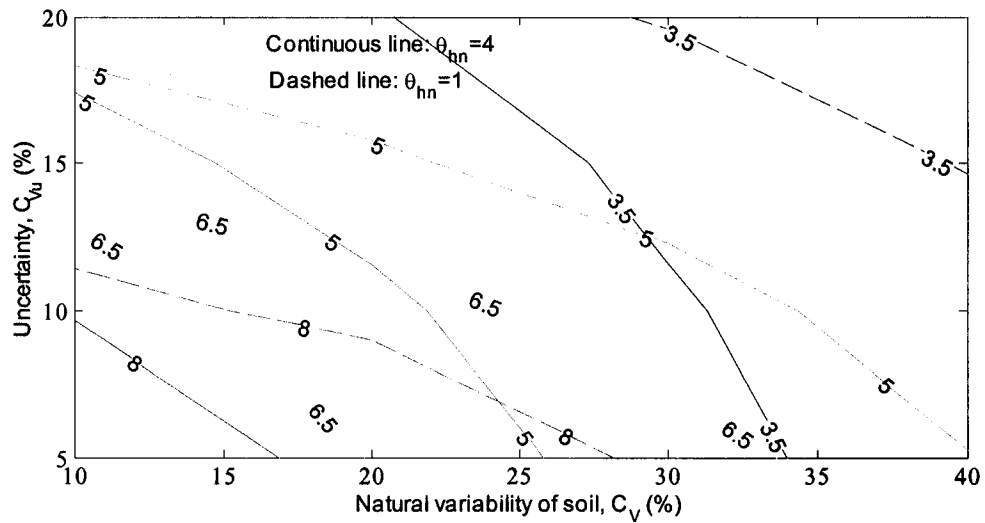


Figure 4.26 Contours of partial design factors vs. natural variability of soil, C_V and uncertainty from other sources, C_{Vu} , for design using characteristic bearing capacity (see Section 4.4.4.1).

For Gamma distributed soil strength



For Beta distributed soil strength

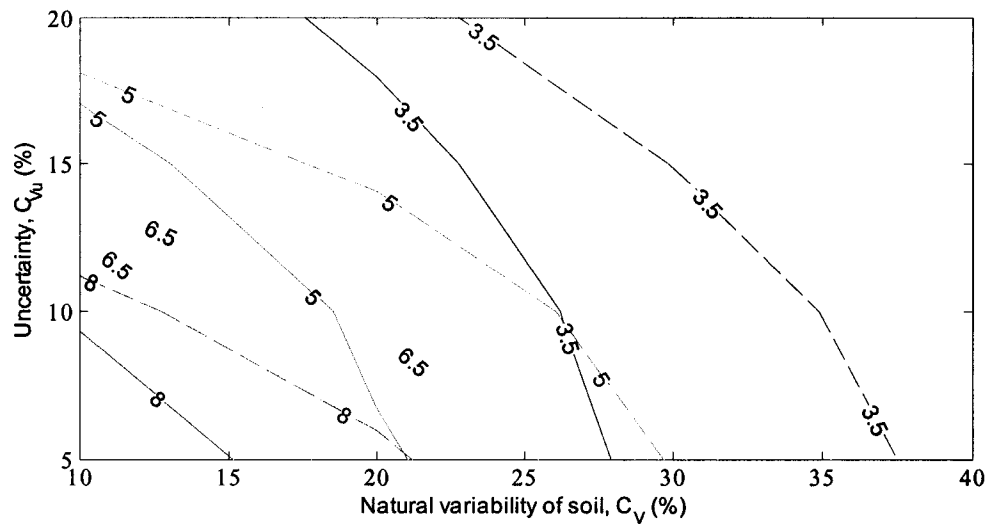


Figure 4.27 Contours of reliability index, β , obtained using a constant partial factor of 0.5. A target reliability index of 3.5 was used in Calibration of National Building Code of Canada, NBCC (see NRC, 1995 [142]; Becker, 1996a [15]).

4.5. DIFFERENTIAL SETTLEMENT AND DAMAGE LEVELS

4.5.1 Introduction

The main purpose of this study was to evaluate the effects of soil heterogeneity on ultimate bearing capacity of foundation. However, even under vertical loading, a foundation placed on spatially variable soil exhibits rotations. The effects of these rotations were studied in this section using the damage criteria concept (described in Section 4.5.2). These criteria for rotations may not correspond to their realistic application in practise. They were used in this work for demonstration purposes. As mentioned in Section 4.5.2, often uniform settlements of a structure do not cause structural malfunction. Footing rotations or differential settlements may, however, cause problems (e.g. Bowles, 1997 [20]).

A relatively high ratio of $E/c_u = 1500$ was used in the previous sections. This high ratio leads to relatively small rotations, but serves well the analysis for ultimate bearing capacity. Since E/c_u differs for various soil types, this study considered two ratios – $E/c_u = 300$ and $E/c_u = 1500$ – to calculate foundation rotations. Deformation modulus, E , was assumed to be a variable perfectly correlated with soil shear strength.

4.5.2 Damage Criteria

In addition to the shear failure criterion, foundation settlements must be estimated and controlled with great care for buildings, bridges, towers, power plants, and similar high cost structures. Settlements are generally made up of immediate, consolidation and

secondary compression (creep) components. The analysis approach used here is only appropriate to account for immediate settlements. Consolidation and viscous analyses are required to capture the second and third components of settlement.

It is convenient to express possible structural damage in the form of a few discrete damage states, selected as a function of feasibility of repairs (e.g. Park and Ang 1987 [148]), serviceability or structural distress (e.g. Grant et al. 1974 [71]). The latter approach was adopted here. Three levels of structural damage, representing three serviceability limit states, were expressed in terms of footing rotations, as follows:

- Minor damage – for rotations greater than $1/500$
- Medium damage – for rotations greater than $1/300$, and
- Major damage – for rotations greater than $1/150$

The probability that a certain level of damage will occur, or will be exceeded, under different load intensity may be expressed in the form of a cumulative distribution function (CDF) similar to the bearing capacity problem presented in the previous section. The CDF function corresponding to each damage level was constructed by first obtaining the empirical distribution for exceedance of each criterion from the results of Monte Carlo simulations. For each analysed case, plots similar to Figure 4.11b were obtained (also see Figures B.3 to B.5). Using these plots, it is possible to obtain empirical probability distribution of bearing pressure at each damage criterion by reading the bearing pressures at absolute values of the damage rotations ($1/500$, $1/300$, and $1/150$) from each curve (each curve is one finite element analysis for Monte Carlo simulations). A lognormal fit was used for this distribution. Thus, for the method of moments, it is sufficient to identify the mean

and coefficient of variation of resulting bearing capacity to define the theoretical probability distribution for each criterion. It is also possible to express this in terms of fragility curves (e.g. Shinozuka et al. 2000 [187]; Popescu et al., 2002 [170]). The latter approach is presented by Popescu et al. (2002 [168]).

4.5.3 Experiment Design

The design layout of experiments is outlined in Section 4.4.1. The following ranges of soil spatial characteristics were taken: $C_V = 10\%$ to 40% , Gamma and Beta probability distribution for soil shear strength, and $\theta_{mn} = 1$ to 4 . Two ratios of $E/c_u = 300$ and 1500 were considered. As mentioned, a range of the vertical correlation distance was considered for $E/c_u = 1500$, but was screened out for $E/c_u = 300$.

4.5.4 Statistical Analysis and Results

The mean and coefficient of variation of bearing pressure at major medium and minor damage criteria were obtained from results of Monte Carlo simulations. They are reported in Table 4.14 and Table 4.15 for $E/c_u = 300$ and $E/c_u = 1500$, respectively. The response surface methodology was used to analyse and fit a regression model to the results.

Table 4.14 Parametric study for $E/c_u = 300$, design layout of Monte Carlo simulations and results for damage levels.

Exp. #	Factor 1 Coeff. of variation, C_V (%)	Factor 2 Normalized horizontal correlation distance, θ_{hn}	Factor 3 Prob. distrib.	Normalized bearing pressure					
				Mean			Coefficient of variation		
				Minor damage, R_{minor}	Medium damage, R_{medium}	Major damage, R_{major}	Minor damage, $C_{V-minor}$ (%)	Medium damage, $C_{V-medium}$ (%)	Major damage, $C_{V-major}$ (%)
1	10	1	Gamma	0.59	0.66	0.74	22	20	17
2	40	1	Gamma	0.28	0.38	0.49	62	43	29
3	10	4	Gamma	0.60	0.66	0.74	23	20	17
4	40	4	Gamma	0.29	0.39	0.49	63	50	38
5	10	1	Beta	0.56	0.64	0.72	24	21	18
6	40	1	Beta	0.24	0.32	0.42	79	61	46
7	10	4	Beta	0.59	0.67	0.74	25	21	18
8	40	4	Beta	0.26	0.35	0.46	77	61	47
9	25	2.5	Gamma	0.41	0.51	0.59	43	31	24
10	25	2.5	Beta	0.38	0.48	0.57	53	37	28

Table 4.15 Parametric study for $E/c_u = 1500$, design layout of Monte Carlo simulations and results for damage levels.

Exp #	Factor 1	Factor 2	Factor 3	Factor 4	Mean bearing capacity ratio			Coefficient of variation		
	Coeff. of variat., C_V (%)	Norm. horiz. correl. dist., θ_{hn}	Norm. vert. correl. dist., θ_{vn}	Prob. dist.	Minor damage, R_{minor}	Medium damage, R_{medium}	Major damage, $R_{BC-major}$	Minor damage, $C_{V-minor}$ (%)	Medium damage, $C_{V-medium}$ (%)	Major damage, $C_{V-major}$ (%)
1	10	1	0.25	Gamma	0.79	0.85	0.91	14	10	7
2	40	1	0.25	Gamma	0.54	0.60	0.68	22	21	18
3	10	4	0.25	Gamma	0.82	0.88	0.93	11	9	6
4	40	4	0.25	Gamma	0.56	0.63	0.70	28	27	25
5	10	1	1	Gamma	0.80	0.86	0.92	13	9	6
6	40	1	1	Gamma	0.55	0.61	0.68	24	23	20
7	10	4	1	Gamma	0.81	0.87	0.92	13	9	7
8	40	4	1	Gamma	0.58	0.64	0.72	31	31	29
9	10	2.5	0.625	Gamma	0.80	0.86	0.92	12	9	7
10	40	2.5	0.625	Gamma	0.54	0.60	0.67	28	26	24
11	25	1	0.625	Gamma	0.64	0.70	0.78	20	18	13
12	25	4	0.625	Gamma	0.68	0.74	0.81	24	21	18
13	25	2.5	0.25	Gamma	0.66	0.74	0.81	19	17	14
14	25	2.5	1	Gamma	0.63	0.70	0.78	21	20	16
15	25	2.5	0.625	Gamma	0.64	0.72	0.79	22	18	15
16	10	1	0.25	Beta	0.78	0.85	0.90	14	11	8
17	40	1	0.25	Beta	0.47	0.54	0.60	34	27	25
18	10	4	0.25	Beta	0.81	0.88	0.93	14	11	9
19	40	4	0.25	Beta	0.53	0.60	0.67	41	38	35
20	10	1	1	Beta	0.78	0.84	0.90	15	11	8
21	40	1	1	Beta	0.48	0.55	0.62	34	29	26
22	10	4	1	Beta	0.81	0.87	0.92	15	12	10
23	40	4	1	Beta	0.53	0.61	0.68	45	39	36
24	10	2.5	0.625	Beta	0.81	0.88	0.93	14	11	8
25	40	2.5	0.625	Beta	0.55	0.62	0.69	38	34	30
26	25	1	0.625	Beta	0.64	0.70	0.78	22	19	14
27	25	4	0.625	Beta	0.66	0.73	0.80	29	26	23
28	25	2.5	0.25	Beta	0.65	0.72	0.78	27	25	21
29	25	2.5	1	Beta	0.63	0.70	0.77	24	23	19
30	25	2.5	0.625	Beta	0.66	0.74	0.81	25	21	18

4.5.4.1. Regression equations for damage levels

Similar to ultimate bearing capacity, regression equations were obtained for the damage levels. The coefficient of variation of soil shear strength was found to be the main factor affecting mean limit bearing pressure at the three damage levels. The shape of the probability distribution of shear strength characterizing the portion of loose pockets of soil also influenced the results. For $E/c_u = 1500$, the following equations were obtained for mean limit bearing pressure ratio at the three damage levels. Mean limit bearing pressure ratio is defined as the mean limit bearing pressure at damage criteria divided by the ultimate bearing capacity obtained deterministically from uniform soil assuming mean soil shear strength. In general format, the equation can be written as,

$$R_{minor} / R_{medium} / R_{major} = a + bC_v + c\theta_{hn} + dC_v^2 \quad \text{Eq. 4.15}$$

where a , b , c , d are given in Table 4.16 and Table 4.17, and C_v is in percents. The predicted R^2 for all fitted equations (models) were from 0.97 to 0.98. Figure 4.28 and Figure 4.29 show the scatter plots for Monte Carlo simulations and predicted (Eq. 4.15) values of bearing pressures at minor and major damage levels.

Table 4.16 Parameters a, b, c, d in Eq. 4.15 for Gamma probability distribution and $E/c_u = 1500$

	a	b	c	d
Minor damage	0.890	-0.0126	0.0113	8.66×10^{-5}
Medium damage	0.939	-0.0113	0.0118	6.11×10^{-5}
Major damage	0.963	-0.00756	0.0109	0

Table 4.17 Parameters a, b, c, d in Eq. 4.15 for Beta probability distribution and $E/c_u = 1500$

	a	b	c	d
Minor damage	0.905	0.0139	0.0113	8.66×10^{-5}
Medium damage	0.954	-0.0124	0.0118	6.11×10^{-5}
Major damage	0.978	-0.00875	0.0109	0

Similarly, for the coefficient of variation of limit bearing pressure ratio for damage levels, they can be written as,

$$C_{V\text{-minor}}/C_{V\text{-medium}}/C_{V\text{-major}} = e + fC_V + g\theta_{hn} + hC_V\theta_{hn} \quad \text{Eq. 4.16}$$

where e, f, g, h are given in Table 4.18 and Table 4.19 and all coefficients of variation are expressed in percents. The predicted R^2 for all fitted equations (models) were from 0.97 to 0.98. Figure 4.30 and Figure 4.31 show the scatter plots for Monte Carlo simulations and predicted (Eq. 4.16) values of coefficient of variation of bearing pressures at minor and major damage levels.

Table 4.18 Parameters e, f, g, h in Eq. 4.16 for Gamma probability distribution and $E/c_u = 1500$

	e	f	g	h
Minor damage	10.3	0.259	-1.02	0.0898
Medium damage	6.07	0.301	-0.925	0.0993
Major damage	2.34	0.298	-0.544	0.0948

Table 4.19 Parameters e, f, g, h in Eq. 4.16 for Beta probability distribution and $E/c_u = 1500$

	e	f	g	h
Minor damage	8.61	0.575	-1.02	0.0898
Medium damage	6.19	0.489	-0.925	0.0993
Major damage	2.48	0.481	-0.544	0.0948

For each damage level, cumulative distributions of bearing resistance (similar to the one for ultimate bearing capacity in Section 4.4.3) were constructed and various probability distributions were fitted for all the cases (an example is presented in Appendix B). The lognormal distribution fits well in most cases. Therefore, the mean and coefficients of variation in Eq. 4.15 and Eq. 4.16 could be used to construct cumulative distributions of limit bearing pressure at each damage level. Likewise, these distributions could be used in reliability analysis of foundations.

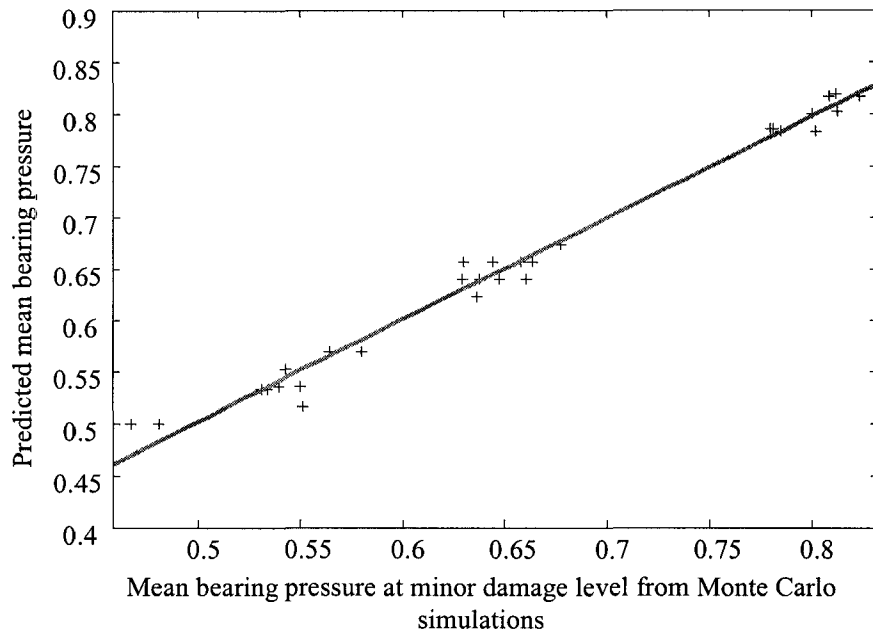


Figure 4.28 Scatter plot for Monte Carlo simulations and predicted (Eq. 4.15) values of mean bearing pressure at minor damage level.

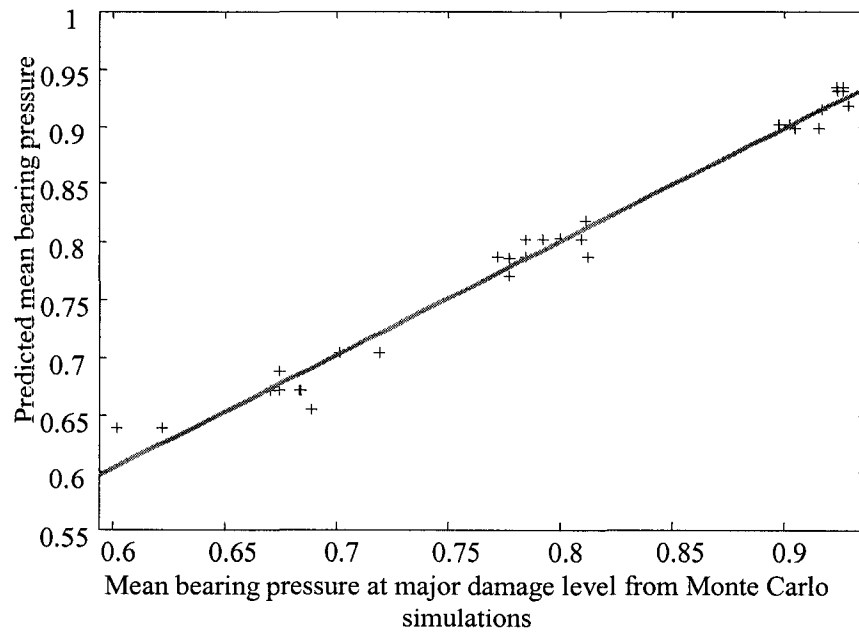


Figure 4.29 Scatter plot for Monte Carlo simulations and predicted (Eq. 4.15) values of mean bearing pressure at major damage level.

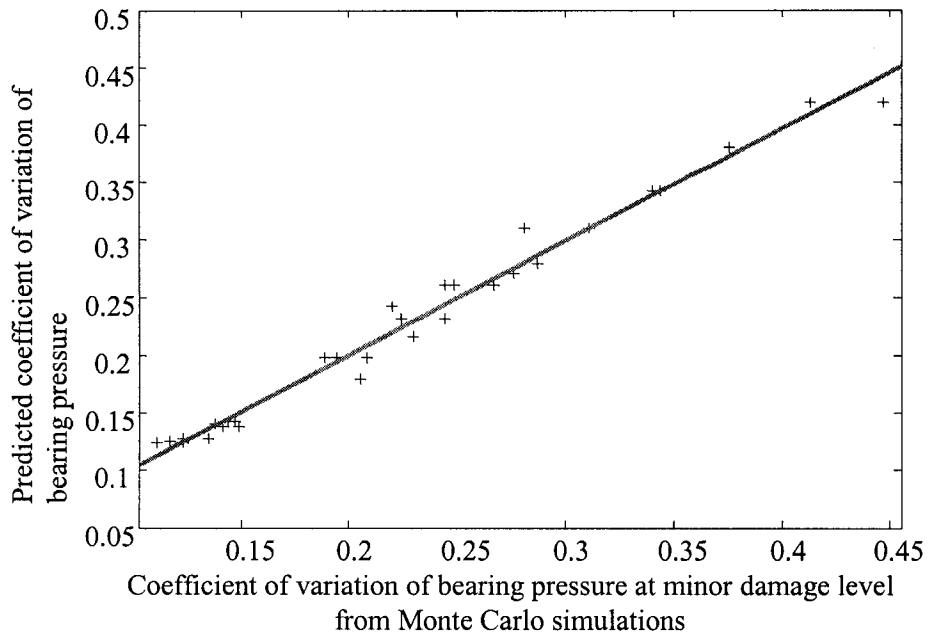


Figure 4.30 Scatter plot for Monte Carlo simulations and predicted (Eq. 4.16) values of coefficient of variation bearing pressure at minor damage level.

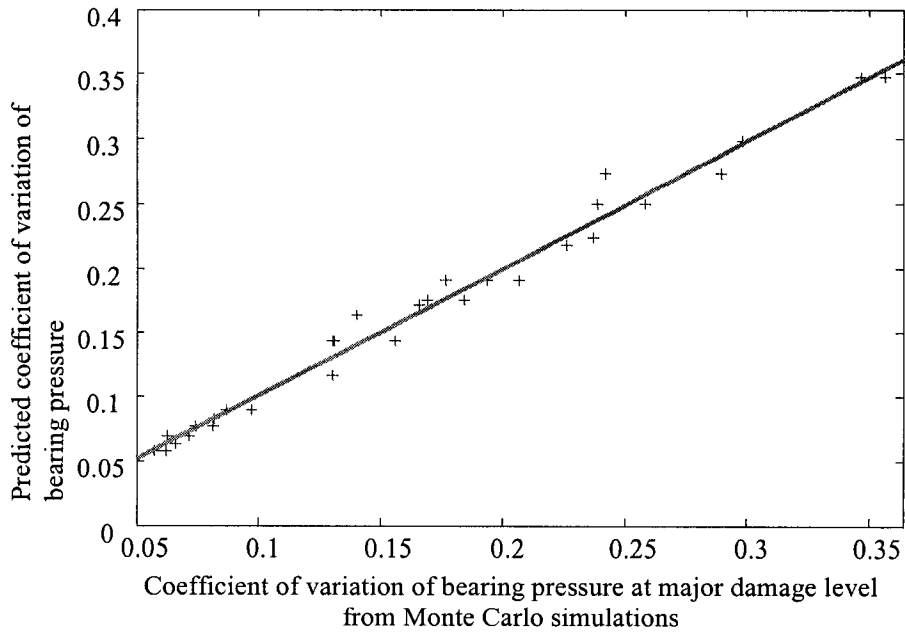


Figure 4.31 Scatter plot for Monte Carlo simulations and predicted (Eq. 4.16) values of coefficient of variation bearing pressure at major damage level.

For $E/c_u = 300$, the regression equations were obtained for limit bearing pressure at damage levels similar to $E/c_u = 1500$. The following simplified equations can be written for mean bearing pressure and its coefficient of variation at the three damage levels (for cases with $E/c_u = 300$),

$$R_{minor} / R_{medium} / R_{major} = a + bC_V \quad \text{Eq. 4.17}$$

$$C_{V-minor} / C_{V-medium} / C_{V-major} (\%) = c + dC_V \quad \text{Eq. 4.18}$$

where a , b , c , d are given in Table 4.20 and Table 4.21. The predicted R^2 for all fitted equations except for $C_{V-major}$ were larger than 0.95. The equation for $C_{V-major}$ had a predicted $R^2 = 0.86$ and $R^2 = 0.95$. The damage levels were defined based on foundation rotations. These equations demonstrate that the foundation rotations were probably influenced by soil variability near the foundation particularly for the lower E/c_u . Therefore, the correlation distance in the range studied was not a significant factor in Eq. 4.17 and Eq. 4.18.

Table 4.20 Parameters for estimating mean limit bearing pressure at different damage levels (Eq. 4.17, for cases with $E/c_u = 300$)

Damage levels	Gamma Probability distribution		Beta Probability distribution	
	a	b	a	b
Minor	0.689	-0.0102	0.681	-0.0109
Medium	0.749	-0.00913	0.759	-0.0107
Major	0.821	-0.00840	0.828	-0.00981

Table 4.21 Parameters for estimating coefficient of variation of bearing resistance at different damage levels (Eq. 4.18, for cases with $E/c_u = 300$)

Damage levels	Gamma Probability distribution		Beta Probability distribution	
	c	d	c	d
Minor	9.59	1.33	7.63	1.77
Medium	11.0	0.873	7.40	1.31
Major	11.5	0.536	8.00	0.933

4.6. APPLICATION TO DESIGN AND RELIABILITY ANALYSIS

The results presented in Section 4.4 were used to calibrate partial design factors. The results in Section 4.5 can also be used in the same framework to calibrate partial design factors for damage criteria (serviceability criteria). It is also possible to estimate mean bearing pressure and its coefficient of variation at failure and several damage levels using the equations provided in Sections 4.4 and 4.5. These values can be used in reliability level II and III analyses. Calibration of partial design factors is an example of using these values in reliability level II analysis. This section presents a possible integration of the results obtained in this study with more vigorous reliability analysis.

Assuming uniform soil properties and weightless soil, bearing capacity of a shallow foundation can be defined as,

$$q^{\text{det}} = N_c c_u \quad \text{Eq. 4.19}$$

where N_c is the bearing capacity factor ($N_c = 5.14$ for a Tresca soil – Prandtal solution) and c_u is the soil shear strength. Based on the study presented here, the effects of soil heterogeneity can be accounted for by,

$$q = Xq^{\text{det}} = XN_c c_u \quad \text{Eq. 4.20}$$

where X is normalized bearing capacity (or pressure). X is a random variable; its mean can be obtained using Eq. 4.4 & Eq. 4.5 and its coefficient of variation can be obtained using Eq. 4.6 & Eq. 4.7. The empirical probability distributions of bearing capacity were studied. It was found that a lognormal distribution often fit well. Use of lognormal distribution is also common in these applications – e.g. construction of fragility curves (Shinozuka et al., 2000 [187]). Thus, a logarithmic distribution can be assumed for X . As discussed in the literature review, there are other sources of uncertainty. For instance, there is uncertainty in N_c due to the complex behaviour of soil and there is uncertainty in mean c_u due to measurement errors. Assuming independence between different sources of uncertainty, it is easy to obtain the cumulative probability distribution of bearing capacity if the probability distributions of other uncertainties are known. The cumulative probability distribution of q is,

$$F(q) = \iiint_{X.N_c.c_u < q} XN_c c_u f(X)g(N_c)h(c_u) \, dX.dN_c.dc_u \quad \text{Eq. 4.21}$$

where f , g , and h are probability density functions, *pdf*, of their arguments. Similar to bearing capacity, the cumulative probability distributions can be obtained for bearing pressures at damage levels. Popescu et al. (2002) [170] performed such calculations to

obtain fragility curves at ultimate state and damage levels accounting for additional uncertainty due to measurement errors.

4.7. SUMMARY

The effects of soil heterogeneity on the bearing capacity of strip foundations under undrained conditions were examined using a Monte Carlo simulation method, including digital generation of non-Gaussian random fields and nonlinear finite element analyses with stochastic input. A parametric study was performed to investigate the effects of (1) degree of variability, (2) scales of fluctuation, (3) probability distribution of soil strength, and (4) soil deformability on predicted bearing capacity and differential settlements. The analysis cases were designed using a Design of Experiment (DOE) method. Main parameters (mean and coefficient of variation) of resulting bearing distribution at the ultimate state and three damage levels were derived based on statistical analyses using the response surface methodology. The results were summarized and studied in terms of cumulative probability distribution curves that express the probability of exceeding a certain degree of structural damage. The three serviceability states associated with differential settlements, and a limit state associated with bearing capacity failure were analysed. Regression equations are provided to account for the effects of probabilistic characteristics of soil on bearing resistance of soil. They can be used in foundation design and reliability analysis. The following main results are derived,

- Behaviour of soil and soil-structure systems in the nonlinear regime is strongly affected by the natural spatial variability of soil strength within geologically distinct and uniform layers.
- Increasing soil variability and the amount of loose pockets in the soil mass (controlled by the left tail of the probability distribution of soil strength) strongly diminished bearing capacity of soil and increased differential settlements.
- The average bearing capacity of heterogeneous soils obtained from Monte Carlo simulations resulted in consistently lower values than those predicted assuming uniform soil strength. Soil shear strength variability and its distribution (amount of loose pockets) were the most significant factors.
- The predicted bearing capacity had a lower coefficient of variation than that of the soil shear strength. This can be attributed to the effects of local averaging (Vanmarcke, 1983 [209]). Variability of bearing capacity originates from soil shear strength variability. The horizontal correlation distance and probability distribution (amount of loose pockets) of soil shear strength variability affects the variability of bearing capacity.
- The study demonstrated how the effects of natural soil variability can be combined with other sources of scatter to estimate the total uncertainty in the bearing capacity.
- A methodology was developed to account for the effects of natural soil variability in a limit state design method. Partial resistance factors were

calibrated for a target reliability index ($\beta = 3.5$) considering the effects of soil natural variability as well as other sources of scatter (uncertainty).

- Characteristic bearing capacity values of a heterogeneous soil deposit, corresponding to a failure probability of 5%, were obtained. The required reduction factors to obtain characteristic values were contoured in Figure 4.24 for the ranges of probabilistic characteristics considered here.

CHAPTER 5

LATERAL LOADING OF A BURIED PIPE

5.1. INTRODUCTION

5.1.1 Description

A study of the effects of soil heterogeneity on lateral loading of a buried pipeline was conducted using Monte Carlo simulation methodology. Results of simulations accounting for the spatial variability of soil strength were compared to deterministic analyses assuming uniform soil properties. Soil response to movement of buried pipelines and corresponding failure mechanisms are still not well known for uniform soil. Due to the complex behaviour of pipeline and the large number of factors affecting pipe response, this study had a limited scope compared to the one on foundation and can be assumed as a starting point for future research. Only one configuration for a buried pipeline was considered. The effects of soil shear strength variability and correlation distances were briefly studied. Based on the results, recommendations were set forward for future work. Numerical, experimental and theoretical aspects of soil-pipe analysis are discussed in Section 2.3.

The response of oil and gas pipelines to soil movements is an important consideration in pipeline design and route selection. These soil movements may be due to landslides, seismic activity such as faulting or lateral spreading, or a variety of other causes. These soil movements displace the buried pipeline as exemplified in Figure 5.1. This is a displacement controlled loading scenario (e.g. ASCE, 1984 [5]; Paulin, 1998 [149]). The load transfer behaviour between a pipe and the surrounding soil is not well understood. A simplified approach to complex loading is to account for soil-pipe interaction in three distinct directions: axial, transverse lateral and transverse vertical (also see Section 2.3.1). In this study, only lateral movements of soil were considered. For simplification, it was assumed that the backfill soil has the same characteristics as native soil.

5.1.2 Objectives and Limitations

Many factors, including soil shear strength, burial depth, pipe diameter and soil weight contribute to the response of buried pipelines subjected to soil movement. The failure mechanism of a pipeline also changes with the aforementioned parameters. In this study, only one configuration for buried pipelines was considered. The following objectives were pursued:

- validate the capability of finite element method to capture the failure mechanism of a buried pipeline;
- demonstrate the capability of the proposed methodology to capture the effects of soil heterogeneity;

- investigate the effects of degree of variability of the soil strength, C_v , and correlation distances on the response of pipeline; and
- investigate the effects of soil heterogeneity on the behaviour and failure mechanisms of pipelines.

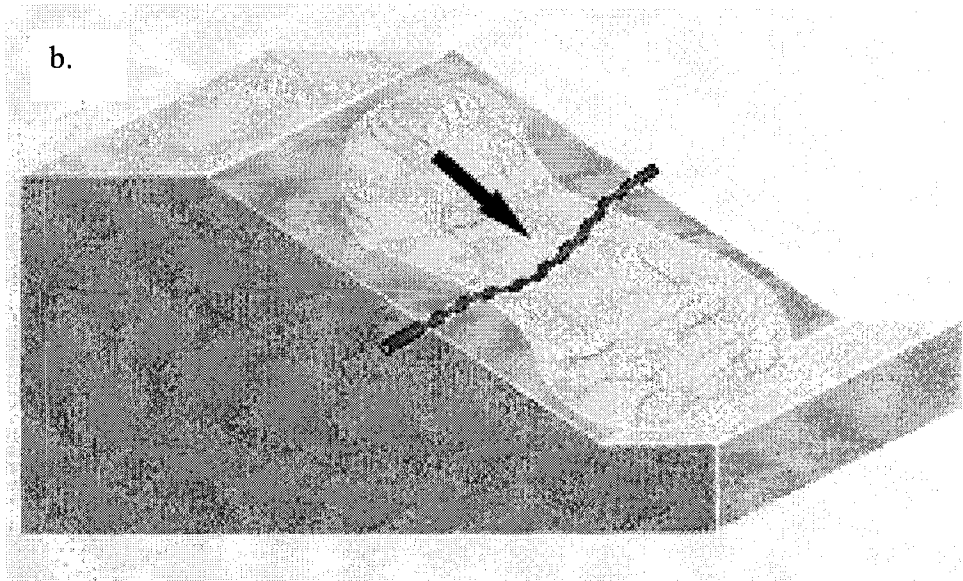


Figure 5.1 Lateral movements of soil: (a) an observed landslide in cohesive material; and (b) schematic representation of landslide.

5.2. DETERMINISTIC FINITE ELEMENT ANALYSIS

5.2.1 Finite Element Analysis Set-up

5.2.1.1. Finite element mesh

One embedment ratio was analysed with $H/D = 1.5$ (shallow cover), where H is the springline burial depth and D is the pipe diameter. The finite element mesh and boundary conditions used are shown in Figure 5.2. The soil was discretized using 482 quadratic plane strain finite elements with 8 nodes and reduced integration (CPE8R in ABAQUS). During the course of projects conducted at C-CORE, it was concluded that these second order elements yielded higher accuracy than linear elements at the same computational effort for pipeline analysis. A rigid pipe section was modelled using 20 3-node quadratic beam structural elements (B22). These beam elements model a rigid pipe; therefore, their plane stress behaviour does not affect the analysis. Also, there is no nodal rotation in the pipeline section due to rigid behaviour; this satisfies the shape function compatibility between beam and 2D elements.

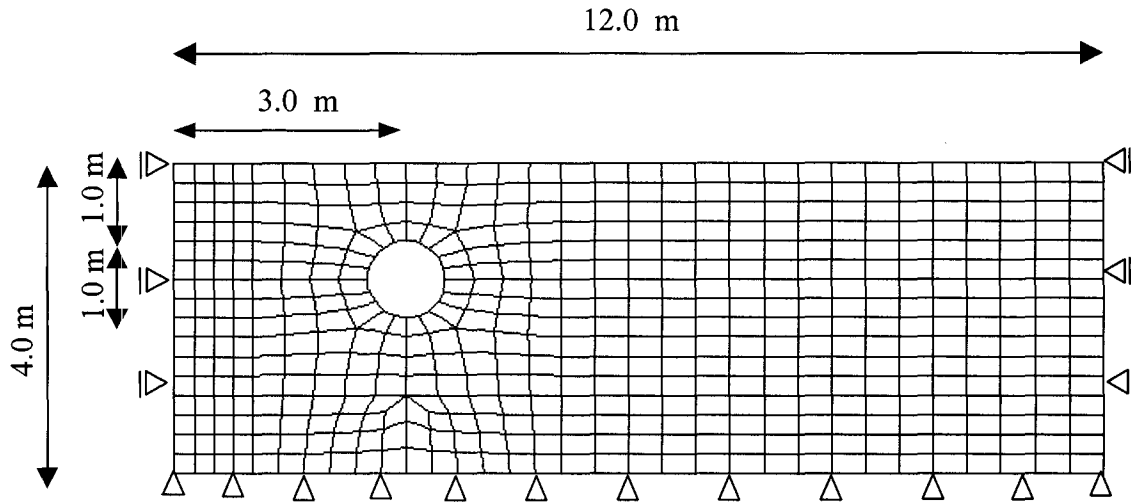


Figure 5.2 Typical finite element mesh and boundary conditions.

The contact surface approach implemented in ABAQUS/Standard, allowing for separation and sliding of finite amplitude and arbitrary relative rotation of the contact surfaces, was used to simulate the pipe/soil interface. The contact was assumed frictional, with isotropic Coulomb friction. The shear stress between the surfaces in contact was limited by a critical stress $\tau_{crit} = \mu p$, where p is the normal contact pressure, and μ is the friction coefficient. For clay materials, a maximum value was also assumed for the shear stress at the interface, τ_{max} , irrespective of the normal contact pressure. The critical shear stress is expressed as $\tau_{crit} = \min(\mu p, \tau_{max})$. Practical values of τ_{max} for pipe/soil interface are approximately one third of the undrained shear strength (e.g. Paulin et al., 1998 [150]). In this study, the interface between the soil and pipe was assumed to be adhesive; hence, $\tau_{max} = 0.33c_u$ and a large friction coefficient of $\mu = 1$ were assumed.

5.2.1.2. *Material properties*

A clay material under undrained conditions was assumed. The soil material properties were as follows:

Average undrained shear strength, $c_u^{av} = 50\text{kPa}$

Deformation modulus, $E = 300 c_u$

Poisson's ratio, $\nu = 0.49$, to simulate an almost incompressible behaviour

Total unit weight $\gamma = 18 \text{ kN/m}^3$

The pipe was modelled using a linear elastic material with very high stiffness to simulate a rigid pipeline.

5.2.1.3. *Analysis procedure*

First, a geostatic step was performed to establish the initial stress state in the soil. Next, the desired pipe movement was imposed as displacement controlled. Nodal displacements were prescribed in the horizontal direction, while the pipe was free to move in the vertical direction. Large deformations and finite strain analysis options were used throughout the study.

The program generated the interaction forces only at contact nodes in the soil, so called the "slave" surface. Due to the large relative deformations at soil/pipe interface, it was difficult to follow the position of soil nodes relative to the pipe and, therefore, those nodes were not appropriate for calculating the forces on the pipe. The predicted soil/pipe interaction forces could be obtained using two methods: (1) from driving forces as nodal reactions – for nodes with imposed displacements, and (2) from element forces, using the

balance of the internal element forces over each node at the pipe/soil interface. The first method is deemed to provide correct numerical results, while the second may be affected by numerical errors induced by adding element forces that can differ by several orders of magnitude. The first methodology was employed here.

5.2.2 Finite Element Results

The predicted interaction forces are presented as normalized pressure–normalized displacement curves, in which the normalized pressure is calculated as,

$$p_n = \frac{F}{c_u D} \quad \text{Eq. 5.1}$$

where F is the interaction force per meter of pipe, D is the pipe diameter, and c_u is the undrained shear strength of clay. The pipeline displacement was normalized with respect to the pipe diameter. In this study, the pipeline diameter was one metre.

5.2.2.1. Predicted force displacement results

Predicted force displacement curves are shown in Figure 5.3 for two cases – one with and one without self-weight effects. The results were compared to the results of Rowe and Davis (1982a) [179]. This reference used weightless soil. Figure 5.3 shows very good agreement between predicted weightless ultimate capacity and those obtained by Rowe and Davis. The effects of weight on the bearing capacity factor of pipeline increases as the $\gamma h/c_u$ ratio increases. This was demonstrated by performing the same analysis on soft clay with shear strength of 10 kPa as shown in Figure 5.3b. It is also known that increases in burial

depth of pipeline results in an increase in the bearing capacity factor. This can be attributed to changes in failure mechanism and stress level at pipeline. Figure 5.4 shows some of these effects. These issues are currently being studied through deterministic analysis assuming uniform soil properties (Popescu et al., 2002 [168]). As previously mentioned, only one configuration, as shown in Figure 5.2, was considered for stochastic analysis and the research can be further expanded to a more general parametric study.

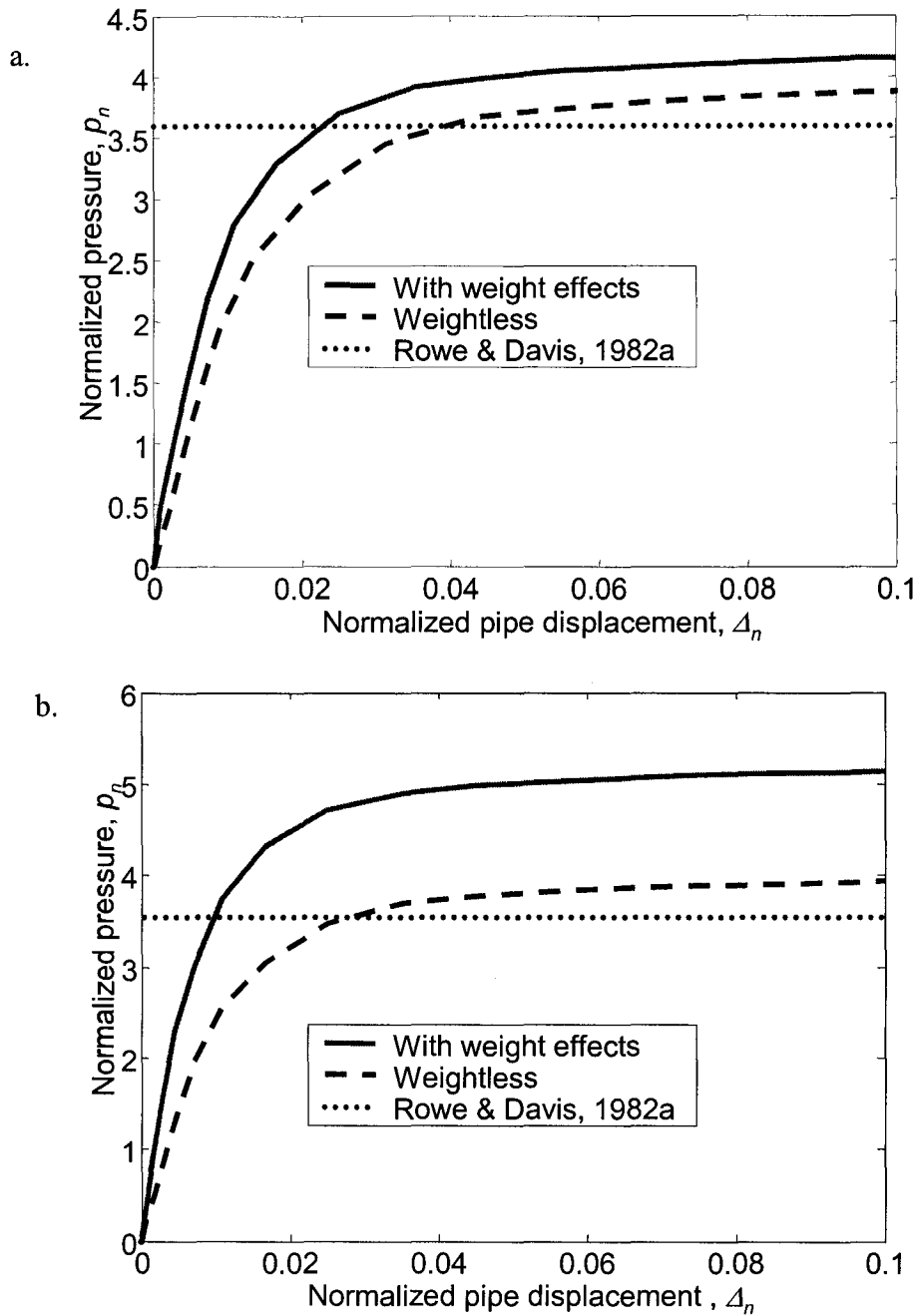


Figure 5.3 Predicted normalized pressure-normalized displacement for pipeline as shown in Figure 5.2 and comparison with Rowe & Davis (1982a) results: a. firm clay used in stochastic analysis with $c_u = 50$ kPa; b. soft clay with $c_u = 10$ kPa.

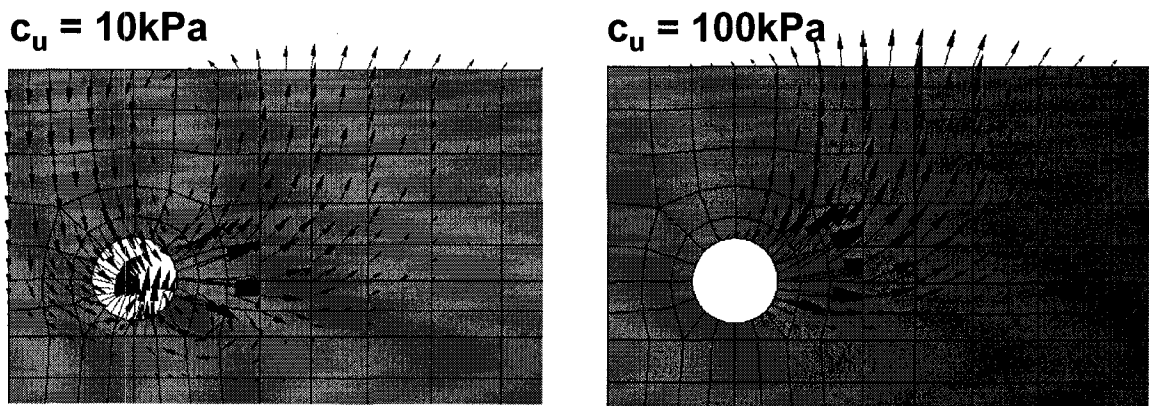
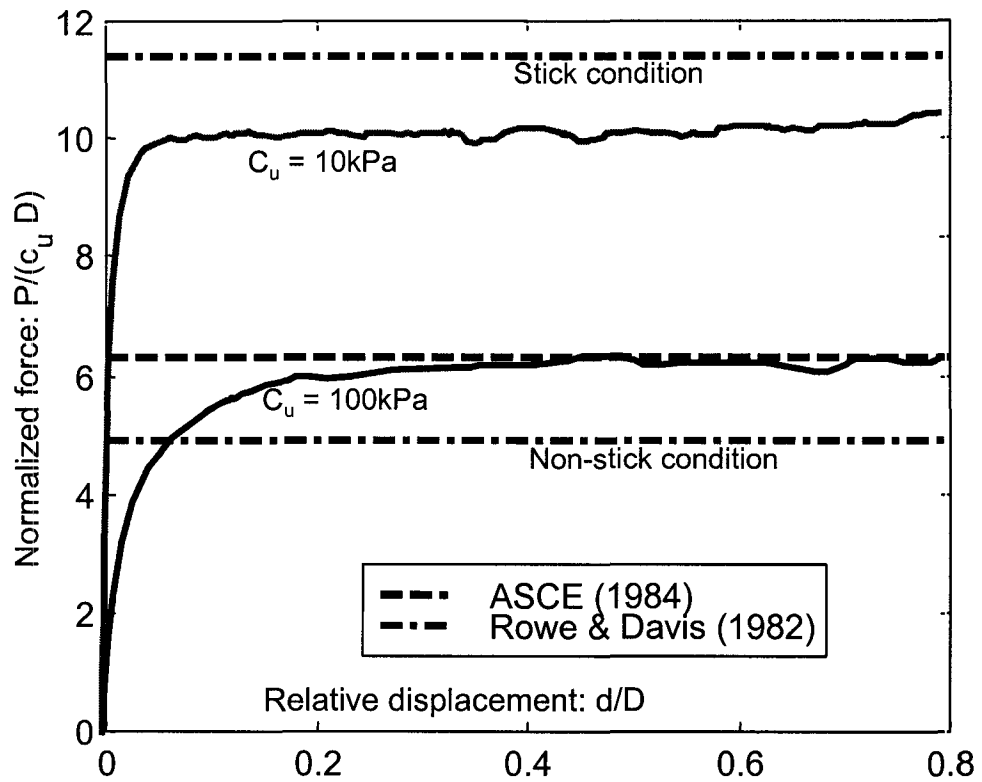


Figure 5.4 Effects of undrained shear strength on soil failure mechanism and p-y curves (H/D ratio of 2.5) – adapted from Popescu et al. 2002 [168].

5.2.2.2. Failure mechanism

Figure 5.5 shows contours of plastic shear strain due to lateral loading of pipeline as described in Section 5.2.1. It illustrates the failure mechanism of firm clay ($c_u = 50$ kPa, $E = 300 \times c_u = 15000$ kPa) under lateral loading of a rigid pipeline.

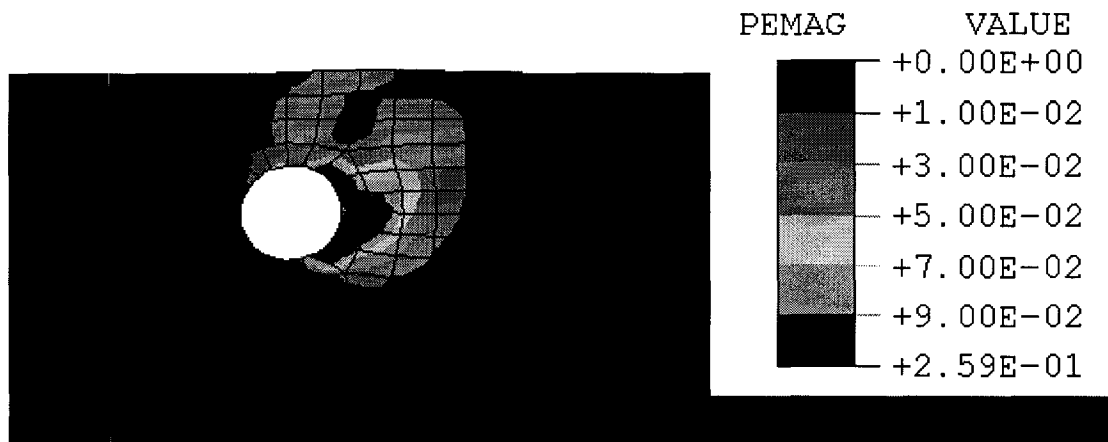


Figure 5.5 Contours of plastic shear strain magnitude (PEMAG) demonstrating failure mechanism of firm clay subjected to lateral loading of rigid pipeline (uniform soil).

5.2.3 Validation of the Numerical Model

5.2.3.1. Validation of finite element model based on full-scale experimental results

Using the continuum finite element method, a numerical model was constructed for pipe-soil interaction involving large relative displacements. The analysis procedure accounted for the nonlinear behaviour of soil materials, relative slip and separation at the pipe-soil interface. The calculations were performed in terms of large displacements/finite strains. The model was calibrated and validated based on full-scale experimental data (e.g.

Paulin, 1998 [149]). Various soil materials, soil-pipe relative flexibility and loading mechanisms were considered in the numerical program (see e.g. Nobahar et al., 2000 [141]; Popescu et al., 2001 & 2002 [160 & 161]; Guo et al., 2002 [80]).

For verification, numerical modelling results were compared with experimental data from a large-scale model study. The finite element mesh used in this verification is shown in Figure 5.6. Comparisons between finite element predictions using Tresca model and experimental measurements in terms of force-displacement curves are presented in Figure 5.7 for firm clay and soft clay. A range of results was obtained based on the range of shear strength estimated from different triaxial tests performed on the same soil (shaded area in Figure 5.7). The values are not shown due to the confidentiality of test results. Figure 5.8 presents the comparison of calculated plastic deformation zone in stiff clay and the observed deformation at the end of the test after excavation.

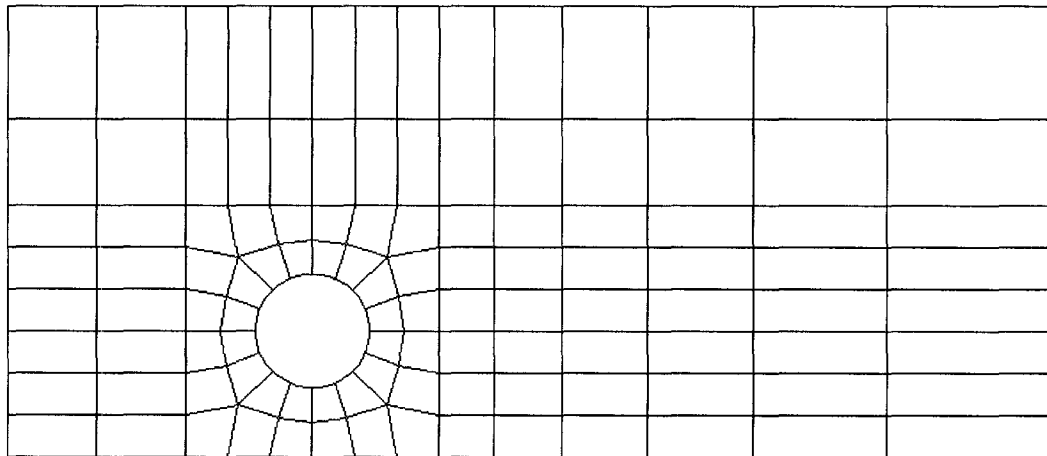


Figure 5.6 Finite element mesh for validation modelled according to large-scale experimental tank size.

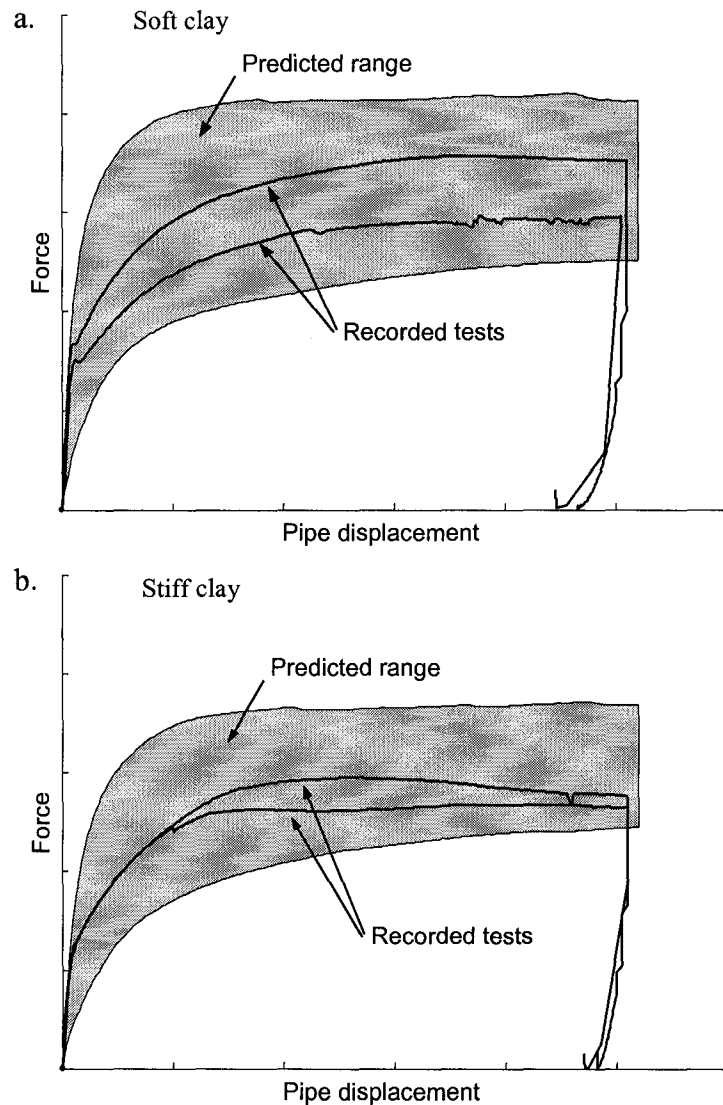


Figure 5.7 Recorded and predicted range of force-displacement relations for large-scale tests in clay, using the Tresca model: a. soft clay; b. stiff clay.

Popescu et al. (1999) [166], Nobahar et al. (2000) [141], and Popescu et al. (2001) [160] implemented more advanced models such as Cam-Clay model (with associated plastic flow rule) for clay materials and the extended non-associated Mohr-Coulomb plasticity model accounting for softening/hardening of sand to back-analysis the results of large-scale tests. Two-dimensional, nonlinear finite element analyses of large scale tests of

lateral loading of a rigid pipe were performed for numerical model validation, using the soil materials employed in the full-scale experiments: stiff and soft clays, and dense and loose sands. Comparisons between numerical predictions and full-scale experimental results proved that the finite element model was able to closely simulate the observed phenomena in terms of force-displacement relations (Figure 5.9) and failure mechanisms (Figure 5.10). Popescu et al. (1999) [166], Nobahar et al. (2000) [141] and Popescu et al. (2002) [168] presented a summary of the numerical results and model calibration, as well as a discussion of the limitations of the soil constitutive models used in these studies.

5.2.3.2. *Summary*

This section presents comparisons and validation of numerical analysis of pipe-soil interaction. As discussed in the literature review, there is a wide range of factors and equations suggested by researchers to calculate soil-pipe interaction response. The Tresca model, discussed in Section 3.5.2.3, was used here. In a plane strain condition, this model predicts interaction forces that are 15% lower than those obtained using von-Mises model and it is theoretically more rational (see Section 3.5.2). Force-displacement relations for the configuration used in stochastic analysis are presented in Figure 5.3.

Comparisons between numerical modelling and large-scale model tests on pipelines buried in both sand and clay show that the proposed numerical procedure can reasonably reproduce pipe-soil interaction forces under different soil conditions, when soil parameters are correctly estimated.

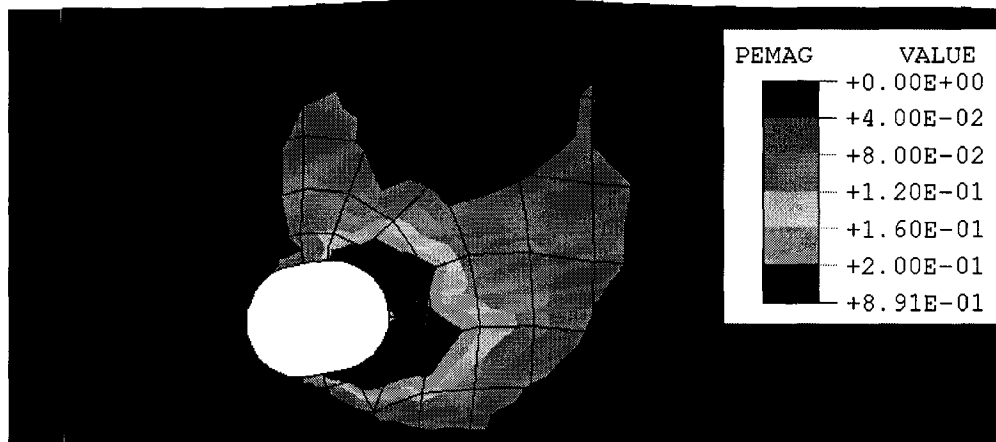
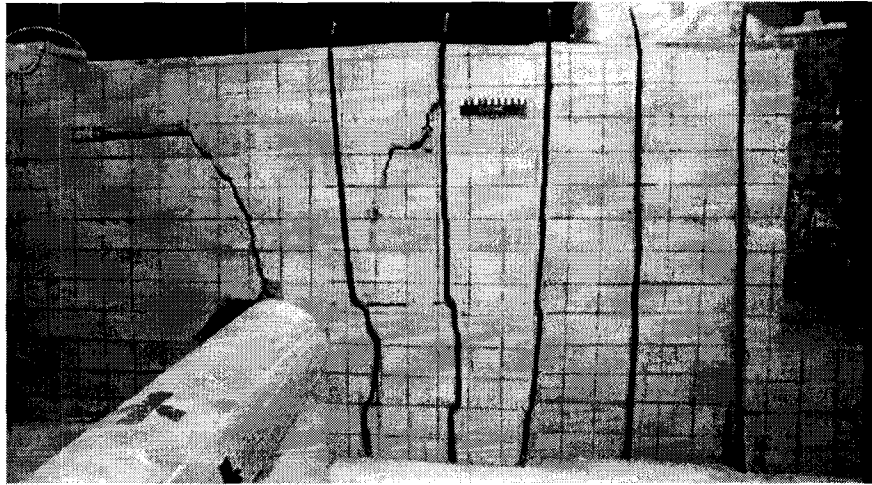


Figure 5.8 Comparison of predicted and observed failure in stiff clay: a. observed (after Paulin et al. 1998 [150]); b. predicted using a finite element model of the experimental tests; c. predicted using finite element model used for stochastic analysis.

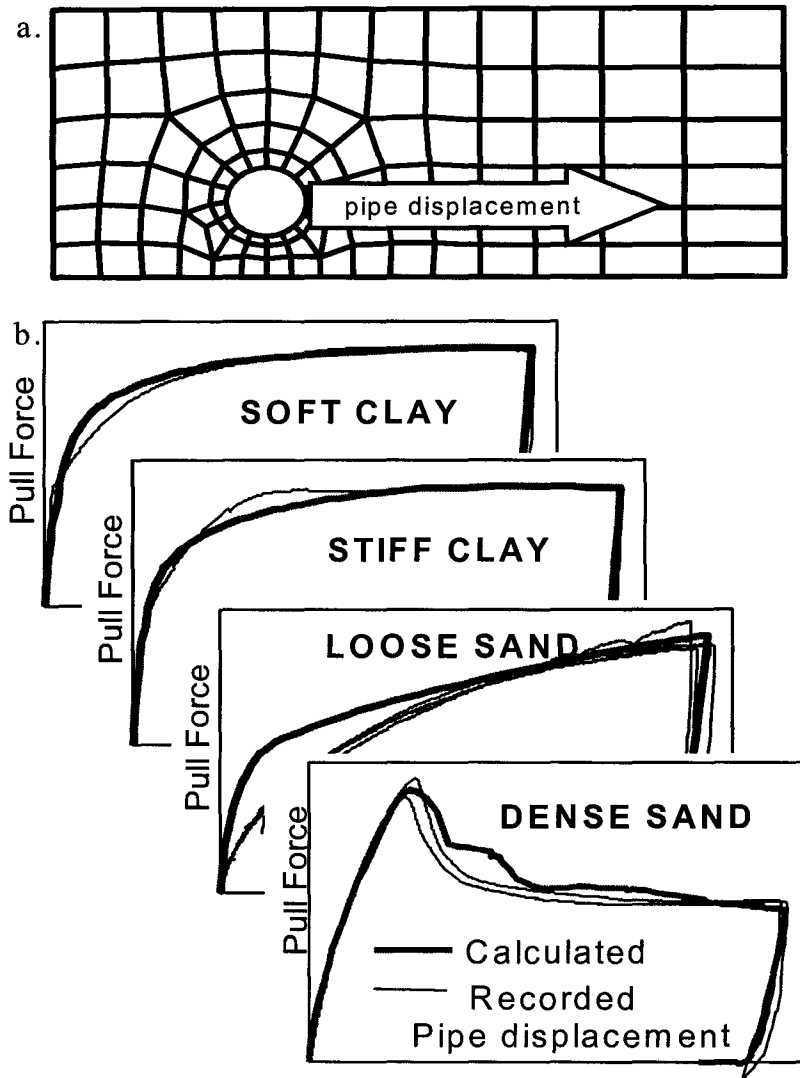


Figure 5.9 Validation of a numerical model for pipe/soil interaction: a. finite element mesh; b. comparison of recorded and predicted force-displacement relations (from Popescu et al., 2002 [169]).

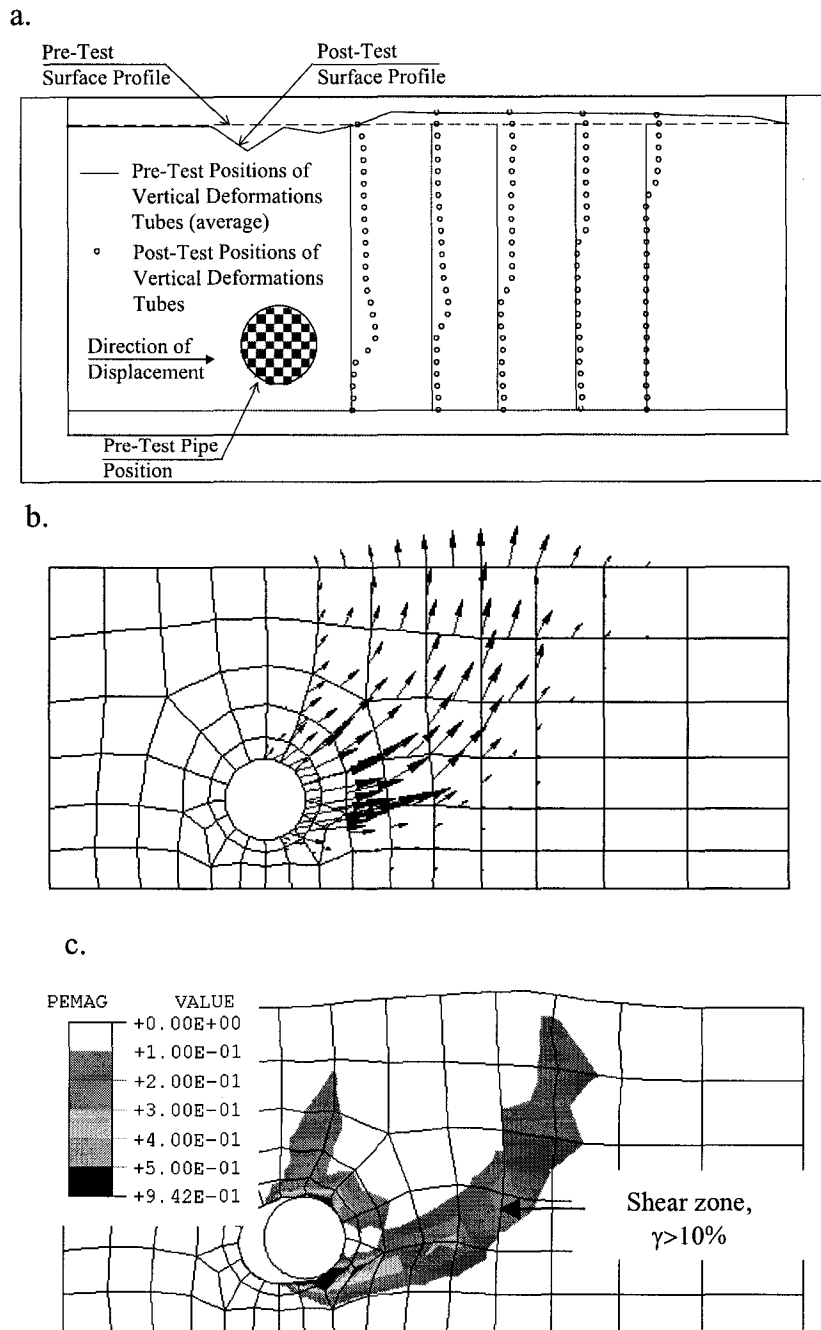


Figure 5.10 Comparison of predicted and observed behaviour of dense sand: a. post-tests deformation tubes (after Paulin et al. 1998 [150], printed with permission from the Canadian Geotechnical Society); b. predicted displacements; c. predicted contours of plastic strain magnitude (after Nobahar et al., 2000 [141]).

5.3. STOCHASTIC FINITE ELEMENT ANALYSIS

5.3.1 Selection of Probabilistic Characteristics for Soil Variability

The range of soil variability adopted in this study for the undrained soil strength was $C_V = 20\%$ to 80% . This range was selected based on the literature review (Section 2.1.1.3). Pipelines are buried in all types of soil having low or high shear strength; thus, a possible range of inherent variability of soil strength is wider for pipelines than for foundations. A separable correlation structure based on the exponentially decaying model was assumed, with a range of scales of fluctuations: $\theta_{hn} = 2.5$ to 5 , and $\theta_{vn} = 0.25$ to 1.5 (where θ_{hn} , θ_{vn} are correlation distances normalized with respect to the pipe diameter). Due to the limited scope of this study, a limited range of correlation distances was analysed. A Gamma probability distribution skewed to the right was assumed for the soil shear strength (Figure 3.2). The average shear strength, c_u^{av} was 50 kPa. The soil deformation modulus for undrained behaviour was assumed as $E = 300c_u$.

Table 5.1 presents the cases analysed for lateral loading of the pipeline. A factorial design was followed, but only variation of two parameters, namely the degree of soil variability and the vertical correlation distance, was considered. For two cases, the horizontal correlation distance varied as well (cases 6 and 7).

Table 5.1 Stochastic cases analysed for lateral loading of pipeline

Experiment #	Coefficient of variation, C_V (%)	Normalized horizontal correlation distance, θ_{hn}	Normalized vertical correlation distance, θ_{vn}
	Factor 1	Factor 2	Factor 3
1	20	5	0.5
2	80	5	0.5
3	20	5	1.5
4	80	5	1.5
5	50	5	1
6	50	2.5	0.25
7	50	1	0.25

5.3.2 Monte Carlo Simulation Results

5.3.2.1 Comparison with deterministic analysis

For Monte Carlo simulations, a total of 4200 finite element analyses with stochastic input were performed (600 for each case shown in Table 5.1). For each analysis, the pipe response in terms of force vs. displacement was obtained, as discussed in Section 5.2.1.3. Figure 5.11 shows a sample realization of soil strength, the predicted failure mechanism using finite element method, and the corresponding force-displacement curve. The results were normalized in terms of normalized pressure vs. normalized displacement. For case 5 in Table 5.1, the results of Monte Carlo simulations are shown in Figure 5.12a. As shown in Figure 5.12b, the results were processed to obtain the average, and 5% and 95% fractile at each displacement. The results of lateral loading of the same pipe using uniform soil with shear strength, $c_u = 50$ kPa are presented for comparison (Figure 5.12b). The Monte Carlo simulations, accounting for spatial variability of soil strength, yielded interaction forces that

were generally lower than those predicted by the deterministic analysis. However, the effects of soil heterogeneity on pipeline seemed to be smaller than that of shallow foundation. This can be attributed to the observation that pipe failure in uniform soil is asymmetric for uniform soil in contrast to foundation failure. Therefore, soil heterogeneity does not significantly change the failure mechanism. The contours of plastic shear strains are shown for pipeline in Figure 5.11b (compare to Figure 5.5). It should be noted that in pipeline, a lower interaction force is usually desirable for design purposes to decrease the stresses and strains in pipe steel section.

5.3.2.2. *Probabilistic analysis*

The results of Monte Carlo simulations were statistically studied for each case (Table 5.1). The pipe interaction forces were obtained at a reference normalized pipe displacement, $\Delta_n = 0.1$ ($\Delta_n = \delta/D$). The empirical probability distributions of failure loads were constructed for all cases. Their means and standard deviations were estimated and different probability distributions were fitted to the results (an example of lognormal fit, for case 6, is shown in Figure 5.13). Lognormal distribution fit reasonably well the results in all studied cases.

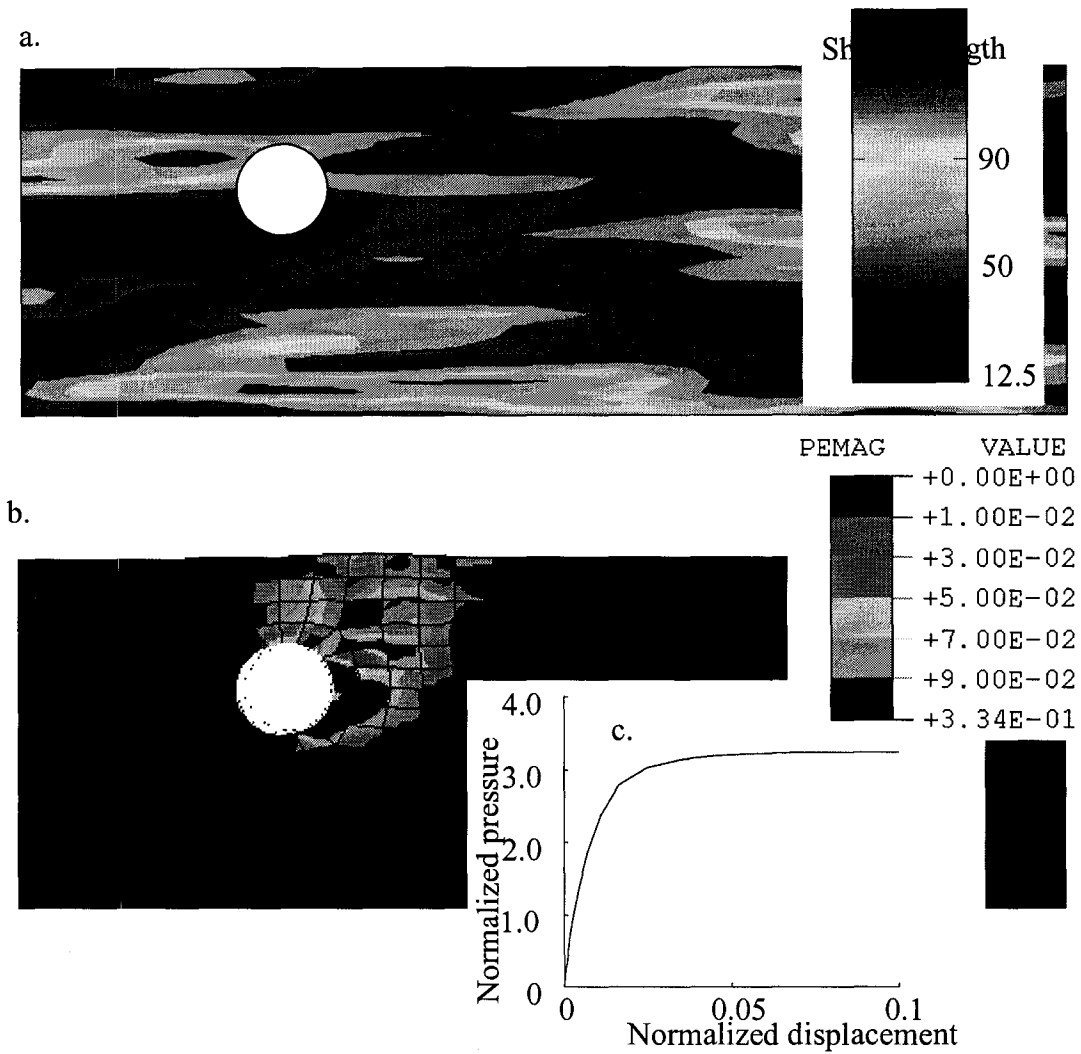


Figure 5.11 A sample finite element analysis with spatially variable input soil: a. contours of undrained shear strength over domain of analysis (with average shear strength of 50 kPa); b. contours of plastic shear strain (PEMAG) demonstrating failure mechanism for the corresponding soil realization; (c) predicted normalized force-displacement relationship for the corresponding soil realization.

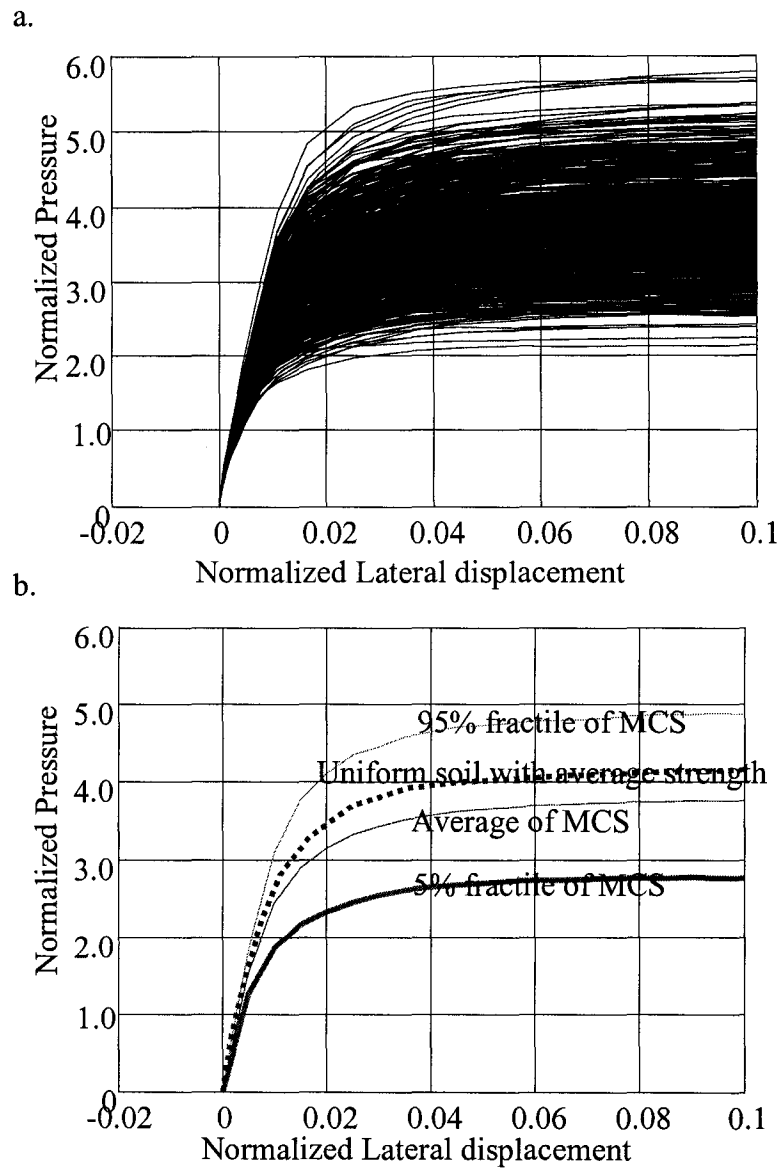


Figure 5.12 Results of Monte Carlo simulations (MCS) and comparison with results obtained for uniform soil with shear strength, $c_u = 50$ kPa.

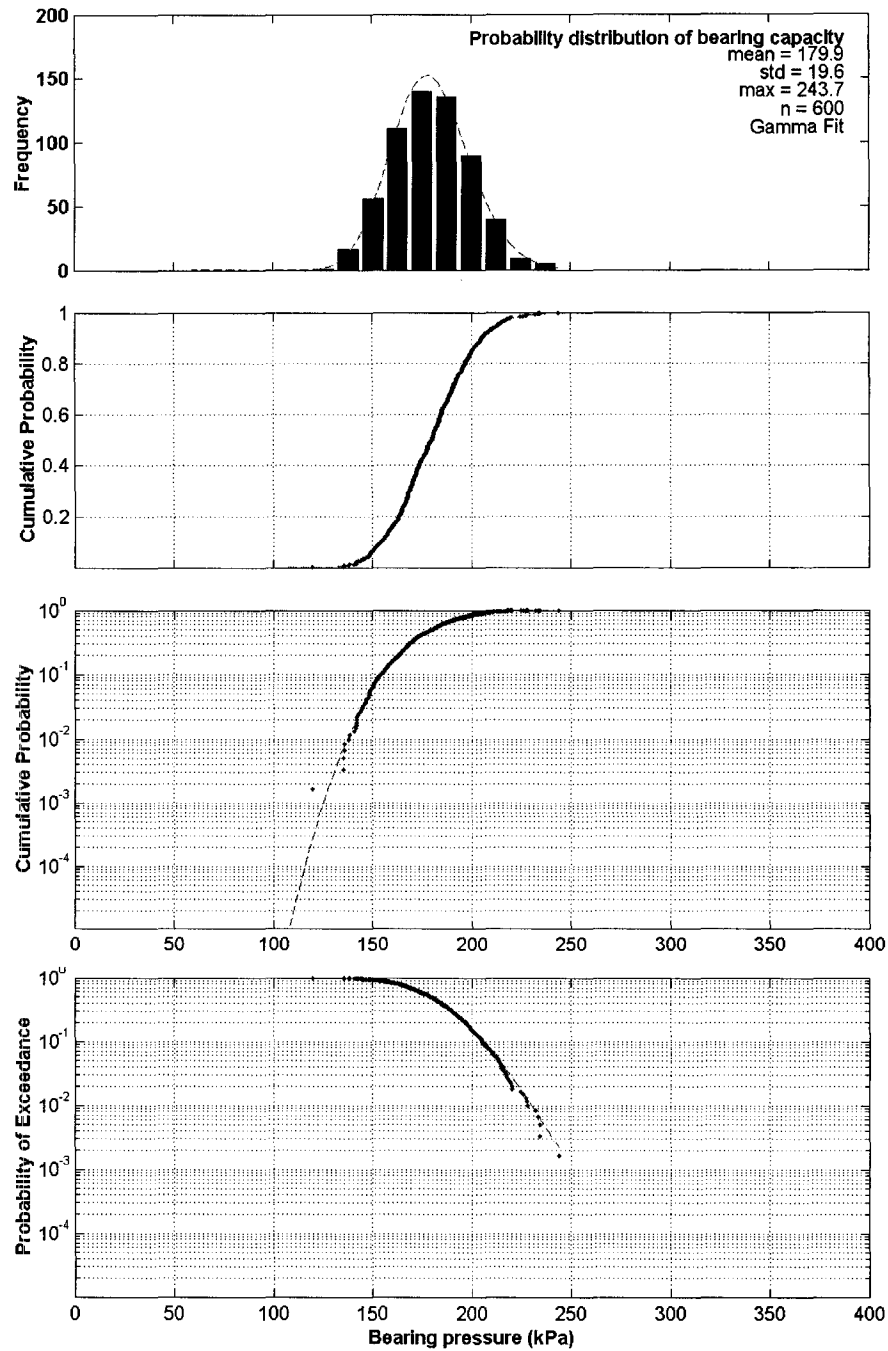


Figure 5.13 Lateral loading of pipeline in heterogeneous clay (case 6 in Table 5.1) – empirical probability distribution of interaction pressures and fitted lognormal distribution (The results are obtained for $c_u^{av} = 50$ kPa and are not normalized).

5.4. ILLUSTRATIVE STUDY FOR A PIPE LOADED IN CLAY

5.4.1 Statistical Analysis of Results – Rigid Pipe; 2D Analysis

For all studied cases, the mean bearing ratio and coefficient of variation were normalized and are reported in Table 5.2. To obtain the mean bearing ratio, similar to the foundation case, the pressure obtained at the reference settlement was normalized by the corresponding pressure of a pipe in uniform soil with shear strength, $c_u = 50$ kPa (comparative study). This ratio shows the amount of decrease/increase in the average bearing pressure in stochastic analyses (Monte Carlo simulations) compared to that of a deterministic analysis using the same soil shear strength (i.e. the average shear strength used in the Monte Carlo simulations). Results showed that the decrease in mean pressure calculated by Monte Carlo simulations was smaller than the decrease found in foundation analysis; this was previously discussed in Section 5.3.2.1. The bearing pressure coefficient of variation, C_V was smaller than that of the soil shear strength, indicating the effect of local averaging. Similar to the foundation case, the vertical correlation distance in the range considered here was found to have non-significant effects on the bearing pressure (compare C_V of cases 1 and 3 and cases 2 and 4 in Table 5.2). An explanation could reside in the fact that the failure surfaces develop in the horizontal direction, similar to the case of bearing capacity of a shallow foundation. For cases 6 and 7, smaller correlation distances in both directions were considered, resulting in noticeable decreases in C_V of bearing pressure

(cases 5 to 7). The C_V of bearing pressure reflected the variability of average shear strength on surfaces in which failure occurred.

Table 5.2 Results of lateral loading of pipe in terms of normalized mean and coefficient of variation of bearing pressure

Exp. #	Factor 1	Factor 2	Factor 3	Bearing pressure at $\Delta_n = 0.1$	
	Coefficient of variation of soil strength, C_V (%)	Normalized horizontal correlation distance, θ_{hn}	Normalized horizontal correlation distance, θ_{vn}	Mean bearing pressure ratio, R_{BC} (*)	Bearing pressure, C_V
1	20	5	0.5	0.95	6.7%
2	80	5	0.5	0.73	32.3%
3	20	5	1.5	0.95	7.0%
4	80	5	1.5	0.72	34.2%
5	50	5	1	0.88	17.4%
6	50	2.5	0.25	0.86	10.9%
7	50	1	0.25	0.86	8.6%

* The mean bearing ratio defined as the pressure obtained at the reference settlement normalized by the corresponding pressure of a pipe in uniform soil with shear strength, $c_u = 50$ kPa

5.4.1.1. Regression equations

As illustrated, the results obtained for parameters in Table 5.2 were statistically studied and a response surface, similar to that obtained for the foundation in Section 4.4, was fitted to the results. However, the ranges of studied parameters were limited, and therefore, the equations and results presented here are mainly for illustration purposes and are valid only in the specific range and set-up considered here. Only cases 1 to 5 were statistically designed and used in obtaining the regression equations.

For mean bearing pressure ratio, the following equations were derived from fitting to the results in Table 5.2,

$$R_{BC} = 1.03 - 0.00376C_V \quad \text{Eq. 5.2}$$

For bearing pressure C_V ,

$$C_{VBC} (\%) = -2.0 + 0.44C_V (\%) \quad \text{Eq. 5.3}$$

The contribution of the vertical correlation distance in the predicted C_V of bearing pressure was small for the limited studied range ($C_V = 20\%$ to 80% ; $\theta_{hn} = 5$; $\theta_{vn} = 0.5$ to 1.5) and for the deterministic set-up here; therefore, it was omitted for response fit in Eq. 5.3. It should be noted again that only cases 1 to 5 were used in regression; thus, the above equations are only approximately valid for the studied ranges. It is well known that correlation distances affect the coefficient of variation of response. For example, for correlation distances of infinity, both soil strength and pipe response will have identical variation. The effects of correlation distances on variability of response (bearing pressure) are demonstrated using the results of cases 6 and 7 (Table 5.2). These effects should be investigated through a more detailed parametric study.

5.4.2 Lateral Loading of Flexible Pipeline, 3D Effects

Soil bearing capacity on a laterally loaded pipeline buried in heterogeneous soil is quantified as a random variable in Section 5.4.1 assuming plane strain condition in a plane normal to pipe axis. These results can be used to define spring characteristics in structural models to analyze the effects of soil heterogeneity for a pipeline subjected to lateral soil movements; in structural models, the soil continuum is represent using springs (see Figure

2.13). Structural models as discussed in the literature review (Section 2.3.1) are state of practice in pipeline engineering. Here, the application of the study to a practical problem is demonstrated.

A pipeline subjected to subscour deformation is considered. The soil deposit under ice-scour undergoes large deformations (e.g. Poorooshasb and Clark, 1990 [158]). Practical methods were developed by C-CORE to predict subscour soil deformation under a research program named PRISE. PRISE, the Pressure Ridge Ice Scour Experiment, was a jointly funded program to develop the capability to design pipelines and other seabed installations in regions scoured by ice, taking into account the sediment deformations and stress changes which may be caused during a scour event, Clark et al. (1998) [34]. Here, a pipeline buried in an overconsolidated clayey deposit subjected to ice-scour loading with characteristics given in Table 5. 3 were considered. Soil movements at pipeline springline were calculated based on C-CORE routines (Table 5. 4; see Woodworth-Lynas, 1996 [220]) as illustrated in Figure 5. 14a. It was necessary to simplify the complex sub-scour loading mechanism to allow for a meaningful comparison. Thus, only horizontal movements of soil and one loading condition were considered here.

The lateral bearing capacity of uniform soil was estimated based on ASCE (1984) [5]. For heterogeneous soil, the lateral bearing capacity was assumed as a random variable with mean and coefficient of variation calculated according to Equations 5-2 & 5-3 and the lateral bearing capacity in uniform soil. The lateral bearing capacity along the pipeline, which defines the lateral spring capacity, is modelled as a 1D random field. The assumed parameters for soil heterogeneity and spring characteristics are given in Table 5. 4. One

sample function of the random field representing spring characteristics was generated and a finite element analysis was performed. The results obtained for uniform and heterogeneous soil are compared in Figure 5. 14b&c in terms of longitudinal strains for points 1&2 of the pipeline section as shown in Figure 5. 14a. It can be seen that soil heterogeneity has changed the symmetric pattern of strain distribution in the pipeline. Also due to non-uniformity of the soil reaction, the strains in the case analysed are significantly larger than those obtained for a pipeline buried in assumed uniform soil. When assuming uniform soil, both compression and tensile strains are satisfactory, based on DNV's (2000) [53] criteria. However, both strains are above the acceptable limits for heterogeneous soil (Figure 5. 14).

Table 5. 3 Parameters used for the pipeline in Section 5.4.2

Pipeline Characteristics		
Parameter	Value/Type	Explanation/ Reference
Pipeline grade	X52	Typical steel
Yield strength for X52	358 MPa @ 0.5% strain	Ramber_Osgood hardening model (Walker and Williams, 1995 [216])
Ultimate strength for X52	430 MPa	
Outside pipe diameter including concrete coating	1.0 m	Practical values selected for the example
Steel wall thickness	22.8 mm	
Pipeline internal pressure	2.0 MPa	
Depth from soil surface to pipeline springline, H_s	2.5 m	
Tensile strain limit	2.5%	DNV(2000) [53]. Tensile strain limit often is set due too welding flexibility. Compression strain limit is a function of pipeline thickness and internal pressure.
Compression strain limit	0.65%	

Table 5. 4 Soil and gouge characteristics

Soil Characteristics		
Type	Clay	A typical example based on C-CORE routines
Backfill material over pipeline	Clay	
Undrained shear strength, c_u	100 kPa	
Unit weight, γ	18 kN/m ³	
Coefficient of variation of soil undrained shear strength	50%	Practical values selected for the example
Horizontal correlation distance	5m	
Vertical correlation distance	1m	
Lateral bearing capacity factor for uniform soil, $N_{ch(\text{uniform})}$	4.6	ASCE (1984)
Lateral bearing capacity factor for heterogeneous soil, $N_{ch(\text{heterogeneous})}$	3.87	Using Equation 5-2, $N_{ch(\text{heterogeneous})} = R_{BC} \times N_{ch(\text{uniform})}$
Coefficient of variation of lateral bearing capacity	20%	Using Equation 5-3
Gouge Characteristics		
Gouge Orientation	Perpendicular to pipeline	Practical values selected for the example
Gouge width, B	16 m	
Gouge depth, d	1.5 m	
Keel angle	15 (degrees)	
Maximum horizontal movement, u_o	2.94 m	C-CORE routines (see Woodworth-Lynas, 1996 [220] and Figure 1a)

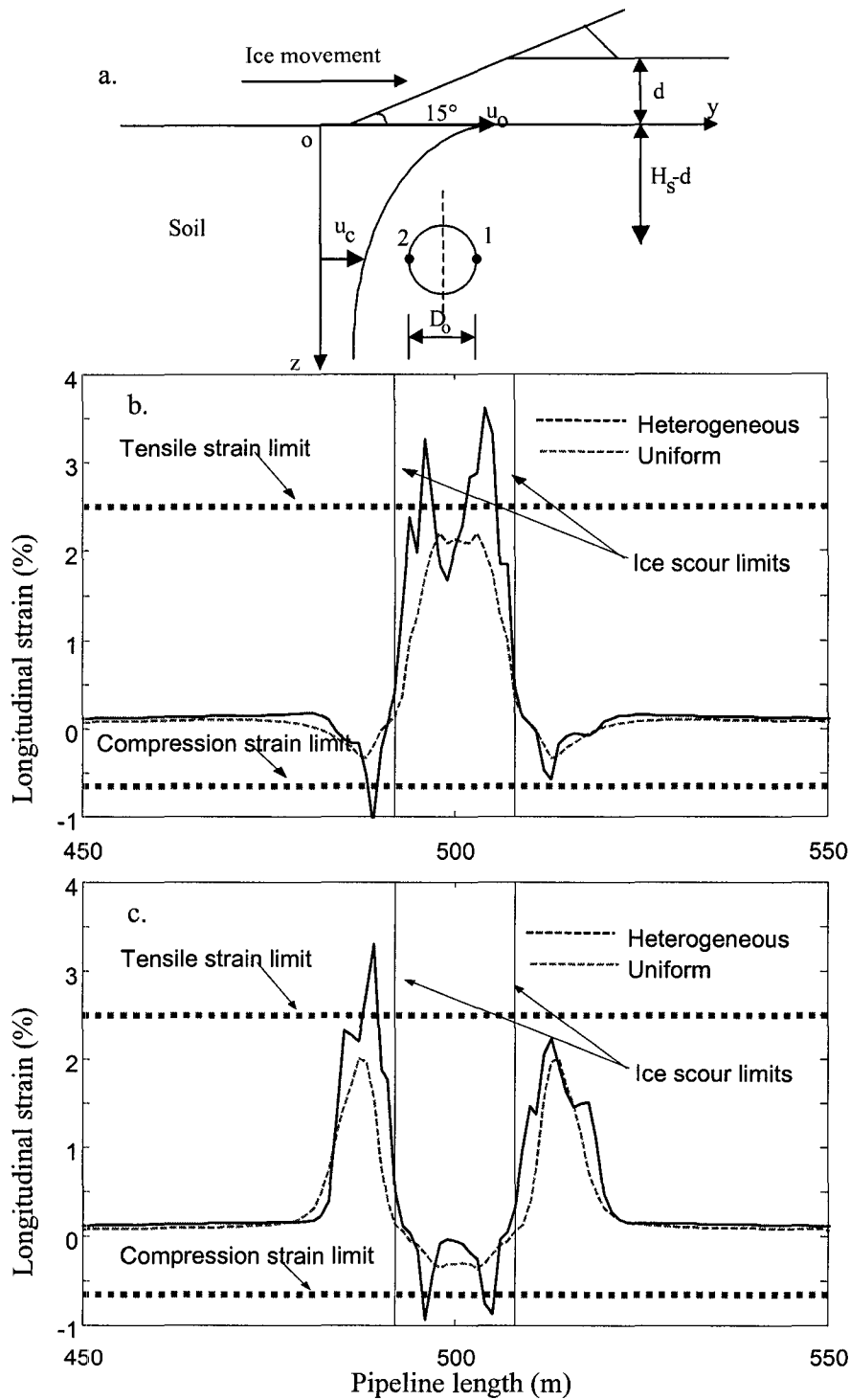


Figure 5.14 (a) schematic subscour soil deformation; (b&c) longitudinal strain distributions in the pipe section at point 1&2 – soil cover from scour base to top of pipe = 0.5 m, scour depth = 1.5 m, scour width = 16 m

5.5. CONCLUSIONS

A procedure for calculating the effects of soil heterogeneity on the pipe-soil interaction was established and the applicability of the proposed methodology was demonstrated. The methodology was similar to foundation and combined digital generation of stochastic fields with deterministic analysis through a Monte Carlo simulation. This was discussed in more detail in Chapter 3.

Similar to the case of foundations, it was found that average bearing pressure of a pipe laterally loaded in heterogeneous soil was smaller than that of a pipe in uniform soil with shear strength equal to the average shear strength in Monte Carlo simulations. However, the decrease in average pressure was modest. The failure mechanism of laterally loaded buried pipe was not significantly affected by soil heterogeneity. This can be attributed to the observation that the failure mechanism of a foundation on heterogeneous soil is unsymmetrical in contrast to a foundation on uniform soil, while for shallow buried pipeline, the failure mechanism is unsymmetrical for both uniform and heterogeneous soil. The failure mechanism of pipeline changes by burial depth, stress level at springline (middle of the pipe), interaction factors, etc. Therefore, this observation may not be true for all cases. A more thorough study of laterally loaded buried pipelines is required, including an investigation of the effects of deterministic parameters such as burial depth, interaction factors, stress level at springline, and probabilistic characteristics.

Similar to foundations, the predicted bearing pressures had a smaller variability than that of the soil shear strength. Coefficient of variation of bearing capacity originates from soil shear strength variability. For the limited number of parameters and ranges

considered in this study, the effects of soil heterogeneity on lateral loading of pipeline were analysed. Empirical probability distributions of bearing pressure were obtained and statistically processed. Results showed that a lognormal distribution fit those results well. The results, presented in terms of mean and coefficient of variation (Table 5.2), can be used in a probabilistic framework to analyse the reliability of a pipeline similar to that outlined for foundations.

CHAPTER 6

SUMMARY AND CONCLUSIONS

6.1. SUMMARY

This chapter presents a summary of the observed effects of soil heterogeneity on a strip foundation and a laterally loaded pipe, as well as the corresponding design recommendations and suggestions for future work. This thesis outlines the application of a Monte Carlo simulation methodology, described in Chapter 3, to study the effects of soil heterogeneity on nonlinear problems in geotechnical engineering with consideration of soil-structure interaction and plastic behaviour. The methodology used conventional finite element analysis with spatially variable soil input parameters. A large number of finite element analyses were performed and processed by automation of the procedures. The method and automation procedure can easily be extended to other geotechnical problems such as those related to slope stability, piles, coupled analysis, etc.

The Monte Carlo simulation approach used here is too complicated and numerically expensive for routine design. However, the aim of this study was to determine the effects of spatial variability of soil on foundation response and consequently provide necessary design recommendations and guidelines for engineering application. This provided a replacement approach for simple assessment of the effects of soil heterogeneity.

6.1.1 Shallow Foundations

A series of parametric studies involving over 7200 nonlinear finite element analyses was performed. The effects of probabilistic characteristics of soil spatial variability – degree of soil variability, probability distribution and correlation distances – and Young's modulus on the behaviour and responses of a shallow foundation were investigated. The range of soil variability adopted in this study for the undrained soil strength was $C_V = 10\%$ to 40% . A separable correlation structure based on the exponentially decaying model was assumed, with ranges of scales of fluctuations $\theta_{hm} = 1$ to 4 , and $\theta_{vn} = 0.25$ to 1 . Two different probability distribution functions were assumed for the soil strength: (1) a Gamma distribution skewed to the right, and (2) a symmetrical Beta distribution. The soil deformation modulus for undrained behaviour was assumed to be perfectly correlated with soil shear strength, $E = \alpha c_u$, with α ranging from 300 to 1500 . The parametric study was pre-designed using statistical methods for efficiency. The results were statistically analysed to quantify the effects of each probabilistic characteristic of soil spatial variability (Section 4.4 and Section 4.5) and were qualitatively investigated for the effects of soil heterogeneity on failure mechanism. One failure criterion and three serviceability criteria were considered. Serviceability criteria are defined based on foundation rotations (see damage criteria – Section 4.5.2). Foundations placed on heterogeneous soil have significant rotations even under vertical loading due to non-uniformity of deformation modulus and soil strength. For each criterion, the researcher obtained empirical probability distribution of bearing resistance. Several probability distributions were fitted to the results, and for most cases, the lognormal distribution fit was the best. Response surfaces (regression

equations) were determined for the predicted mean and degree of variability. The fitted equations can be used for the studied ranges to estimate the effects of soil heterogeneity in reliability analysis.

This thesis also presents an approach to estimating the required partial resistance factor, which can satisfy the desired reliability level, accounting for uncertainties caused by soil heterogeneity and other sources. Contours of required resistance factors are presented for the range studied for reliability index, $\beta = 3.5$.

6.1.2 Lateral Loading of Buried Pipeline

Experimental and numerical studies have been performed on the behaviour of buried pipeline in the last decade (see Section 2.3). In this study, a numerical model for lateral loading of pipeline was developed. It was validated based on large-scale experimental tests and comparison with previous studies. The finite element model was then adapted for analysis of spatially variable soil.

A limited study on the effects of soil heterogeneity on lateral loading of a shallow buried pipeline was conducted. One pipe diameter with one cover depth was considered (one configuration). The range of variability for the undrained soil strength was $C_v = 20\%$ to 80% . A separable correlation structure based on the exponentially decaying model was assumed, with ranges of scales of fluctuations: $\theta_{hn} = 2.5$ to 5.0 , and $\theta_{vn} = 0.25$ to 1.5 . 600 finite element analyses were performed for each case. Ultimate failure criteria were also considered. The ultimate pressure was obtained at normalized displacement of 0.1 . At this displacement, all pressure-displacement curves were flat. The empirical probability

distributions of ultimate bearing pressure were constructed and statistically studied. Mean and coefficient of variation of ultimate pressure were obtained. Similar to the foundation problem, a lognormal distribution can be reconstructed from mean and C_V for reliability analysis.

6.2. CONCLUSIONS

The following conclusions can be drawn from the results obtained when the developed methodology, described in Chapter 3, was applied to the geotechnical problems described in Chapters 4 and 5:

1. Behaviour of soil and soil-structure systems in the nonlinear regime was strongly affected by the natural spatial variability of soil strength within geologically distinct and uniform layers.

In heterogeneous soil, the failure mechanism of the foundation changes to an asymmetric one, which passes through loose pockets of soil. The presence of loose pockets of soil and an asymmetric failure mechanism led to earlier shear failure than predicted by the deterministic analysis, which assumed perfect symmetry. These changes were less pronounced in lateral loading of a pipeline. This may be attributed to the observation that in uniform soil, the failure mechanism of a shallow buried pipe is initially asymmetric, while for the foundation it is symmetric.

2. Increasing soil variability and the amount of loose pockets in the soil mass (controlled by the left tail of the probability distribution of soil strength)

strongly diminished bearing capacity of soil and increased differential settlements.

3. The predicted ultimate bearing capacity had lower variability than that of the input for the soil shear strength.

This can be attributed to the effects of local averaging (see the variance function: Vanmarcke, 1983 [210]). The point-to-point variability is not identical to the variability of the response; the response variability depends on variability of the average soil strength over the length of failure surface. The coefficient of variation of the responses depends on soil shear strength variability. In addition to this factor, the correlation distances and probability distribution (amount of loose pockets) of soil shear strength affects the value of the coefficient of variation.

4. The main parameters affecting foundation and pipe response were determined. Regression equations were provided to account for the effects of soil heterogeneity on soil-structure interaction – namely bearing capacity and bearing pressures at damage criteria of foundation and lateral loading of buried pipeline (Sections 4.4, 4.5 and 5.4).

The regression equations were presented as simple functions (response surfaces) of soil probabilistic characteristics, which can be used in foundation design and reliability analysis. These regressions are only valid for the range studied.

5. Characteristic bearing capacity accounting for natural variability of soil properties were obtained for the ranges studied (Section 4.4.3.3).

6. Different methodologies accounting for the effects of soil spatial variability in reliability analysis and routine design were illustrated (e.g. Section 3.6 and Section 4.6). These methodologies also considered the combination of the effects of soil spatial variability and uncertainties from other sources in reliability analysis.
7. A methodology was developed to account for the effects of soil natural variability in a limit state design method (reliability level I – Section 3.6.4). Considering the effects of soil heterogeneity as well as other sources of uncertainty, partial resistance factors were calibrated for a target reliability index, $\beta = 3.5$ (Section 4.4.4.3).

It was demonstrated that due to large uncertainty in geotechnical design and ambiguity in determining a characteristic value, a fixed partial design factor cannot guarantee an adequate level of safety unless very conservative values are selected. Therefore, using a lump-sum variable partial design factor is advised. This factor accounts for different sources of uncertainty and can be applied directly to estimated average shear strength. It is possible to use a constant partial design factor if a prescribed procedure, similar to the one demonstrated in Section 4.4.4, is used in determining characteristic resistance.

8. The results of this study can be used to calibrate partial design factors and obtain nominal values with certain reliability for the three serviceability criteria through a level II reliability analysis, similar to the one for the ultimate bearing capacity limit.

9. The results of this study can be used in a full reliability analysis through numerical integration (see Section 4.6 and Popescu et al., 2002 [170]).

6.3. FUTURE WORK

There are still many unknowns regarding the nature of soil heterogeneity and its consequences. Quantification of the effects of soil heterogeneity requires a large amount of effort and research. In future studies, the following tasks can be done among others,

1. The current study used a 2D model to analyse the effects of soil heterogeneity, but soil spatial variability is actually a 3D phenomenon. Therefore, a 3D analysis is required to address the problem more accurately. When faster computers are available, this can be more easily done using the methodology and automation program developed in this study.
2. The work done here can be extended for a wider range of parameters. Particularly for pipeline, the study was limited. Many factors affect the behaviour of pipeline, including burial depth, pipe diameter, soil weight, and interaction factors, etc. These factors should first be investigated through extensive parametric study of uniform soil. Then based on the deterministic results, a parametric study of the effects of soil heterogeneity on lateral loading of pipeline can be developed. This study can also be extended for other loading conditions of pipeline (e.g. upward, downward, axial, and complex loading).

3. This study focused on the behaviour of cohesive soil in undrained conditions using a total stress analysis. This study can be further developed to include frictional material. In the course of the study, a calibration model was developed to estimate hardening/softening rules for frictional materials from direct shear box tests. Mohr-Coulomb constitutive model in ABAQUS/Standard was customized and developed to account for softening/hardening of soil. The model was validated based on large-scale tests (see Nobahar et al., 2000 & 2001 [141 & 139]). However, the application of the hardening/softening rules for frictional materials in stochastic analysis faced severe numerical limitations and can be studied in future work.

REFERENCES

1. AASHTO (1992). Standard specification for highway bridges. 15th ed., American Association of State Highway and Transportation Officials, Washington D.C.
2. Agyris, J.H., and Kelsey, S. (1954). "Energy theorems and structural analysis." *Aircraft Engineering*, vol. 26 & 27.
3. Allen, D.E. (1975). "Limit states design - a probabilistic study." *Canadian Journal of Civil Engineering*, 2, 36-49.
4. ANSI (1980). Development of a probability based load criterion for American National Standard A58. American National Standards Institute, National Bureau of Standards, Washington, Special Publication 577.
5. ASCE (1984). Guidelines for the Seismic Design of Oil and Gas Pipeline Systems. Committee on Gas and Liquid Fuel Lifelines, Technical Council on Lifeline Earthquake Engineering, ASCE, New York.
6. Assimaki, D., Pecker, A., Popescu, R., and Prevost, J. (2002). "Effects of spatial variability of soil properties on surface ground motion." *Journal of Earthquake Engineering* (submitted).
7. ASTM (1989). Standard test method for deep, quasi-static, cone and friction-cone penetration tests of soil (D3441-86). Annual Book of Standards, vol. 4.08, American Society for Testing and Materials, Philadelphia, pp. 414-419.
8. Altaee, A., and Boivin, R. (1995). "Laterally displaced pipelines: finite element analysis." *Proceedings of 14th International Conference on Offshore Mechanics and Arctic Engineering*, vol. 5, pp. 209-216.
9. Altaee, A., Fellenius, B.H., and Salem, H. (1996). "Finite element modelling of lateral pipeline-soil interaction." *Proceedings of 15th International Conference on Offshore Mechanics and Arctic Engineering*, OMAE, Houston, TX, USA, vol. 5, Pipeline Technology, pp. 333-341.
10. Atkinson, A.C., and Donev, A.N. (1992). "Optimum experimental designs." Oxford University Press, 328 pages.
11. Baecher, G.B. and Ingra, T.S. (1981). "Stochastic FEM in settlement predictions." *Journal of the Geotechnical Engineering Division, ASCE*, 107(4), 449-463.

12. Baikie, L.D. (1998). "Comparison of limits states design methods for bearing capacity of shallow foundations." *Canadian Geotechnical Journal*, 35, 175-182.
13. Barker, R.M., and Puckett, J.A. (1997). *Design of highway bridges*. John Wiley & Sons, Inc., 1169 pages.
14. Bauer, J., and Pula W. (2000). "Reliability with respect to settlement limit-states of shallow foundations on linearly-deformable subsoil." *Computers and Geotechnics*, 26, 281-308.
15. Becker, D.E. (1996a). "Eighteenth Canadian Geotechnical Colloquium: Limit states design for foundations. Part I. An overview of the foundation design process." *Canadian Geotechnical Engineering*, 33, 956-983.
16. Becker, D.E. (1996b). "Eighteenth Canadian geotechnical colloquium: Limit states Design For Foundations. Part II. Development for the national building code of Canada." *Canadian Geotechnical Journal*, 33, 984-1007.
17. Been, K., Clark, J.I., and Livingstone, W.R. (1993). "Verification and calibration studies for the new CAN/CSA-S472 foundations of offshore structures." *Canadian Geotechnical Journal*, 30(3), 515-525.
18. Boyd, R.D. (1994). "Managing risk." Keynote paper of ICE Conference on Risk and Reliability in Ground Engineering, 27(5), 30-33.
19. Brenner, C.E. (1991). "Stochastic finite element methods: Literature review." Technical report, Inst. Of Engineering Mechanics, Univ. of Innsbruck, Austria, pp. 35-91.
20. Bowles, J. E. (1997). *Foundation analysis and design*. 5th edition, McGraw-Hill International Editions.
21. Britto, A.M., and Gunn, M.J. (1987). *Critical state soil mechanics via finite elements*. John Wiley & Sons, New York, 488 pages.
22. Brzakala, W., and Pula, W. (1996). "A probabilistic analysis of foundation settlements." *Computer and Geotechnics*, 18(4), 291-309.
23. Bruschi, R., Monti, P., Bolzoni, G., and Tagliaferri, R. (1995). "Finite Element Method as Numerical Laboratory for Analysing Pipeline Response Under Internal Pressure, Axial Load, Bending Moment." *Proceedings of 14th Offshore Mechanics and Arctic Engineering, OMAE, Houston, TX, USA, vol. 5, Pipeline Technology*, pp.389-401.

24. Cardoso, A.S., and Fernandes, M.M. (2001). "Characteristic values of ground parameters and probability of failure in design according to Eurocode 7." *Geotechnique*, 51(6), 519-531.
25. CGS (1992). *Canadian foundation engineering manual*, 3rd edition. Canadian Geotechnical Society, Bitech Publishers Ltd., Vancouver.
26. Chen, W.F. (1975). *Limit analysis and soil plasticity*. Elsevier, New York, 638 p.
27. Chen, W.F., and Han, D.J. (1988). *Plasticity for Structural Engineers*. Springer-Verlag Inc., New York, 606 pages.
28. Cherubini, C., Giasi, I., and Rethati, L. (1993). "The coefficient of variation of some geotechnical parameters." *Proceedings of Conference on Probabilistic Methods in Geotechnical Engineering*. Edited by Li, K.S., and Lo, S-C.R., A.A. Balkema, Rotterdam, 179-183.
29. Cherubini, C. (2000). "Reliability evaluation of shallow foundation bearing capacity on c' ϕ ' soils." *Canadian Geotechnical Journal*, 37, 264-269.
30. Chiasson, P., Lafleur, J., Soulie, M., Law, K.T. (1995). "Characterizing spatial variability of a clay by geostatistics." *Canadian Geotechnical Journal*, 32(1), 1-10.
31. Choot, G.E. (1980). *Stochastic under seepage analysis in dams*. Ph.D. Thesis, MIT, Cambridge, Massachusetts.
32. Christian, J.T. (1977). *Numerical methods in geotechnical engineering*. McGraw Hill Book Company.
33. Christian, J.T., Ladd, C.C., and Baecher, G.B. (1994). "Reliability applied to slope stability analysis." *Journal of Geotechnical and Geoenvironmental Engineering*, 120(2), 2180-2207.
34. Clark J.I., Phillips R., and Paulin M., (1998). "Ice scour research for the safe design of pipelines: 1975-1997." *Proceedings of Ice Scour & Arctic Marine Pipelines Workshop*. 13th International Symposium on Okhotsk Sea & Sea Ice, Mombetsu, Japan.
35. Coduto, D.P. (2001). *Foundation design, principles and practices*. Second Edition, Prentice-Hall, Inc., 883 pages.
36. Cornell, J. (2002). *Experiments with mixtures: Designs, models, and the analysis of mixture data*. Third Edition, John Wiley & Sons, New York, 649 pages.

37. Courant, R. (1943). "Variational methods for the solution of problems of equilibrium and vibrations." *Bulletin of American Mathematical Society*, vol. 49, pp. 1-23.
38. Cox, D.C., and Baybutt, P. (1981). "Methods for uncertainty analysis: a comparative survey." *Risk Analysis*, 1(4), 251-258.
39. Cressie, N. (1991). *Statistics for spatial data*. John Wiley & Sons, Inc., New York, 900 pages.
40. CSA (1981). *Guidelines for the development of limit states design*. Canadian Standards Association, Rexdale, Ontario, CSA Special Publication S408-1981.
41. CSA (1992). *General requirements, design criteria, the environmental, and loads*. Canadian Standard Association, Rexdale, Ont. Publication No. CAN/CSA-S471-92.
42. Day, R.A. (2001). "Factored material properties and limit state loads – unlikely extreme or impossible pretense." *Geotechnical Engineering*, 149(4), 209-210.
43. Davidson, H.L., and Chen, W.F. (1976). "Nonlinear analysis in soil and solid mechanics." In *numerical methods in Geomechanics* (ed. C.S. Desai), pp. 205-218.
44. DeGroot, D.J. (1996). "Analyzing spatial variability of in situ properties." *Uncertainty in the Geologic Environment, from Theory to Practice*. Special ASCE Publication, No. 58, 210-238.
45. DeGroot, D.J., and Baecher, G.B. (1993). "Estimating autocovariance of in-situ soil properties." *Journal of Geotechnical and Geoenvironmental Engineering*, 119(1), 147-166.
46. Deodatis, G. (1989). "Stochastic FEM sensitivity analysis of nonlinear dynamic problems." *Probabilistic Engineering Mechanics*, 4(3), 135-141.
47. Deodatis, G. (1996). "Simulation of ergodic multi-variate stochastic processes." *Journal of Engineering Mechanics*, 122(8), 778-787.
48. Der Kiureghian, A., and Ke, J.B. (1985). "Finite-element based reliability analysis of frame structures." *Proc. Fourth International Conference on Structural Safety and Reliability*, 1, Kobe, Japan, 395-404.
49. Der Kiureghian, A. and Ke, J.B. (1988). "The stochastic finite element method in structural reliability." *Probabilistic Engineering Mechanics*, 3(2): 83-91.
50. *Design-Expert software* (2000). Version 6 user guide. Copyright by Stat-Ease, Inc.

51. Deutsch, C.V. (2002). Geostatistical reservoir. Oxford University Press, Oxford, N.Y.
52. DI (1965). Code of practice for foundation engineering. DS 415, Dansk Ingeniorforening, Copenhagen.
53. DNV (2000). Submarine Pipeline Systems, Offshore Standard OS-F101. Det Norske Veritas, Veritasveien, N-1322 Hovik, Norway, 204 pages.
54. Duncan, J.M. (2000). "Factors of Safety and Reliability in Geotechnical Engineering." Journal of Geotechnical and Geoenvironmental Engineering, ASCE, 126(4), 307-316.
55. Ejezie, S., and Harrop-Williams, K. (1984). "Probabilistic characterization of Nigerian soils." In Probabilistic Characterization of Soil Properties, Bridge Between Theory and Practice, ASCE, 140-156.
56. Elkateb, T., Chalaturmy, R., and Robertson, P.K. (2000). "Quantification of soil heterogeneity." 53rd Canadian Geotechnical Conference, Montreal, pp. 1131-1138.
57. English, R.J. and Schofield, A.N. (1973). "Centrifuge Tests Buckle Rigid Pipes." New Civil Engineer, 8, p. 23.
58. ENV (1993). Geotechnical design, general rules. European Committee for Standardization (CEN), Eurocode.
59. ENV (1994). Eurocode 7: Geotechnical design. Part 1: General rules. Brussels: CEN, European Committee for Standardization.
60. ENV (1999). Eurocode 1: Basis of design and actions on structures. Part 1: Basis of design. Brussels: CEN, European Committee for Standardization.
61. Failmezger, A. (2001). "Discussions on Factor of safety and reliability in geotechnical engineering." Journal of Geotechnical and Geoenvironmental Engineering, pp. 703-704.
62. Fenton, G.A. (1999a). "Estimation for stochastic soil models." Journal of Geotechnical and Geoenvironmental Engineering, 125(6), 470-485.
63. Fenton, G.A. (1999b). "Random field modeling of CPT data." Journal of Geotechnical and Geoenvironmental Engineering, 125(6), 486-498.
64. Fenton, G.A., and Griffiths, D.V. (1996). "Statistics of free surface flow through stochastic earth dam." Journal of Geotechnical Engineering, 122(6), 427-436.

65. Fenton, G.A. and Griffiths D.V. (2002). "Probabilistic foundation settlement on spatially random soil." *Journal of Geotechnical and Geoenvironmental Engineering*, ASCE, 128(5), 381-390.
66. Fenton, A.G., and Griffiths, D.V. (2003). "Bearing capacity prediction of spatially random $c-\phi$ soils." *Canadian Geotechnical Journal*, 40, 54-65.
67. Fenton G.A. and Vanmarcke E.H. (1998). "Spatial Variation in liquefaction risk." *Geotechnique*, 48(6), 819-831.
68. Fernando, N.S.M. and Carter, J.P. (1998). "Elastic analysis of buried pipes under surface patch loadings." *Journal of Geotechnical and Geoenvironmental Engineering*, ASCE, 124(8), 720-728.
69. Fredlund, D.G., and Dahlman, A.E. (1972). "Statistical geotechnical properties of glacial lake Edmonton sediments." In *Statistics and Probability in Civil Engineering*, Hong Kong University Press.
70. Gelhar, L.W. (1993). *Stochastic subsurface hydrology*. Prentice Hall, NJ, 390p.
71. Grant, R. Christian, J. and Vanmarcke, E. (1974). "Differential settlement of buildings." *Journal of Geotechnical Engineering Division*, ASCE, GT9, 973-991.
72. Green, R. (1989). "Limit states design: some thoughts." In *Proceedings of the Symposium on Limit States Design in Foundation Engineering*, Canadian Geotechnical Society -Southern Ontario Section, Toronto, pp. 91-116.
73. Griffith, D.V. (1982). "Computation of bearing capacity factors using finite elements." *Canadian Geotechnical Journal*, 18(4), 599-603.
74. Griffiths, D.V. and Fenton, G.A. (1993). "Seepage beneath water retaining structures founded on spatially random soil." *Geotechnique*, 43(4), 577-587.
75. Griffiths, D.V., and Fenton, G.A. (1997). "Three-dimensional seepage through spatially random soil." *Journal of Geotechnical Engineering*, 123(2), 153-160.
76. Griffiths, D.V. and Fenton, G.A. (2000). "Influence of soil strength spatial variability on the stability of an undrained clay slope by finite elements." *Geotechnical Special Publications No. 101, Slope Stability 2000*, The Geoinstitute of the American Society of Civil Engineers.
77. Griffiths, D.V. and Fenton, G.A. (2001). "Bearing capacity of spatially random soil: the undrained clay Prandtl problem revisited." *Geotechnique*, 51(4), 351-360.

78. Griffiths, D.V., Fenton, G.A., and Manoharan, N. (2002). "Bearing capacity of rough rigid strip footing on cohesive soil: probabilistic study." *Journal of Geotechnical and Geoenvironmental Engineering*, 128(9), 743-755.
79. Gui, S., Zhang, R., Turner, J.P., and Xue, X. (2000). "Probabilistic slope stability analysis with stochastic soil hydraulic conductivity." *Journal of Geotechnical and Geoenvironmental Engineering*, 126(1), 1-9.
80. Guo, P.J., and Popescu, R. (2002). "Trench effects on pipe/soil interaction." *Proceedings of 2nd Canadian Specialty Conference on Computer Applications in Geotechnique*, pp. 261-268.
81. Hachich, W. (1981). *Seepage-related reliability of embankment dams*. Ph.D. Thesis, MIT, Cambridge, Massachusetts.
82. Han, S.W. and Wen, Y.K. (1997a). "Method of reliability-based seismic design. I: Equivalent nonlinear systems." *Journal of Structural Engineering*, 123(3), 264-270.
83. Han, S.W., and Wen, Y.K. (1997b). "Method of reliability-based seismic design. II: Equivalent nonlinear systems." *Journal of Structural Engineering*, 123(3), 264-271.
84. Hansen, J.B. (1953). *Earth pressure calculations*. The Danish Technical Press, Copenhagen.
85. Hansen, J.B. (1956). *Limit designs and safety factors in soil mechanics*. Danish Geotechnical Institute, Copenhagen, Bulletin No. 1.
86. Hansen, J.B. (1970). "A revised and extended formula for bearing capacity." *Danish Geotech. Inst., Copenhagen, Bulletin 28*, pp. 5-11.
87. Harr, M.E. (1977). *Mechanics of particulate media: a probabilistic approach*. McGraw-Hill, New York, 543 pages.
88. Harr, M.E. (1984). "Reliability-based design in civil engineering." 1984 Henry M. Shaw Lecture, Dept. of Civil Engineering, North Carolina, State University, Raleigh, NC.
89. Harr, M.E. (1987). *Reliability-based design in civil engineering*. McGraw-Hill Book Company, New York.
90. Hasofer, A.M., and Lind, N.C. (1974). "Exact and invariant second-moment code format." *Journal of Engineering Mechanics Division, ASCE*, 100(1), 111-121.

91. Hegazy, Y., Mayne, P.W., and Rouhani, S. (1996). "Geostatistical assessment of spatial variability in piezocone tests." *Uncertainty in the Geologic Environment, from Theory to Practice*, Special ASCE Publication, No. 58, 254-268.
92. Hibbitt, Karlsson and Sorensen (1998). *ABAQUS/STANDARD User's manual*, vol. 1,2,3, Getting started with ABAQUS and ABAQUS/POST.
93. Hibbitt, Karlsson & Sorensen, Inc. 1998a. *ABAQUS version 5.8 - Theory Manual*.
94. Hibbitt, Karlsson and Sorensen, Inc. (2001). *ABAQUS electronic documentations*.
95. Honegger, D., and Nyman, J. (2001). *Manual for the Seismic Design and Assessment of Natural Gas Transmission Pipelines*. Pipeline Research Committee International Project, PR-268-9823.
96. Hrennikoff, A. (1941). "Solution of problems in elasticity by the frame work method." *Journal of Applied Mechanics*, 8(4), 59-82.
97. Javanmard, M. and Valsangkar, A.J. (1988). "Physical and finite element analysis of buried flexible pipelines." *Centrifuge '98*, Balkema, Rotterdam, pp.687-692.
98. Jefferies, M.G. (1989). "Observed strength distributions in some arctic clays." In *proceedings of 8th Int. Conf. Mech. and Arctic Engineering*, pp. 125-132, The Hague.
99. Karadeniz, H. (1997). "Interface beam element for the analyses of soil-structure interactions and pipelines." *Proc. 7th Int. Offshore and Polar Engrg Conf.*, vol. 2, pp. 286-292.
100. Kettle, R.J. (1984). "Soil-Pipeline Interaction: A Review of the Problem. Pipelines and Frost Heave." *Proceedings of a Seminar at Caen, France, April*, pp. 35-37.
101. Kim, S.H and Na, S.W. (1997). "Response surface method using vector projected sampling points." *Structural Safety*, 19(1), 3-19.
102. Kulhawy, F.H. (1992). *On evaluation of static soil properties*. In *stability and performance of slopes and embankments II (GSP31)*. Edited by Seed, R.B. and Boulanger, R.W., American Society of Civil Engineers, New York, pp. 95-115.
103. Kulhawy, F.H., and Trautmann, C.H. (1996). "Estimation of in situ test uncertainty." In *Uncertainty in the geologic environment*. Edited by C.D. Shackelford, P.P. Nelson, and M.J. Roth. American Society of Civil Engineers, New York, pp. 269-286.

104. Kusakabe, O. (1984). "Centrifuge model tests on the influence of an axisymmetric excavation on buried pipe." Proceedings, International Symposium on Geotechnical Centrifuge Model Testing, T. Kimura (ed.), Tokyo, pp. 87-93.
105. Lacasse, S., and Nadim, F. (1996). "Uncertainties in characterizing soil properties." Publ. No. 201, Norwegian Geotechnical Institute, Oslo, Norway, pp. 49-75.
106. Lambe, T.W., and Whitman, R. (1969). Soil mechanics in engineering practice. Chichester/New York, John Wiley & Sons.
107. Lee, I.K., White, W., and Ingles, O.G. (1983). Geotechnical Engineering. Pitman, London, England.
108. Li, K.S., Lee, I.K., and Lo, S-C.R. (1993). "Limit state design in geotechnics." Proceeding of Conference on Probabilistic Methods in Geotechnical Engineering, pp. 29-42.
109. Li, K.S., and Lo, S-C.R. (1993). Probabilistic Methods in Geotechnical Engineering. Proceedings of Conference, A.A. Balkema, Rotterdam, 333 pages.
110. Li, K.S., and Lam, J. (2001). "Discussions on "Factor of safety and reliability in geotechnical engineering." Journal of Geotechnical and Geoenvironmental Engineering, pp. 714-715.
111. Lin, Y., (1996). "Limit state design load dependence in offshore structure." C-CORE, Memorial University of Newfoundland, St. John's, NL, Canada.
112. Lind, N.C. (1971). "Consistent partial safety factors." American Society of Civil Engineers: Journal of the Structural Division, 97(6), 1651-1669.
113. Lumb, P. (1966). "The variability of natural soils." Canadian Geotechnical Journal, 3, 74-97.
114. Lumb, P. (1972). "Precision and accuracy of soil tests." In Statistics and Probability in Civil Engineering, Hong Kong University Press.
115. Lumb, P. (1974). "Application of statistics in soil mechanics." In Soil Mechanics - New Horizons, Elsevier Publication Inc., New York, pp. 44-111.
116. MathWorks (2000) MATLAB – Statistics Toolbox, The MathWorks Inc., Natick, MA.
117. Mackenzie, T.R. (1955). Strength of Deadman Anchors in Clay. M.Sc. Thesis, Princeton University, Princeton, USA.

118. MacGregor, J.G. (1976). "Safety and Limit states design for reinforced concrete." *Canadian Journal of Civil Engineering*, 3, 484-513.
119. Matsuo, M., and Kuroda, K., (1974). "Probabilistic approach to design of embankments." *Soils and Foundations*, vol. 14, no. 4.
120. McHenry, D. (1943). "A lattice analogy for the solution of plane stress problems." *Journal of Institution of Civil Engineers*, 21, 59-82.
121. Melchers, R.E. (1993). Human error in structural reliability. In *reliability theory and its application to structures and soil mechanics*, Edited by Nijhoff, M., NATO Advanced Study Institute, Bomholm, Demark, pp. 453-464.
122. Merifield, R.S., Sloan, S.W., and Yu, H.S. (1999). "Rigorous plasticity solutions for the bearing capacity of two-layered clays." *Geotechnique*, 49(4), 471-490.
123. Meyerhof, G.G., (1955). "Influence of roughness of base and ground water conditions on the ultimate bearing capacity of foundations." *Geotechnique*, 5, 227-242.
124. Meyerhof, G.G., (1963). "Some recent research on the bearing capacity of foundations." *Canadian geotechnical Journal*, 1(1), 16-26.
125. Meyerhof, G.G. (1982). "Limit state design in geotechnical engineering." *Structural Safety* 1, 67-71.
126. Meyerhof, G.G., (1984). "Safety factor sand Limit state Analysis." *Canadian Geotechnical Journal*, 21(1), 1-7.
127. Meyerhof, G.G. (1993). "Development of geotechnical limit state design." *International symposium on Limit state design in geotechnical engineering, Copenhagen*, pp. 1-12.
128. Meyerhof, G.G., (1995). "Development of geotechnical limit state design." *Canadian Geotechnical Journal*, 32(1), 128-136.
129. Mohamed, A., Soares, R., and Venturini, W.S. (2001). "Partial safety factors for homogeneous reliability of nonlinear reinforced concrete columns." *Structural Safety*, 23, 137 –156.
130. Montgomery, D.C. (1997). "Design and analysis of experiments." *John Wiley & sons*, 704 pages.
131. Morse, R.K. (1972). "The importance of proper soil units for statistical analysis." In *Statistics and Probability in Civil Engineering*, Hong Kong University Press.

132. Nagtegaal, J.C., Parks, D.M., and Rice, J.R. (1974). "On numerically accurate finite element solutions in the fully plastic range." *Computer Methods in Applied Mechanics and Engineering*, 4, 153-177.
133. NEN 3650 Nederlandse Norm (1991). *Eisen voor Stalen Transportleidingssystemen (Requirements for Steel Pipeline Transportation Systems)*. Publikatie Uitsluitend ter Kritiek.
134. Ng, P.C.F. (1994). *Behaviour of Buried Pipelines Subjected to External Loading*. Ph.D. Thesis, University of Sheffield, Department of Civil and Structural Engineering, Sheffield, England.
135. Nobahar, A. (1999). "Study on application of LSD method in marine geotechnical engineering." Term paper for Marine Geotechnique course, 75 pages, C-CORE, St. John's, Newfoundland.
136. Nobahar, A. (2000). "Assessment of LSD method for foundation design." Term paper for Probabilistic Methods in Engineering, 77 pages, Memorial University, St. John's, Newfoundland.
137. Nobahar, A., and Popescu, R. (2000). "Spatial variability of soil properties _ effects on foundation design." *Proceedings of 53rd Canadian Geotechnical Conference*, pp. 1311-1317.
138. Nobahar, A., and Popescu, R. (2001a). "Some effects of soil heterogeneity on bearing capacity of shallow foundations." *Proc. ASCE Spec. Conf. 2001: A Geo-Odyssey*, Blacksburg, VA.
139. Nobahar, A. and Popescu, R. (2001b). "Hardening/Softening Rule for Sand." *Proc. 18th Canadian Congress of Applied Mechanics, CANCAM*, pp. 223-224.
140. Nobahar, A., and Popescu, R. (2001c). "Soil heterogeneity – Effects on bearing capacity." *Proc. 18th Canadian Congress of Applied Mechanics, CANCAM* , pp. 225-226.
141. Nobahar, A., Popescu, R., and Konuk, I. (2000). "Estimating progressive mobilization of soil strength." *Proceedings of 53rd Canadian Geotechnical Conference*, pp. 1311-1317.
142. NRC (1995). *National Building Code*. National Research Council of Canada, Ottawa.
143. Ochi, M.K. (1990). *Applied probability and stochastic processes*. John Wiley & Sons, Inc., 499 pages.

144. Orchant, C.J., Kulhawy, F.H., and Trautmann, C.H. (1988). "Reliability-based foundation design for transmission line structures: critical evaluation of in situ test methods." Electric Power Research Institute, Palo Alto, California, Report EL-5507(2), pp. 4-63.
145. Paice, G.M., Griffiths, D.V. and Fenton, G.A. (1994). "Influence of spatially random soil stiffness on foundation settlements." Proceeding of Settlement, pp. 628-639.
146. Paice, G.M., Griffiths, D.V. and Fenton, G.A. (1996). "Finite element modeling of settlement on spatially random soil." Journal of Geotechnical Engineering, 122(9), 777-779.
147. Palmer, A. (1996). "The limits of reliability theory and the reliability of limit state theory applied to pipelines." Offshore Technology Conference, pp. 619-626.
148. Park, Y.J., Ang, A.H-S., and Wenn, Y.K. (1987). "Damage limiting a seismic design of buildings." Earthquake Spectra, 3(1), 1-26.
149. Paulin, M.J. (1998). An Investigation into Pipelines Subjected to Lateral Soil Loading. Ph.D. Thesis, Memorial University of Newfoundland, St. John's, Canada.
150. Paulin, M.J., Phillips, R., Clark, J.I., Trigg, A., and Konuk, I. (1998). "A full-scale investigation into pipeline/soil interaction." Proc. International Pipeline Conf., ASME, pp. 779-788, Calgary, AB.
151. Peters, N.E., Bonelli, J.E. (1982). Chemical composition of bulk precipitation in the north-central and northeastern United States, December 1980 through February 1981. U.S. Geological Survey, Circular 874.
152. Phillips, R. (1986). Ground Deformation in the Vicinity of a Trench Heading. Ph.D. Thesis, Cambridge University, Cambridge, England, December.
153. Phoon, K.K., and Kulhawy, F.H. (1996). On quantifying inherent soil variability. Geotechnical Earthquake Engineering and Soil Dynamics, Geotechnical Special Publication No. 75, ASCE, pp. 326-340.
154. Phoon, K.K., and Kulhawy, F.H. (1999a). "Characterization of geotechnical variability." Canadian Geotechnical Journal, 36(5), 612-624.
155. Phoon, K.K., and Kulhawy, F.H. (1999b). "Evaluation of geotechnical property variability." Canadian Geotechnical Journal, 36(5), 625-639.

156. Phoon, K.K., Kulhawy, F.H., and Grigoriu, M.D. (2000). "Reliability -based design for transmission line structure foundations." *Computers and Geotechnics*, 26, 169-185.
157. Phoon, K.K., Quek, S.T., Chow, Y.K., and Lee, S.L. (1990). "Reliability analysis of pile settlement." *Journal of Geotechnical Engineering*, 116(11), 1717-1735.
158. Poorooshasb, F., and Clark, J.I. (1990). "Ice scouring and the design of offshore pipelines." Invited Workshop, April, Calgary, Alberta, pp. 193-235.
159. Popescu, R. (1995). Stochastic variability of soil properties: data analysis, digital simulation, effects on system behaviour. Ph.D. thesis, Princeton University, Princeton, NJ.
160. Popescu, R., Guo, P., and Nobahar, A. (2001). "3D Finite Element Analysis of Pipe/Soil Interaction." Final Report for Geological Survey of Canada, Chevron Corp. and Petro Canada, C-CORE Contract Report 01-C8.
161. Popescu, R., Phillips, R., Konuk, I., Guo, P., and Nobahar, A. (2002). "Pipe-Soil Interaction: Large Scale Tests and Numerical Modelling", Proc. Int. Conf. on Physical Modelling in Geotech., ICPMG02, St. John's, NL.
162. Popescu, R., Prevost, J.H., and Deodatis, G. (1997). "Effects of spatial variability on soil liquefaction: some design recommendations." *Geotechnique*, 47(5), 1019-1036.
163. Popescu, R., Prevost, J.H., and Deodatis, G. (1998a). "Spatial variability of soil properties: two case studies." *Geotechnical Earthquake Engineering and Soil Dynamics Geotechnical Special Publication ASCE*, No. 75, pp. 568-579.
164. Popescu, R., Deodatis, G., and Prevost, J.H. (1998b). "Simulation of homogeneous non-Gaussian stochastic vector fields." *Probabilistic Engineering Mechanics*, 13(1), 1-13.
165. Popescu, R., Prevost, J.H., and Deodatis, G. (1998c). "Characteristic Percentile of Soil Strength for Dynamic Analyses." *Geotechnical Earthquake Engineering and Soil Dynamics, Geotechnical Special Publication No. 75, ASCE*, pp. 1461-1471.
166. Popescu, R., Philips, R., Konuk, I., and Deacu, D. (1999). "Numerical and physical modeling of pipe-soil interaction" Proc. 52nd Canadian Geotech. Conf., Regina. SK, pp. 437-444.

167. Popescu, R., and Konuk, I. (2001). "3D Finite Element Analysis of Rigid Pipe Interaction with Clay." Proc. 10th Int. Conf. Computer Meth. Adv. Geomech., Tucson, AZ, vol. 2, pp. 1203-1208.
168. Popescu, R., Konuk, I., Gou, P., and Nobahar, A. (2002). "Some aspects in numerical analysis of pipe-soil Interaction." 2nd Canadian Specialty Conference on Computer Applications in Geotechnique, pp. 290-297.
169. Popescu, R., Phillips, R., Konuk, I., Guo, P., and Nobahar, A. (2002). "Pipe-Soil Interaction: Large Scale Tests and Numerical Modelling." ICPMG, St. John's, NL.
170. Popescu, R., Deodatis, G., and Nobahar, A. (2002). "Bearing capacity of heterogeneous soils - A probabilistic approach." 56th Canadian Geotechnical Conference, pp. 1021-1028.
171. Prevost, J.H. (1990). Modeling the Behavior of Geomaterials, Princeton University Press.
172. Prevost, J.H., Popescu, R., and Deodatis, G. (1997). "Spatial Variability of Soil Properties - Analysis and Effects on Soil Liquefaction." Proc. Int. Conf. Int. Assoc. for Computer Meth. and Advances in Geomech., (invited lecture), Wuhan, China, pp. 225-233.
173. Przewłocki, J. (2000). "Two-dimensional random field of mechanical soil properties." Journal of Geotechnical and Geoenvironmental Engineering, 26(4), 373-377.
174. Rahman, M.S., and Yeh, C.H. (1999). "Variability of seismic response of soils using stochastic finite element method." Soil dynamics and Earthquake Engineering, 18, 229-245.
175. Ranjan, G., and Aurora, V.B. (1980). "Model Studies on Anchors Under Horizontal Pull in Clay." Proceedings, 3rd Australia, New Zealand Conference on Geomechanics. vol. 1, pp. 65-70.
176. Reissner, E. (1958). "Deflection of plates on Viscoelastic Foundation." Transactions ASME, J. Appl. Mech., 80, pp. 144-145.
177. Righetti, G., and Harrop-Williams, K. (1988). "Finite element analysis of random soil media." Journal of Geotechnical Engineering, ASCE, 14(1), 59-75.
178. Rizakalla, M., Poorooshab, F., and Clark, J. I. (1992). Centrifuge modelling of lateral pipeline/soil interaction. Proc. 11 the Offshore Mechanics and Arctic Engineering Symposium.

179. Rowe, R.K., and Davis E.H. (1982a). "The behavior of anchor plates in clay." *Geotechnique*, 32(1), 9-23.
180. Rowe, R.K., and Davis E.H. (1982b). "The behavior of anchor plates in sand." *Geotechnique*, 32(1), 25-41.
181. Schultze, E. (1971). "Frequency distributions and correlations of soil properties." In 1st International Conf. Appl. Stat. Prob. Soil Struct. Engr., pp. 371-387.
182. Shinozuka, M. (1987). "Stochastic fields and their digital simulation." In *Stochastic Methods in Structural Dynamics*, G.I. Schueller and M. Shinozuka, eds., Martinus Nijhoff Publishers, Boston, Mass., pp. 93-133.
183. Shinozuka, M., and Dasgupta, G. (1986). "Stochastic finite element methods in dynamics." *Proc. 3rd Conference of Dynamic Response of Structures*, ASCE, University of California, L.A., CA, pp. 44-54.
184. Shinozuka, M., and Deodatis, G. (1988). "Response variability of stochastic finite element systems." *Journal of Eng. Mech.*, 114(3), 499-519.
185. Shinozuka, M., and Deodatis, G. (1991). "Simulation of stochastic processes by spectral representation." *Appl. Mech. Rev.*, 44(7), 191-203.
186. Shinozuka, M., and Deodatis, G. (1996). "Simulation of multi-dimensional Gaussian stochastic fields by spectral representation." *Appl. Mech. Reviews*, ASME, 49(1), 29-53.
187. Shinozuka, M., Feng, M.Q., Lee, J., and Naganuma, T. (2000). "Statistical analysis of fragility curves." *Journal of Engineering Mechanics*, ASCE, 126(12), 1224-1231.
188. Sloan, S.W. (1988). "Lower bound limit analysis using finite elements and linear programming." *International Journal for Numerical and Analytical Methods in Geomechanics*, 12, 61-77.
189. Sloan, S. W., and Randolph, M.F. (1982). "Numerical prediction of collapse loads using finite element methods." *International Journal for Numerical and Analytical Methods in Geomechanics*, 6, 47-76.
190. Smith, C.C. (1991). *Thaw Induced Settlement of Pipelines in Centrifuge Model Tests*. Ph.D. Thesis, Cambridge University, Cambridge, England, September.
191. Soulie, M., Montes, P., and Silvestri, V. (1990). "Modelling spatial variability of soil parameters." *Canadian Geotechnical Journal*, 27, 617-630.

192. Syngge, J.L. (1957). "The hypercircle in mathematical physics." Cambridge University Press, London.
193. Taiebat, H.A., and Carter J.P. (2000). "Numerical studies of the bearing capacity of shallow foundations on cohesive soil subjected to combined loading." *Geotechnique*, 50(4), 409-418.
194. Taiebat, H.A., and Carter J.P. (2002). "Bearing capacity of strip and circular foundations on undrained clay subjected to eccentric loads." *Geotechnique*, 52(1), 61-63.
195. Tandjiria, V., Teh, C.I., and Low, B.K. (2000). "Reliability analysis of laterally loaded piles using response surface methods." *Structural Safety*, 22, 335-355.
196. Tang, W. H. (1984). "Principles of probabilistic characterization of soil properties." *Probabilistic Characterization of Soil Properties: Bridge Between Theory and Practice*, ASCE, Atlanta, pp. 74-89.
197. Tang, W.H. (1993). "Recent development in geotechnical reliability." *Probabilistic methods in geotechnical engineering*. Edited by Li, K.S., and Lo, S-C.R., A.A. Balkema, Rotterdam, pp. 3-27.
198. Terzaghi, K. (1943). *Theoretical soil mechanics*. John Wiley & Sons, New York, 510 pages.
199. Terzaghi, K., and Peck, R.P. (1948). *Soil mechanics in engineering practice*. First Edition, John Wiley & Sons, New York.
200. Terzaghi, K., and Peck, R.P. (1967). *Soil mechanics in engineering practice*. Second Edition, John Wiley & Sons, New York.
201. Terzaghi, K., Peck, R.P., and Mesri, G. (1996). *Soil mechanics in engineering practice*. Third Edition, John Wiley & Sons, New York.
202. Thoft-Christian, P., and Baker, M.J., (1982). *Structural reliability theory and its applications*. Springer-Verlag, Berlin, Germany, 267 pages.
203. Tohda, J., Takada, N., and Mikasa, M. (1985). "Earth pressure on underground rigid pipe in a centrifuge." *Proceedings, International Conference on Advances in Underground Pipeline Engineering*, J.K. Jeyapalan (ed.), ASCE, Wisconsin, pp. 567-575.
204. Tohda, J., Li, L., and Yoshimura, H. (1994). "FE elastic analysis of earth pressure on buried flexible pipelines." *Centrifuge '94*, Balkema, Rotterdam, pp. 727-732.

205. Tresca, H. (1868). "Memoire sur L'Ecoulement des Corps Solids." Men, Pres. Par Div. Sav, vol. 18.
206. Ural, D.N. (1996). "Spatial variability of soil parameters." Special ASCE publication, No. 58, pp. 341-352.
207. Valsangkar, A.J., and Britto, A.M. (1979). Centrifuge Tests of Flexible Circular Pipes Subjected to Surface Loading. Transport and Road Research Laboratory Supplementary Report 530.
208. Vanmarcke, E.H. (1977). "Probabilistic modeling of soil profiles." Journal of Geotechnical Engineering Division, ASCE, 109(5), 1203-1214.
209. Vanmarcke, E.H. (1983). "Random fields: analysis and synthesis." MIT Press, Cambridge, 382 pages.
210. Vanmarcke, E.H., and Grigoriu, M. (1983). "Stochastic finite element analysis of simple beams." Journal of Engineering Mechanics, ASCE, 109(5), 1203-1214.
211. Venkatraman, B., and Patel, S.A. (1970). Structural mechanics with introduction to elasticity and plasticity. McGraw-Hill Book Company, 648 pages.
212. Vesic, A.S. (1973). "Analysis of ultimate loads of shallow foundations." ASCE Journal of Soil Mechanics and Foundation Engineering Division, 99(1), 45-73.
213. Vesic, A.S. (1975). "Bearing capacity of shallow foundations." Foundation Engineering Handbook, Van Nostrand Reinhold Company, New York, pp. 121-147.
214. Vlazov, V.Z., and Leontiev, U.N. (1966). Beams, Plates and Shells on Elastic Foundations. Israel Program for Scientific Translations, Jerusalem.
215. Von Mises, R. (1913). "Mechanik der festen korper in Plastichdefirmablen Zustand." Goettinger-Nachr, Math-Phys, K1.
216. Walker, A.C. and Williams K.A.J. (1995). "Strain based design of pipelines." 14th OMAE, vol. 4, pp.345-350, Denmark.
217. Wantland, G.P., O'Neill, M.B., Coelogyne, E.H., and Reese, L.C. (1982). "Pipeline lateral stability in soft clay." Journal of Petroleum Technology, 34(1), 217-220.
218. Whitman, R.V. (1984). "Evaluating calculated risk in geotechnical engineering." The Seventeenth Terzaghi Lecture, Journal of Geotechnical Engineering, ASCE, 110(2), 145-188.

219. Winkler, E. (1867). *Die Leher von der Elastizitat und Festigkeit*. Dominicus, Prague. Dominicus, Prague.
220. Woodworth-Lynas, C., Nixon, D., Phillips, R., Palmer, A. (1996). "Subgouge deformations and the security of arctic marine pipelines." OTC 8222.
221. Workman, G.H. (1992). "Design study of submerged sidebend response." Proc. 11th Int. Conf. Offs. Mech. Arctic Engrg., Calgary, Alberta, vol. 5, pp. 367-373.
222. Yamazaki, F., and Shinozuka, M. (1988). "Digital generation of non-Gaussian stochastic fields." *Journal of Engineering Mechanics*, 114(7), 1183-1197.
223. Yang, Q.S., and Poorooshab, H.B. (1997). "Numerical modeling of seabed ice scour." *Computers and Geotechnics*, 21(1), 1-20.
224. Yeh, C.H., and Rahman, M.S. (1998). "Stochastic finite element methods for the seismic response of soils." *International Journal for Numerical and Analytical Methods in Geomechanics*, 22, 819-850.
225. Yin, J-H., Paulin, M.J., Clark, J.I., and Poorooshab, F. (1993). "Preliminary finite element analysis of lateral pipeline/soil interaction and comparison to centrifuge model test results." Proc. 12th Int. Conf. Offshore Mechanics Arctic Engrg, vol.5, pp. 143-155.
226. Yoosef-Ghodsi, N., Cheng, J.J.R, Murray, D.W., Doblanko, R., and Wilkie, S. (2000). "Analytical Simulation and Field Measurement for a Wrinkle on the Norman Wells Pipeline." *Proceedings, International Pipeline Conference*, vol. 2, ASME, Calgary, AB, Canada, pp. 931-938. Paper IPC00 0009.
227. Yoshizaki, K., Ando, H., and Oguchi, N. (1998). "Large Deformation Behaviour of Pipe Bends Subjected to In-Plane Bending." *Proceedings, International Pipeline Conference*, ASME, Calgary, AB, Canada, vol. 2, pp. 733-740."
228. Z662 (1999). *Oil and Gas Pipeline Systems*. Canadian Standards Association, 329 pages.
229. Zienkiewicz, O.C., and Corneau, I.C. (1972). "Visco-plastic Solution in the finite element process." *Arch. Mech.*, 24, 873-888.
230. Zienkiewicz, O.C., and Corneau, I.C. (1974). "Visco-plasticity, plasticity and creep in elastic solids: a united numerical solution approach." *International Journal for Numerical Methods in Engineering*, 8, 832-845.

231. Zienkiewicz, O.C., Humpheson, C., and Lewis, R.W. (1975). "Associated and non-linear associated visco-plasticity and plasticity in soil mechanics." *Geotechnique*, vol. 25, No. 4, pp. 671-689.
232. Zienkiewicz, O.C., Norris, V.A., Winnicki, L.A., Naylor, D.J., and Lewis, R.W. (1978). "A united approach to the soil mechanics problems of offshore foundations." In *Numerical Methods in Offshore Engineering*, John Wiley & Sons, New York, pp. 361-364.
233. Zhou, J.Z., and Harvey, D.P. (1996). "A model for dynamic analysis of buried and partially buried piping systems." *Pressure Vessels and Piping Systems*, PPV, vol. 331, ASME, pp. 21-29.
234. Zhu, F., (1998). Centrifuge modelling and numerical analysis of bearing capacity of ring foundations on sand. Ph.D. thesis, Memorial University of Newfoundland.
235. Zhuang, Z., and O'Donoghue, P.E. (1998). "Analysis model to simulate the cracked pipe buried in soil." *Acta Mechanica Sinica*, 14(2), 147-156.

APPENDIX A. A SAMPLE FINITE ELEMENT INPUT FILE, A DETERMINISTIC FINITE ELEMENT ANALYSIS WITH STOCHASTIC INPUT

Parameters used in this analysis for soil shear strength are:

$C_V = 25\%$, $\theta_{hn} = 2.5$, $\theta_{vn} = 0.25$, Gamma distribution, and $E/c_u = 300$

*HEADING

nfs-CPE4R-0.25*0.5m elements- Cu100-displacement-E150.0Mpa

Concrete high

Mohr coulomb-tresca

Bearing capacity of strip foundation

**-----SOIL -----

**

** NODES DEFINING

*****All dimension in meter and stress is kPa

*NODE, NSET=NA1

1001,0.0

1061,30,0

5001,0,10

5061,30,10.0

101,13,10

301,13,16

109,17,10

309,17,16

*NGEN, NSET=NBOT

1001,1061,1

*NGEN, NSET=NTOP

5001,5061,1

*NGEN, NSET=NFB

101,109

*NGEN, NSET=NFT

301,309

*Nset, NSET=NLOAD

105

*NFILL, BIAS=1., NSET=NSOIL

NBOT,NTOP,40,100

*NFILL, BIAS=1.0, NSET=NF

NFB,NFT,2,100

*NSET, NSET=NSIDE, GENERATE

1001, 5001,100

```

1061,5061,100
*NSET, NSET=NEND
101,109
*****
** SOIL ELEMENT DEFINING
*****
*ELEMENT, TYPE=CPE4R, ELSET=ELSOIL
1001,1001,1002,1102,1101
*ELGEN,ELSET=ELSOIL
1001,60,1,1,40,100,100
*ELSET,ELSET=ELST, GENERATE
4901,4960
*ELEMENT, TYPE=CPE4, ELSET=ELCON
101,101,102,202,201
*ELGEN,ELSET=ELCON
101,8,1,1,2,100,100
*ELSET,ELSET=ELCONB, GENERATE
101,108
*ELSET,ELSET=ELS1001
1001
*ELSET,ELSET=ELS1002
1002
*ELSET,ELSET=ELS1003
1003
*ELSET,ELSET=ELS1004
1004
*ELSET,ELSET=ELS1005
1005
*ELSET,ELSET=ELS1006
1006
*ELSET,ELSET=ELS1007
1007
*ELSET,ELSET=ELS1008
1008
*ELSET,ELSET=ELS1009
1009
*ELSET,ELSET=ELS1010
1010
*ELSET,ELSET=ELS1011
1011
...
...
(Due to the large size of the file – over 2400 element sets and materials – only
some parts of the input file are shown)
...
...

```

*ELSET,ELSET=ELS4952
4952
*ELSET,ELSET=ELS4953
4953
*ELSET,ELSET=ELS4954
4954
*ELSET,ELSET=ELS4955
4955
*ELSET,ELSET=ELS4956
4956
*ELSET,ELSET=ELS4957
4957
*ELSET,ELSET=ELS4958
4958
*ELSET,ELSET=ELS4959
4959
*ELSET,ELSET=ELS4960
4960

*SOLID SECTION,ELSET=ELS1001 ,MATERIAL=MSOIL1001

*MATERIAL,NAME=MSOIL1001

*ELASTIC

22924.5 , 0.49

*MOHR COULOMB

0.0

*MOHR COULOMB HARDENING

76.4

*SOLID SECTION,ELSET=ELS1002 ,MATERIAL=MSOIL1002

*MATERIAL,NAME=MSOIL1002

*ELASTIC

22104.6 , 0.49

*MOHR COULOMB

0.0

*MOHR COULOMB HARDENING

73.7

*SOLID SECTION,ELSET=ELS1003 ,MATERIAL=MSOIL1003

*MATERIAL,NAME=MSOIL1003

*ELASTIC

21116.9 , 0.49

*MOHR COULOMB

0.0

*MOHR COULOMB HARDENING

70.4

*SOLID SECTION,ELSET=ELS1004 ,MATERIAL=MSOIL1004

*MATERIAL,NAME=MSOIL1004

*ELASTIC

20151.6 , 0.49
 *MOHR COULOMB
 0.0
 *MOHR COULOMB HARDENING
 67.2
 *SOLID SECTION,ELSET=ELS1005 ,MATERIAL=MSOIL1005
 *MATERIAL,NAME=MSOIL1005
 *ELASTIC
 19333.2 , 0.49
 *MOHR COULOMB
 0.0
 *MOHR COULOMB HARDENING
 64.4
 *SOLID SECTION,ELSET=ELS1006 ,MATERIAL=MSOIL1006
 *MATERIAL,NAME=MSOIL1006
 *ELASTIC
 18705.7 , 0.49
 *MOHR COULOMB
 0.0
 *MOHR COULOMB HARDENING
 62.4
 *SOLID SECTION,ELSET=ELS1007 ,MATERIAL=MSOIL1007
 *MATERIAL,NAME=MSOIL1007
 *ELASTIC
 18257.6 , 0.49
 *MOHR COULOMB
 0.0
 ...
 (Due to the large size of the file – over 2400 element sets and materials – only
 some parts of the input file are shown)
 ...
 *SOLID SECTION,ELSET=ELS4958 ,MATERIAL=MSOIL4958
 *MATERIAL,NAME=MSOIL4958
 *ELASTIC
 36566.3 , 0.49
 *MOHR COULOMB
 0.0
 *MOHR COULOMB HARDENING
 121.9
 *SOLID SECTION,ELSET=ELS4959 ,MATERIAL=MSOIL4959
 *MATERIAL,NAME=MSOIL4959
 *ELASTIC
 38514.5 , 0.49
 *MOHR COULOMB
 0.0
 *MOHR COULOMB HARDENING

```

128.4
*SOLID SECTION,ELSET=ELS4960 ,MATERIAL=MSOIL4960
*MATERIAL,NAME=MSOIL4960
*ELASTIC
40334.6 , 0.49
*MOHR COULOMB
0.0
*MOHR COULOMB HARDENING
134.4
*SOLID SECTION,ELSET=ELCON,MATERIAL=MCON
*MATERIAL,NAME=MCON
*ELASTIC,TYPE=ISO
4.0E7,0.3
*****
** CONTACT
** Soil-foundation contact
** The joint between two surfaces are released.
*****
*SURFACE DEFINITION, NAME=SOILT
ELST, S3
*SURFACE DEFINITION, NAME=CON
101,S4
201,S4
ELCONB,S1
108,S2
208,S2
*CONTACT PAIR, INTERACTION=SOIL
CON,SOILT
*SURFACE INTERACTION, NAME=SOIL
1.
*FRICTION, TAUMAX=33.4
1.0
*RESTART, WRITE, frequency=1
*BOUNDARY
NBOT, ENCASTRE
NSIDE,1,1
*STEP, INC=10000, NLGEOM, UNSYMM=YES, amplitude=ramp
*STATIC
1e-1,1,1e-12,0.25
*CONTROLS,ANALYSIS=DISCONTINUOUS
*CONTROLS, PARAMETERS=LINE SEARCH
10
*BOUNDARY
nload,2,2,-0.25
*EL PRINT, frequency=0
*NODE PRINT, NSET=NLOAD, FREQUENCY=1,summary=no, total=yes

```

```
U2,RF2
*NODE PRINT, NSET=NEND, FREQUENCY=1,summary=no, total=yes
U2
**EL PRINT, ELSET=EMID, position=centroidal, summary=no,total=yes,
**FREQUENCY=0
**PEMAG
*NODE PRINT, FREQUENCY=0
*END STEP
```

APPENDIX B. AUTOMATION OF MONTE CARLO SIMULATIONS

B.1. INTRODUCTION

For each case (meaning each experiment, i.e. each set of coefficient of variation, probability distribution, and horizontal and vertical correlation distances), a large number of finite element analyses with stochastic input were performed, as described in Section 3.5.4. This meant that more than 7200 finite element analyses were performed during the course of this study.

For each set of probabilistic characteristics of soil probability (each experiment), a set of Monte Carlo simulations was performed. This required generation of sample functions of stochastic fields, mapping the generated field to finite element input, execution of finite element runs, post-processing of finite element results to organize the relevant responses, calculation of probabilistic characteristics of the response based on statistical inference.

B.2. AUTOMATION OF THE GENERATION OF STOCHASTIC SAMPLE FUNCTIONS

For the parametric studies, a large number of sample functions of stochastic fields with various probabilistic characteristics were required. The procedure was automated using Microsoft Excel® spreadsheets, Microsoft Visual Basic® for Application and MATLAB®. An interactive spreadsheet was created as shown in Figure B.1. The user could change parameters b_1 and b_2 to obtain the desired correlation distances in each direction. The values of M , N , and κ_{iu} could be changed to obtain the desired “stochastic

field mesh size Δx & Δy , and desired stochastic domain size L_x & L_y as shown in Figure B.1. The spectral density values were controlled by the spreadsheet to be acceptable at the cut-off frequency number for given inputs. Next, the Visual Basic subroutine “stoc_gen” was executed to generate input files for generating random files (this subroutine was linked to MATLAB for more efficiency). The input files were generated for each combination of the defined horizontal and vertical correlation distances (There were $3 \times 3 = 9$ cases in Figure B.1). The input files were stored in the location defined in the spreadsheet. Subsequently, the stochastic field generation program “SINOGA” was run automatically to generate the desired stochastic sample functions.

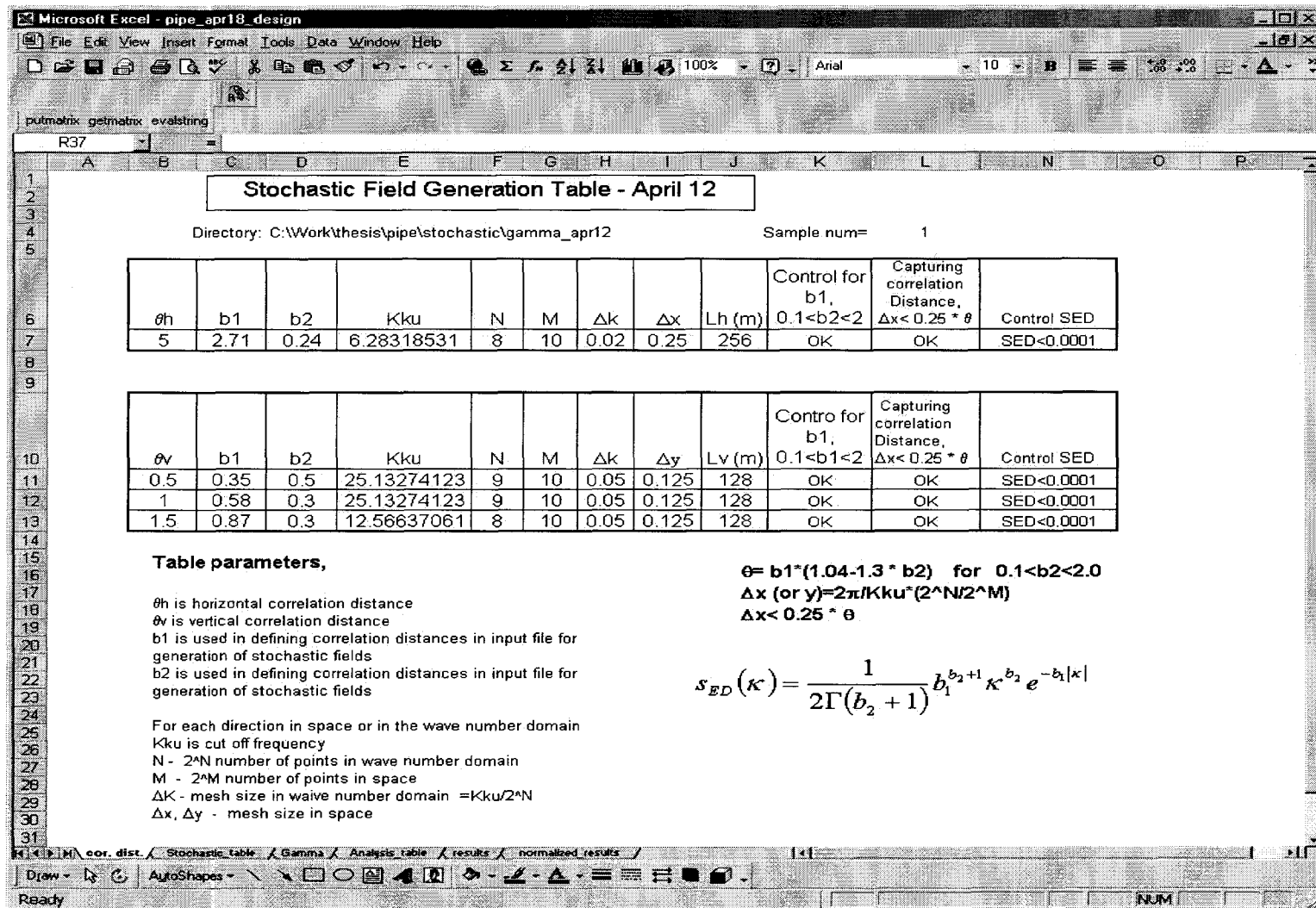


Figure B.1 Generation table for sample functions of stochastic fields.

B.3. FINITE ELEMENT ANALYSES: INPUT FILES, EXECUTION AND POST-PROCESSING

As described in the previous section, an Excel spreadsheet was used to organize the simulation of stochastic fields. In the same Excel workbook, another sheet was used to define the analysis cases according to experiment design (see Section 3.3). The advantages of the spreadsheet (its organization and visibility) were combined with the numerical and programming capabilities of MATLAB by using Excel with built-in Visual Basic programming options.

A MATLAB routine, “inpgen_spfn” was used to generate MATLAB input files and specified directories for Monte Carlo simulations. Due to numerical cost, the analyses were usually performed on a UNIX workstation. Next, two MATLAB programs – “main_spfn” for foundation and “main_pipe” for pipe – were programmed to map the generated stochastic sample functions to the finite element meshes and then construct finite element input files (ABAQUS inps), run the analyses for each case (usually 100 to 1000 finite element runs with stochastic input) and post-process the results. The programs “main_spfn” or “main_pipe” performed the following tasks,

- Read corresponding generated sample functions of stochastic fields and mapped them to the finite element mesh. Every generated sample function of a stochastic field is contoured in Figure B.2.
- Constructed corresponding finite element input files.
- Ran the finite element analysis with stochastic input for each sample function

- Read foundation/pipe result outputs. For example, for foundation, load-displacement and load-rotation relations were read for each finite element run and stored in separate files. Plots of load-settlement and load-differential settlement were drawn for each run. An example is shown in Figure B.3.

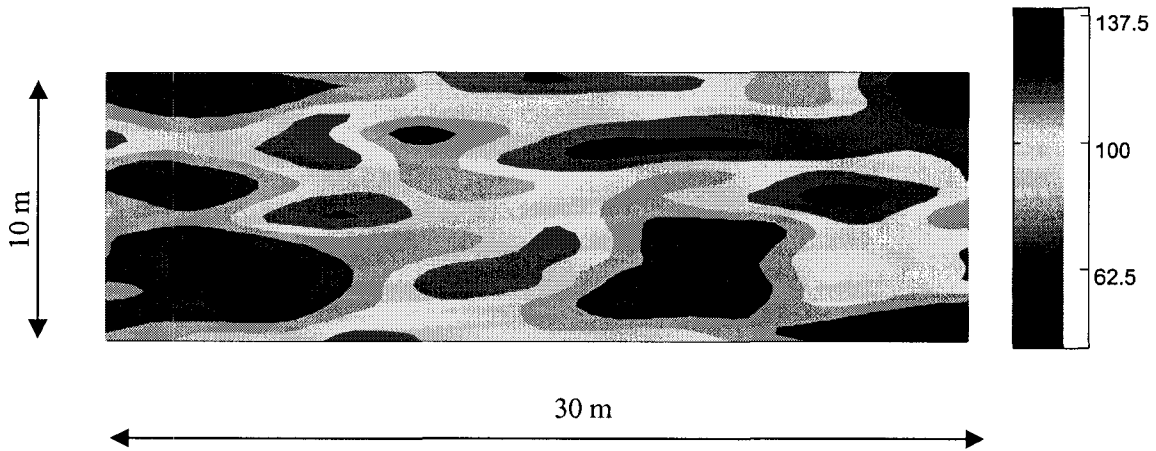


Figure B.2 A generated sample function of a stochastic field read by MATLAB routine, “main_spfn” – contours show spatially variable parameter, here undrained shear strength (in kPa), the distribution over the domain of interest.

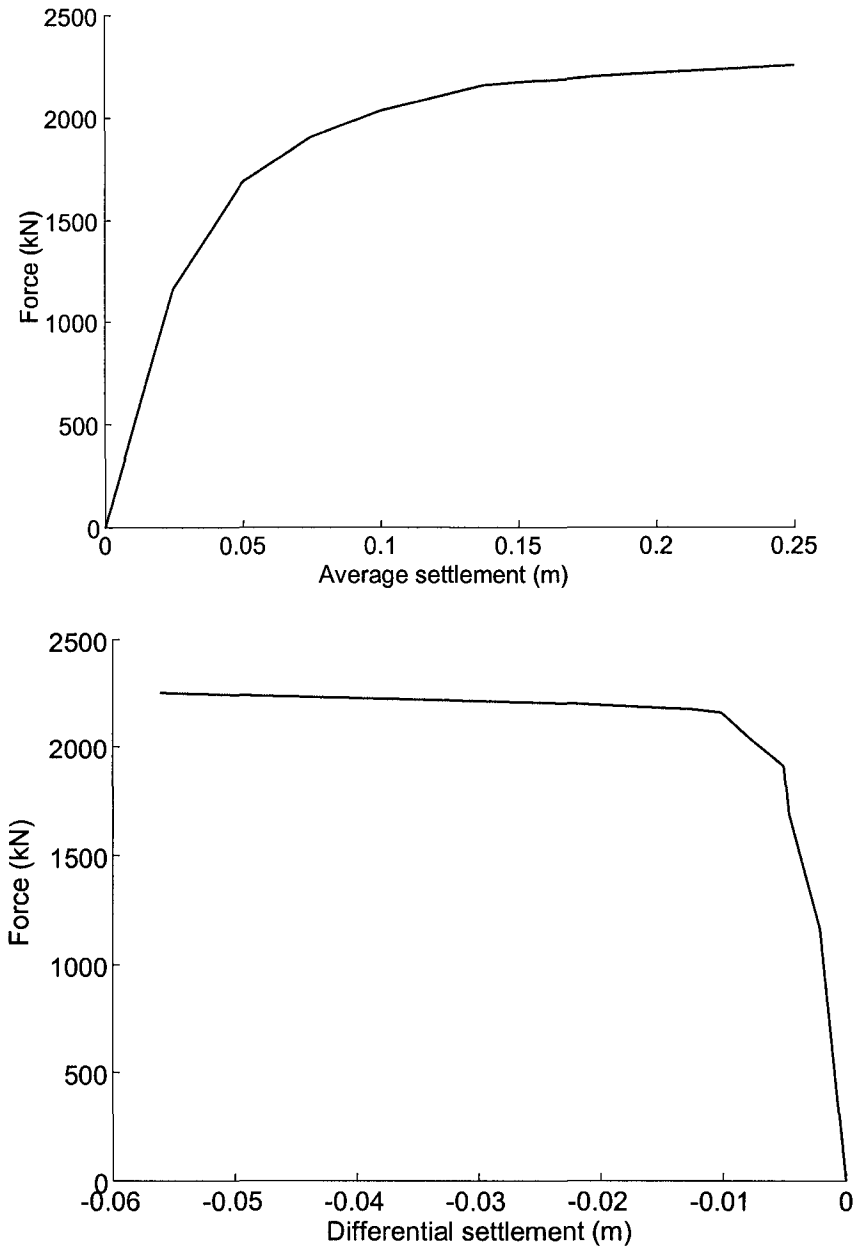


Figure B.3 A sample of foundation responses read by MATLAB routine, “main_spfn”.

B.4. AUTOMATION OF PROBABILISTIC ANALYSIS

Finally, the results of Monte Carlo simulations were processed for each experiment (group of sample functions). This post-processing was also automated using MATLAB routines. The functions named “call_post_spfn” and “call_post_pipe” were used for

foundation and pipe analysis, respectively. Each function called two main post processing subroutines, “post_spatial_foundation” & “resp_post_spfn” for foundation and “post_pipe” & “resp_post_pipe” for pipe and performed the following analysis,

- Read the foundation/pipe responses in terms of the load-displacement and/or load-differential settlement
- Stored and plotted all the foundation/pipe responses in one MATLAB matrix and one plot as shown in Figure B.4. It also estimated the foundation/pipe response (load/pressure) in equal increment displacement/rotation segments.
- Stored and plotted the mean, percentiles and standard deviation at each displacement/rotation increment as shown in Figure B.5.
- Obtained the desired response(s) (e.g. average pressure beneath foundation) for each finite element run at the given criteria (reference settlement for ultimate bearing capacity and reference differential settlements for damage criteria). It fit three different probability distribution functions (Lognormal, Normal and Gamma) on the obtained empirical probability distribution. It was potentially capable of fitting other probability distributions. A complete set of graphs is shown in Figures B. 6 to 17 for a case with the following probabilistic characteristics: Gamma distributed soil shear strength, $C_V = 25\%$, $\theta_{hn} = 2.5$, $\theta_{vn} = 0.25$, and $E/c_u = 1500$. Subsequently, it calculated the mean, standard deviation and the desired percentiles of the response. Using fitted probability distributions, it was possible to extrapolate and estimate the response at lower probabilities. The calculated results were then

transferred to an Excel spreadsheet. These results were used in a Design-Expert spreadsheet described in Section 3.3 for statistical calculations.

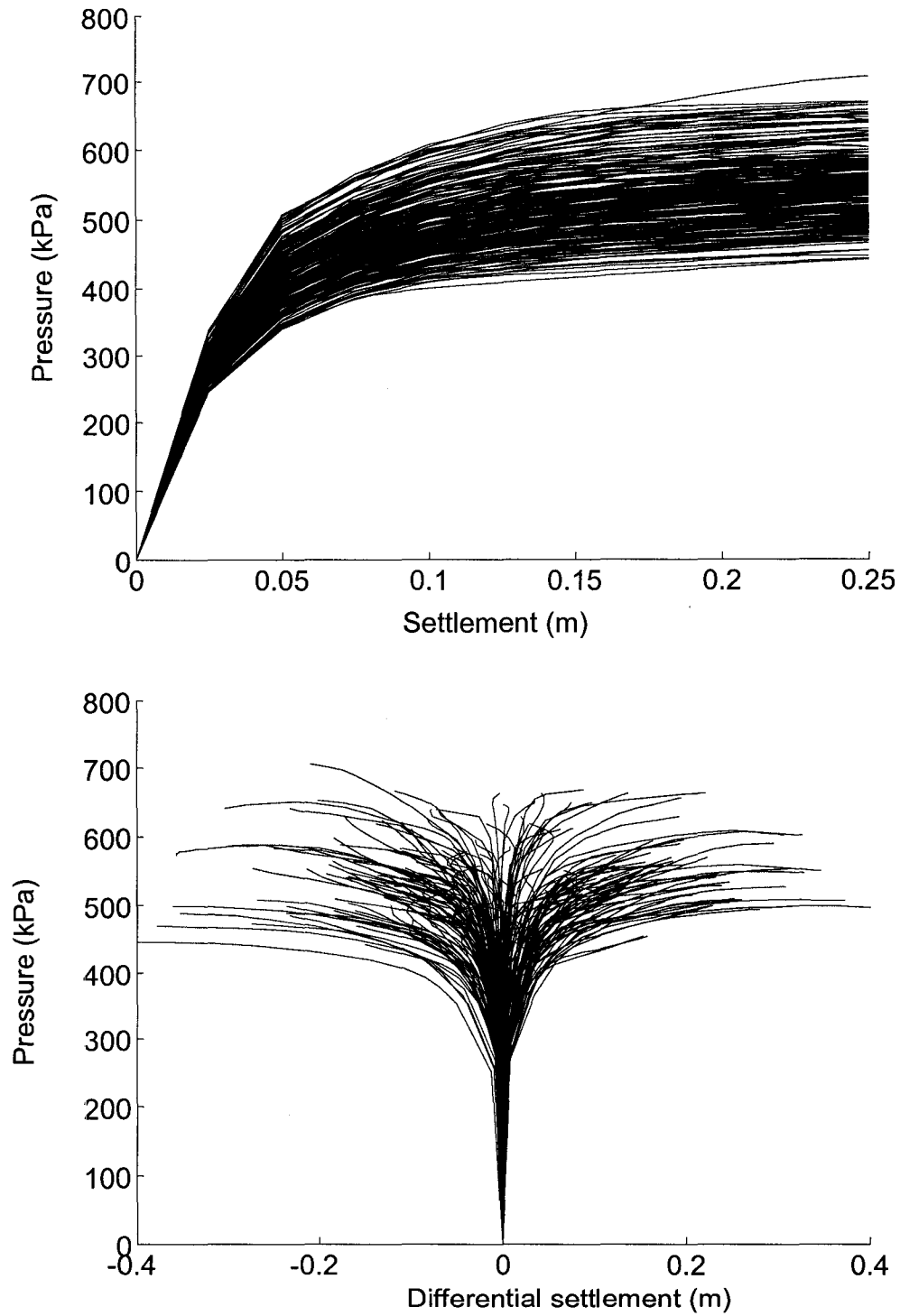


Figure B.4 Samples plot of pressure vs. settlement and differential settlement.

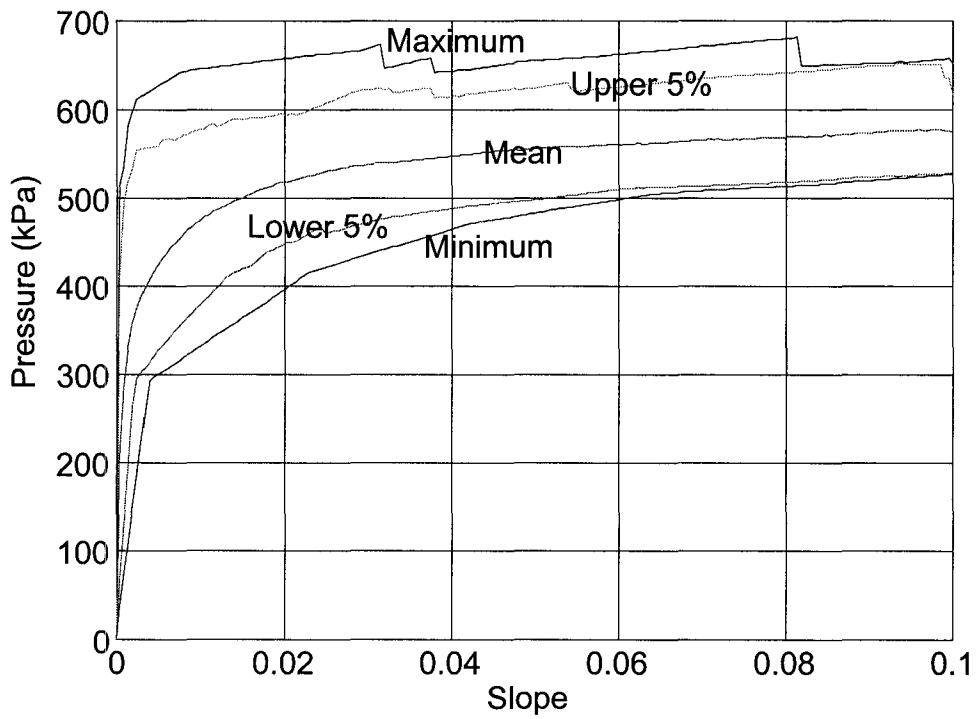
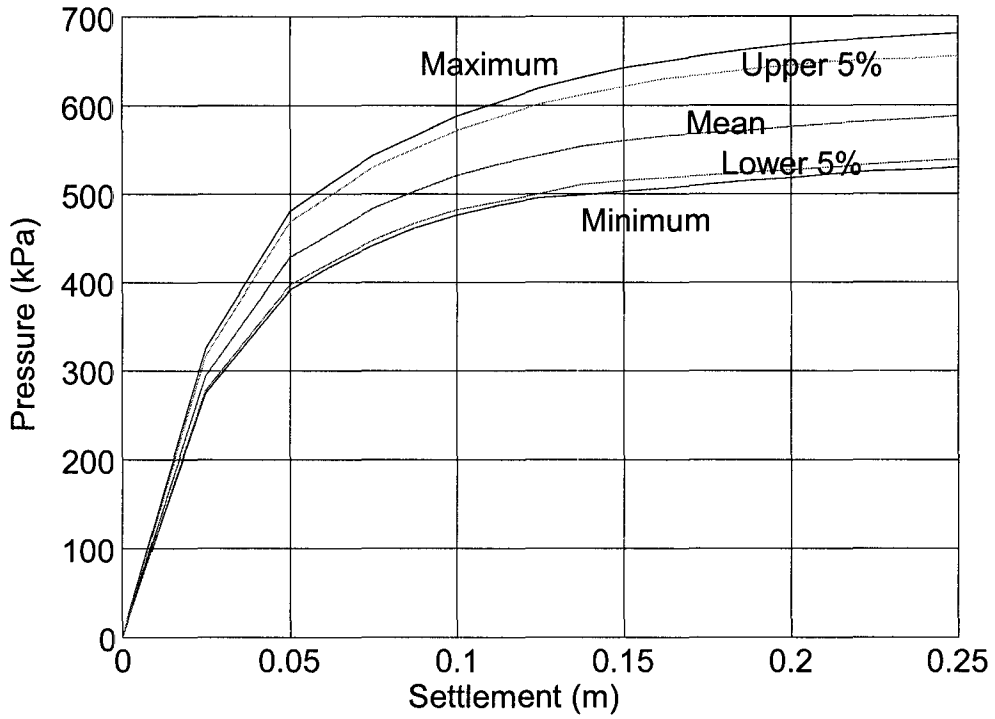


Figure B.5 A sample of plots provided by post processing program.

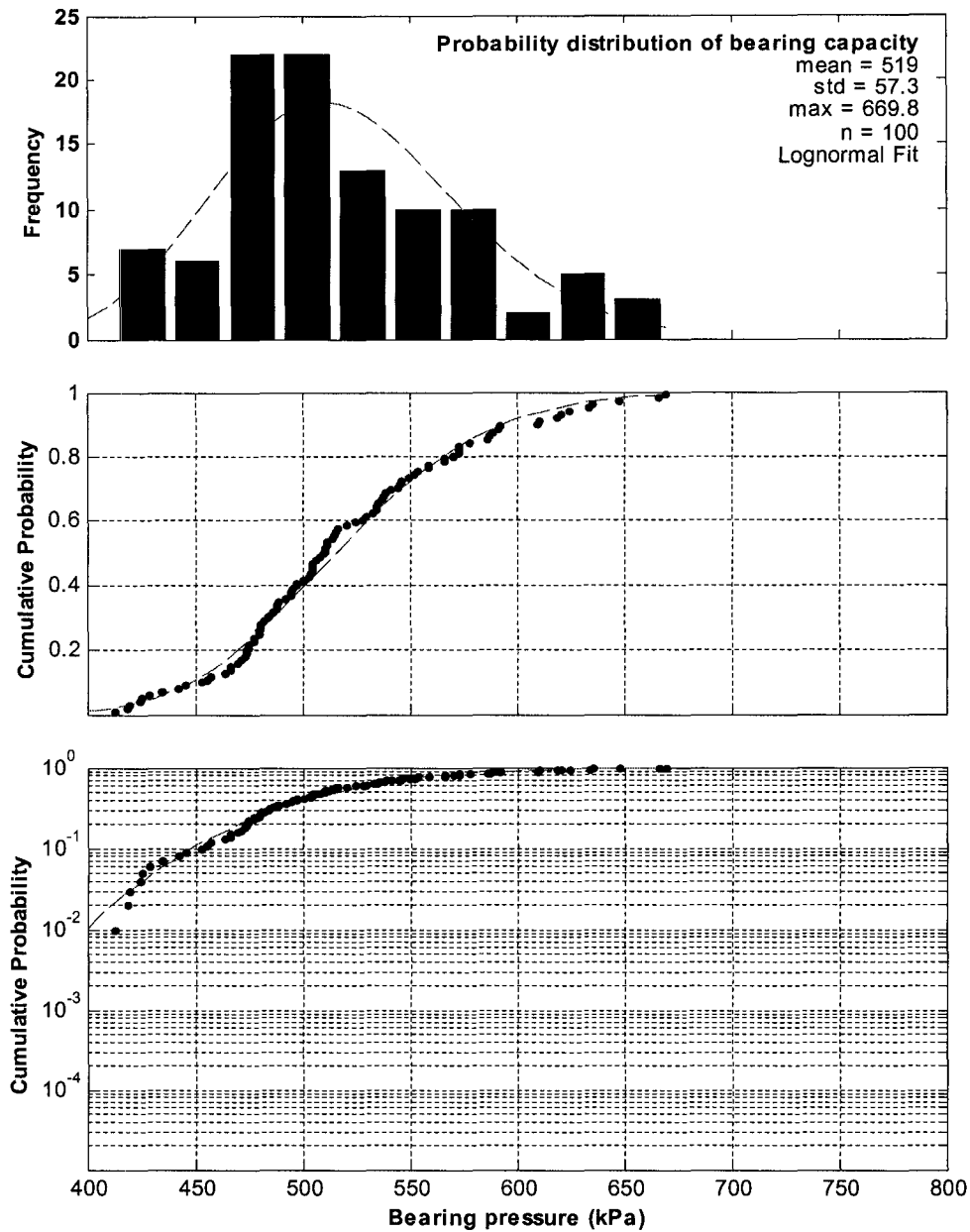


Figure B.6 An example of empirical probability distribution of foundation bearing capacity at reference settlement criterion (ultimate bearing capacity) using Lognormal fit for an experiment with Gamma distributed soil shear strength, $C_V = 25\%$, $\theta_{hn} = 2.5$, $\theta_{vn} = 0.25$, and $E/c_u = 1500$.

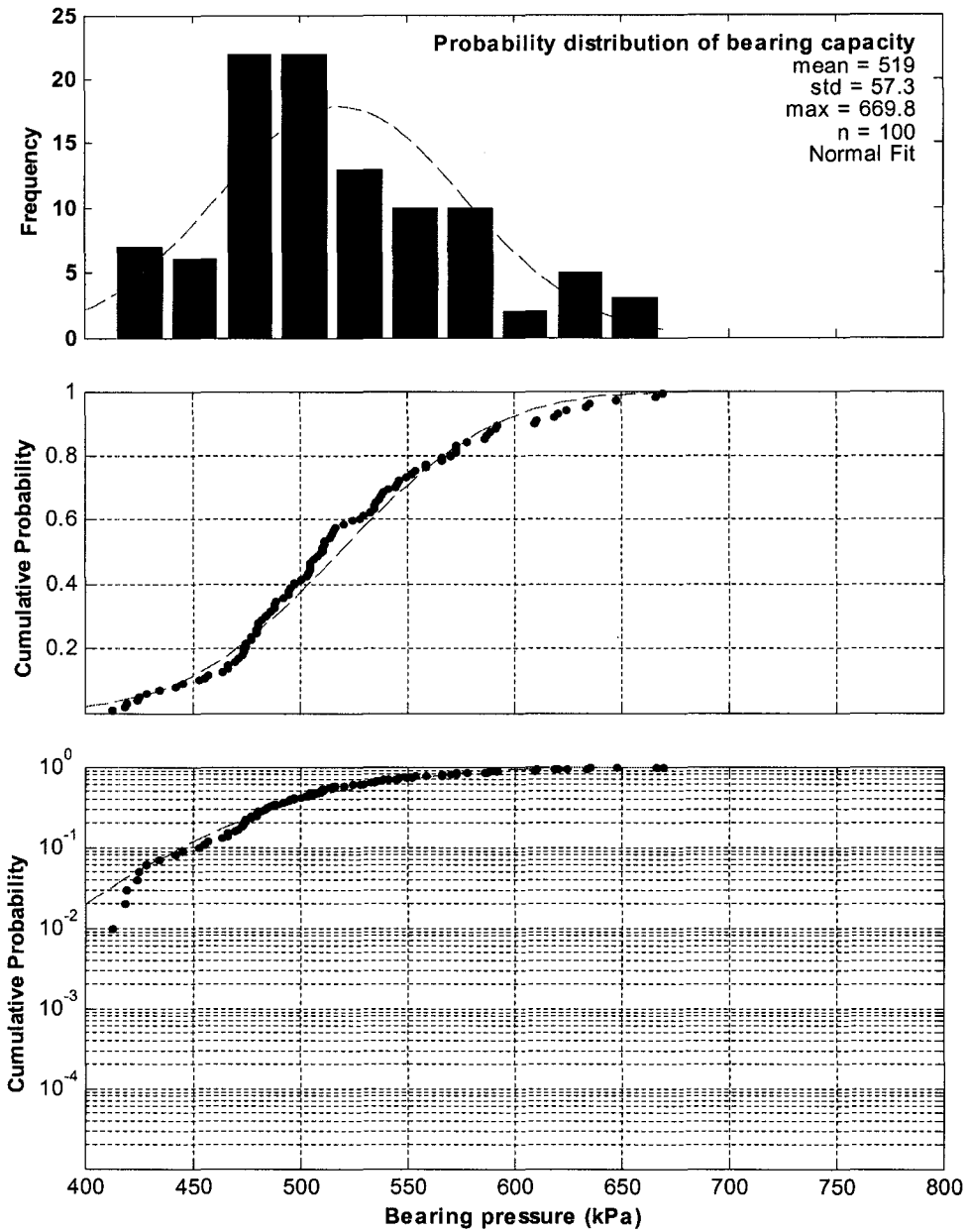


Figure B.7 An example of empirical probability distribution of foundation bearing capacity at reference settlement criterion (ultimate bearing capacity) using Normal fit for an experiment with Gamma distributed soil shear strength, $C_V = 25\%$, $\theta_{hn} = 2.5$, $\theta_{vn} = 0.25$, and $E/c_u = 1500$.

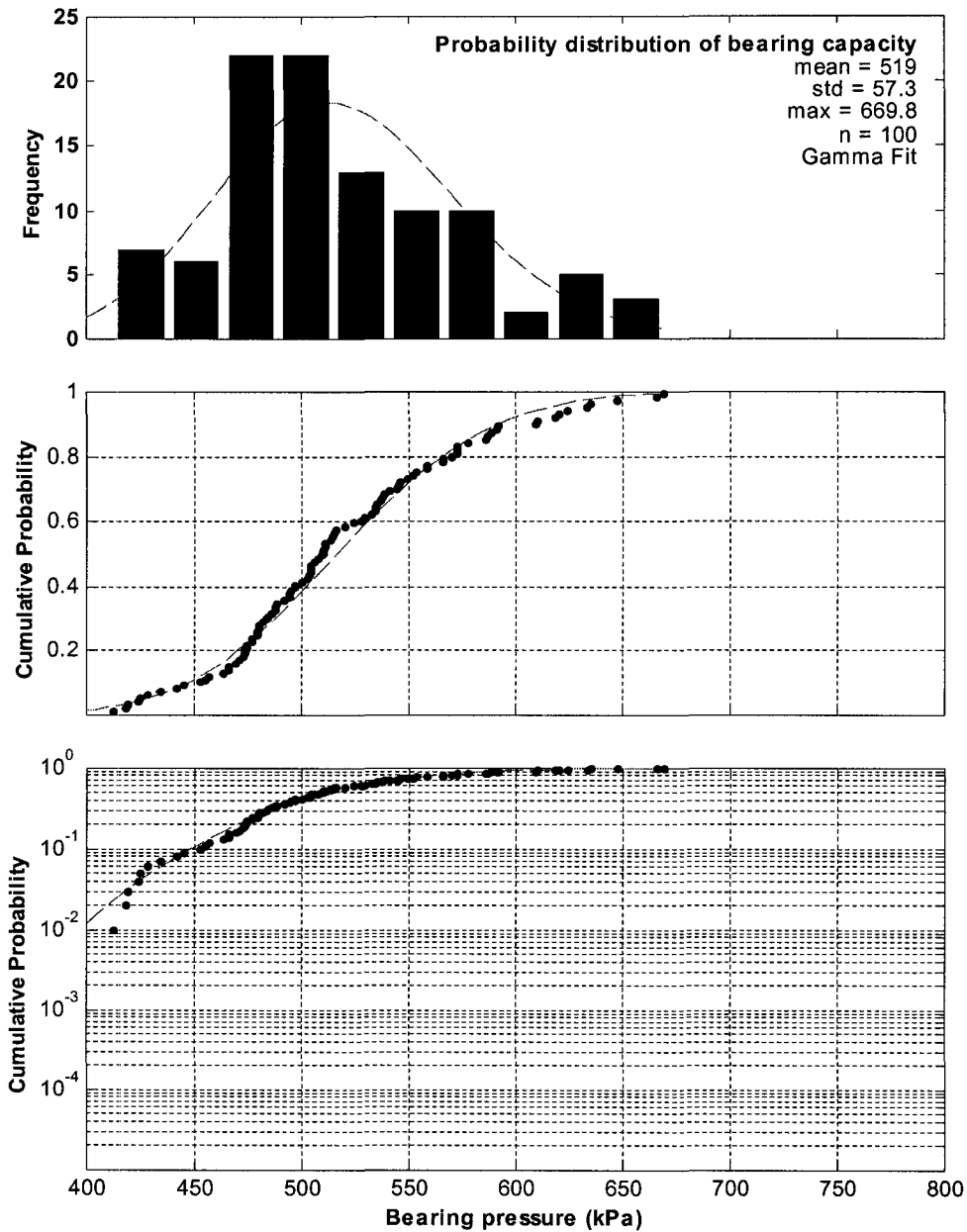


Figure B.8 An example of empirical probability distribution of foundation bearing capacity at reference settlement criterion (ultimate bearing capacity) using Gamma fit for an experiment with Gamma distributed soil shear strength, $C_V = 25\%$, $\theta_{hn} = 2.5$, $\theta_{vn} = 0.25$, and $E/c_u = 1500$.

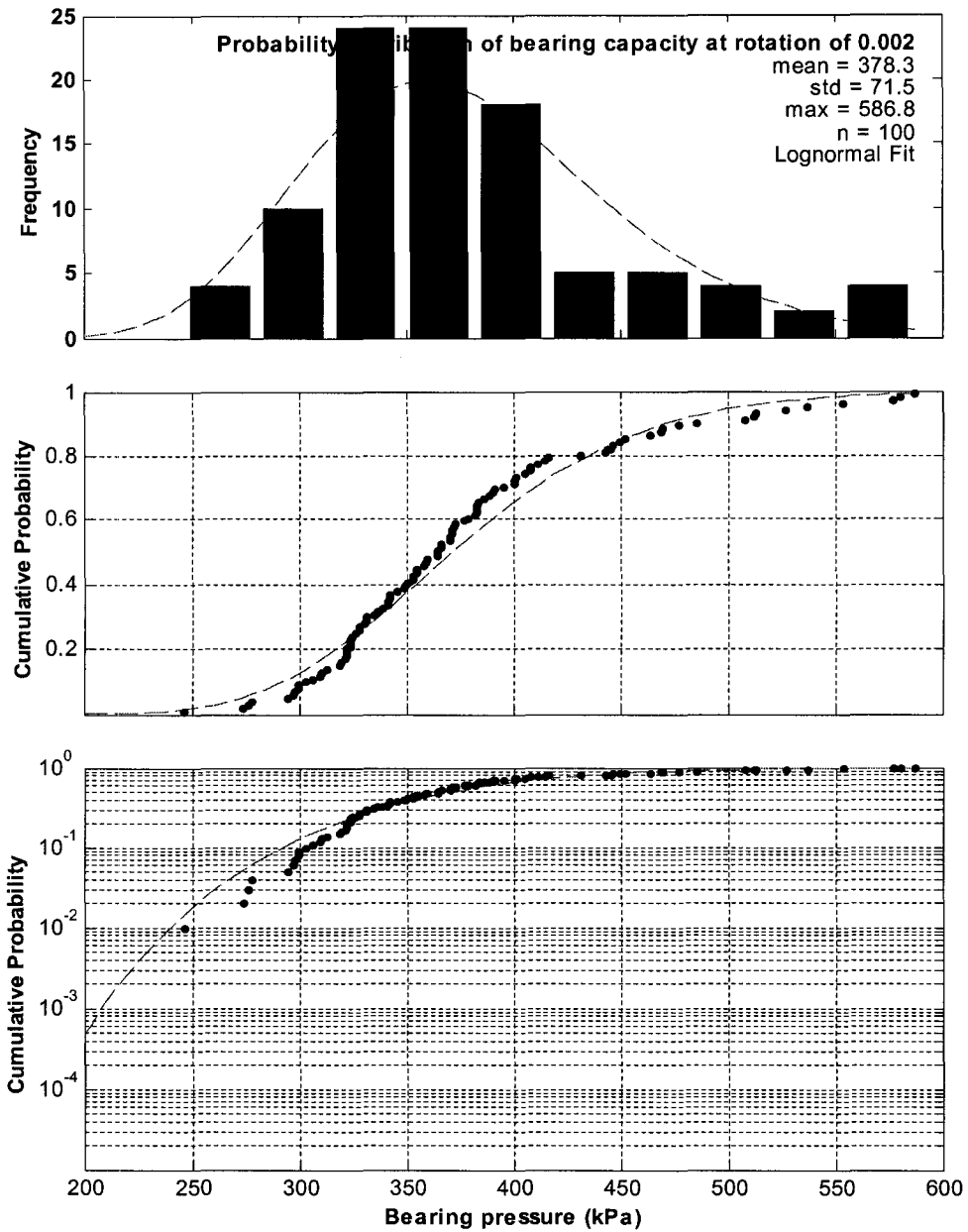


Figure B.9 An example of empirical probability distribution of foundation bearing capacity at minor damage level criterion using Lognormal fit for an experiment with Gamma distributed soil shear strength, $C_V = 25\%$, $\theta_{hn} = 2.5$, $\theta_{vn} = 0.25$, and $E/c_u = 1500$.

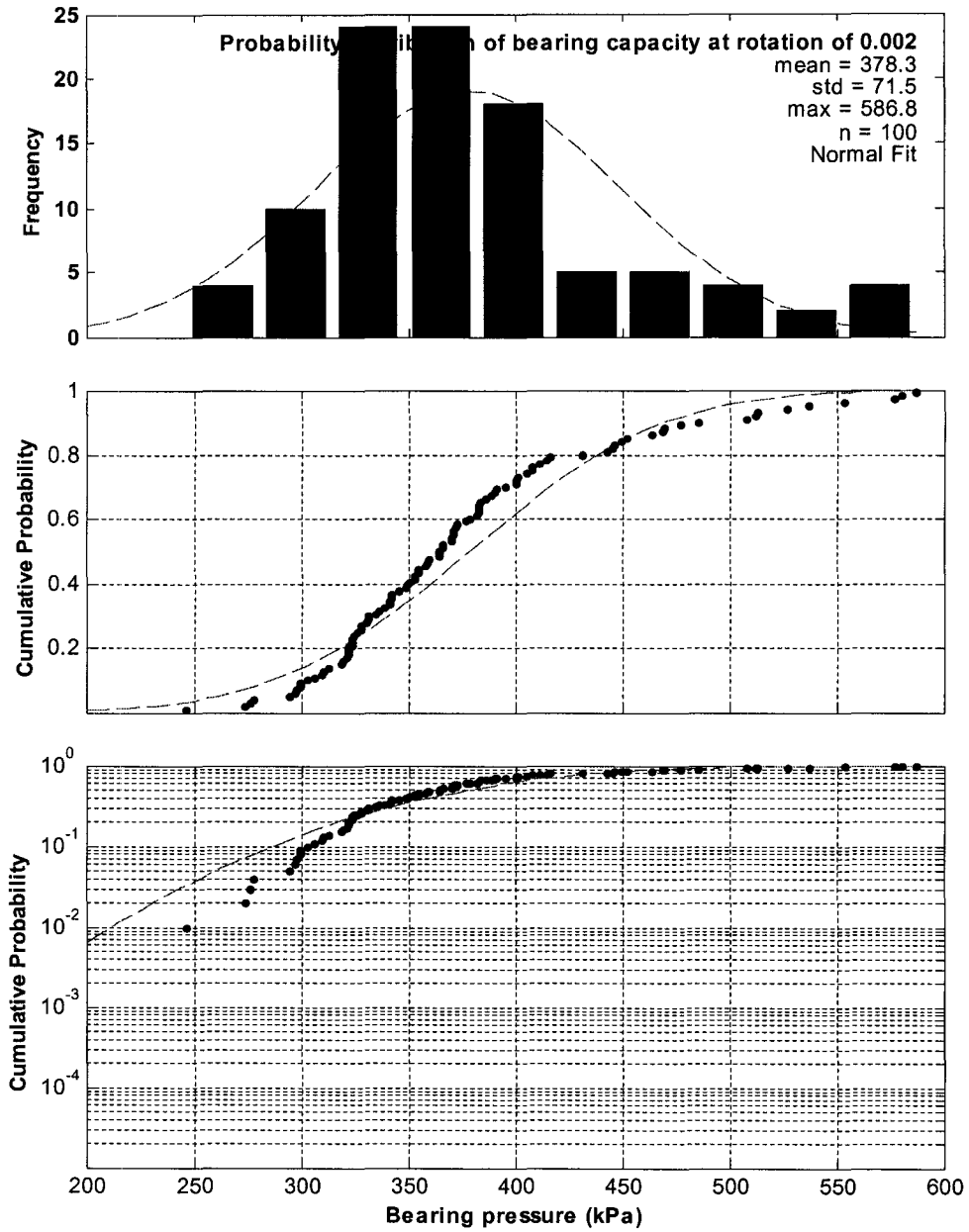


Figure B.10 An example of empirical probability distribution of foundation bearing capacity at minor damage level criterion using Normal fit for an experiment with Gamma distributed soil shear strength, $C_V = 25\%$, $\theta_{hn} = 2.5$, $\theta_{vn} = 0.25$, and $E/c_u = 1500$.

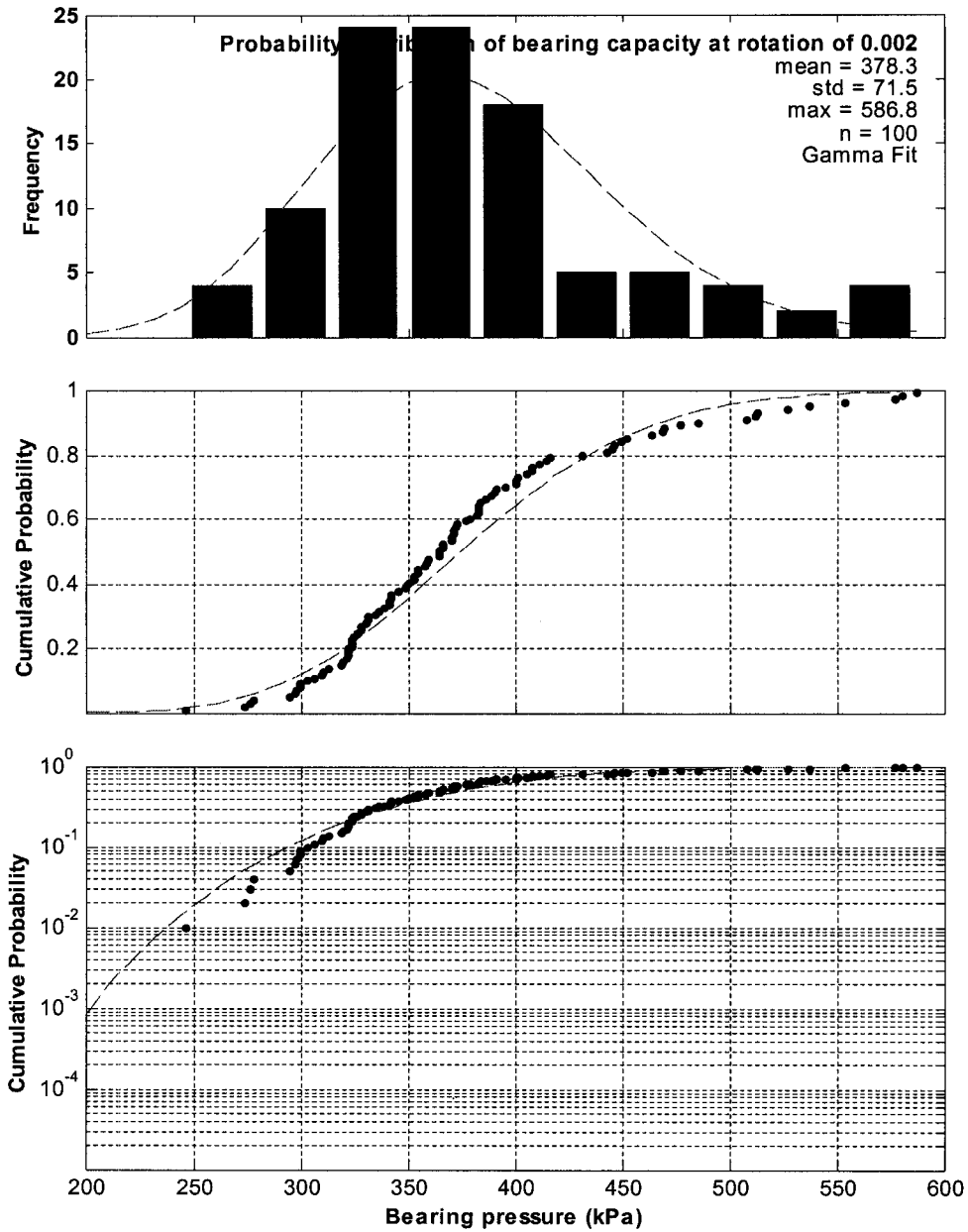


Figure B.11 An example of empirical probability distribution of foundation bearing capacity at minor damage level criterion using Gamma fit for an experiment with Gamma distributed soil shear strength, $C_V = 25\%$, $\theta_{hn} = 2.5$, $\theta_{vn} = 0.25$, and $E/c_u = 1500$.

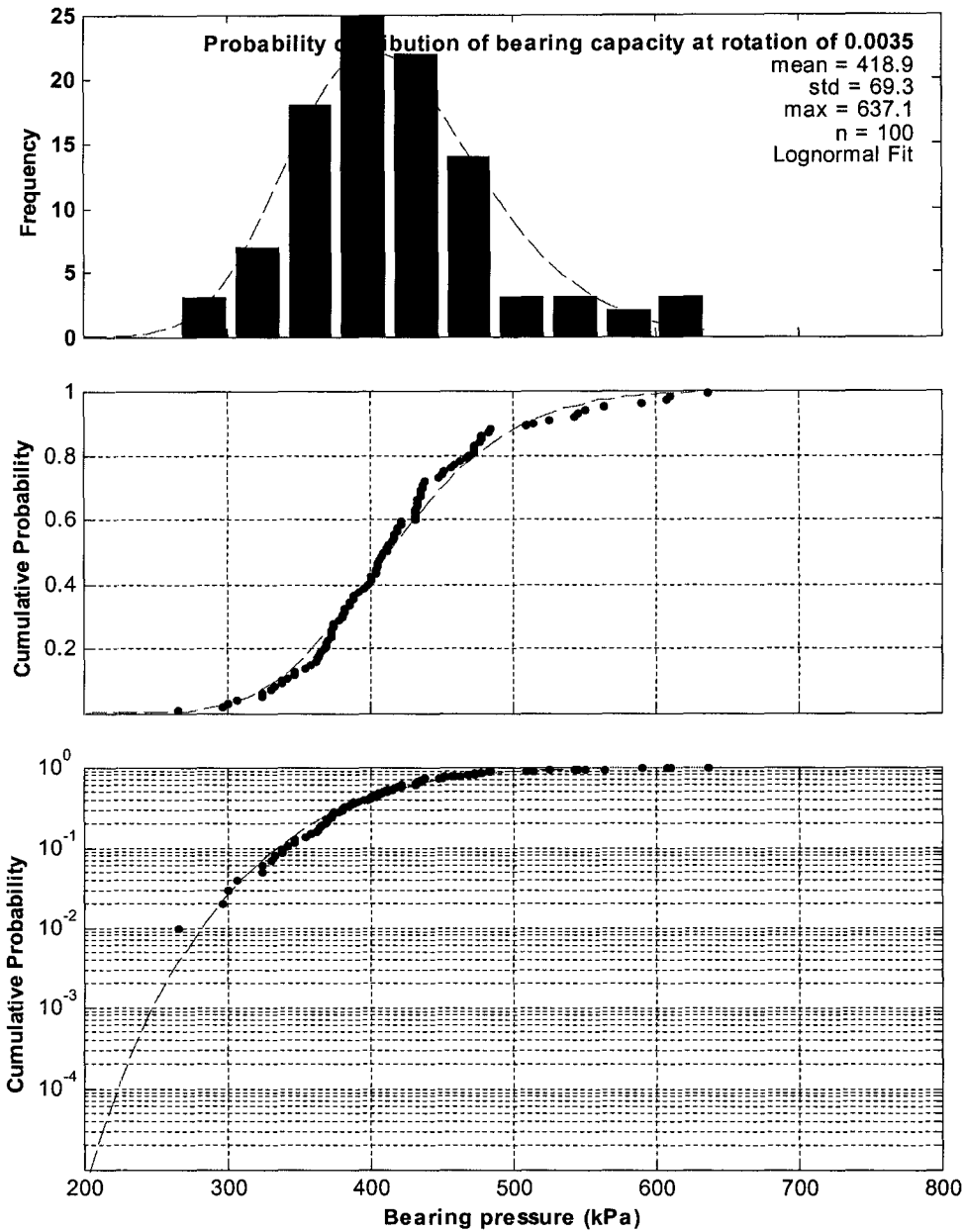


Figure B.12 An example of empirical probability distribution of foundation bearing capacity at medium damage level criterion using Lognormal fit for an experiment with Gamma distributed soil shear strength, $C_v = 25\%$, $\theta_{hn} = 2.5$, $\theta_{vn} = 0.25$, and $E/c_u = 1500$.

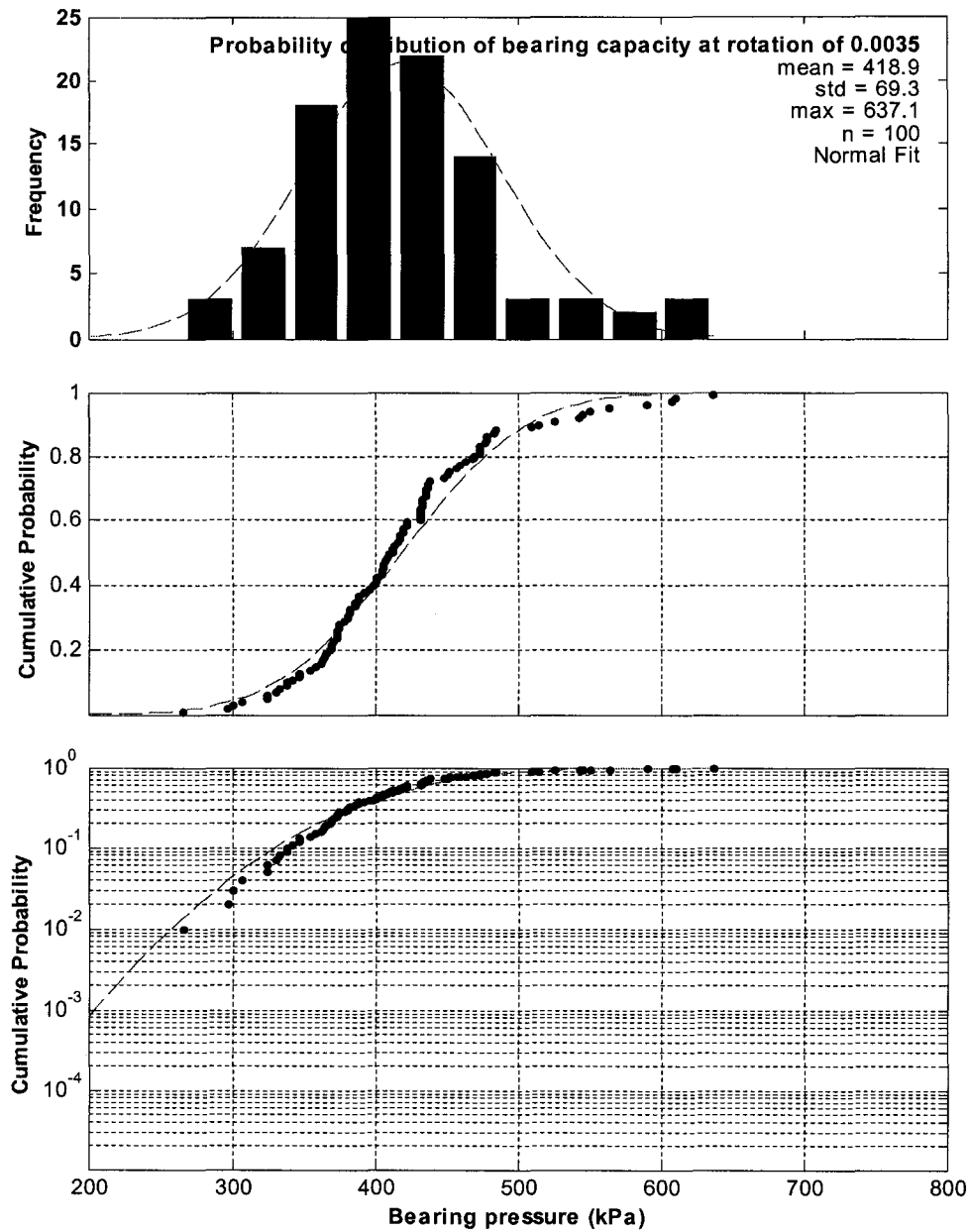


Figure B.13 An example of empirical probability distribution of foundation bearing capacity at medium damage level criterion using Normal fit for an experiment with Gamma distributed soil shear strength, $C_V = 25\%$, $\theta_{hn} = 2.5$, $\theta_{vn} = 0.25$, and $E/c_u = 1500$.

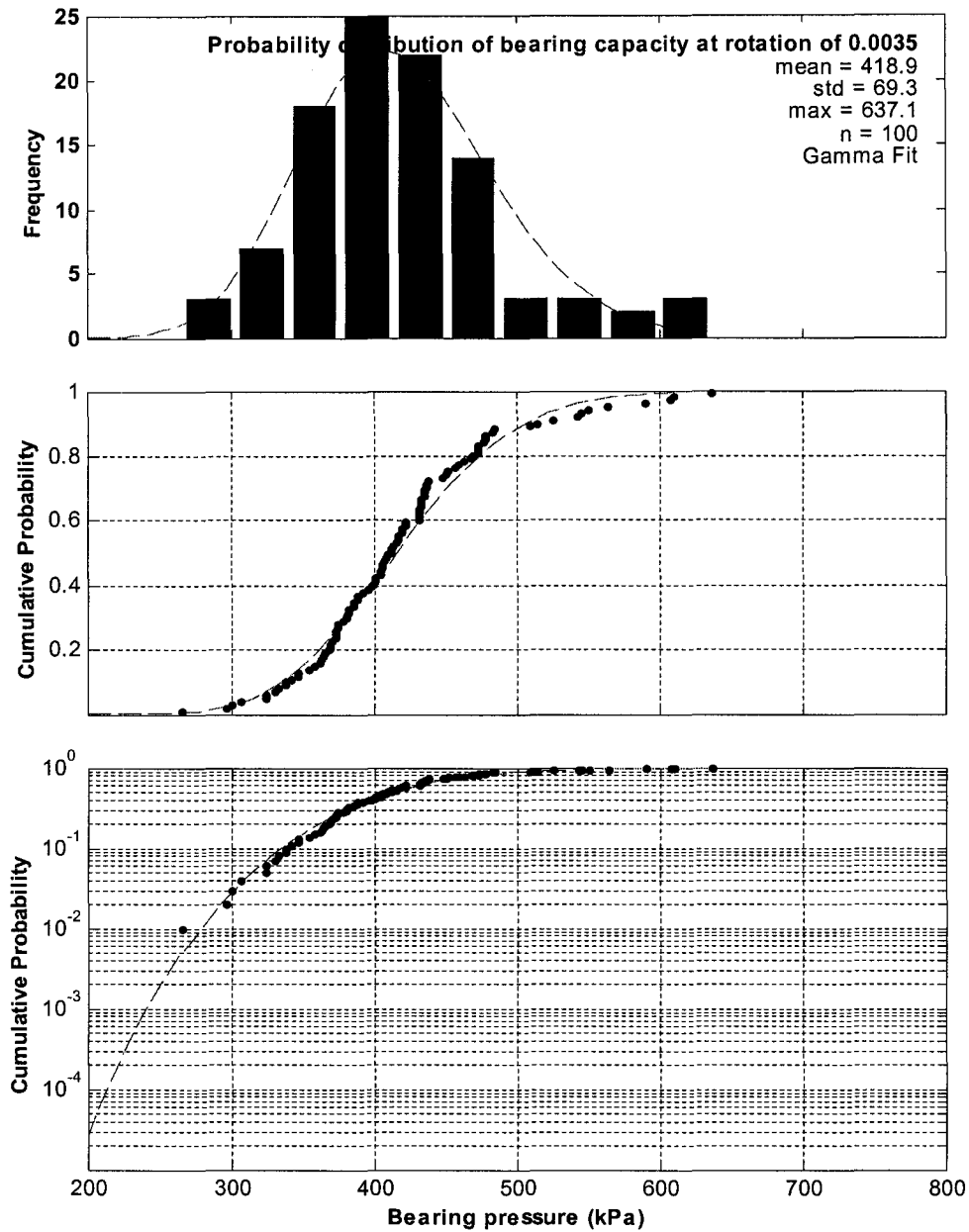


Figure B.14 An example of empirical probability distribution of foundation bearing capacity at medium damage level criterion using Gamma fit for an experiment with Gamma distributed soil shear strength, $C_V = 25\%$, $\theta_{hn} = 2.5$, $\theta_{vn} = 0.25$, and $E/c_u = 1500$.

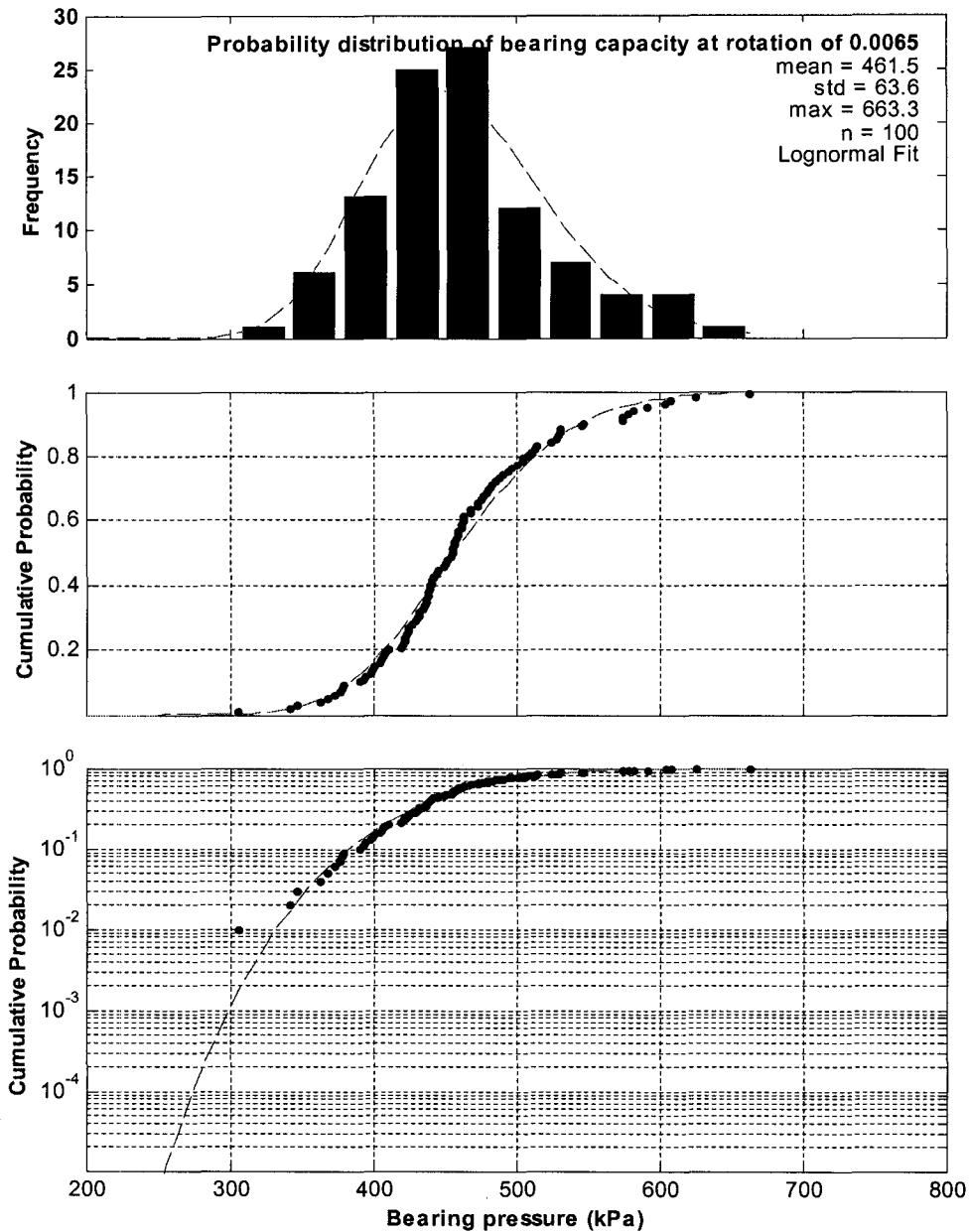


Figure B.15 An example of empirical probability distribution of foundation bearing capacity at major damage level criterion using Lognormal fit for an experiment with Gamma distributed soil shear strength, $C_V = 25\%$, $\theta_{hn} = 2.5$, $\theta_{vn} = 0.25$, and $E/c_u = 1500$.

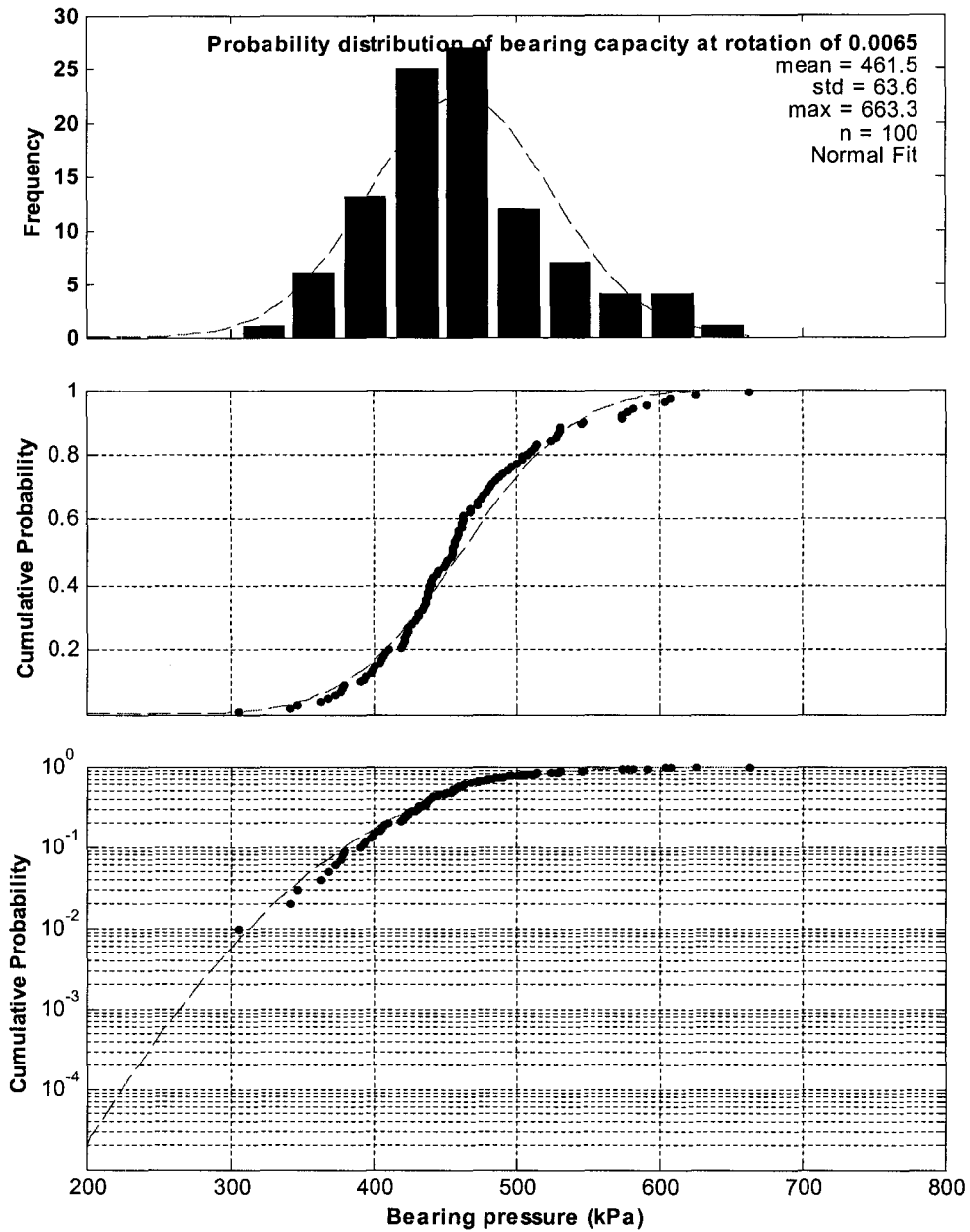


Figure B.16 An example of empirical probability distribution of foundation bearing capacity at major damage level criterion using Normal fit for an experiment with Gamma distributed soil shear strength, $C_V = 25\%$, $\theta_{hn} = 2.5$, $\theta_{vn} = 0.25$, and $E/c_u = 1500$.

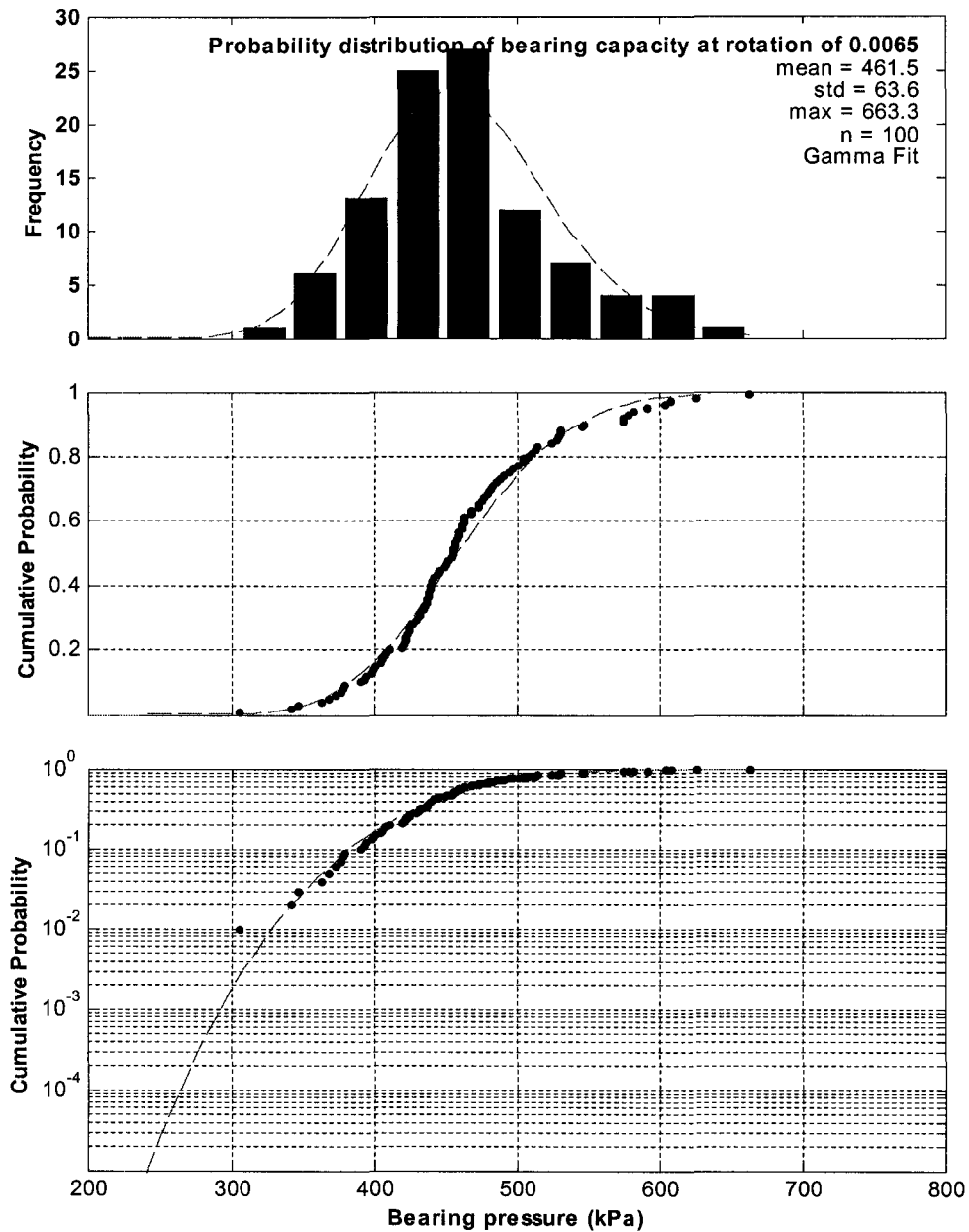


Figure B.17 An example of empirical probability distribution of foundation bearing capacity at major damage level criterion using Gamma fit for an experiment with Gamma distributed soil shear strength, $C_V = 25\%$, $\theta_{hn} = 2.5$, $\theta_{vn} = 0.25$, and $E/c_u = 1500$.

APPENDIX C. CALIBRATION OF RESISTANCE FACTORS FOR HETEROGENEOUS SOIL USING RELIABILITY THEORY

In reliability theory, load and resistance are considered to be random variables that can be described by their probability distributions. If the probability distributions of load and resistance are known, the risk or probability of failure can be obtained from direct integration assuming independence between R and S ,

$$P_f = P(R < S) = \int_0^{\infty} \left[\int_0^s f_R(r) dr \right] f_S(s) ds \quad \text{Eq. C.1}$$

However, the actual probability distribution of load and resistance are rarely available with precision. So it is common to fit a probability distribution to the available data or assumed a probability distribution for data based on some physical evidence or past experience. Normal and lognormal probability distributions are the most common probability distributions for this type of analysis. The probability of failure, P_f can be written as,

$$P_f = P(R < S) = P(z = R - S < 0) \quad \text{Eq. C.2}$$

Assuming normal distribution for R and S , the probability of failure is purely a function of the number of standard deviations between the average of z and zero (see Lind (1971) [112]; Allen, 1975 [3]). The number of standard deviations that the mean lies above zero or the failure limit is defined as the reliability index, β (Allen, 1975 [3]),

$$\beta = \frac{\bar{R} - \bar{S}}{\sqrt{\sigma_R^2 + \sigma_S^2}} \quad \text{Eq. C.3}$$

Using Lind (1971) [112] linearization,

$$\sqrt{\sigma_R^2 + \sigma_S^2} = \theta(\sigma_R + \sigma_S) \sim \frac{3}{4}(\sigma_R + \sigma_S) \quad \text{Eq. C.4}$$

The above approximation is a very good approximation for practical ratios of $\frac{\sigma_R}{\sigma_S}$

(see Section 3.6.4 for definition of θ). Thus, to obtain partial factors to secure a certain reliability level, the design criteria can be written as,

$$\bar{R} \geq \bar{S} + \beta\sqrt{\sigma_R^2 + \sigma_S^2} \quad \text{Eq. C.5}$$

Using approximation from Eq. C.4,

$$\bar{R}(1 - \theta\beta V_R) \geq \bar{S}(1 + \theta\beta V_S) \quad \text{Eq. C.6}$$

For heterogeneous soil and phenomena governed by nonlinear constitutive laws, the average geotechnical system resistance, \bar{R} , is in general different from the resistance obtained assuming a uniform soil with soil strength equal to the average strength of the heterogeneous soil, R_u . The average geotechnical system resistance for heterogeneous soil can be written as,

$$\bar{R} = \frac{R_u}{k_H} \quad \text{Eq. C.7}$$

Often, instead of average of resistance (e.g. shear strength), a conservatively assessed strength known as nominal or characteristic value is used in civil engineering design,

$$R_n = \frac{R_U}{k_R} = \frac{\bar{R}k_H}{k_R} \quad \text{or} \quad \bar{R} = \frac{R_n k_R}{k_H} \quad \text{Eq. C.8}$$

Substituting the above equation into Eq. C.6,

$$\frac{k_R}{k_H} (1 - \theta\beta V_R) R_n \geq (1 + \theta\beta V_S) \bar{S} \quad \text{Eq. C.9}$$

Comparing the above equation with LRFD definition of load and resistance factor ($\Phi R_n \geq \alpha S_n$) – looking at left side of equations, the partial resistance factor can be defined as,

$$\Phi = \frac{1 - \theta\beta V_R}{k_H} . k_R \sim \frac{4 - 3\beta V_R}{4k_H} . k_R \quad \text{Eq. C.10}$$

The right side of Eq. C.9 deals with loads and can be used to infer the partial load factors. The load factors are not addressed in this study.

